

FOR IMMEDIATE RELEASE

February 11, 2021

Biden-Harris Administration Launches American Innovation Effort to Create Jobs and Tackle the Climate Crisis

White House Forms Climate Innovation Working Group, Outlines Innovation Agenda

Today, the Biden-Harris Administration is initiating an ambitious innovation effort to create American jobs while tackling the climate crisis, which includes the launch of a new research working group, an outline of the Administration's innovation agenda. The announcements kickstart the Administration's undertaking to spur the creation of new jobs, technology, and tools that empower the United States to innovate and lead the world in addressing the climate crisis.

President Biden is fulfilling his promise to accelerate R&D investments, creating a new Climate Innovation Working Group as part of the National Climate Task Force to advance his commitment to launching an Advanced Research Projects Agency-Climate (ARPA-C). The working group will help coordinate and strengthen federal government-wide efforts to foster affordable, game-changing technologies that can help America achieve the President's goal of net zero economy-wide emissions by 2050 and can protect the American people from the impacts of droughts and flooding, bigger wildfires, and stronger hurricanes. The working group will be co-chaired by the White House Office of Domestic Climate Policy, Office of Science of Technology and Policy, and Office of Management and Budget.

"We are tapping into the imagination, talent, and grit of America's innovators, scientists, and workers to spearhead a national effort that empowers the United States to lead the world in tackling the climate crisis," **said Gina McCarthy, President Biden's National Climate Advisor**. "At the same time, we are positioning America to create good-paying, union jobs in a just and equitable way in communities across the nation that will be at the forefront of new manufacturing for clean energy and new technology, tools, and infrastructure that will help us adapt to a changing climate."

As the opportunity for American leadership in climate innovation is vast, the Administration is outlining key planks of an agenda the Climate Innovation Working Group will help advance:

- zero net carbon buildings at zero net cost, including carbon-neutral construction materials;
- energy storage at one-tenth the cost of today's alternatives;
- advanced energy system management tools to plan for and operate a grid powered by zero carbon power plants;
- very low-cost zero carbon on-road vehicles and transit systems;
- new, sustainable fuels for aircraft and ships, as well as improvements in broader aircraft and ship efficiency and transportation management;
- affordable refrigeration, air conditioning, and heat pumps made without refrigerants that warm the planet;
- carbon-free heat and industrial processes that capture emissions for making steel, concrete, chemicals, and other important industrial products;
- carbon-free hydrogen at a lower cost than hydrogen made from polluting alternatives;
- innovative soil management, plant biologies, and agricultural techniques to remove carbon dioxide from the air and store it in the ground;

- direct air capture systems and retrofits to existing industrial and power plant exhausts to capture carbon dioxide and use it to make alternative products or permanently sequester it deep underground.

In addition to supporting technologies that are near commercialization, the Climate Innovation Working Group will also emphasize research to bolster and build critical clean energy supply chains in the United States and strengthen American manufacturing. As it coordinates climate innovation across the federal government, it will focus on programs at land-grant universities, Historically Black Colleges and Universities, and other minority-serving institutions.

“Today is an important day for tackling the climate crisis through cutting-edge science, technology, and innovation. The Office of Science and Technology Policy is ready to help turbocharge climate-related innovation, and we look forward to engaging with scientists, engineers, students, and innovators all across America to build a future in which not only jobs and economic benefits but also opportunities to participate in climate innovation are shared equitably by all Americans,” **said Kei Koizumi, Acting Director of the White House Office of Science and Technology Policy.**

###



Heat stored in the Earth system: where does the energy go?

Karina von Schuckmann¹, Lijing Cheng^{2,28}, Matthew D. Palmer³, James Hansen⁴, Caterina Tassone⁵,
 Valentin Aich⁵, Susheel Adusumilli⁶, Hugo Beltrami⁷, Tim Boyer⁸, Francisco José Cuesta-Valero^{7,27},
 Damien Desbruyères⁹, Catia Domingues^{10,11}, Almudena García-García⁷, Pierre Gentile¹²,
 John Gilson¹³, Maximilian Gorfer¹⁴, Leopold Haimberger¹⁵, Masayoshi Ishii¹⁶, Gregory C. Johnson¹⁷,
 Rachel Killick³, Brian A. King¹⁰, Gottfried Kirchengast¹⁴, Nicolas Kolodziejczyk¹⁸, John Lyman¹⁷,
 Ben Marzeion¹⁹, Michael Mayer^{15,29}, Maeva Monier²⁰, Didier Paolo Monselesan²¹, Sarah Purkey⁶,
 Dean Roemmich⁶, Axel Schweiger²², Sonia I. Seneviratne²³, Andrew Shepherd²⁴, Donald A. Slater⁶,
 Andrea K. Steiner¹⁴, Fiammetta Straneo⁶, Mary-Louise Timmermans²⁵, and Susan E. Wijffels^{21,26}

¹Mercator Ocean International, Ramonville St.-Agne, France

²Institute of Atmospheric Physics, Chinese Academy of Sciences, Beijing, China

³Met Office Hadley Centre, Exeter, UK

⁴Columbia University Earth Institute, New York, USA

⁵WMO/GCOS, Geneva, Switzerland

⁶Scripps Institution of Oceanography, University of California San Diego, San Diego, California, USA

⁷Climate and Atmospheric Sciences Institute, St. Francis Xavier University, Antigonish, Nova Scotia, Canada

⁸NOAA's National Centers for Environmental Information, Silver Spring, Maryland, USA

⁹Ifremer, University of Brest, CNRS, IRD, Laboratoire d'Océanographie Physique et Spatiale, Brest, France

¹⁰National Oceanographic Centre, Southampton, UK

¹¹ARC Centre of Excellence for Climate Extremes, University of Tasmania, Hobart, Tasmania, Australia

¹²Earth and Environmental Engineering in the School of Engineering and Applied Sciences,

Columbia University, New York, New York, USA

¹³SCRIPPS Institution of Oceanography, University of California San Diego, La Jolla, California, USA

¹⁴Wegener Center for Climate and Global Change and Institute of Physics, University of Graz, Graz, Austria

¹⁵Department of Meteorology and Geophysics, University of Vienna, Vienna, Austria

¹⁶Department of Atmosphere, Ocean and Earth System Modeling Research,
 Meteorological Research Institute, Nagamine, Tsukuba, Japan

¹⁷NOAA, Pacific Marine Environmental Laboratory, Seattle, USA

¹⁸University of Brest, CNRS, IRD, Ifremer, Laboratoire d'Océanographie Physique et Spatiale,
 IUEM, Brest, France

¹⁹Institute of Geography and MARUM – Center for Marine Environmental Sciences,
 University of Bremen, Bremen, Germany

²⁰CELAD/Mercator Ocean International, Ramonville-Saint-Agne, France

²¹CSIRO Oceans and Atmosphere, Hobart, Tasmania, Australia

²²Polar Science Center, Applied Physics Laboratory, University of Washington, Seattle, WA, USA

²³Institute for Atmospheric and Climate Science, ETH Zurich, Zürich, Switzerland

²⁴Center for Polar Observation and Modeling, University of Leeds, Leeds, UK

²⁵Department of Earth and Planetary Sciences, Yale University, New Haven, Connecticut, USA

²⁶Woods Hole Oceanographic Institution, Massachusetts, USA

²⁷Environmental Sciences Program, Memorial University of Newfoundland, NL, Canada

²⁸Center for Ocean Mega-Science, Chinese Academy of Sciences, Qingdao, 266071, China

²⁹European Centre for Medium-Range Weather Forecasts, Reading, UK

Correspondence: Karina von Schuckmann (karina.von.schuckmann@mercator-ocean.fr)

Received: 30 December 2019 – Discussion started: 20 March 2020

Revised: 15 August 2020 – Accepted: 18 August 2020 – Published: 7 September 2020

Abstract. Human-induced atmospheric composition changes cause a radiative imbalance at the top of the atmosphere which is driving global warming. This Earth energy imbalance (EEI) is the most critical number defining the prospects for continued global warming and climate change. Understanding the heat gain of the Earth system – and particularly how much and where the heat is distributed – is fundamental to understanding how this affects warming ocean, atmosphere and land; rising surface temperature; sea level; and loss of grounded and floating ice, which are fundamental concerns for society. This study is a Global Climate Observing System (GCOS) concerted international effort to update the Earth heat inventory and presents an updated assessment of ocean warming estimates as well as new and updated estimates of heat gain in the atmosphere, cryosphere and land over the period 1960–2018. The study obtains a consistent long-term Earth system heat gain over the period 1971–2018, with a total heat gain of $358 \pm 37 \text{ ZJ}$, which is equivalent to a global heating rate of $0.47 \pm 0.1 \text{ W m}^{-2}$. Over the period 1971–2018 (2010–2018), the majority of heat gain is reported for the global ocean with 89 % (90 %), with 52 % for both periods in the upper 700 m depth, 28 % (30 %) for the 700–2000 m depth layer and 9 % (8 %) below 2000 m depth. Heat gain over land amounts to 6 % (5 %) over these periods, 4 % (3 %) is available for the melting of grounded and floating ice, and 1 % (2 %) is available for atmospheric warming. Our results also show that EEI is not only continuing, but also increasing: the EEI amounts to $0.87 \pm 0.12 \text{ W m}^{-2}$ during 2010–2018. Stabilization of climate, the goal of the universally agreed United Nations Framework Convention on Climate Change (UNFCCC) in 1992 and the Paris Agreement in 2015, requires that EEI be reduced to approximately zero to achieve Earth's system quasi-equilibrium. The amount of CO_2 in the atmosphere would need to be reduced from 410 to 353 ppm to increase heat radiation to space by 0.87 W m^{-2} , bringing Earth back towards energy balance. This simple number, EEI, is the most fundamental metric that the scientific community and public must be aware of as the measure of how well the world is doing in the task of bringing climate change under control, and we call for an implementation of the EEI into the global stocktake based on best available science. Continued quantification and reduced uncertainties in the Earth heat inventory can be best achieved through the maintenance of the current global climate observing system, its extension into areas of gaps in the sampling, and the establishment of an international framework for concerted multidisciplinary research of the Earth heat inventory as presented in this study. This Earth heat inventory is published at the German Climate Computing Centre (DKRZ, <https://www.dkrz.de/>, last access: 7 August 2020) under the DOI https://doi.org/10.26050/WDC/GCOS_EHI_EXP_v2 (von Schuckmann et al., 2020).

1 Introduction

In the Paris Agreement of the United Nations Framework Convention on Climate Change (UNFCCC), article 7 demands that “Parties should strengthen [...] scientific knowledge on climate, including research, systematic observation of the climate system and early warning systems, in a manner that informs climate services and supports decision-making”. This request of the UNFCCC expresses the need of climate monitoring based on best available science, which is globally coordinated through the Global Climate Observing System (GCOS). In the current Implementation Plan of GCOS, main observation gaps are addressed and it states that “closing the Earth's energy balance [...] through observations remain outstanding scientific issues that require high-quality climate records of Essential Climate Variables (ECVs).” (GCOS, 2016). GCOS is asking the broader scientific community to establish the observational requirements needed to meet the targets defined in the GCOS Implementation Plan and to identify how climate observations could be

enhanced and continued into the future in order to monitor the Earth's cycles and the global energy budget. This study addresses and intends to respond to this request.

The state, variability and change of Earth's climate are to a large extent driven by the energy transfer between the different components of the Earth system (Hansen, 2005; Hansen et al., 2011). Energy flows alter clouds, and weather and internal climate modes can temporarily alter the energy balance on subannual to multidecadal timescales (Palmer and McNeall, 2014; Rhein et al., 2013). The most practical way to monitor climate state, variability and change is to continually assess the energy, mainly in the form of heat, in the Earth system (Hansen et al., 2011). All energy entering or leaving the Earth climate system does so in the form of radiation at the top of the atmosphere (TOA) (Loeb et al., 2012). The difference between incoming solar radiation and outgoing radiation, which is the sum of the reflected shortwave radiation and emitted longwave radiation, determines the net radiative flux at TOA. Changes of this global radiation balance at TOA – the so-called Earth energy imbalance (EEI)

– determine the temporal evolution of Earth’s climate: If the imbalance is positive (i.e., less energy going out than coming in), energy in the form of heat is accumulated in the Earth system, resulting in global warming – or cooling if the EEI is negative. The various facets and impacts of observed climate change arise due to the EEI, which thus represents a crucial measure of the rate of climate change (von Schuckmann et al., 2016). The EEI is the portion of the forcing that has not yet been responded to (Hansen, 2005). In other words, warming will continue even if atmospheric greenhouse gas (GHG) amounts are stabilized at today’s level, and the EEI defines additional global warming that will occur without further change in forcing (Hansen et al., 2017). The EEI is less subject to decadal variations associated with internal climate variability than global surface temperature and therefore represents a robust measure of the rate of climate change (von Schuckmann et al., 2016; Cheng et al., 2017a).

The Earth system responds to an imposed radiative forcing through a number of feedbacks, which operate on various different timescales. Conceptually, the relationships between EEI, radiative forcing and surface temperature change can be expressed as (Gregory and Andrews, 2016)

$$\Delta N_{\text{TOA}} = \Delta F_{\text{ERF}} - |\alpha_{\text{FP}}| \Delta T_{\text{S}}, \quad (1)$$

where ΔN_{TOA} is Earth’s net energy imbalance at TOA (in W m^{-2}), ΔF_{ERF} is the effective radiative forcing (W m^{-2}), ΔT_{S} is the global surface temperature anomaly (K) relative to the equilibrium state and α_{FP} is the net total feedback parameter ($\text{W m}^{-2} \text{K}^{-1}$), which represents the combined effect of the various climate feedbacks. Essentially, α_{FP} in Eq. (1) can be viewed as a measure of how efficient the system is at restoring radiative equilibrium for a unit surface temperature rise. Thus, ΔN_{TOA} represents the difference between the applied radiative forcing and Earth’s radiative response through climate feedbacks associated with surface temperature rise (e.g., Hansen et al., 2011). Observation-based estimates of ΔN_{TOA} are therefore crucial both to our understanding of past climate change and for refining projections of future climate change (Gregory and Andrews, 2016; Kuhlbrodt and Gregory, 2012). The long atmospheric lifetime of carbon dioxide means that ΔN_{TOA} , ΔF_{ERF} and ΔT_{S} will remain positive for centuries, even with substantial reductions in greenhouse gas emissions, and lead to substantial committed sea-level rise (Cheng et al., 2019a; Hansen et al., 2017; Nauels et al., 2017; Palmer et al., 2018).

However, this conceptual picture is complicated by the presence of unforced internal variability in the climate system, which adds substantial noise to the real-world expression of this equation (Gregory et al., 2020; Marvel et al., 2018; Palmer and McNeall, 2014). For example, at timescales from interannual to decadal periods, the phase of the El Niño–Southern Oscillation contributes to both positive or negative variations in EEI (Cheng et al., 2019a; Loeb et al., 2018; Johnson and Birnbaum, 2017; Loeb et al., 2012). At multidecadal and longer timescales, systematic changes

in ocean circulation can significantly alter the EEI as well (Baggenstos et al., 2019).

Timescales of the Earth climate response to perturbations of the equilibrium Earth energy balance at TOA are driven by a combination of climate forcing and the planet’s thermal inertia: the Earth system tries to restore radiative equilibrium through increased thermal radiation to space via the Planck response, but a number of additional Earth system feedbacks also influence the planetary radiative response (Lembo et al., 2019; Myhre et al., 2013). Timescales of warming or cooling of the climate depend on the imposed radiative forcing, the evolution of climate and Earth system feedbacks, with ocean and cryosphere in particular leading to substantial thermal inertia (Clark et al., 2016; Marshall et al., 2015). Consequently, it requires centuries for Earth’s surface temperature to respond fully to a climate forcing.

Contemporary estimates of the magnitude of the Earth’s energy imbalance range between about 0.4 and 0.9 W m^{-2} (depending on estimate method and period; see also conclusion) and are directly attributable to increases in carbon dioxide and other greenhouse gases in the atmosphere from human activities (Ciais et al., 2013; Myhre et al., 2013; Rhein et al., 2013; Hansen et al., 2011). The estimate obtained from climate models (CMIP6) as presented by Wild (2020) amounts to $1.1 \pm 0.8 \text{ W m}^{-2}$. Since the period of industrialization, the EEI has become increasingly dominated by the emissions of radiatively active greenhouse gases, which perturb the planetary radiation budget and result in a positive EEI. As a consequence, excess heat is accumulated in the Earth system, which is driving global warming (Hansen et al., 2005, 2011). The majority (about 90 %) of this positive EEI is stored in the ocean (Rhein et al., 2013) and can be estimated through the evaluation of ocean heat content (OHC, e.g., Abraham et al., 2013). According to previous estimates, a small proportion (~ 3 %) contributes to the melting of Arctic sea ice and land ice (glaciers, the Greenland and Antarctic ice sheets). Another 4 % goes into heating of the land and atmosphere (Rhein et al., 2013).

Knowing where and how much heat is stored in the different Earth system components from a positive EEI, and quantifying the Earth heat inventory, is of fundamental importance to unravel the current status of climate change, as well as to better understand and predict its implications, and to design the optimal observing networks for monitoring the Earth heat inventory. Quantifying this energy gain is essential for understanding the response of the climate system to radiative forcing and hence to reduce uncertainties in climate predictions. The rate of ocean heat gain is a key component for the quantification of the EEI, and the observed surface warming has been used to estimate the equilibrium climate sensitivity (e.g., Knutti and Rugenstein, 2015). However, further insight into the Earth heat inventory, particularly to further unravel where the heat is going, can have implications on the understanding of the transient climate responses to climate change and consequently reduces uncertainties in cli-

mate predictions (Hansen et al., 2011). In this paper, we focus on the inventory of heat stored in the Earth system. The first four sections will introduce the current status of estimate of heat storage change in the ocean, atmosphere, land and cryosphere, respectively. Uncertainties, current achieved accuracy, challenges and recommendations for future improved estimates are discussed for each Earth system component and in the conclusion. In the last chapter, an update of the Earth heat inventory is established based on the results of Sects. 1–4, followed by a conclusion.

2 Heat stored in the ocean

The storage of heat in the ocean leads to ocean warming (IPCC, 2020) and is a major contributor to sea-level rise through thermal expansion (WCRP, 2018). Ocean warming alters ocean stratification and ocean mixing processes (Bindoff et al., 2020), affects ocean currents (Hoegh-Guldberg, 2020; Rhein et al., 2018; Yang et al., 2016), impacts tropical cyclones (Hoegh-Guldberg, 2020; Trenberth et al., 2018; Woollings et al., 2012), and is a major player in ocean deoxygenation processes (Breitburg et al., 2018) and carbon sequestration into the ocean (Bopp et al., 2013; Frölicher et al., 2018). Together with ocean acidification and deoxygenation, ocean warming can lead to dramatic changes in ecosystems, biodiversity, population extinctions, coral bleaching and infectious disease, as well as redistribution of habitat (García Molinos et al., 2016; Gattuso et al., 2015; Ramírez et al., 2017). Implications of ocean warming are also widespread across Earth's cryosphere (Jacobs et al., 2002; Mayer et al., 2019; Polyakov et al., 2017; Serreze and Barry, 2011; Shi et al., 2018). Examples include the basal melt of ice shelves (Adusumilli et al., 2020; Pritchard et al., 2012; Wilson et al., 2017) and marine-terminating glaciers (Straneo and Cenedese, 2015), as well as the retreat and speedup of outlet glaciers in Greenland (King et al., 2018) and in Antarctica (Shepherd et al., 2018a) and of tidewater glaciers in South America and in the High Arctic (Gardner et al., 2013).

Opportunities and challenges in forming OHC estimates depend on the availability of in situ subsurface temperature measurements, particularly for global-scale evaluations. Subsurface ocean temperature measurements before 1900 had been obtained from shipboard instrumentation, culminating in the global-scale Challenger expedition (1873–1876) (Roemmich and Gilson, 2009). From 1900 up to the mid-1960s, subsurface temperature measurements relied on shipboard Nansen bottle and mechanical bathythermograph (MBT) instruments (Abraham et al., 2013), only allowing limited global coverage and data quality. The inventions of the conductivity–temperature–depth (CTD) instruments in the mid-1950s and the expendable bathythermograph (XBT) observing system about 10 years later increased the oceanographic capabilities for widespread and accurate (in the case

of the CTD) measurements of in situ subsurface water temperature (Abraham et al., 2013; Goni et al., 2019).

With the implementation of several national and international programs, and the implementation of the moored arrays in the tropical ocean in the 1980s, the Global Ocean Observing System (GOOS, <https://www.goosocean.org/>, last access: 7 August 2020) started to grow. Particularly the global World Ocean Circulation Experiment (WOCE) during the 1990s obtained a global baseline survey of the ocean from top to bottom (King et al., 2001). However, measurements were still limited to fixed point platforms, major shipping routes, and naval and research vessel cruise tracks, leaving large parts of the ocean undersampled. In addition, detected instrumental biases in MBTs, XBTs and other instruments pose a further challenge for the global scale OHC estimate (Abraham et al., 2013; Ciais et al., 2013; Rhein et al., 2013), but significant progress has been made recently to correct biases and provide high-quality data for climate research (Boyer et al., 2016; Cheng et al., 2016; Goni et al., 2019; Gouretski and Cheng, 2020). Satellite altimeter measurements of sea surface height began in 1992 and are used to complement in situ-derived OHC estimates, either for validation purposes (Cabanes et al., 2013) or to complement the development of global gridded ocean temperature fields (Guinehut et al., 2012; Willis et al., 2004). Indirect estimates of OHC from remote sensing through the global sea-level budget became possible with satellite-derived ocean mass information in 2002 (Dieng et al., 2017; Llovel et al., 2014; Loeb et al., 2012; Meyssignac et al., 2019; von Schuckmann et al., 2014).

After the OceanObs conference in 1999, the international Argo profiling float program was launched with first Argo float deployments in the same year (Riser et al., 2016; Roemmich and Gilson, 2009). By the end of 2006, Argo sampling had reached its initial target of data sampling roughly every 3° between 60° S and 60° N. However, due to technical evolution, only 40 % of Argo floats provided measurements down to 2000 m depth in the year 2005, but that percentage increased to 60 % in 2010 (von Schuckmann and Le Traon, 2011). The starting point of the Argo-based best estimate for near-global-scale (60° S–60° N) OHC is either defined in 2005 (von Schuckmann and Le Traon, 2011) or in 2006 (Wijffels et al., 2016). The opportunity for improved OHC estimation provided by Argo is tremendous and has led to major advancements in climate science, particularly on the discussion of the EEI (Hansen et al., 2011; Johnson et al., 2018; Loeb et al., 2012; Trenberth and Fasullo, 2010; von Schuckmann et al., 2016; Meyssignac et al., 2019). The near-global coverage of the Argo network also provides an excellent test bed for the long-term OHC reconstruction extending back well before the Argo period (Cheng et al., 2017b). Moreover, these evaluations inform further observing system recommendations for global climate studies, i.e., gaps in the deep ocean layers below 2000 m depth, in marginal seas, in shelf areas and in the polar regions (e.g., von Schuckmann et

al., 2016), and their implementations are underway, for example for deep Argo (Johnson et al., 2019).

Different research groups have developed gridded products of subsurface temperature fields for the global ocean using statistical models (Gaillard et al., 2016; Good et al., 2013; Ishii et al., 2017; Levitus et al., 2012) or combined observations with additional statistics from climate models (Cheng et al., 2017b). An exhaustive list of the pre-Argo products can be found in, for example, Abraham et al. (2013), Boyer et al. (2016), WCRP (2018) and Meyssignac et al. (2019). Additionally, specific Argo-based products are listed on the Argo web page (<http://www.argo.ucsd.edu/>, last access: 7 August 2020). Although all products rely more or less on the same database, near-global OHC estimates show some discrepancies which result from the different statistical treatments of data gaps, the choice of the climatology, and the approach used to account for the MBT and XBT instrumental biases (Boyer et al., 2016; Wang et al., 2018). Argo-based products show smaller differences, likely resulting from different treatments of currently undersampled regions (e.g., von Schuckmann et al., 2016). Ocean reanalysis systems have been also used to deliver estimates of near-global OHC (Meyssignac et al., 2019; von Schuckmann et al., 2018), and their international assessments show increased discrepancies with decreasing in situ data availability for the assimilation (Palmer et al., 2017; Storto et al., 2018). Climate models have also been used to study global and regional ocean heat changes and the associated mechanisms, with observational datasets providing valuable benchmarks for model evaluation (Cheng et al., 2016; Gleckler et al., 2016).

International near-global OHC assessments have been performed previously (e.g., Abraham et al., 2013; Boyer et al., 2016; Meyssignac et al., 2019; WCRP, 2018). These assessments are challenging, as most of the gridded temperature fields are research products, and only few are distributed and regularly updated operationally (e.g., <https://marine.copernicus.eu/>, last access: 7 August 2020). This initiative relies on the availability of data products, their temporal extensions and direct interactions with the different research groups. A complete view of all international temperature products can be only achieved through a concerted international effort and over time. In this study, we do not achieve a holistic view of all available products but present a starting point for future international regular assessments of near-global OHC. For the first time, we propose an international ensemble mean and standard deviation of near-global OHC (Fig. 1) which is then used to build an Earth climate system energy inventory (Sect. 5). The ensemble spread gives an indication of the agreement among products and can be used as a proxy for uncertainty. The basic assumption for the error distribution is Gaussian with a mean of zero, which can be approximated by an ensemble of various products. However, it does not account for systematic errors that may result in biases across the ensemble and does not represent the full uncertainty. The uncertainty can also be estimated in

Table 1. Linear trends (weighted least square fit; see for example von Schuckmann and Le Traon, 2011) as derived from the ensemble mean as presented in Fig. 1 for different time intervals, as well as different integration depth. The uncertainty on the trend estimate is given for the 95 % confidence level. Note that values are given for the ocean surface area between 60° S and 60° N and are limited to the 300 m bathymetry of each product. See text and Fig. 1 caption for more details on the OHC estimates.

Period	0–300 m (W m ^{−2})	0–700 m (W m ^{−2})	0–2000 m (W m ^{−2})	700–2000 m (W m ^{−2})
1960–2018	0.3 ± 0.03	0.4 ± 0.1	0.5 ± 0.1	0.2 ± 0.03
1993–2018	0.4 ± 0.04	0.6 ± 0.1	0.9 ± 0.1	0.3 ± 0.03
2005–2018	0.4 ± 0.1	0.6 ± 0.1	1.0 ± 0.2	0.4 ± 0.1
2010–2018	0.5 ± 0.1	0.7 ± 0.1	1.3 ± 0.3	0.5 ± 0.1

other ways including some purely statistical methods (Levitus et al., 2012) or methods explicitly accounting for the error sources (Lyman and Johnson, 2013), but each method has its caveats, for example the error covariances are mostly unknown, so adopting a straightforward method with a “data democracy” strategy has been chosen here as a starting point.

However, future evolution of this initiative is needed to include missing and updated in situ-based products, ocean reanalyses and indirect estimates (for example satellite based). The continuity of this activity will help to further unravel uncertainties due to the community’s collective efforts on detecting/reducing errors, and it then provides up-to-date scientific knowledge of ocean heat uptake.

Products used for this assessment are referenced in the caption of Fig. 2. Estimates of OHC have been provided by the different research groups under homogeneous criteria. All estimates use a coherent ocean volume limited by the 300 m isobath of each product and are limited to 60° S–60° N since most observational products exclude high-latitude ocean areas because of the low observational coverage, and only annual averages have been used. 60° S–60° N constitutes ~ 91 % of the global ocean surface area, and limiting to 300 m isobath neglects the contributions from coastal and shallow waters, so the resultant OHC trends will be underestimated if these ocean regions are warming. For example, neglecting shallow waters can account for 5 %–10 % for 0–2000 m OHC trends (von Schuckmann et al., 2014). A first initial test using Cheng et al. (2017b) data indicates that OHC 0–2000 m trends can be underestimated by ~ 10 % if the ocean warming in the area polewards of 60° latitude is not taken into account (not shown). This is a caveat of the assessment in this review and will be addressed in the future.

The assessment is based on three distinct periods to account for the evolution of the observing system, i.e., 1960–2018 (i.e., “historical”), 1993–2018 (i.e., “altimeter era”) and 2005–2018 (i.e., “golden Argo era”). In addition, ocean warming rates over the past decade are specifically discussed according to an apparent acceleration of global sur-

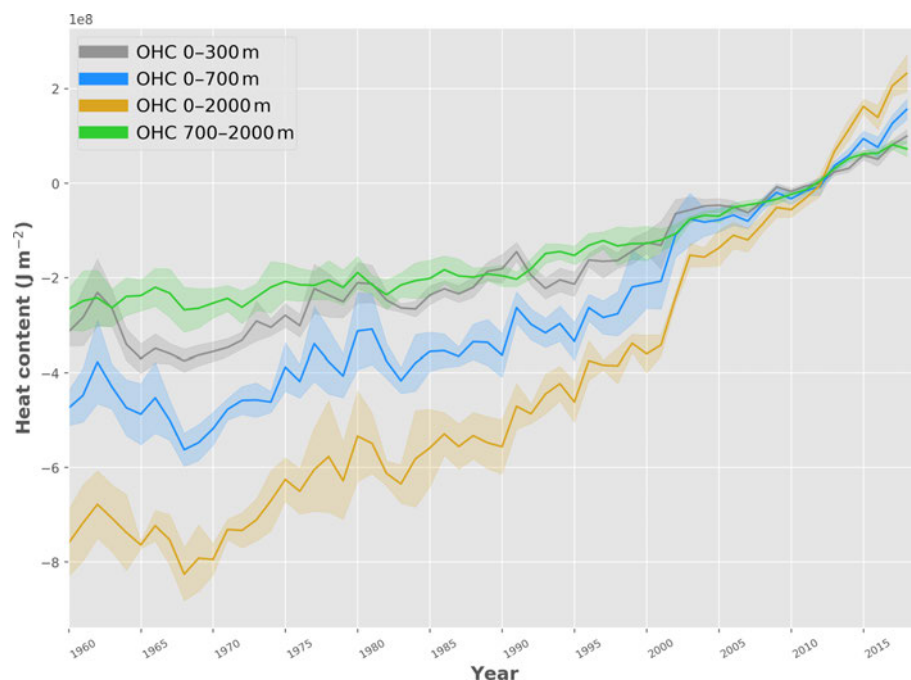


Figure 1. Ensemble mean time series and ensemble standard deviation (2σ , shaded) of global ocean heat content (OHC) anomalies relative to the 2005–2017 climatology for the 0–300 m (gray), 0–700 m (blue), 0–2000 m (yellow) and 700–2000 m depth layer (green). The ensemble mean is an outcome of an international assessment initiative, and all products used are referenced in the legend of Fig. 2. The trends derived from the time series are given in Table 1. Note that values are given for the ocean surface area between 60° S and 60° N and are limited to the 300 m bathymetry of each product.

face warming since 2010 (WMO, 2020; Blunden and Arndt, 2019). All time series reach the end in 2018 – which was one of the principal limitations for the inclusion of some products. Our final estimates of OHC for the upper 2000 m over different periods are the ensemble average of all products, with the uncertainty range defined by the standard deviation (2σ) of the corresponding estimates used (Fig. 1).

The first and principal result of the assessment (Fig. 1) is an overall increase in the trend for the two more recent study periods, e.g., the altimeter era (1993–2018) and golden Argo era (2005–2018), relative to the historical era (1960–2018), which is in agreement with previous results (e.g., Abraham et al., 2013). The trend values are all given in Table 1. A major part of heat is stored in the upper layers of the ocean (0–300 m and 0–700 m depth). However, heat storage at intermediate depth (700–2000 m) increases at a comparable rate as reported for the 0–300 m depth layer (Table 1, Fig. 2). There is a general agreement among the 15 international OHC estimates (Fig. 2). However, for some periods and depth layers the standard deviation reaches maximal values up to about 0.3 W m^{-2} . All products agree on the fact that ocean warming rates have increased in the past decades and doubled since the beginning of the altimeter era (1993–2018 compared with 1960–2018) (Fig. 2). Moreover, there is a clear indication that heat sequestration into the deeper ocean layers below 700 m depth took place over the past 6 decades

linked to an increase in OHC trends over time (Fig. 2). In agreement with observed accelerated Earth surface warming over the past decade (WMO, 2020; Blunden and Arndt, 2019), ocean warming rates for the 0–2000 m depth layer also reached record rates of $1.3 (0.9) \pm 0.3 \text{ W m}^{-2}$ for the ocean (global) area over the period 2010–2018.

For the deep OHC changes below 2000 m, we adapted an updated estimate from Purkey and Johnson (2010) (PG10) from 1991 to 2018, which is a constant linear trend estimate ($1.15 \pm 0.57 \text{ ZJ yr}^{-1}$, $0.07 \pm 0.04 \text{ W m}^{-2}$). Some recent studies strengthened the results in PG10 (Desbruyères et al., 2016; Zanna et al., 2019). Desbruyères et al. (2016) examined the decadal change of the deep and abyssal OHC trends below 2000 m in the 1990s and 2000s, suggesting that there has not been a significant change in the rate of decadal global deep/abyssal warming from the 1990s to the 2000s and the overall deep ocean warming rate is consistent with PG10. Using a Green function method, Zanna et al. (2019) reported a deep ocean warming rate of $\sim 0.06 \text{ W m}^{-2}$ during the 2000s, consistent with PG10 used in this study. Zanna et al. (2019) shows a fairly weak global trend during the 1990s, inconsistent with observation-based estimates. This mismatch might come from the simplified or misrepresentation of surface-deep connections using ECCO reanalysis data and the use of time-mean Green functions in Zanna et al. (2019), as well as from the limited spatial resolution of the observational net-

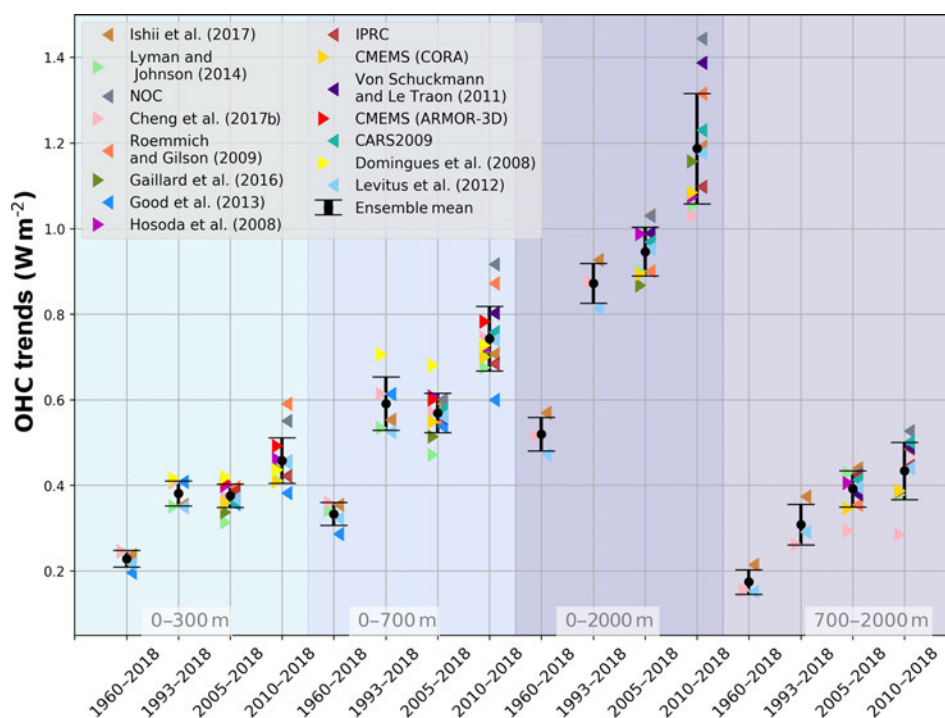


Figure 2. Linear trends of global ocean heat content (OHC) as derived from different temperature products (colors). References are given in the figure legend, except for IPRC (<http://apdrc.soest.hawaii.edu/projects/Argo/>, last access: 7 August 2020), CMEMS (CORa and ARMOR-3D, <http://marine.copernicus.eu/science-learning/ocean-monitoring-indicators>, last access: 7 August 2020), CARS2009 (<http://www.marine.csiro.au/~dunn/cars2009/>, last access: 7 August 2020) and NOC (National Oceanographic Institution, Desbruyères et al., 2016). The ensemble mean and standard deviation (2σ) are given in black. The shaded areas show trends from different depth layer integrations, i.e., 0–300 m (light turquoise), 0–700 m (light blue), 0–2000 m (purple) and 700–2000 m (light purple). For each integration depth layer, trends are evaluated over the three study periods, i.e., historical (1960–2018), altimeter era (1993–2018) and golden Argo era (2005–2018). In addition, the most recent period 2010–2018 is included. See text for more details on the international assessment criteria. Note that values are given for the ocean surface area (see text for more details).

work for relatively short time spans. Furthermore, combining hydrographic and deep-Argo floats, a recent study (Johnson et al., 2019) reported an accelerated warming in the South Pacific Ocean in recent years, but a global estimate of the OHC rate of change over time is not available yet.

Before 1990, we assume zero OHC trend below 2000 m, following the methodology in IPCC-AR5 (Rhein et al., 2013). The zero-trend assumption is made mainly because there are too few observations before 1990 to make an estimate of OHC change below 2000 m. But it is a reasonable assumption because OHC 700–2000 m warming was fairly weak before 1990 and heat might not have penetrated down to 2000 m (Cheng et al., 2017b). Zanna et al. (2019) also shows a near-zero OHC trend below 2000 m from the 1960s to 1980s. The derived time series is used for the Earth energy inventory in Sect. 5. A centralized (around the year 2006) uncertainty approach has been applied for the deep (> 2000 m depth) OHC estimate following the method of Cheng et al. (2017b), which allows us to extract an uncertainty range over the period 1993–2018 within the given [lower ($1.15 - 0.57 \text{ ZJ yr}^{-1}$), upper ($1.15 + 0.57 \text{ ZJ yr}^{-1}$)] range of the deep

OHC trend estimate. We then extend the obtained uncertainty estimate back from 1993 to 1960, with 0 OHC anomaly.

3 Heat available to warm the atmosphere

While the amount of heat accumulated in the atmosphere is small compared to the ocean, warming of the Earth's near-surface air and atmosphere aloft is a very prominent effect of climate change, which directly affects society. Atmospheric observations clearly reveal a warming of the troposphere over the last decades (Santer et al., 2017; Steiner et al., 2020) and changes in the seasonal cycle (Santer et al., 2018). Changes in atmospheric circulation (Cohen et al., 2014; Fu et al., 2019) together with thermodynamic changes (Fischer and Knutti, 2016; Trenberth et al., 2015) will lead to more extreme weather events and increase high-impact risks for society (Coumou et al., 2018; Zscheischler et al., 2018). Therefore, a rigorous assessment of the atmospheric heat content in context with all Earth's climate subsystems is important for a full view on the changing climate system.

The atmosphere transports vast amounts of energy laterally and strong vertical heat fluxes occur at the atmosphere's lower boundary. The pronounced energy and mass exchanges within the atmosphere and with all other climate components is a fundamental element of Earth's climate (Peixoto and Oort, 1992). In contrast, long-term heat accumulation in the atmosphere is limited by its small heat capacity as the gaseous component of the Earth system (von Schuckmann et al., 2016).

Recent work revealed inconsistencies in earlier formulations of the atmospheric energy budget (Mayer et al., 2017; Trenberth and Fasullo, 2018), and hence a short discussion of the updated formulation is provided here. In a globally averaged and vertically integrated sense, heat accumulation in the atmosphere arises from a small imbalance between net energy fluxes at the top of the atmosphere (TOA) and the surface (denoted s). The heat budget of the vertically integrated and globally averaged atmosphere (indicated by the global averaging operator $\langle \cdot \rangle$) reads as follows (Mayer et al., 2017):

$$\left\langle \frac{\partial \text{AE}}{\partial t} \right\rangle = \langle N_{\text{TOA}} \rangle - \langle F_s \rangle - \langle F_{\text{snow}} \rangle - \langle F_{\text{PE}} \rangle, \quad (2)$$

where, in mean-sea-level altitude (z) coordinates used here for integrating over observational data, the vertically integrated atmospheric energy content AE per unit surface area [J m^{-2}] reads

$$\text{AE} = \int_{z_s}^{z_{\text{TOA}}} \rho \left(c_v T + g(z - z_s) + L_e q + \frac{1}{2} V^2 \right) dz. \quad (3)$$

In Eq. (2), AE represents the total atmospheric energy content, N_{TOA} the net radiation at TOA, F_s the net surface energy flux defined as the sum of net surface radiation and latent and sensible heat flux, and F_{snow} the latent heat flux associated with snowfall (computed as the product of latent heat of fusion and snowfall rate). Here, we take constant latent heat of vaporization (at 0°C) in the latent heat flux term that is contained in F_s , but variations in latent heat flux arising from the deviation of evaporated water from 0°C are contained in F_{PE} , which additionally accounts for sensible heat of precipitation (referenced to 0°C). That is, F_{PE} expresses a modification of F_s arising from global evaporation and precipitation occurring at temperatures different from 0°C .

Snowfall is the fraction of precipitation that returns originally evaporated water to the surface in a frozen state. In that sense, F_{snow} represents a heat transfer from the surface to the atmosphere: it warms the atmosphere through additional latent heat release (associated with freezing of vapor) and snowfall consequently arrives at the surface in an energetic state lowered by this latent heat. This energetic effect is most obvious over the open ocean, where falling snow requires the same amount of latent heat to be melted again and thus cools the ocean. Over high latitudes, F_{snow} can attain values up to 5 W m^{-2} , but its global average value is smaller than

1 W m^{-2} (Mayer et al., 2017). Although its global mean energetic effect is relatively small, it is systematic and should be included for accurate diagnostics. Moreover, snowfall is an important contributor to the heat and mass budget of ice sheets and sea ice (see Sect. 4).

F_{PE} represents the net heat flux arising from the different temperatures of rain and evaporated water. This flux can be sizable regionally, but it is small in a global average sense (warming of the atmosphere $\sim 0.3 \text{ W m}^{-2}$ according to Mayer et al., 2017).

Equation (3) provides a decomposition of the atmospheric energy content AE into sensible heat energy (sum of the first two terms, internal heat energy and gravity potential energy), latent heat energy (third term) and kinetic energy (fourth term), where ρ is the air density, c_v the specific heat for moist air at constant volume, T the air temperature, g the acceleration of gravity, L_e the temperature-dependent effective latent heat of condensation (and vaporization) L_v or sublimation L_s (the latter relevant below 0°C), q the specific humidity of the moist air, and V the wind speed. We neglect atmospheric liquid water droplets and ice particles as separate species, as their amounts and especially their trends are small.

In the AE derivation from observational datasets based on Eq. (3), we accounted for the intrinsic temperature dependence of the latent heat of water vapor by assigning L_e to L_v if ambient temperatures are above 0°C and to L_s (adding in the latent heat of fusion L_f) if they are below -10°C , respectively, with a gradual (half-sine weighted) transition over the temperature range between. The reanalysis evaluations similarly approximated L_e by using values of L_v , L_s , and L_f , though in slightly differing forms. The resulting differences in AE anomalies from any of these choices are negligibly small, however, since the latent heat contribution at low temperatures is itself very small.

As another small difference, the AE estimations from observations neglected the kinetic energy term in Eq. (3) (fourth term), while the reanalysis evaluations accounted for it. This as well leads to negligible AE anomaly differences, however, since the kinetic energy content and trends at a global scale are more than three orders of magnitude smaller than for the sensible heat (Peixoto and Oort, 1992). Aligning with the terminology of ocean heat content (OHC) and given the dominance of the heat-related terms in Eq. (3), we hence refer to the energy content AE as atmospheric heat content (AHC) hereafter.

Turning to the actual datasets used, atmospheric energy accumulation can be quantified using various data types, as summarized in the following. Atmospheric reanalyses combine observational information from various sources (radiosondes, satellites, weather stations, etc.) and a dynamical model in a statistically optimal way. This data type has reached a high level of maturity, thanks to continuous development work since the early 1990s (Hersbach et al., 2018). Especially reanalyzed atmospheric state quantities like temperature, winds and moisture are considered to be of high

quality and suitable for climate studies, although temporal discontinuities introduced from the ever-changing observation system remain a matter of concern (Berrisford et al., 2011; Chiodo and Haimberger, 2010).

Here we use the current generation of atmospheric reanalyses as represented by ECMWF's fifth-generation reanalysis ERA5 (Hersbach et al., 2018, 2020), NASA's Modern-Era Retrospective analysis for Research and Applications version 2 (MERRA2) (Gelaro et al., 2017) and JMA's 55-year-long reanalysis JRA-55 (Kobayashi et al., 2015). All these are available over 1980 to 2018 (ERA5 also in 1979), while JRA-55 is the only one covering the full early timeframe 1960 to 1979. We additionally used a different version of JRA-55 that assimilates only conventional observations also over the satellite era from 1979 onwards, which away from the surface only leaves radiosondes as data source and which is available to 2012 (JRA-55C). The advantage of this product is that it avoids potential spurious jumps associated with satellite changes. Moreover, JRA-55C is fully independent of satellite-derived Global Positioning System (GPS) radio occultation (RO) data that are also separately used and described below together with the observational techniques.

In addition to these four reanalyses, the datasets from three different observation techniques have been used for complementary observational estimates of the atmospheric heat content. We use the Wegener Center (WEGC) multisatellite RO data record, WEGC OPSv5.6 (Angerer et al., 2017), as well as its radiosonde (RS) data record derived from the high-quality Vaisala sondes RS80/RS92/VS41, WEGC Vaisala (Ladstädter et al., 2015). WEGC OPSv5.6 and WEGC Vaisala provide thermodynamic upper air profiles of air temperature, specific humidity and density from which we locally estimate the vertical AHC based on the first three integral terms of Eq. (3) (Kirchengast et al., 2019). In atmospheric domains not fully covered by the data (e.g., in the lower part of the boundary layer for RO or over the polar latitudes for RS), the profiles are vertically completed by collocated ERA5 information. The local vertical AHC results are then averaged into regional monthly means, which are finally geographically aggregated to global AHC. Applying this estimation approach in the same way to reanalysis profiles subsampled at the observation locations accurately leads to the same AHC anomaly time series records as the direct estimation from the full gridded fields.

The third observation-based AHC dataset derives from a rather approximate estimation approach using the microwave sounding unit (MSU) data records (Mears and Wentz, 2017). Because the very coarse vertical resolution of the brightness temperature measurements from MSU does not enable integration according to Eq. (3), this dataset is derived by replicating the method used in IPCC AR5 WGI Assessment Report 2013 (Rhein et al., 2013; chap. 3, Box 3.1 therein). We used the most recent MSU Remote Sensing System (RSS) V4.0 temperature dataset (Mears and Wentz, 2017), however, instead of MSU RSS V3.3 (Mears and Wentz, 2009a, b) that

was used in the IPCC AR5. In order to derive global time series of AHC anomalies, the approach simply combines weighted MSU lower tropospheric temperature and lower stratospheric temperature changes (TLT and TLS channels) converted to sensible heat content changes via global atmospheric mass, as well as an assumed fractional increase in latent heat content according to water vapor content increase driven by temperature at a near-Clausius–Clapeyron rate ($7.5\% \text{ }^{\circ}\text{C}^{-1}$).

Figure 3 shows the resulting global AHC change inventory over 1980 to 2018 in terms of AHC anomalies of all data types (top), mean anomalies and time-average uncertainty estimates including long-term AHC trend estimates (middle), and annual-mean AHC tendency estimates (bottom). The mean anomaly time series (middle left), preceded by the small JRA-55 anomalies over 1960–1979, is used as part of the overall heat inventory in Sect. 5 below. Results including MSU in addition are separately shown (right column), since this dataset derives from a fairly approximate estimation as summarized above and hence is given lower confidence than the others deriving from rigorous AHC integration and aggregation. Since MSU data were the only data for AHC change estimation in the IPCC AR5 report, bringing it into context is considered relevant, however.

The results clearly show that the AHC trends have intensified from the earlier decades represented by the 1980–2010 trends of near 1.8 TW (consistent with the trend interval used in the IPCC AR5 report). We find the trends about 2.5 times higher over 1993–2018 (about 4.5 TW) and about 3 times higher in the most recent 2 decades over 2002–2018 (near 5.3 TW), a period that is already fully covered also by the RO and RS records (which estimate around 6 TW). Checking the sensitivity of these long-term trend estimates to El Niño–Southern Oscillation (ENSO) interannual variations, by comparing to trends fitted to ENSO-corrected AHC anomalies (with ENSO regressed out via the Nino 3.4 index), confirms that the estimates are robust (trends consistent within about 10 %, slightly higher with ENSO correction).

The year-to-year annual-mean tendencies in AHC, reaching amplitudes as high as 50 to 100 TW (or 0.1 to 0.2 W m^{-2} , if normalized to the global surface area), indicate the strong coupling of the atmosphere with the uppermost ocean. This is mainly caused by the ENSO interannual variations that lead to net energy changes in the climate system including the atmosphere (Loeb et al., 2012; Mayer et al., 2013) and substantial reshuffling of heat energy between the atmosphere and the upper ocean (Cheng et al., 2019b; Johnson and Birnbaum, 2017; Mayer et al., 2014, 2016).

4 Heat available to warm land

Although the land component of the Earth's energy budget accounts for a small proportion of heat in comparison with the ocean, several land-based processes sensitive to the mag-

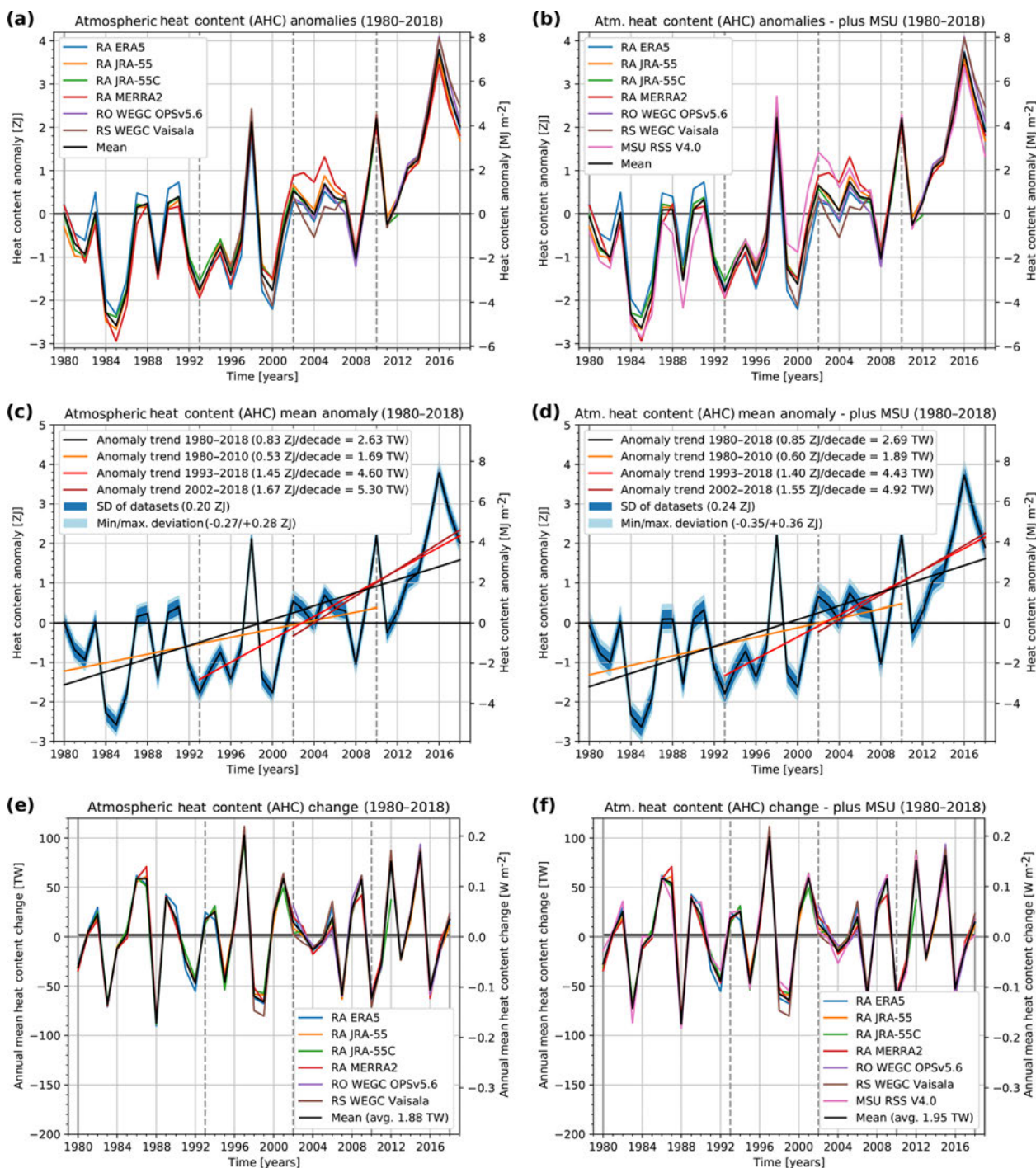


Figure 3. Annual-mean global AHC anomalies over 1980 to 2018 of four different reanalyses and two (a, c, e) or three (b, d, f, plus MSU) different observational datasets shown together with their mean (a, b), the mean AHC anomaly shown together with four representative AHC trends and ensemble spread measures of its underlying datasets (c, d), and the annual-mean AHC change (annual tendency) shown for each year over 1980 to 2018 for all datasets and their mean (e, f). The in-panel legends identify the individual datasets shown (a, b and e, f) and the chosen trend periods together with the associated trend values and spread measures (c, d), with the latter including the time-average standard deviation and minimum/maximum deviations of the individual datasets from the mean.

nitude of the available land heat play a crucial role in the future evolution of climate. Among others, the stability and extent of the continental areas occupied by permafrost soils depend on the land component. Alterations of the thermal conditions at these locations have the potential to release long-term stored CO₂ and CH₄ and may also destabilize the recalcitrant soil carbon (Bailey et al., 2019; Hicks Pries et al., 2017). Both of these processes are potential tipping points (Lenton et al., 2008, 2019; Lenton, 2011) leading to possible positive feedback on the climate system (Leifeld et al., 2019; MacDougall et al., 2012). Increased land energy is related to decreases in soil moisture that may enhance the occurrence of extreme temperature events (Jeong et al., 2016; Seneviratne et al., 2006, 2014, 2010; Xu et al., 2019). Such extreme events carry negative health effects for the most vulnerable sectors of human and animal populations and ecosystems (Matthews et al., 2017; McPherson et al., 2017; Sherwood and Huber, 2010; Watts et al., 2019). Given the importance of properly determining the fraction of EEI flowing into the land component, recent works have examined the CMIP5 simulations and revealed that Earth system models (ESMs) have shortcomings in modeling the land heat content of the last half of the 20th century (Cuesta-Valero et al., 2016). Numerical experiments have pointed to an insufficient depth of the land surface models (LSMs) (MacDougall et al., 2008, 2010; Stevens, 2007) and to a zero heat-flow bottom boundary condition (BBC) as the origin of the limitations in these simulations. An LSM of insufficient depth limits the amount of energy that can be stored in the subsurface. The zero heat-flow BBC neglects the small but persistent long-term contribution from the flow of heat from the interior of the Earth, which shifts the thermal regime of the subsurface towards or away from the freezing point of water, such that the latent heat component is misrepresented in the northern latitudes (Hermoso de Mendoza et al., 2020). Although the heat from the interior of the Earth is constant at timescales of a few millennia, it may conflict with the setting of the LSM initial conditions in ESM simulations. Modeling experiments have also allowed us to estimate the heat content in land water reservoirs (Vanderkelen et al., 2020), accounting for 0.3 ± 0.3 ZJ from 1900 to 2020. Nevertheless, this estimate has not been included here because it is derived from model simulations and its magnitude is small in relation to the rest of the components of the Earth's heat inventory.

4.1 Borehole climatology

The main premise of borehole climatology is that the subsurface thermal regime is determined by the balance of the heat flowing from the interior of the Earth (the bottom boundary condition) and the heat flowing through the interface between the lower atmosphere and the ground (the upper boundary condition). If the thermal properties of the subsurface are known, or if they can be assumed constant over short-depth intervals, then the thermal regime of the subsur-

face can be determined by the physics of heat diffusion. The simplest analogy is the temperature distribution along a (infinitely wide) cylinder with known thermal properties and constant temperature at both ends. If upper and lower boundary conditions remain constant (i.e., internal heat flow is constant and there are no persistent variations on the ground surface energy balance), then the thermal regime of the subsurface is well known and it is in a (quasi-)steady state. However, any change to the ground surface energy balance would create a transient, and such a change in the upper boundary condition would propagate into the ground, leading to changes in the thermal regime of the subsurface (Beltrami, 2002a). These changes in the ground surface energy balance propagate into the subsurface and are recorded as departures from the quasi-steady thermal state of the subsurface. Borehole climatology uses these subsurface temperature anomalies to reconstruct the ground surface temperature changes that may have been responsible for creating the subsurface temperature anomalies we observe. That is, it is an attempt to reconstruct the temporal evolution of the upper boundary condition. Ground surface temperature histories (GSTHs) and ground heat flux histories (GHFHs) have been reconstructed from borehole temperature profile (BTP) measurements at regional and larger scales for decadal and millennial timescales (Barkaoui et al., 2013; Beck, 1977; Beltrami, 2001; Beltrami et al., 2006; Beltrami and Bourlon, 2004; Cermak, 1971; Chouinard and Mareschal, 2009; Davis et al., 2010; Demezhko and Gornostaeva, 2015; Harris and Chapman, 2001; Hartmann and Rath, 2005; Hopcroft et al., 2007; Huang et al., 2000; Jaume-Santero et al., 2016; Lachenbruch and Marshall, 1986; Lane, 1923; Pickler et al., 2018; Roy et al., 2002; Vasseur et al., 1983). These reconstructions have provided independent records for the evaluation of the evolution of the climate system well before the existence of meteorological records. Because subsurface temperatures are a direct measure, which unlike proxy reconstructions of past climate do not need to be calibrated with the meteorological records, they provide an independent way of assessing changes in climate. Such records are useful tools for evaluating climate simulations prior to the observational period (Beltrami et al., 2017; Cuesta-Valero et al., 2019, 2016; García-García et al., 2016; González-Rouco et al., 2006; Jaume-Santero et al., 2016; MacDougall et al., 2010; Stevens et al., 2008), as well as for assessing proxy data reconstructions (Beltrami et al., 2017; Jaume-Santero et al., 2016).

Borehole reconstructions have, however, certain limitations. Due to the nature of heat diffusion, temperature changes propagated through the subsurface suffer both a phase shift and an amplitude attenuation (Smerdon and Stieglitz, 2006). Although subsurface temperatures continuously record all changes in the ground surface energy balance, heat diffusion filters out the high frequency variations of the surface signal with depth; thus the annual cycle is detectable up to approximately 16 m of depth, while millen-

nial changes are recorded approximately to a depth of 500 m. Therefore, reconstructions from borehole temperature profiles represent changes at decadal-to-millennial timescales. Additionally, borehole data are sparse, since the logs were usually recorded from holes of opportunity at mining exploration sites. As a result, the majority of profiles were measured in the Northern Hemisphere, although recent efforts have been taken to increase the sampling rate in South America (Pickler et al., 2018) and Australia (Suman et al., 2017). Despite this uneven sampling, the spatial distribution of borehole profiles has been able to represent the evolution of land surface conditions at global scales (Beltrami and Bourlon, 2004; Cuesta-Valero et al., 2020; González-Rouco et al., 2006, 2009; Pollack and Smerdon, 2004). Another factor that reduces the number of borehole profiles suitable for climate analyses is the presence of nonclimatic signals in the measured profiles, mainly caused by groundwater flow and changes in the lithology of the subsurface. Therefore, all profiles are screened before the analysis in order to remove questionable logs. Despite all these limitations, the borehole methodology has been shown to be reliable based on observational analyses (Bense and Kooi, 2004; Chouinard and Mareschal, 2007; Pollack and Smerdon, 2004; Verdoya et al., 2007) and pseudoproxy experiments (García Molinos et al., 2016; González-Rouco et al., 2006, 2009).

4.2 Land heat content estimates

Global continental energy content has been previously estimated from geothermal data retrieved from a set of quality-controlled borehole temperature profiles. Ground heat content was estimated from heat flux histories derived from BTP data (Beltrami, 2002b; Beltrami et al., 2002, 2006). Such results have formed part of the estimate used in AR3, AR4 and AR5 IPCC reports (see Box 3.1, chap. 3 Rhein et al., 2013). A continental heat content estimate was inferred from meteorological observations of surface air temperature since the beginning of the 20th century (Huang, 2006). Nevertheless, all global estimates were performed nearly 2 decades ago. Since, those days, advances in borehole methodological techniques (Beltrami et al., 2015; Cuesta-Valero et al., 2016; Jaume-Santero et al., 2016), the availability of additional BTP measurements and the possibility of assessing the continental heat fluxes in the context of the FluxNet measurements (Gentine et al., 2020) require a comprehensive summary of all global ground heat fluxes and continental heat content estimates.

The first estimates of continental heat content used borehole temperature versus depth profile data. However, the dataset in those analyses included borehole temperature profiles of a wide range of depths, as well as different data acquisition dates. That is, each borehole profile contained the record of the accumulation of heat in the subsurface for different time intervals. In addition, the borehole data were analyzed for a single ground surface temperature model using

a single constant value for each of the subsurface thermal properties.

Although the thermal signals are attenuated with depth, which may partially compensate for data shortcomings, uncertainties were introduced in previous analyses that may have affected the estimates of subsurface heat change. A continental heat content estimate was carried out using a gridded meteorological product of surface air temperature by Huang (2006). Such work yielded similar values to the estimates from geothermal data (see Table 2). This estimate, however, assumed that surface air and ground temperatures are perfectly coupled everywhere, and it used a single value for the thermal conductivity of the ground. Studies have shown that the coupling of the surface air and ground temperatures is mediated by several processes that may influence the ground surface energy balance and, therefore, the air–ground temperature coupling (García-García et al., 2019; Melo-Aguilar et al., 2018; Stieglitz and Smerdon, 2007). In a novel attempt to reconcile continental heat content from soil heat-plate data from the FluxNet network with estimates from geothermal data and a deep bottom boundary land surface model simulation, Gentine et al. (2020) obtained a much larger magnitude from the global land heat flux than all previous estimates. Cuesta-Valero et al. (2020) has recently updated the estimate of the global continental heat content using a larger borehole temperature database (1079 logs) that includes more recent measurements and a stricter data quality control. The updated estimate of continental heat content change also takes into account the differences in borehole logging time and restricts the data to the same depth range for each borehole temperature profile. Such depth range restriction ensures that the subsurface accumulation of heat at all BTP sites is synchronous. In addition to the standard method for reconstructing heat fluxes with a single constant value for each subsurface thermal property, Cuesta-Valero et al. (2020) also developed a new approach that considers a range of possible subsurface thermal properties – several models, each at a range of resolutions yielding a more realistic range of uncertainties for the fraction of the EEI flowing into the land subsurface.

Global land heat content estimates from FluxNet data, geothermal data and model simulations point to a marked increase in the amount of energy flowing into the ground in the last few decades (Figs. 4, 5 and Table 2). These results are consistent with the observations of ocean, cryosphere and atmospheric heat storage increases during the same time period as well as with EEI at the top of the atmosphere.

5 Heat utilized to melt ice

The energy uptake by the cryosphere is given by the sum of the energy uptake within each one of its components: sea ice, the Greenland and Antarctic ice sheets, glaciers other than those that are part of the ice sheets (“glaciers”, here-

Table 2. Ground surface heat flux and global continental heat content. Uncertainties in parenthesis.

Reference	Time period	Heat flux (m W m ⁻²)	Heat content (ZJ)	Source of data
Beltrami (2002b)	1950–2000	33	7.1	Geothermal
Beltrami et al. (2002)	1950–2000	39.1 (3.5)	9.1 (0.8)	Geothermal
Beltrami et al. (2002)	1900–2000	34.1 (3.4)	15.9 (1.6)	Geothermal
Beltrami (2002b)	1765–2000	20.0 (2.0)	25.7 (2.6)	Geothermal
Huang (2006)	1950–2000	–	6.7	Meteorological
Gentine et al. (2020)	2004–2015	240 (120)	–	FluxNet, geothermal, LSM
Cuesta-Valero et al. (2020)	1950–2000	70 (20)	16 (3)	Geothermal
Cuesta-Valero et al. (2020)	1993–2018	129 (28)	14 (3)	Geothermal
Cuesta-Valero et al. (2020)	2004–2015	136 (28)	6 (1)	Geothermal

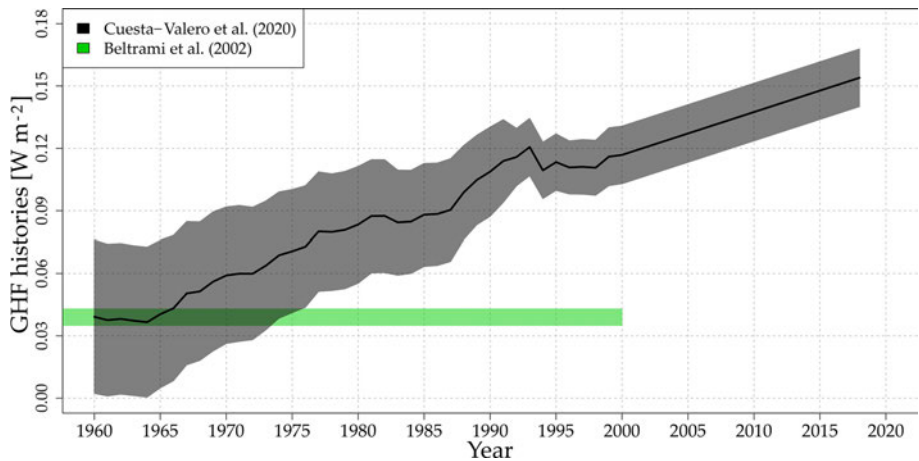


Figure 4. Global mean ground heat flux history (black line) and 95 % confidence interval (gray shadow) from BTP measurements from Cuesta-Valero et al. (2020). Results for 1950–2000 from Beltrami et al. (2002) (green bar) are provided for comparison purposes.

after), snow, and permafrost. The basis for the heat uptake by the cryosphere presented here is provided by a recent estimate for the period 1979 to 2017 (Straneo et al., 2020). This study concludes that heat uptake over this period is dominated by the mass loss from Arctic sea ice, glaciers, and the Greenland and Antarctic ice sheets. The contributions from thawing permafrost and shrinking snow cover are either negligible, compared to these other components, or highly uncertain. (Note that warming of the land in regions where permafrost is present is accounted for in the land warming; however, the energy to thaw the permafrost is not.) Antarctic sea ice shows no explicit trend over the period described here (Parkinson, 2019). Here, we extend the estimate of Straneo et al. (2020) backwards in time to 1960 and summarize the method, the data and model outputs used. The reader is referred to Straneo et al. (2020) for further details.

Within each component of the cryosphere, energy uptake is dominated by that associated with melting, including both the latent heat uptake and the warming of the ice to its freezing point. As a result, the energy uptake by each component is directly proportional to its mass loss (Straneo et al., 2020).

For consistency with previous estimates (Ciais et al., 2013), we use a constant latent heat of fusion of $3.34 \times 10^5 \text{ J kg}^{-1}$, a specific heat capacity of $2.01 \times 10^3 \text{ J/(kg } ^\circ\text{C)}$ and an ice density of 920 kg m^{-3} .

For Antarctica, we separate contributions from grounded ice loss and floating ice loss building on recent separate estimates for each. Grounded ice loss from 1992 to 2017 is based on a recent study that reconciles mass balance estimates from gravimetry, altimetry and input–output methods from 1992 to 2017 (Shepherd et al., 2018b). For the 1972–1991 period, we used estimates from Rignot et al. (2019), which combined modeled surface mass balance with ice discharge estimates from the input/output method. Floating ice loss between 1994 and 2017 is based on thinning rates and iceberg calving fluxes estimated using new satellite altimetry reconstructions (Adusumilli et al., 2020). For the 1960–1994 period, we also considered mass loss from declines in Antarctic Peninsula ice shelf extent (Cook and Vaughan, 2010) using the methodology described in Straneo et al. (2020).

To estimate grounded ice mass loss in Greenland, we use the Ice Sheet Mass Balance Intercomparison Exercise for the

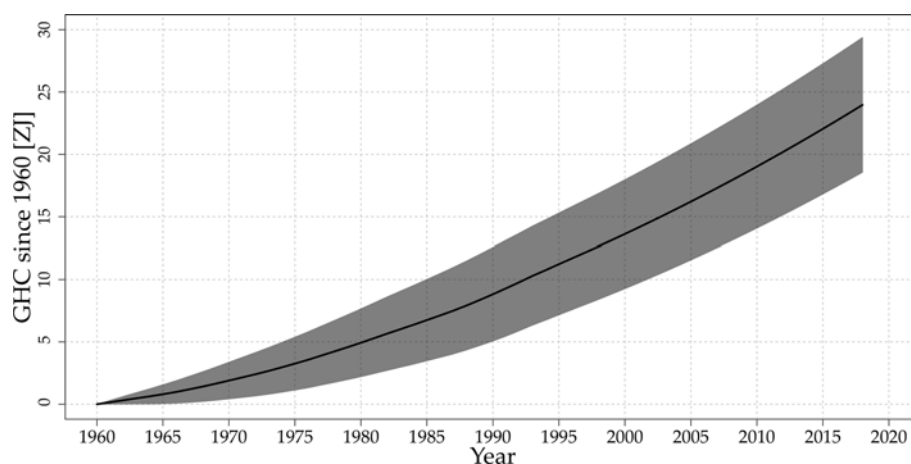


Figure 5. Global cumulative heat storage within continental landmasses since 1960 CE (black line) and 95 % confidence interval (gray shadow) estimated from ground heat flux results displayed in Fig. 4. Data obtained from Cuesta-Valero et al. (2020).

time period 1992–2017 (Shepherd et al., 2019) and the difference between surface mass balance and ice discharge for the period 1979–1991 (Mankoff et al., 2019; Mouginot et al., 2019; Noël et al., 2018). Due to a lack of observations, from 1960–1978 we assume no mass loss. For floating ice mass change, we collated reports of ice shelf thinning and/or collapse together with observed tidewater glacier retreat (Straneo et al., 2020). Based on firn modeling we assessed that warming of Greenland’s firn has not yet contributed significantly to its energy uptake (Ligtenberg et al., 2018; Straneo et al., 2020).

For glaciers we combine estimates for glaciers from the Randolph Glacier Inventory outside of Greenland and Antarctica, based on direct and geodetic measurements (Zemp et al., 2019), with estimates based on a glacier model forced with an ensemble of reanalysis data (Marzeion et al., 2015) and GRACE-based estimates (Bamber et al., 2018). An additional contribution from uncharted glaciers or glaciers that have already disappeared is obtained from Parkes and Marzeion (2018). Greenland and Antarctic peripheral glaciers are derived from Zemp et al. (2019) and Marzeion et al. (2015).

Finally, while estimates of Arctic sea ice extent exist over the satellite record, sea ice thickness distribution measurements are scarce, making it challenging to estimate volume changes. Instead we use the Pan-Arctic Ice Ocean Modeling and Assimilation System (PIOMAS) (Schweiger et al., 2011; Zhang and Rothrock, 2003) which assimilates ice concentration and sea surface temperature data and is validated with most available thickness data (from submarines, oceanographic moorings, and remote sensing) and against multidecadal records constructed from satellite (for example, Labe et al., 2018; Laxon et al., 2013; Wang et al., 2016). A longer reconstruction using a slightly different model version, PIOMAS-20C (Schweiger et al., 2019), is used to cover the 1960 to 1978 period that is not covered by PIOMAS.

These reconstructions reveal that all four components contributed similar amounts (between 2 and 5 ZJ) over the 1960–2017 period, amounting to a total energy uptake by the cryosphere of 14.7 ± 1.9 ZJ. Compared to earlier estimates, and in particular the 8.83 ZJ estimate from Ciais et al. (2013), this larger estimate is a result both of the longer period of time considered and, also, the improved estimates of ice loss across all components, especially the ice shelves in Antarctica. Approximately half of the cryosphere’s energy uptake is associated with the melting of grounded ice, while the remaining half is associated with the melting of floating ice (ice shelves in Antarctica and Greenland, Arctic sea ice).

6 The Earth heat inventory: where does the energy go?

The Earth has been in radiative imbalance, with less energy exiting the top of the atmosphere than entering, since at least about 1970, and the Earth has gained substantial energy over the past 4 decades (Hansen, 2005; Rhein et al., 2013). Due to the characteristics of the Earth system components, the ocean with its large mass and high heat capacity dominates the Earth heat inventory (Cheng et al., 2016, 2017b; Rhein et al., 2013; von Schuckmann et al., 2016). The rest goes into grounded and floating ice melt, as well as warming the land and atmosphere.

In agreement with previous studies, the Earth heat inventory based on most recent estimates of heat gain in the ocean (Sect. 1), the atmosphere (Sect. 2), land (Sect. 3) and the cryosphere (Sect. 4) shows a consistent long-term heat gain since the 1960s (Fig. 6). Our results show a total heat gain of 358 ± 37 ZJ over the period 1971–2018, which is equivalent to a heating rate of 0.47 ± 0.1 W m⁻², and it applied continuously over the surface area of the Earth (5.10×10^{14} m²). For comparison, the heat gain obtained in IPCC AR5 amounts to 274 ± 78 ZJ and 0.4 W m⁻² over the period 1971–2010

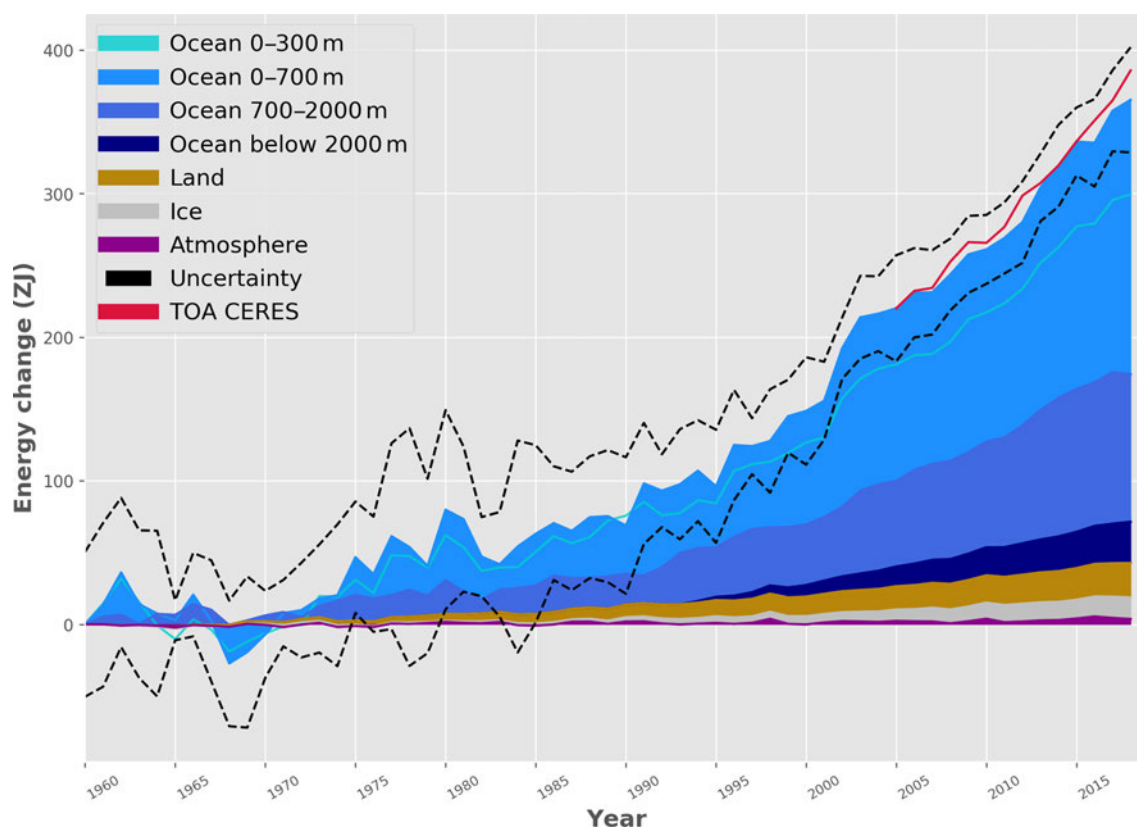


Figure 6. Earth heat inventory (energy accumulation) in ZJ ($1 \text{ ZJ} = 10^{21} \text{ J}$) for the components of the Earth's climate system relative to 1960 and from 1960 to 2018 (assuming constant cryosphere increase for the year 2018). See Sects. 1–4 for data sources. The upper ocean (0–300 m, light blue line, and 0–700 m, light blue shading) accounts for the largest amount of heat gain, together with the intermediate ocean (700–2000 m, blue shading) and the deep ocean below 2000 m depth (dark blue shading). Although much lower, the second largest contributor is the storage of heat on land (orange shading), followed by the gain of heat to melt grounded and floating ice in the cryosphere (gray shading). Due to its low heat capacity, the atmosphere (magenta shading) makes a smaller contribution. Uncertainty in the ocean estimate also dominates the total uncertainty (dot-dashed lines derived from the standard deviations (2σ) for the ocean, cryosphere and land; atmospheric uncertainty is comparably small). Deep ocean ($> 2000 \text{ m}$) is assumed to be zero before 1990 (see Sect. 1 for more details). The dataset for the Earth heat inventory is published at the German Climate Computing Centre (DKRZ, <https://www.dkrz.de/>) under the DOI https://doi.org/10.26050/WDCC/GCOS_EHI_EXP_v2. The net flux at TOA from the NASA CERES program is shown in red (<https://ceres.larc.nasa.gov/data/>, last access: 7 August 2020; see also for example Loeb et al., 2012) for the period 2005–2018 to account for the golden period of best available estimates. We obtain a total heat gain of $358 \pm 37 \text{ ZJ}$ over the period 1971–2018, which is equivalent to a heating rate (i.e., the EEI) of $0.47 \pm 0.1 \text{ W m}^{-2}$ applied continuously over the surface area of the Earth ($5.10 \times 10^{14} \text{ m}^2$). The corresponding EEI over the period 2010–2018 amounts to $0.87 \pm 0.12 \text{ W m}^{-2}$. A weighted least square fit has been used taking into account the uncertainty range (see also von Schuckmann and Le Traon, 2011).

(Rhein et al., 2013). In other words, our results show that since the IPCC AR5 estimate has been performed, heat accumulation has continued at a comparable rate. The major player in the Earth inventory is the ocean, particularly the upper (0–700 m) and intermediate (700–2000 m) ocean layers (see also Sect. 1, Fig. 2).

Although the net flux at TOA as derived from remote sensing is anchored by an estimate of global OHC (Loeb et al., 2012), and thus does not provide a completely independent result for the total EEI, we additionally compare net flux at TOA with the Earth heat inventory obtained in this study (Fig. 6). Both rates of change compare well, and we obtain

$0.7 \pm 0.1 \text{ W m}^{-2}$ for the remote sensing estimate at TOA and $0.8 \pm 0.1 \text{ W m}^{-2}$ for the Earth heat inventory over the period 2005–2018.

Rates of change derived from Fig. 6 are in agreement with previously published results for the different periods (Fig. 7). Major disagreements occur for the estimate of Balmaseda et al. (2013) which is obtained from an ocean re-analysis and known to provide higher heat gain compared to results derived strictly from observations (Meyssignac et al., 2019). Over the last quarter of a decade this Earth heat inventory reports – in agreement with previous publications – an increased rate of Earth heat uptake reaching up to

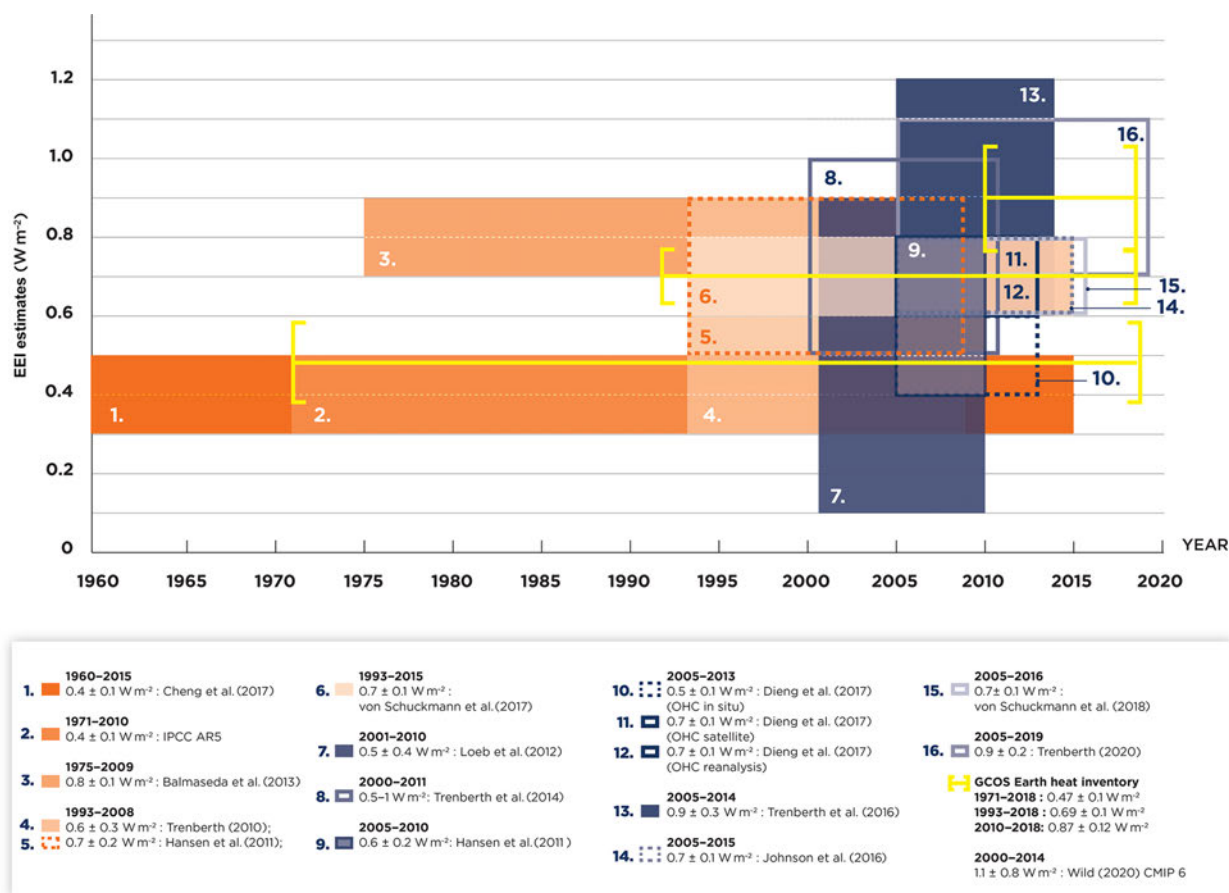


Figure 7. Overview on EEI estimates as obtained from previous publications; references are listed in the figure legend. For IPCC AR5, Rhein et al. (2013) is used. The color bars take into account the uncertainty ranges provided in each publication, respectively. For comparison, the estimates of our Earth heat inventory based on the results of Fig. 6 have been added (yellow lines) for the periods 1971–2018, 1993–2018 and 2010–2018, and the trends have been evaluated using a weighted least square fit (see von Schuckmann and Le Traon, 2011, for details on the method).

0.9 W m^{-2} (Fig. 7). This period is also characterized with an increase in the availability and quality of the global climate observing system, particularly for the past 2 decades. The heat inventory as obtained in this study reveals an EEI of $0.87 \pm 0.12 \text{ W m}^{-2}$ over the period 2010–2018 – a period which experienced record levels of Earth surface warming and is ranked as the warmest decade relative to the reference period 1850–1900 (WMO, 2020). Whether this increased rate can be attributed to an acceleration of global warming and Earth system heat uptake (e.g., Cheng et al., 2019a; WMO, 2020; Blunden and Arndt, 2019), an induced estimation bias due to the interplay between natural and anthropogenically driven variability (e.g., Cazenave et al., 2014), or underestimated uncertainties in the historical record (e.g., Boyer et al., 2016) needs further investigation.

The new multidisciplinary estimate obtained from a concerted international effort provides an updated insight in where the heat is going from a positive EEI of $0.47 \pm 0.1 \text{ W m}^{-2}$ for the period 1971–2018. Over the period 1971–

2018 (2010–2018), 89 % (90 %) of the EEI is stored in the global ocean, from which 52 % (52 %) is repartitioned in the upper 700 m depth, 28 % (30 %) at intermediate layers (700–2000 m) and 9 % (8 %) in the deep ocean layer below 2000 m depth. Atmospheric warming amounts to 1 % (2 %) in the Earth heat inventory, the land heat gain amounts to 6 % (5 %) and the heat uptake by the cryosphere amounts to 4 % (3 %). These results show general agreement with previous estimates (e.g., Rhein et al., 2013). Over the period 2010–2018, the EEI amounts to $0.87 \pm 0.12 \text{ W m}^{-2}$, indicating a rapid increase in EEI over the past decade. Note that a near-global (60° N – 60° S) area for the ocean heat uptake is used in this study, which could induce a slight underestimation, and needs further evaluation in the future (see Sect. 1). However, a test using a single dataset (Cheng et al., 2017b) indicates that the ocean contribution within 1960–2018 can increase by 1 % if the full global ocean domain is used (not shown).

7 Data availability

The time series of the Earth heat inventory are published at DKRZ (<https://www.dkrz.de/>, last access: 7 August 2020) under the DOI https://doi.org/10.26050/WDCC/GCOS_EHI_EXP_v2 (von Schuckmann et al., 2020). The data contain an updated international assessment of ocean warming estimates as well as new and updated estimates of heat gain in the atmosphere, cryosphere and land over the period 1960–2018. This published dataset has been used to build the basis for Fig. 6 of this paper. The ocean warming estimate is based on an international assessment of 15 different in situ data-based ocean products as presented in Sect. 1. The new estimate of the atmospheric heat content is fully described in Sect. 2 and is based on a combined use of atmospheric reanalyses, multisatellite data and radiosonde records, and microwave sounding techniques. The land heat storage time series as presented in Sect. 3 relies on borehole data. The heat available to account for cryosphere loss is presented in Sect. 4 and is based on a combined use of model results and observations to obtain estimates of major cryosphere components such as polar ice sheets, Arctic sea ice and glaciers.

8 Conclusions

The UN 2030 Agenda for Sustainable Development states that climate change is “one of the greatest challenges of our time ...” and warns “... the survival of many societies, and of the biological support systems of the planet, is at risk” (UNGA, 2015). The outcome document of the Rio+20 Conference, *The Future We Want*, defines climate change as “an inevitable and urgent global challenge with long-term implications for the sustainable development of all countries” (UNGA, 2012). The Paris Agreement builds upon the United Nations Framework Convention on Climate Change (UN, 1992) and for the first time all nations agreed to undertake ambitious efforts to combat climate change, with the central aim to keep global temperature rise this century well below 2 °C above preindustrial levels and to limit the temperature increase even further to 1.5 °C (UN, 2015). Article 14 of the Paris Agreement requires the Conference of the Parties serving as the meeting of the Parties to the Paris Agreement (CMA) to periodically take stock of the implementation of the Paris Agreement and to assess collective progress towards achieving the purpose of the agreement and its long-term goals through the so-called global stocktake based on best available science.

The EEI is the most critical number defining the prospects for continued global warming and climate change (Hansen et al., 2011; von Schuckmann et al., 2016), and we call for an implementation of the EEI into the global stocktake. The current positive EEI is understood to be foremost and primarily a result of increasing atmospheric greenhouse gases

(IPCC, 2013), which have – according to the IPCC special report on Global Warming of 1.5 °C – already “caused approximately 1.0 °C of global warming above preindustrial levels, with a likely range of 0.8 °C to 1.2 °C” (IPCC, 2018). The IPCC special report further states with high confidence that “global warming is likely to reach 1.5 °C between 2030 and 2052 if it continues to increase at the current rate”. The EEI is the portion of the forcing that the Earth’s climate system has not yet responded to (Hansen et al., 2005) and defines additional global warming that will occur without further change in forcing (Hansen et al., 2017). Our results show that EEI is not only continuing, but also increasing. Over the period 1971–2018 average EEI amounts to $0.47 \pm 0.1 \text{ W m}^{-2}$, but it amounts to $0.87 \pm 0.12 \text{ W m}^{-2}$ during 2010–2018 (Fig. 8). Concurrently, acceleration of sea-level rise (WCRP, 2018; Legelais et al., 2020), accelerated surface warming, record temperatures and sea ice loss in the Arctic (Richter-Menge et al., 2019; WMO, 2020; Blunden and Arndt, 2020) and ice loss from the Greenland ice sheet (King et al., 2020), and intensification of atmospheric warming near the surface and in the troposphere (Steiner et al., 2020) have been – for example – recently reported. To what degree these changes are intrinsically linked needs further evaluations.

Global atmospheric CO₂ concentration reached $407.38 \pm 0.1 \text{ ppm}$ averaged over 2018 (Friedlingstein et al., 2019) and $409.8 \pm 0.1 \text{ ppm}$ in 2019 (Blunden and Arndt, 2020). WMO (2020) reports CO₂ concentrations at the Mauna Loa measurement platform of 411.75 ppm in February 2019 and 414.11 ppm in February 2020. Stabilization of climate, the goal of the universally agreed UNFCCC (UN, 1992) and the Paris Agreement (UN, 2015), requires that EEI be reduced to approximately zero to achieve Earth’s system quasi-equilibrium. The change of heat radiation to space for a given greenhouse gas change can be computed accurately. The amount of CO₂ in the atmosphere would need to be reduced from 410 to 353 ppm (i.e., a required reduction of $-57 \pm 8 \text{ ppm}$) to increase heat radiation to space by 0.87 W m^{-2} , bringing Earth back towards energy balance (Fig. 8), where we have used the analytic formulae of Hansen et al. (2000) for this estimation. Atmospheric CO₂ was last 350 ppm in the year 1988, and the global Earth surface temperature was then +0.5 °C relative to the preindustrial period (relative to the 1880–1920 mean) (Hansen et al., 2017; Friedlingstein et al., 2019). In principle, we could reduce other greenhouse gases and thus require a less stringent reduction of CO₂. However, as discussed by Hansen et al. (2017), some continuing increase in N₂O, whose emissions are associated with food production, seems inevitable, so there is little prospect for much net reduction of non-CO₂ greenhouse gases, and thus the main burden for climate stabilization falls on CO₂ reduction. This simple number, EEI, is the most fundamental metric that the scientific community and public must be aware of as the measure of how well the world is doing in the task of bringing climate change under control (Fig. 8).

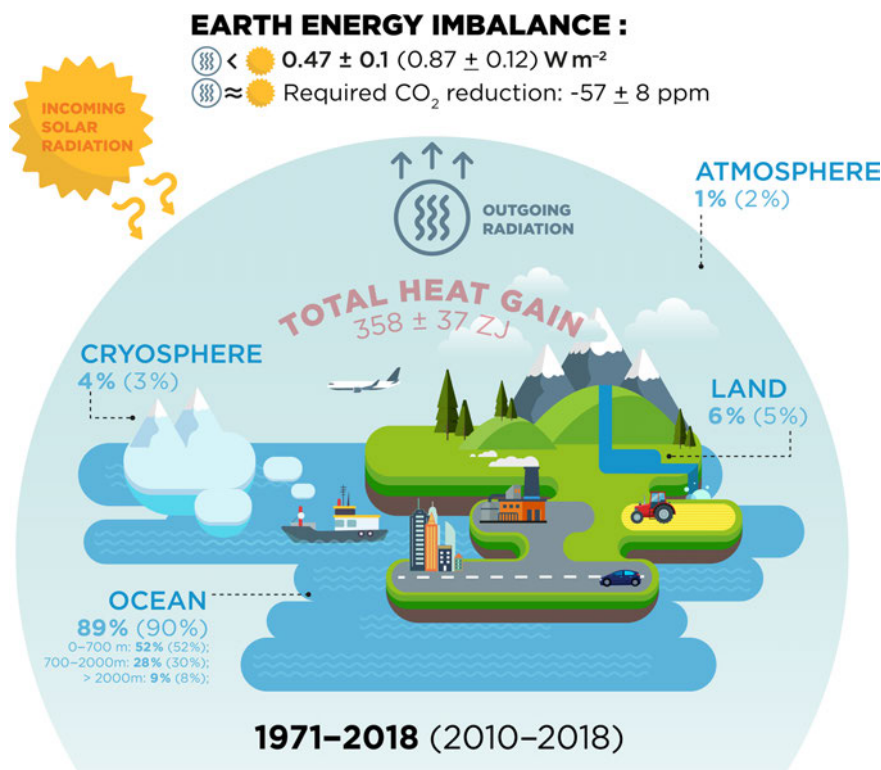


Figure 8. Schematic presentation on the Earth heat inventory for the current anthropogenically driven positive Earth energy imbalance at the top of the atmosphere (TOA). The relative partition (in %) of the Earth heat inventory presented in Fig. 6 for the different components is given for the ocean (upper: 0–700 m, intermediate: 700–2000 m, deep: > 2000 m), land, cryosphere (grounded and floating ice) and atmosphere, for the periods 1971–2018 and 2010–2018 (for the latter period values are provided in parentheses), as well as for the EEI. The total heat gain (in red) over the period 1971–2018 is obtained from the Earth heat inventory as presented in Fig. 6. To reduce the 2010–2018 EEI of $0.87 \pm 0.12 \text{ W m}^{-2}$ towards zero, current atmospheric CO_2 would need to be reduced by $-57 \pm 8 \text{ ppm}$ (see text for more details).

This community effort also addresses gaps for the evolution of future observing systems for a robust and continued assessment of the Earth heat inventory and its different components. Immediate priorities include the maintenance and extension of the global climate observing system to assure a continuous monitoring of the Earth heat inventory and to reduce the uncertainties. For the global ocean observing system, the core Argo sampling needs to be sustained and complemented by remote sensing data. Extensions such as into the deep ocean layer need to be further fostered (Desbruyères et al., 2017; Johnson et al., 2015), and technical developments for the measurements under ice and in shallower areas need to be sustained and extended. Moreover, continued efforts are needed to further advance bias correction methodologies, uncertainty evaluations and data processing of the historical dataset.

In order to allow for improvements on the present estimates of changes in the continental heat and to ensure that the database is continued into the future, an international, coordinated effort is needed to increase the number of subsurface temperature data from BTPs at additional locations around the world, in particular in the Southern Hemisphere. Addi-

tionally, repeated monitoring (after a few decades) of existing boreholes should help reduce uncertainties at individual sites. Such data should be shared through an open platform.

For the atmosphere, the continuation of operational satellite- and ground-based observations is important, but the foremost need is sustaining and enhancing a coherent long-term monitoring system for the provision of climate data records of essential climate variables. GNSS radio occultation observations and reference radiosonde stations within the Global Climate Observing System (GCOS) Reference Upper Air Network (GRUAN) are regarded as climate benchmark observations. Operational radio occultation missions for continuous global climate observations need to be maintained and expanded, ensuring global coverage over all local times, as the central node of a global climate observing system.

For the cryosphere, sustained remote sensing for all of the cryosphere components is key to quantifying future changes over these vast and inaccessible regions but must be complemented by in situ observations for calibration and validation. For sea ice, the albedo, the area and ice thickness are all essential, with ice thickness being particularly chal-

lenging to quantify with remote sensing alone. For ice sheets and glaciers, reliable gravimetric measurements, ice thickness and extent, snow/ice thickness and density are essential to quantify changes in mass balance of grounded and floating ice. We highlight Antarctic sea ice change and warming of ice as terms that are poorly constrained or have not significantly contributed to this assessment but may become important over the coming decades. Similarly, there exists the possibility for rapid change associated with positive ice dynamical feedbacks at the marine margins of the Greenland and Antarctic ice sheets. Sustained monitoring of each of these components will, therefore, serve the dual purpose of furthering the understanding of the dynamics and quantifying the contribution to Earth's energy budget. In addition to data collection, open access to the data and data synthesis products as well as coordinated international efforts are key to the continued monitoring of the ice loss from the cryosphere and related energy uptake.

Sustained and improved observations to quantify Earth's changing energy inventory are also critical to the development of improved physical models of the climate system, including both data assimilation efforts that help us to understand past changes and predictions (Storto et al., 2019) and climate models used to provide projections of future climate change (Eyring et al., 2019). For example, atmospheric reanalyses have shown to be a valuable tool for investigating past changes in the EEI (Allan et al., 2014) and ocean reanalyses have proven useful in estimating rates of ocean heating on annual and subannual timescales by reducing observational noise (Trenberth et al., 2016). Furthermore, both reanalyses and climate models can provide information to assess current observing capabilities (Fujii et al., 2019) and improve uncertainty estimates in the different components of Earth's energy inventory (Allison et al., 2019). Future priorities for expanding the observing system to improve future estimates of EEI should be cognizant of the expected evolution of the climate change signal, drawing on evidence from observations, models and theory (Meyssignac et al., 2019; Palmer et al., 2019).

A continuous effort to regularly update the Earth heat inventory is important to quantify how much and where heat accumulated from climate change is stored in the climate system. The Earth heat inventory crosses multidisciplinary boundaries and calls for the inclusion of new science knowledge from the different disciplines involved, including the evolution of climate observing systems and associated data products, uncertainty evaluations, and processing tools. The results provide indications that a redistribution and conversion of energy in the form of heat is taking place in the different components of the Earth system, particularly within the ocean, and that EEI has increased over the past decade. The outcomes have further demonstrated how we are able to evolve our estimates for the Earth heat inventory while bringing together different expertise and major climate science advancements through a concerted international effort.

All of these component estimates are at the leading edge of climate science. Their union has provided a new and unique insight on the inventory of heat in the Earth system, its evolution over time and a revision of the absolute values. The data product of this effort is made available and can be thus used for model validation purposes.

This study has demonstrated the unique value of such a concerted international effort, and we thus call for a regular evaluation of the Earth heat inventory. This first attempt presented here has been focused on the global area average only, and evolving into regional heat storage and redistribution, the inclusion of various timescales (e.g., seasonal, year to year) and other climate study tools (e.g., indirect methods, ocean reanalyses) would be an important asset of this much needed regular international framework for the Earth heat inventory. This would also respond directly to the request of GCOS to establish the observational requirements needed to monitor the Earth's cycles and the global energy budget. The outcome of this study will therefore directly feed into GCOS' assessment of the status of the global climate observing system due in 2021, which is the basis for the next implementation plan. These identified observation requirements will guide the development of the next generation of in situ and satellite global climate observations by all national meteorological services and space agencies and other oceanic and terrestrial networks.

Author contributions. Overall coordination of this initiative has been driven by KvS, LC, MDP, CT and VA.

Author contributions to the ocean section include KvS, LC, TB, DD, CD, JG, MI, GCJ, REK, BAK, NK, JL, MM, DPM, SP, DR and SEW.

Author contributions to the atmosphere section include GK, MG, AKS, MM and LH.

Author contributions for the land section include AGG, FJCV, HB, SIS and PG.

Author contributions for the cryosphere section include FS, SA, DAS, MLT, BM, AS and AS.

All authors have contributed to the Earth energy inventory section, with specific contributions from KvS, AGG, FJCV, JH and MM.

All authors have contributed to the conclusion, with specific contributions from KvS, JH, CT, VA, LC, MDP, GK, AKS, AGG, FJCV, HB and FS.

Acknowledgements. This research benefited from long-term attention by GCOS and builds on initial work carried out under the WCRP core projects CLIVAR, GEWEX, CliC and SPARC.

We would like to thank the anonymous reviewers for their comments, which helped to improve the manuscript.

We also would like to thank Marianne Nail (<https://girlsmakesense.com/>, last access: 7 August 2020) for her support to the graphical development of Figs. 7 and 8.

We acknowledge the WEGC EOPAC team for providing the OPSv5.6 RO data (available online at

<https://doi.org/10.25364/WEGC/OPS5.6:2019.1>, EOPAC Team, 2019) as well as quality-processed Vaisala RS data, UCAR/CDAAC (Boulder, CO, USA) for access to RO phase and orbit data, RSS (Santa Rosa, CA, USA) for providing MSU V4.0 data, ECMWF (Reading, UK) for access to operational analysis and forecast data, ERA5 reanalysis data, and RS data from the ERA-Interim archive, JMA (Tokyo, Japan) for provision of the JRA55 and JRA55C reanalysis data, and NASA GMAO (Greenbelt, MD, USA) for access of the MERRA-2 reanalysis data.

Financial support. Matthew D. Palmer and Rachel E. Killick were supported by the Met Office Hadley Centre Climate Programme funded by the BEIS and Defra. PML authors were supported by contribution number 5053. Catia M. Domingues was supported by an ARC Future Fellowship (FT130101532). Lijing Cheng is supported by the Key Deployment Project of Centre for Ocean Mega-Research of Science, CAS (COMS2019Q01). Maximilian Gorfer was supported by WEGC atmospheric remote sensing and climate system research group young scientist funds. Michael Mayer was supported by Austrian Science Fund project P33177. This work was supported by grants from the National Sciences and Engineering Research Council of Canada Discovery Grant (NSERC DG 140576948) and the Canada Research Chairs Program (CRC 230687) to Hugo Beltrami. Almudena García-García and Francisco José Cuesta-Valero are funded by Beltrami's CRC program, the School of Graduate Studies at Memorial University of Newfoundland and the Research Office at St. Francis Xavier University. Fiamma Straneo was supported by NSF OCE 1657601. Susheel Adusumilli was supported by NASA grant 80NSSC18K1424.

Review statement. This paper was edited by David Carlson and reviewed by two anonymous referees.

References

- Abraham, J. P., Baringer, M., Bindoff, N. L., Boyer, T., Cheng, L. J., Church, J. A., Conroy, J. L., Domingues, C. M., Fasullo, J. T., Gilson, J., Goni, G., Good, S. A., Gorman, J. M., Gouretski, V., Ishii, M., Johnson, G. C., Kizu, S., Lyman, J. M., Macdonald, A. M., and Willis, J. K.: A review of global ocean temperature observations: Implications for ocean heat content estimates and climate change, *Rev. Geophys.*, 51, 450–483, <https://doi.org/10.1002/rog.20022>, 2013.
- Adusumilli, S., Fricker, H. A., Medley, B., Padman, L., and Siegfried, M. R.: Multi-year variability in ocean-driven melting of Antarctica's ice shelves, *Nat. Geosci.*, <https://doi.org/10.1038/s41561-020-0616-z>, online first, 2020.
- Allan, R. P., Liu, C., Loeb, N. G., Palmer, M. D., Roberts, M., Smith, D., and Vidale, P.-L.: Changes in global net radiative imbalance 1985–2012 (I10, trans.), *Geophys. Res. Lett.*, 41, 5588–5597, <https://doi.org/10.1002/2014GL060962>, 2014.
- Allison, L. C., Roberts, C. D., Palmer, M. D., Hermanson, L., Killick, R. E., Rayner, N. A., Smith, D. M., and Andrews, M. B.: Towards quantifying uncertainty in ocean heat content changes using synthetic profiles, *Environ. Res. Lett.*, 14, 084037, <https://doi.org/10.1088/1748-9326/ab2b0b>, 2019.
- Angerer, B., Ladstädter, F., Scherllin-Pirscher, B., Schwärz, M., Steiner, A. K., Foelsche, U., and Kirchengast, G.: Quality aspects of the Wegener Center multi-satellite GPS radio occultation record OPSv5.6, *Atmos. Meas. Tech.*, 10, 4845–4863, <https://doi.org/10.5194/amt-10-4845-2017>, 2017.
- Baggenstos, D., Häberli, M., Schmitt, J., Shackleton, S. A., Birner, B., Severinghaus, J. P., Kellerhals, T., and Fischer, H.: Earth's radiative imbalance from the Last Glacial Maximum to the present, *P. Natl. Acad. Sci. USA*, 116, 14881, <https://doi.org/10.1073/pnas.1905447116>, 2019.
- Bailey, V. L., Pries, C. H., and Lajtha, K.: What do we know about soil carbon destabilization?, *Environ. Res. Lett.*, 14, 083004, <https://doi.org/10.1088/1748-9326/ab2c11>, 2019.
- Balmaseda, M. A., Trenberth, K. E., and Källén, E.: Distinctive climate signals in reanalysis of global ocean heat content, *Geophys. Res. Lett.*, 40, 1754–1759, <https://doi.org/10.1002/grl.50382>, 2013.
- Bamber, J. L., Westaway, R. M., Marzeion, B., and Wouters, B.: The land ice contribution to sea level during the satellite era, *Environ. Res. Lett.*, 13, 063008, <https://doi.org/10.1088/1748-9326/aac2f0>, 2018.
- Barkaoui, A. E., Correia, A., Zarhloule, Y., Rimi, A., Carneiro, J., Boughriba, M., and Verdoya, M.: Reconstruction of remote climate change from borehole temperature measurement in the eastern part of Morocco, *Climatic Change*, 118, 431–441, <https://doi.org/10.1007/s10584-012-0638-7>, 2013.
- Beck, A. E.: Climatically perturbed temperature gradients and their effect on regional and continental heat-flow means, *Tectonophysics*, 41, 17–39, [https://doi.org/10.1016/0040-1951\(77\)90178-0](https://doi.org/10.1016/0040-1951(77)90178-0), 1977.
- Beltrami, H.: Surface heat flux histories from inversion of geothermal data: Energy balance at the Earth's surface, *J. Geophys. Res.-Sol. Ea.*, 106, 21979–21993, <https://doi.org/10.1029/2000JB000065>, 2001.
- Beltrami, H.: Earth's Long-Term Memory, *Science*, 297, 206–207, <https://doi.org/10.1126/science.1074027>, 2002a.
- Beltrami, H.: Climate from borehole data: Energy fluxes and temperatures since 1500, *Geophys. Res. Lett.*, 29, 26–1–26–4, <https://doi.org/10.1029/2002GL015702>, 2002b.
- Beltrami, H. and Bournon, E.: Ground warming patterns in the Northern Hemisphere during the last five centuries, *Earth Planet. Sc. Lett.*, 227, 169–177, <https://doi.org/10.1016/j.epsl.2004.09.014>, 2004.
- Beltrami, H., Bournon, E., Kellman, L., and González-Rouco, J. F.: Spatial patterns of ground heat gain in the Northern Hemisphere, *Geophys. Res. Lett.*, 33, L06717, <https://doi.org/10.1029/2006GL025676>, 2006.
- Beltrami, H., Matharoo, G. S., and Smerdon, J. E.: Impact of borehole depths on reconstructed estimates of ground surface temperature histories and energy storage, *J. Geophys. Res.-Earth*, 120, 763–778, <https://doi.org/10.1002/2014JF003382>, 2015.
- Beltrami, H., Matharoo, G. S., Smerdon, J. E., Illanes, L., and Tarasov, L.: Impacts of the Last Glacial Cycle on ground surface temperature reconstructions over the last millennium, *Geophys. Res. Lett.*, 44, 355–364, <https://doi.org/10.1002/2016GL071317>, 2017.
- Beltrami, H., Smerdon, J. E., Pollack, H. N., and Huang, S.: Continental heat gain in the global climate system, *Geophys.*

- Res. Lett., 29, 8–1–8–3, <https://doi.org/10.1029/2001GL014310>, 2002.
- Bense, V. F. and Kooi, H.: Temporal and spatial variations of shallow subsurface temperature as a record of lateral variations in groundwater flow, *J. Geophys. Res.-Sol. Ea.*, 109, B04103, <https://doi.org/10.1029/2003JB002782>, 2004.
- Berrisford, P., Kållberg, P., Kobayashi, S., Dee, D., Uppala, S., Simmons, A. J., Poli, P., and Sato, H.: Atmospheric conservation properties in ERA-Interim, *Q. J. Roy. Meteor. Soc.*, 137, 1381–1399, <https://doi.org/10.1002/qj.864>, 2011.
- Bindoff, N. L., Cheung, W. W. L., and Kairo, J. G.: Changing Ocean, Marine Ecosystems, and Dependent Communities, in: Special Report: The Ocean and Cryosphere in a Changing Climate Summary for Policymakers, edited by: Pörtner, H. O., Roberts, D. C., Masson-Delmotte, V., Zhai, P., Tignor, M., Poloczanska, E., Mintenbeck, K., Alegría, A., Nicolai, M., Okem, A., Petzold, J., Rama, B., and Weyer, N. M., 447–587, available at: <https://www.ipcc.ch/report/srocc/> (last access: 7 August 2020), in press, 2020.
- Blunden, J. and Arndt, D. S.: State of the Climate in 2019, *B. Am. Meteorol. Soc.*, 100, Si–S305, <https://doi.org/10.1175/2019BAMSStateoftheClimate.1>, 2019.
- Blunden, J. and Arndt, D. S. (Eds.): State of the Climate in 2019, *B. Am. Meteorol. Soc.*, 101, Si–S429, <https://doi.org/10.1175/2020BAMSStateoftheClimate.1>, 2020.
- Bopp, L., Resplandy, L., Orr, J. C., Doney, S. C., Dunne, J. P., Gehlen, M., Halloran, P., Heinze, C., Ilyina, T., Séférian, R., Tjiputra, J., and Vichi, M.: Multiple stressors of ocean ecosystems in the 21st century: projections with CMIP5 models, *Biogeosciences*, 10, 6225–6245, <https://doi.org/10.5194/bg-10-6225-2013>, 2013.
- Boyer, T., Domingues, C. M., Good, S. A., Johnson, G. C., Lyman, J. M., Ishii, M., Gouretski, V., Willis, J. K., Antonov, J., Wijffels, S., Church, J. A., Cowley, R., and Bindoff, N. L.: Sensitivity of Global Upper-Ocean Heat Content Estimates to Mapping Methods, XBT Bias Corrections, and Baseline Climatologies, *J. Climate*, 29, 4817–4842, <https://doi.org/10.1175/JCLI-D-15-0801.1>, 2016.
- Breitbart, D., Levin, L. A., Oschlies, A., Grégoire, M., Chavez, F. P., Conley, D. J., Garçon, V., Gilbert, D., Gutiérrez, D., Isensee, K., Jacinto, G. S., Limburg, K. E., Montes, I., Naqvi, S. W. A., Pitcher, G. C., Rabalais, N. N., Roman, M. R., Rose, K. A., Seibel, B. A., and Zhang, J.: Declining oxygen in the global ocean and coastal waters, *Science*, 359, eaam7240, <https://doi.org/10.1126/science.aam7240>, 2018.
- Cabanes, C., Grouazel, A., von Schuckmann, K., Hamon, M., Turpin, V., Coatanoan, C., Paris, F., Guinehut, S., Boone, C., Ferry, N., de Boyer Montégut, C., Carval, T., Reverdin, G., Pouliquen, S., and Le Traon, P.-Y.: The CORA dataset: validation and diagnostics of in-situ ocean temperature and salinity measurements, *Ocean Sci.*, 9, 1–18, <https://doi.org/10.5194/os-9-1-2013>, 2013.
- Cazenave, A., Dieng, H.-B., Meyssignac, B., von Schuckmann, K., Decharme, B., and Berthier, E.: The rate of sea-level rise, *Nat. Clim. Change*, 4, 358–361, <https://doi.org/10.1038/nclimate2159>, 2014.
- Cermak, V.: Underground temperature and inferred climatic temperature of the past millenium, *Palaeogeogr. Palaeoclimatol.*, 10, 1–19, [https://doi.org/10.1016/0031-0182\(71\)90043-5](https://doi.org/10.1016/0031-0182(71)90043-5), 1971.
- Cheng, L., Trenberth, K. E., Palmer, M. D., Zhu, J., and Abraham, J. P.: Observed and simulated full-depth ocean heat-content changes for 1970–2005, *Ocean Sci.*, 12, 925–935, <https://doi.org/10.5194/os-12-925-2016>, 2016.
- Cheng, L., Trenberth, K., Fasullo, J., Boyer, T., Abraham, J., von Schuckmann, K., and Zhou, J.: Taking the Pulse of the Planet, *Eos Trans. AGU*, 98, <https://doi.org/10.1029/2017EO081839>, 2017a.
- Cheng, L., Trenberth, K. E., Fasullo, J., Boyer, T., Abraham, J., and Zhu, J.: Improved estimates of ocean heat content from 1960 to 2015, *Science Advances*, 3, e1601545, <https://doi.org/10.1126/sciadv.1601545>, 2017b.
- Cheng, L., Abraham, J., Hausfather, Z., and Trenberth, K. E.: How fast are the oceans warming? *Science*, 363, 128–129, <https://doi.org/10.1126/science.aav7619>, 2019a.
- Cheng, L., Trenberth, K. E., Fasullo, J. T., Mayer, M., Balmaseda, M., and Zhu, J.: Evolution of ocean heat content related to ENSO, *J. Climate*, 32, 3529–3556, <https://doi.org/10.1175/JCLI-D-18-0607.1>, 2019b.
- Chiodo, G. and Haimberger, L.: Interannual changes in mass consistent energy budgets from ERA-Interim and satellite data, *J. Geophys. Res.-Atmos.*, 115, D02112, <https://doi.org/10.1029/2009JD012049>, 2010.
- Chouinard, C. and Mareschal, J.-C.: Selection of borehole temperature depth profiles for regional climate reconstructions, *Clim. Past*, 3, 297–313, <https://doi.org/10.5194/cp-3-297-2007>, 2007.
- Chouinard, C. and Mareschal, J.-C.: Ground surface temperature history in southern Canada: Temperatures at the base of the Laurentide ice sheet and during the Holocene, *Earth Planet. Sc. Lett.*, 277, 280–289, <https://doi.org/10.1016/j.epsl.2008.10.026>, 2009.
- Ciais, P., Sabine, C., Bala, G., Bopp, L., Brovkin, V., Canadell, J., Chhabra, A., DeFries, R., Galloway, J., Heimann, M., Jones, C., Quéré, C. Le, Myneni, R. B., Piao, S., and Thornton, P.: The physical science basis. Contribution of working group I to the fifth assessment report of the intergovernmental panel on climate change, *Change, IPCC Climate*, 465–570, <https://doi.org/10.1017/CBO9781107415324.015>, 2013.
- Clark, P. U., Shakun, J. D., Marcott, S. A., Mix, A. C., Eby, M., Kulp, S., Levermann, A., Milne, G. A., Pfister, P. L., Santer, B. D., Schrag, D. P., Solomon, S., Stocker, T. F., Strauss, B. H., Weaver, A. J., Winkelmann, R., Archer, D., Bard, E., Goldner, A., and Plattner, G.-K.: Consequences of twenty-first-century policy for multi-millennial climate and sea-level change, *Nat. Clim. Change*, 6, 360–369, <https://doi.org/10.1038/nclimate2923>, 2016.
- Cohen, J., Screen, J. A., Furtado, J. C., Barlow, M., Whittleston, D., Coumou, D., Francis, J., Dethloff, K., Entekhabi, D., Overland, J., and Jones, J.: Recent Arctic amplification and extreme mid-latitude weather, *Nat. Geosci.*, 7, 627–637, <https://doi.org/10.1038/ngeo2234>, 2014.
- Cook, A. J. and Vaughan, D. G.: Overview of areal changes of the ice shelves on the Antarctic Peninsula over the past 50 years, *The Cryosphere*, 4, 77–98, <https://doi.org/10.5194/tc-4-77-2010>, 2010.
- Coumou, D., Di Capua, G., Vavrus, S., Wang, L., and Wang, S.: The influence of Arctic amplification on mid-latitude summer circulation, *Nat. Commun.*, 9, 2959, <https://doi.org/10.1038/s41467-018-05256-8>, 2018.

- Cuesta-Valero, F. J., García-García, A., Beltrami, H., and Smerdon, J. E.: First assessment of continental energy storage in CMIP5 simulations, *Geophys. Res. Lett.*, 43, 5326–5335, <https://doi.org/10.1002/2016GL068496>, 2016.
- Cuesta-Valero, F. J., García-García, A., Beltrami, H., Zorita, E., and Jaume-Santero, F.: Long-term Surface Temperature (LoST) database as a complement for GCM preindustrial simulations, *Clim. Past*, 15, 1099–1111, <https://doi.org/10.5194/cp-15-1099-2019>, 2019.
- Cuesta-Valero, F. J., García-García, A., Beltrami, H., González-Rouco, J. F., and García-Bustamante, E.: Long-Term Global Ground Heat Flux and Continental Heat Storage from Geothermal Data, *Clim. Past Discuss.*, <https://doi.org/10.5194/cp-2020-65>, in review, 2020.
- Davis, M. G., Harris, R. N., and Chapman, D. S.: Repeat temperature measurements in boreholes from northwestern Utah link ground and air temperature changes at the decadal time scale, *J. Geophys. Res.-Sol. Ea.*, 115, B05203, <https://doi.org/10.1029/2009JB006875>, 2010.
- Demezhko, D. Y. and Gornostaeva, A. A.: Late Pleistocene–Holocene ground surface heat flux changes reconstructed from borehole temperature data (the Urals, Russia), *Clim. Past*, 11, 647–652, <https://doi.org/10.5194/cp-11-647-2015>, 2015.
- Desbruyères, D., McDonagh, E. L., King, B. A., and Thierry, V.: Global and Full-Depth Ocean Temperature Trends during the Early Twenty-First Century from Argo and Repeat Hydrography, *J. Climate*, 30, 1985–1997, <https://doi.org/10.1175/JCLI-D-16-0396.1>, 2017.
- Desbruyères, D. G., Purkey, S. G., McDonagh, E. L., Johnson, G. C., and King, B. A.: Deep and abyssal ocean warming from 35 years of repeat hydrography, *Geophys. Res. Lett.*, 43, 310–356, <https://doi.org/10.1002/2016GL070413>, 2016.
- Dieng, H. B., Cazenave, A., Meyssignac, B., and Ablain, M.: New estimate of the current rate of sea level rise from a sea level budget approach, *Geophys. Res. Lett.*, 44, 3744–3751, <https://doi.org/10.1002/2017GL073308>, 2017.
- Domingues, C. M., Church, J. A., White, N. J., Gleckler, P. J., Wijffels, S. E., Barker, P. M., and Dunn, J. R.: Improved estimates of upper-ocean warming and multi-decadal sea-level rise, *Nature*, 453, 1090–1093, <https://doi.org/10.1038/nature07080>, 2008.
- EOPAC Team: GNSS Radio Occultation Record (OPS 5.6 2001–2018), University of Graz, Austria, <https://doi.org/10.25364/WEGC/OPS5.6:2019.1>, 2019.
- Eyring, V., Cox, P. M., Flato, G. M., Gleckler, P. J., Abramowitz, G., Caldwell, P., Collins, W. D., Gier, B. K., Hall, A. D., Hoffman, F. M., Hurtt, G. C., Jahn, A., Jones, C. D., Klein, S. A., Krasting, J. P., Kwiatkowski, L., Lorenz, R., Maloney, E., Meehl, G. A., and Williamson, M. S.: Taking climate model evaluation to the next level, *Nat. Clim. Change*, 9, 102–110, <https://doi.org/10.1038/s41558-018-0355-y>, 2019.
- Fischer, E. M. and Knutti, R.: Observed heavy precipitation increase confirms theory and early models, *Nat. Clim. Change*, 6, 986–991, <https://doi.org/10.1038/nclimate3110>, 2016.
- Friedlingstein, P., Jones, M. W., O’Sullivan, M., Andrew, R. M., Hauck, J., Peters, G. P., Peters, W., Pongratz, J., Sitch, S., Le Quéré, C., Bakker, D. C. E., Canadell, J. G., Ciais, P., Jackson, R. B., Anthoni, P., Barbero, L., Bastos, A., Bastrikov, V., Becker, M., Bopp, L., Buitenhuis, E., Chandra, N., Chevallier, F., Chini, L. P., Currie, K. I., Feely, R. A., Gehlen, M., Gilfillan, D., Gkritzalis, T., Goll, D. S., Gruber, N., Gutekunst, S., Harris, I., Haverd, V., Houghton, R. A., Hurtt, G., Ilyina, T., Jain, A. K., Joetzjer, E., Kaplan, J. O., Kato, E., Klein Goldewijk, K., Korsbakken, J. I., Landschützer, P., Lauvset, S. K., Lefèvre, N., Lenton, A., Lienert, S., Lombardozzi, D., Marland, G., McGuire, P. C., Melton, J. R., Metzl, N., Munro, D. R., Nabel, J. E. M. S., Nakaoka, S.-I., Neill, C., Omar, A. M., Ono, T., Peregon, A., Pierrot, D., Poulter, B., Rehder, G., Resplandy, L., Robertson, E., Rödenbeck, C., Séférian, R., Schwinger, J., Smith, N., Tans, P. P., Tian, H., Tilbrook, B., Tubiello, F. N., van der Werf, G. R., Wiltshire, A. J., and Zaehle, S.: Global Carbon Budget 2019, *Earth Syst. Sci. Data*, 11, 1783–1838, <https://doi.org/10.5194/essd-11-1783-2019>, 2019.
- Frölicher, T. L., Fischer, E. M., and Gruber, N.: Marine heatwaves under global warming, *Nature*, 560, 360–364, <https://doi.org/10.1038/s41586-018-0383-9>, 2018.
- Fu, Q., Solomon, S., Pahlavan, H. A., and Lin, P.: Observed changes in Brewer–Dobson circulation for 1980–2018, *Environ. Res. Lett.*, 14, 114026, <https://doi.org/10.1088/1748-9326/ab4de7>, 2019.
- Fujii, Y., Rémy, E., Zuo, H., Oke, P., Halliwell, G., Gasparin, F., Benkiran, M., Loose, N., Cummings, J., Xie, J., Xue, Y., Masuda, S., Smith, G. C., Balmaseda, M., Germineaud, C., Lea, D. J., Larnicol, G., Bertino, L., Bonaduce, A., and Usui, N.: Observing System Evaluation Based on Ocean Data Assimilation and Prediction Systems: On-Going Challenges and a Future Vision for Designing and Supporting Ocean Observational Networks, *Front. Mar. Sci.*, 6, <https://doi.org/10.3389/fmars.2019.00417>, 2019.
- Gaillard, F., Reynaud, T., Thierry, V., Kolodziejczyk, N., and von Schuckmann, K.: In Situ–Based Reanalysis of the Global Ocean Temperature and Salinity with ISAS: Variability of the Heat Content and Steric Height, *J. Climate*, 29, 1305–1323, <https://doi.org/10.1175/JCLI-D-15-0028.1>, 2016.
- García Molinos, J., Halpern, B. S., Schoeman, D. S., Brown, C. J., Kiessling, W., Moore, P. J., Pandolfi, J. M., Poloczanska, E. S., Richardson, A. J., and Burrows, M. T.: Climate velocity and the future global redistribution of marine biodiversity, *Nat. Clim. Change*, 6(1), 83–88, <https://doi.org/10.1038/nclimate2769>, 2016.
- García-García, A., Cuesta-Valero, F. J., Beltrami, H., and Smerdon, J. E.: Simulation of air and ground temperatures in PMIP3/CMIP5 last millennium simulations: implications for climate reconstructions from borehole temperature profiles, *Environ. Res. Lett.*, 11, 044022, <https://doi.org/10.1088/1748-9326/11/4/044022>, 2016.
- García-García, A., Cuesta-Valero, F. J., Beltrami, H., and Smerdon, J. E.: Characterization of Air and Ground Temperature Relationships within the CMIP5 Historical and Future Climate Simulations, *J. Geophys. Res.-Atmos.*, 124, 3903–3929, <https://doi.org/10.1029/2018JD030117>, 2019.
- Gardner, A. S., Moholdt, G., Cogley, J. G., Wouters, B., Arendt, A. A., Wahr, J., Berthier, E., Hock, R., Pfeffer, W. T., Kaser, G., Ligtenberg, S. R. M., Bolch, T., Sharp, M. J., Hagen, J. O., van den Broeke, M. R., and Paul, F.: A Reconciled Estimate of Glacier Contributions to Sea Level Rise: 2003 to 2009, *Science*, 340, 852–857, <https://doi.org/10.1126/science.1234532>, 2013.
- Gattuso, J.-P., Magnan, A., Billé, R., Cheung, W. W. L., Howes, E. L., Joos, F., Allemand, D., Bopp, L., Cooley, S. R., Eakin, C. M.,

- Hoegh-Guldberg, O., Kelly, R. P., Pörtner, H.-O., Rogers, A. D., Baxter, J. M., Laffoley, D., Osborn, D., Rankovic, A., Rochette, J., and Turley, C.: Contrasting futures for ocean and society from different anthropogenic CO₂ emissions scenarios, *Science*, 349, aac4722, <https://doi.org/10.1126/science.aac4722>, 2015.
- GCOS: The Global Observing System for Climate: Implementation needs, World Meteorological Organization, Geneva, Switzerland, <https://doi.org/10.13140/RG.2.2.23178.26566>, 2016.
- Gelaro, R., McCarty, W., Suárez, M. J., Todling, R., Molod, A., Takacs, L., Randles, C. A., Darmenov, A., Bosilovich, M. G., Reichle, R., Wargan, K., Coy, L., Cullather, R., Draper, C., Akella, S., Buchard, V., Conaty, A., da Silva, A. M., Gu, W., and Zhao, B.: The Modern-Era Retrospective Analysis for Research and Applications, Version 2 (MERRA-2), *J. Climate*, 30, 5419–5454, <https://doi.org/10.1175/JCLI-D-16-0758.1>, 2017.
- Gentine, P., Garcia-Garcia, A., Meier, R., Cuesta-Valero, F., Hugo, B., Davin, E. L., and Seneviratne, S. I.: Large recent continental heat storage, *Nature*, under revision, 2020.
- Gleckler, P., Durack, P., Ronald, S., Johnson, G., and Forest, C.: Industrial-era global ocean heat uptake doubles in recent decades, *Nat. Clim. Change*, 6, 394–398, <https://doi.org/10.1038/nclimate2915>, 2016.
- Goni, G. J., Sprintall, J., Bringas, F., Cheng, L., Cirano, M., Dong, S., Domingues, R., Goes, M., Lopez, H., Morrow, R., Rivero, U., Rossby, T., Todd, R. E., Trinanes, J., Zilberman, N., Baringer, M., Boyer, T., Cowley, R., Domingues, C. M., and Volkov, D.: More Than 50 Years of Successful Continuous Temperature Section Measurements by the Global Expendable Bathythermograph Network, Its Integrability, Societal Benefits, and Future, *Front. Mar. Sci.*, 6, <https://doi.org/10.3389/fmars.2019.00452>, 2019.
- González-Rouco, J. F., Beltrami, H., Zorita, E., and von Storch, H.: Simulation and inversion of borehole temperature profiles in surrogate climates: Spatial distribution and surface coupling, *Geophys. Res. Lett.*, 33, L01703, <https://doi.org/10.1029/2005GL024693>, 2006.
- González-Rouco, J. F., Beltrami, H., Zorita, E., and Stevens, M. B.: Borehole climatology: a discussion based on contributions from climate modeling, *Clim. Past*, 5, 97–127, <https://doi.org/10.5194/cp-5-97-2009>, 2009.
- Good, S. A., Martin, M. J., and Rayner, N. A.: EN4: Quality controlled ocean temperature and salinity profiles and monthly objective analyses with uncertainty estimates, *J. Geophys. Res.-Oceans*, 118, 6704–6716, <https://doi.org/10.1002/2013JC009067>, 2013.
- Gouretski, V. and Cheng, L.: Correction for Systematic Errors in the Global Dataset of Temperature Profiles from Mechanical Bathythermographs, *J. Atmos. Ocean. Tech.*, 37, 841–855, <https://doi.org/10.1175/JTECH-D-19-0205.1>, 2020.
- Gregory, J. M. and Andrews, T.: Variation in climate sensitivity and feedback parameters during the historical period, *Geophys. Res. Lett.*, 43, 3911–3920, <https://doi.org/10.1002/2016GL068406>, 2016.
- Gregory, J. M., Andrews, T., Ceppi, P., Mauritsen, T., and Webb, M. J.: How accurately can the climate sensitivity to CO₂ be estimated from historical climate change?, *Clim. Dynam.*, 54, 129–157, <https://doi.org/10.1007/s00382-019-04991-y>, 2020.
- Guinehut, S., Dhomp, A.-L., Larnicol, G., and Le Traon, P.-Y.: High resolution 3-D temperature and salinity fields derived from in situ and satellite observations, *Ocean Sci.*, 8, 845–857, <https://doi.org/10.5194/os-8-845-2012>, 2012.
- Hansen, J.: Efficacy of climate forcings, *J. Geophys. Res.*, 110, D18104, <https://doi.org/10.1029/2005JD005776>, 2005.
- Hansen, J., Sato, M., Ruedy, R., Lacis, A., and Oinas, V.: Global warming in the twenty-first century: An alternative scenario, *P. Natl. Acad. Sci. USA*, 97, 9875–9880, <https://doi.org/10.1073/pnas.170278997>, 2000.
- Hansen, J., Nazarenko, L., Ruedy, R., Sato, M., Willis, J., Del Genio, A., Koch, D., Lacis, A., Lo, K., Menon, S., Novakov, T., Perlwitz, J., Russell, G., Schmidt, G. A., and Tausnev, N.: Earth's Energy Imbalance: Confirmation and Implications, *Science*, 308, 1431–1435, <https://doi.org/10.1126/science.1110252>, 2005.
- Hansen, J., Sato, M., Kharecha, P., and von Schuckmann, K.: Earth's energy imbalance and implications, *Atmos. Chem. Phys.*, 11, 13421–13449, <https://doi.org/10.5194/acp-11-13421-2011>, 2011.
- Hansen, J., Sato, M., Kharecha, P., von Schuckmann, K., Beerling, D. J., Cao, J., Marcott, S., Masson-Delmotte, V., Prather, M. J., Rohling, E. J., Shakun, J., Smith, P., Lacis, A., Russell, G., and Ruedy, R.: Young people's burden: requirement of negative CO₂ emissions, *Earth Syst. Dynam.*, 8, 577–616, <https://doi.org/10.5194/esd-8-577-2017>, 2017.
- Harris, R. N., and Chapman, D. S.: Mid-latitude (30°–60° N) climatic warming inferred by combining borehole temperatures with surface air temperatures, *Geophys. Res. Lett.*, 28, 747–750, <https://doi.org/10.1029/2000GL012348>, 2001.
- Hartmann, A. and Rath, V.: Uncertainties and shortcomings of ground surface temperature histories derived from inversion of temperature logs, *J. Geophys. Eng.*, 2, 299–311, <https://doi.org/10.1088/1742-2132/2/4/S02>, 2005.
- Hermoso de Mendoza, I., Beltrami, H., MacDougall, A. H., and Mareschal, J.-C.: Lower boundary conditions in land surface models – effects on the permafrost and the carbon pools: a case study with CLM4.5, *Geosci. Model Dev.*, 13, 1663–1683, <https://doi.org/10.5194/gmd-13-1663-2020>, 2020.
- Hersbach, H., Rosnay, P. de, Bell, B., Schepers, D., Simmons, A., Soci, C., Abdalla, S., Alonso-Balmaseda, M., Balsamo, G., Bechtold, P., Berrisford, P., Bidlot, J.-R., de Boissés, E., Bonavita, M., Browne, P., Buizza, R., Dahlgren, P., Dee, D., Dragani, R., and Zuo, H.: Operational global reanalysis: progress, future directions and synergies with NWP, ERA Report Series (ERA Report), available at: <https://www.ecmwf.int/node/18765> (last access: 7 August 2018), 2018.
- Hersbach, H., Bell, B., Berrisford, P., Hirahara, S., Horányi, A., Muñoz-Sabater, J., Nicolas, J., Peubey, C., Radu, R., Schepers, D., Simmons, A., Soci, C., Abdalla, S., Abellan, X., Balsamo, G., Bechtold, P., Biavati, G., Bidlot, J., Bonavita, M., Chiara, G. D., Dahlgren, P., Dee, D., Diamantakis, M., Dragani, R., Flemming, J., Forbes, R., Fuentes, M., Geer, A., Haimberger, L., Healy, S., Hogan, R. J., Hólm, E., Janisková, M., Keeley, S., Laloyaux, P., Lopez, P., Lupu, C., Radnoti, G., Rosnay, P. de, Rozum, I., Vamborg, F., Villaume, S., and Thépaut, J.-N.: The ERA5 global reanalysis, *Q. J. Roy. Meteor. Soc.*, 146, 1999–2049, <https://doi.org/10.1002/qj.3803>, 2020.
- Hicks Pries, C. E., Castanha, C., Porras, R., and Torn, M. S.: The whole-soil carbon flux in response to warming, *Science*, 355, 1420–1423, <https://doi.org/10.1126/science.aal1319>, 2017.

- Hoegeh-Guldberg, O., Jacob, D., Taylor, M., Bindi, M., Brown, S., Camilloni, I., Diedhiou, A., Djalante, R., Ebi, K. L., Engelbrecht, F., Guiot, J., Hijikata, Y., Mehrotra, S., Payne, A., Seneviratne, S. I., Thomas, A., Warren, R., and Zhou, G.: Impacts of 1.5°C Global Warming on Natural and Human Systems, in: *Global Warming of 1.5°C. An IPCC Special Report on the impacts of global warming of 1.5°C above pre-industrial levels and related global greenhouse gas emission pathways, in the context of strengthening the global response to the threat of climate change, sustainable development, and efforts to eradicate poverty*, edited by: Masson-Delmotte, V., Zhai, P., Pörtner, H.-O., Roberts, D., Skea, J., Shukla, P. R., Pirani, A., Moufouma-Okia, W., Péan, C., Pidcock, R., Connors, S., Matthews, J. B. R., Chen, Y., Zhou, X., Gomis, M. I., Lonnoy, E., Maycock, T., Tignor, M., and Waterfield, T., in press, 2020.
- Hopcroft, P. O., Gallagher, K., and Pain, C. C.: Inference of past climate from borehole temperature data using Bayesian Reversible Jump Markov chain Monte Carlo, *Geophys. J. Int.*, 171, 1430–1439, <https://doi.org/10.1111/j.1365-246X.2007.03596.x>, 2007.
- Hosoda, S., Ohira, T., and Nakamura, T.: A monthly mean dataset of global oceanic temperature and salinity derived from Argo float observations, *JAMSTEC Report of Research and Development*, 8, 47–59, <https://doi.org/10.5918/jamstecr.8.47>, 2008.
- Huang, S.: 1851–2004 annual heat budget of the continental landmasses, *Geophys. Res. Lett.*, 33, L04707, <https://doi.org/10.1029/2005GL025300>, 2006.
- Huang, S., Pollack, H. N., and Shen, P.-Y.: Temperature trends over the past five centuries reconstructed from borehole temperatures, *Nature*, 403, 756–758, <https://doi.org/10.1038/35001556>, 2000.
- IPCC: *Climate Change 2013: The Physical Science Basis. Contribution of Working Group I to the Fifth Assessment Report of the Intergovernmental Panel on Climate Change*, edited by: Stocker, T. F., Qin, D., Plattner, G.-K., Tignor, M., Allen, S. K., Boschung, J., Nauels, A., Xia, Y., Bex, V., and Midgley, P. M., Cambridge University Press, Cambridge, United Kingdom and New York, NY, USA, 1535 pp., 2013.
- IPCC: *Global warming of 1.5°C. An IPCC Special Report on the impacts of global warming of 1.5°C above pre-industrial levels and related global greenhouse gas emission pathways, in the context of strengthening the global response to the threat of climate change, sustainable development, and efforts to eradicate poverty*, edited by: Masson-Delmotte, V., Zhai, P., Pörtner, H. O., Roberts, D., Skea, J., Shukla, P. R., Pirani, A., Moufouma-Okia, W., Péan, C., Pidcock, R., Connors, S., Matthews, J. B. R., Chen, Y., Zhou, X., Gomis, M. I., Lonnoy, E., Maycock, T., Tignor, M., Waterfield, T., 2018.
- IPCC: *IPCC Special Report on the Ocean and Cryosphere in a Changing Climate*, edited by: Portner, H.-O., Roberts, D. C., Masson-Delmotte, V., Zhai, P., Tignor, M., Poloczanska, E., Mintenbeck, K., Alegría, A., Nicolai, M., Okem, A., Petzold, J., Rama, B., and Weyer, N. M., in press, 2020.
- Ishii, M., Fukuda, Y., Hirahara, S., Yasui, S., Suzuki, T., and Sato, K.: Accuracy of Global Upper Ocean Heat Content Estimation Expected from Present Observational Data Sets, *SOLA*, 13, 163–167, <https://doi.org/10.2151/sola.2017-030>, 2017.
- Jacobs, S. S., Giulivi, C. F., and Mele, P. A.: Freshening of the Ross Sea During the Late 20th Century, *Science*, 297, 386–389, <https://doi.org/10.1126/science.1069574>, 2002.
- Jaume-Santero, F., Pickler, C., Beltrami, H., and Mareschal, J.-C.: North American regional climate reconstruction from ground surface temperature histories, *Clim. Past*, 12, 2181–2194, <https://doi.org/10.5194/cp-12-2181-2016>, 2016.
- Jeong, D. I., Sushama, L., Diro, G. T., Khaliq, M. N., Beltrami, H., and Caya, D.: Projected changes to high temperature events for Canada based on a regional climate model ensemble, *Clim. Dynam.*, 46, 3163–3180, <https://doi.org/10.1007/s00382-015-2759-y>, 2016.
- Johnson, G. C., Lyman, J. M., Boyer, T., Cheng, L., Domingues, C. M., Gilson, J., Ishii, M., Killick, R., Monselesan, D., Purkey, S. G., and Wijffels, S. E.: Ocean heat content [in State of the Climate in 2017], *B. Am. Meteorol. Soc.*, 99, S72–S77, 2018.
- Johnson, G. C. and Birnbaum, A. N.: As El Niño builds, Pacific Warm Pool expands, ocean gains more heat, *Geophys. Res. Lett.*, 44, 438–445, <https://doi.org/10.1002/2016GL071767>, 2017.
- Johnson, G. C., Lyman, J. M., and Purkey, S. G.: Informing Deep Argo Array Design Using Argo and Full-Depth Hydrographic Section Data, *J. Atmos. Ocean. Tech.*, 32, 2187–2198, <https://doi.org/10.1175/JTECH-D-15-0139.1>, 2015.
- Johnson, G. C., Lyman, J. M., and Loeb, N. G.: Improving estimates of Earth's energy imbalance, *Nat. Clim. Change*, 6, 639–640, <https://doi.org/10.1038/nclimate3043>, 2016.
- Johnson, G. C., Purkey, S. G., Zilberman, N. V., and Roemmich, D.: Deep Argo Quantifies Bottom Water Warming Rates in the Southwest Pacific Basin, *Geophys. Res. Lett.*, 46, 2662–2669, <https://doi.org/10.1029/2018GL081685>, 2019.
- King, B. A., Firing, E., and Joyce, T.: Chapter 3.1 Shipboard observations during WOCE, *Int. Geophys.*, 77, 99–122, [https://doi.org/10.1016/S0074-6142\(01\)80114-5](https://doi.org/10.1016/S0074-6142(01)80114-5), 2001.
- King, M. D., Howat, I. M., Jeong, S., Noh, M. J., Wouters, B., Noël, B., and van den Broeke, M. R.: Seasonal to decadal variability in ice discharge from the Greenland Ice Sheet, *The Cryosphere*, 12, 3813–3825, <https://doi.org/10.5194/tc-12-3813-2018>, 2018.
- King, M. D., Howat, I. M., Candela, S. G., Noh, M. J., Jeong, S., Noël, B. P. Y., van den Broeke, M. R., Wouters, B., and Negrete, A.: Dynamic ice loss from the Greenland Ice Sheet driven by sustained glacier retreat, *Commun. Earth Environ.*, 1, 1, <https://doi.org/10.1038/s43247-020-0001-2>, 2020.
- Kirchengast, G., Ladstädter, F., Steiner, A. K., Gorfer, M., Lippl, F., and Angerer, B.: Climate trends and variability in atmosphere heat content and atmosphere-ocean heat exchanges: space geodesy is key, *IUGG General Assembly 2019 Pres.*, available at: https://www.czech-in.org/cmPortalV15/CM_W3_Searchable/iugg19/#!sessiondetails/0000119801_0 (last access: 7 August 2020), 2019.
- Knutti, R. and Rugenstein, M. A. A.: Feedbacks, climate sensitivity and the limits of linear models, *Philos. T. R. Soc. A*, 373, 20150146, <https://doi.org/10.1098/rsta.2015.0146>, 2015.
- Kobayashi, S., Ota, Y., Harada, Y., Ebata, A., Morioka, M., Onoda, H., Onogi, K., Kamahori, H., Kobayashi, C., Endo, H., Miyaoka, K., and Takahashi, K.: The JRA-55 Reanalysis: General Specifications and Basic Characteristics, *J. Meteorol. Soc. Jpn. Ser. II*, 93, 5–48, <https://doi.org/10.2151/jmsj.2015-001>, 2015.
- Kuhlbrodt, T. and Gregory, J. M.: Ocean heat uptake and its consequences for the magnitude of sea level rise and climate change, *Geophys. Res. Lett.*, 39, L18608, <https://doi.org/10.1029/2012GL052952>, 2012.

- Labe, Z., Magnusdottir, G., and Stern, H.: Variability of Arctic Sea Ice Thickness Using PIOMAS and the CESM Large Ensemble, *J. Climate*, 31, 3233–3247, <https://doi.org/10.1175/JCLI-D-17-0436.1>, 2018.
- Lachenbruch, A. H. and Marshall, B. V.: Changing Climate: Geothermal Evidence from Permafrost in the Alaskan Arctic, *Science*, 234, 689–696, 1986.
- Ladstädter, F., Steiner, A. K., Schwärz, M., and Kirchengast, G.: Climate intercomparison of GPS radio occultation, RS90/92 radiosondes and GRUAN from 2002 to 2013, *Atmos. Meas. Tech.*, 8, 1819–1834, <https://doi.org/10.5194/amt-8-1819-2015>, 2015.
- Lane, A. C.: Geotherms of Lake Superior Copper Country, *GSA Bulletin*, 34, 703–720, <https://doi.org/10.1130/GSAB-34-703>, 1923.
- Laxon, S. W., Giles, K. A., Ridout, A. L., Wingham, D. J., Willatt, R., Cullen, R., Kwok, R., Schweiger, A., Zhang, J., Haas, C., Hendricks, S., Krishfield, R., Kurtz, N., Farrell, S., and Davidson, M.: CryoSat-2 estimates of Arctic sea ice thickness and volume, *Geophys. Res. Lett.*, 40, 732–737, <https://doi.org/10.1002/grl.50193>, 2013.
- Leifeld, J., Wüst-Galley, C., and Page, S.: Intact and managed peatland soils as a source and sink of GHGs from 1850 to 2100, *Nat. Clim. Change*, 9, 945–947, <https://doi.org/10.1038/s41558-019-0615-5>, 2019.
- Lembo, V., Folini, D., Wild, M., and Lionello, P.: Inter-hemispheric differences in energy budgets and cross-equatorial transport anomalies during the 20th century, *Clim. Dynam.*, 53, 115–135, <https://doi.org/10.1007/s00382-018-4572-x>, 2019.
- Lenton, T., Rockström, J., Gaffney, O., Rahmstorf, S., Richardson, K., Steffen, W., and Schellnhuber, H.: Climate tipping points – too risky to bet against, *Nature*, 575, 592–595, <https://doi.org/10.1038/d41586-019-03595-0>, 2019.
- Lenton, T. M.: Early warning of climate tipping points, *Nat. Clim. Change*, 1, 201–209, <https://doi.org/10.1038/nclimate1143>, 2011.
- Lenton, T. M., Held, H., Kriegler, E., Hall, J. W., Lucht, W., Rahmstorf, S., and Schellnhuber, H. J.: Tipping elements in the Earth's climate system, *P. Natl. Acad. Sci. USA*, 105, 1786–1793, <https://doi.org/10.1073/pnas.0705414105>, 2008.
- Levitus, S., Antonov, J. I., Boyer, T. P., Baranova, O. K., Garcia, H. E., Locarnini, R. A., Mishonov, A. V., Reagan, J. R., Seidov, D., Yarosh, E. S., and Zweng, M. M.: World ocean heat content and thermosteric sea level change (0–2000 m), 1955–2010, *Geophys. Res. Lett.*, 39, <https://doi.org/10.1029/2012GL051106>, 2012.
- Ligtenberg, S. R. M., Kuipers Munneke, P., Noël, B. P. Y., and van den Broeke, M. R.: Brief communication: Improved simulation of the present-day Greenland firn layer (1960–2016), *The Cryosphere*, 12, 1643–1649, <https://doi.org/10.5194/tc-12-1643-2018>, 2018.
- Llovel, W., Willis, J. K., Landerer, F. W., and Fukumori, I.: Deep-ocean contribution to sea level and energy budget not detectable over the past decade, *Nat. Clim. Change*, 4, 1031–1035, <https://doi.org/10.1038/nclimate2387>, 2014.
- Loeb, N. G., Lyman, J. M., Johnson, G. C., Allan, R. P., Doelling, D. R., Wong, T., Soden, B. J., and Stephens, G. L.: Observed changes in top-of-the-atmosphere radiation and upper-ocean heating consistent within uncertainty, *Nat. Geosci.*, 5, 110–113, <https://doi.org/10.1038/ngeo1375>, 2012.
- Loeb, N. G., Thorsen, T. J., Norris, J. R., Wang, H., and Su, W.: Changes in Earth's Energy Budget during and after the “Pause” in Global Warming: An Observational Perspective, *Climate*, 6, <https://doi.org/10.3390/cli6030062>, 2018.
- Lyman, J. M. and Johnson, G. C.: Estimating Global Ocean Heat Content Changes in the Upper 1800 m since 1950 and the Influence of Climatology Choice, *J. Climate*, 27, 1945–1957, <https://doi.org/10.1175/JCLI-D-12-00752.1>, 2014.
- MacDougall, A. H., Avis, C. A., and Weaver, A. J.: Significant contribution to climate warming from the permafrost carbon feedback, *Nat. Geosci.*, 5, 719–721, <https://doi.org/10.1038/ngeo1573>, 2012.
- MacDougall, A. H., Beltrami, H., González-Rouco, J. F., Stevens, M. B., and Bournon, E.: Comparison of observed and general circulation model derived continental subsurface heat flux in the Northern Hemisphere, *J. Geophys. Res.-Atmos.*, 115, D12109, <https://doi.org/10.1029/2009JD013170>, 2010.
- MacDougall, A. H., González-Rouco, J. F., Stevens, M. B., and Beltrami, H.: Quantification of subsurface heat storage in a GCM simulation, *Geophys. Res. Lett.*, 35, L13702, <https://doi.org/10.1029/2008GL034639>, 2008.
- Mankoff, K. D., Colgan, W., Solgaard, A., Karlsson, N. B., Ahlström, A. P., van As, D., Box, J. E., Khan, S. A., Kjeldsen, K. K., Mougnot, J., and Fausto, R. S.: Greenland Ice Sheet solid ice discharge from 1986 through 2017, *Earth Syst. Sci. Data*, 11, 769–786, <https://doi.org/10.5194/essd-11-769-2019>, 2019.
- Marshall, J., Scott, J. R., Armour, K. C., Campin, J.-M., Kelley, M., and Romanou, A.: The ocean's role in the transient response of climate to abrupt greenhouse gas forcing, *Clim. Dynam.*, 44, 2287–2299, <https://doi.org/10.1007/s00382-014-2308-0>, 2015.
- Marvel, K., Pincus, R., Schmidt, G. A., and Miller, R. L.: Internal Variability and Disequilibrium Confound Estimates of Climate Sensitivity From Observations, *Geophys. Res. Lett.*, 45, 1595–1601, <https://doi.org/10.1002/2017GL076468>, 2018.
- Marzeion, B., Leclercq, P. W., Cogley, J. G., and Jarosch, A. H.: Brief Communication: Global reconstructions of glacier mass change during the 20th century are consistent, *The Cryosphere*, 9, 2399–2404, <https://doi.org/10.5194/tc-9-2399-2015>, 2015.
- Matthews, T. K. R., Wilby, R. L., and Murphy, C.: Communicating the deadly consequences of global warming for human heat stress, *P. Natl. Acad. Sci. USA*, 114, 3861, <https://doi.org/10.1073/pnas.1617526114>, 2017.
- Mayer, M., Trenberth, K. E., Haimberger, L., and Fasullo, J. T.: The Response of Tropical Atmospheric Energy Budgets to ENSO, *J. Climate*, 26, 4710–4724, <https://doi.org/10.1175/JCLI-D-12-00681.1>, 2013.
- Mayer, M., Haimberger, L., and Balmaseda, M. A.: On the Energy Exchange between Tropical Ocean Basins Related to ENSO, *J. Climate*, 27, 6393–6403, <https://doi.org/10.1175/JCLI-D-14-00123.1>, 2014.
- Mayer, M., Fasullo, J. T., Trenberth, K. E., and Haimberger, L.: ENSO-driven energy budget perturbations in observations and CMIP models, *Clim. Dynam.*, 47, 4009–4029, <https://doi.org/10.1007/s00382-016-3057-z>, 2016.
- Mayer, M., Haimberger, L., Edwards, J. M., and Hyder, P.: Toward Consistent Diagnostics of the Coupled Atmosphere and Ocean Energy Budgets, *J. Climate*, 30, 9225–9246, <https://doi.org/10.1175/JCLI-D-17-0137.1>, 2017.

- Mayer, M., Tietsche, S., Haimberger, L., Tsubouchi, T., Mayer, J., and Zuo, H.: An Improved Estimate of the Coupled Arctic Energy Budget, *J. Climate*, 32, 7915–7934, <https://doi.org/10.1175/JCLI-D-19-0233.1>, 2019.
- McPherson, M., García-García, A., Cuesta-Valero Francisco, J., Beltrami, H., Hansen-Ketchum, P., MacDougall, D., and Ogden Nicholas, H.: Expansion of the Lyme Disease Vector *Ixodes Scapularis* in Canada Inferred from CMIP5 Climate Projections, *Environ. Health Persp.*, 125, 057008, <https://doi.org/10.1289/EHP57>, 2017.
- Mears, C. A. and Wentz, F. J.: Construction of the Remote Sensing Systems V3.2 Atmospheric Temperature Records from the MSU and AMSU Microwave Sounders, *J. Atmos. Ocean. Techn.*, 26, 1040–1056, <https://doi.org/10.1175/2008JTECHA1176.1>, 2009a.
- Mears, C. A. and Wentz, F. J.: Construction of the RSS V3.2 Lower-Tropospheric Temperature Dataset from the MSU and AMSU Microwave Sounders, *J. Atmos. Ocean. Techn.*, 26, 1493–1509, <https://doi.org/10.1175/2009JTECHA1237.1>, 2009b.
- Mears, C. A. and Wentz, F. J.: A Satellite-Derived Lower-Tropospheric Atmospheric Temperature Dataset Using an Optimized Adjustment for Diurnal Effects, *J. Climate*, 30, 7695–7718, <https://doi.org/10.1175/JCLI-D-16-0768.1>, 2017.
- Melo-Aguilar, C., González-Rouco, J. F., García-Bustamante, E., Navarro-Montesinos, J., and Steinert, N.: Influence of radiative forcing factors on ground–air temperature coupling during the last millennium: implications for borehole climatology, *Clim. Past*, 14, 1583–1606, <https://doi.org/10.5194/cp-14-1583-2018>, 2018.
- Meyssignac, B., Boyer, T., Zhao, Z., Hakuba, M. Z., Landerer, F. W., Stammer, D., Köhl, A., Kato, S., L'Ecuyer, T., Ablain, M., Abraham, J. P., Blazquez, A., Cazenave, A., Church, J. A., Cowley, R., Cheng, L., Domingues, C. M., Giglio, D., Gouretski, V., and Zilberman, N.: Measuring Global Ocean Heat Content to Estimate the Earth Energy Imbalance, *Front. Mar. Sci.*, 6, <https://doi.org/10.3389/fmars.2019.00432>, 2019.
- Mouginot, J., Rignot, E., Björk, A. A., van den Broeke, M., Milani, R., Morlighem, M., Noël, B., Scheuchl, B., and Wood, M.: Forty-six years of Greenland Ice Sheet mass balance from 1972 to 2018, *P. Natl. Acad. Sci. USA*, 116, 9239, <https://doi.org/10.1073/pnas.1904242116>, 2019.
- Myhre, G., Shindell, D., Bréon, F.-M., Collins, W., Fuglestedt, J., Huang, J., Koch, D., Lamarque, J.-F., Lee, D., Mendoza, B., Nakajima, T., Robock, A., Stephens, G., Takemura, T., and Zhang, H.: Anthropogenic and natural radiative forcing. In *Climate Change 2013 the Physical Science Basis: Working Group I Contribution to the Fifth Assessment Report of the Intergovernmental Panel on Climate Change*, 9781107057, 659–740, <https://doi.org/10.1017/CBO9781107415324.018>, 2013.
- Nauels, A., Meinshausen, M., Mengel, M., Lorbacher, K., and Wigley, T. M. L.: Synthesizing long-term sea level rise projections – the MAGICC sea level model v2.0, *Geosci. Model Dev.*, 10, 2495–2524, <https://doi.org/10.5194/gmd-10-2495-2017>, 2017.
- Noël, B., van de Berg, W. J., van Wessem, J. M., van Meijgaard, E., van As, D., Lenaerts, J. T. M., Lhermitte, S., Kuipers Munneke, P., Smeets, C. J. P. P., van Uft, L. H., van de Wal, R. S. W., and van den Broeke, M. R.: Modelling the climate and surface mass balance of polar ice sheets using RACMO2 – Part 1: Greenland (1958–2016), *The Cryosphere*, 12, 811–831, <https://doi.org/10.5194/tc-12-811-2018>, 2018.
- Palmer, M. D. and McNeall, D. J.: Internal variability of Earth's energy budget simulated by CMIP5 climate models, *Environ. Res. Lett.*, 9, 034016, <https://doi.org/10.1088/1748-9326/9/3/034016>, 2014.
- Palmer, M. D., Roberts, C. D., Balmaseda, M., Chang, Y.-S., Chepurin, G., Ferry, N., Fujii, Y., Good, S. A., Guinehut, S., Haines, K., Hernandez, F., Köhl, A., Lee, T., Martin, M. J., Masina, S., Masuda, S., Peterson, K. A., Storto, A., Toyoda, T., and Xue, Y.: Ocean heat content variability and change in an ensemble of ocean reanalyses, *Clim. Dynam.*, 49, 909–930, <https://doi.org/10.1007/s00382-015-2801-0>, 2017.
- Palmer, M. D., Durack, P. J., Chidichimo, M. P., Church, J. A., Cravatte, S., Hill, K., Johannessen, J. A., Karstensen, J., Lee, T., Legler, D., Mazloff, M., Oka, E., Purkey, S., Rabe, B., Sallée, J.-B., Sloyan, B. M., Speich, S., von Schuckmann, K., Willis, J., and Wijffels, S.: Adequacy of the Ocean Observation System for Quantifying Regional Heat and Freshwater Storage and Change, *Front. Mar. Sci.*, 6, p. 416, 2019.
- Palmer, M. D., Harris, G. R., and Gregory, J. M.: Extending CMIP5 projections of global mean temperature change and sea level rise due to thermal expansion using a physically-based emulator, *Environ. Res. Lett.*, 13, 084003, <https://doi.org/10.1088/1748-9326/aad2e4>, 2018.
- Parkes, D. and Marzeion, B.: Twentieth-century contribution to sea-level rise from uncharted glaciers, *Nature*, 563, 551–554, <https://doi.org/10.1038/s41586-018-0687-9>, 2018.
- Parkinson, C. L.: A 40-y record reveals gradual Antarctic sea ice increases followed by decreases at rates far exceeding the rates seen in the Arctic, *P. Natl. Acad. Sci. USA*, 116, 14414, <https://doi.org/10.1073/pnas.1906556116>, 2019.
- Peixoto, J. P. and Oort, A. H.: *Physics of climate*, New York, NY (United States), American Institute of Physics, available at: <https://www.osti.gov/servlets/purl/7287064> (last access: 7 August 2020), 1992.
- Pickler, C., Gurza Fausto, E., Beltrami, H., Mareschal, J.-C., Suárez, F., Chacon-Oecklers, A., Blin, N., Cortés Calderón, M. T., Montenegro, A., Harris, R., and Tassara, A.: Recent climate variations in Chile: constraints from borehole temperature profiles, *Clim. Past*, 14, 559–575, <https://doi.org/10.5194/cp-14-559-2018>, 2018.
- Pollack, H. N. and Smerdon, J. E.: Borehole climate reconstructions: Spatial structure and hemispheric averages, *J. Geophys. Res.-Atmos.*, 109, D11106, <https://doi.org/10.1029/2003JD004163>, 2004.
- Polyakov, I. V., Pnyushkov, A. V., Alkire, M. B., Ashik, I. M., Baumann, T. M., Carmack, E. C., Goszczko, I., Guthrie, J., Ivanov, V. V., Kanzow, T., Krishfield, R., Kwok, R., Sundfjord, A., Morison, J., Rember, R., and Yulin, A.: Greater role for Atlantic inflows on sea-ice loss in the Eurasian Basin of the Arctic Ocean, *Science*, 356, 285–291, <https://doi.org/10.1126/science.aai8204>, 2017.
- Pritchard, H. D., Ligtenberg, S. R. M., Fricker, H. A., Vaughan, D. G., van den Broeke, M. R., and Padman, L.: Antarctic ice-sheet loss driven by basal melting of ice shelves, *Nature*, 484, 502–505, <https://doi.org/10.1038/nature10968>, 2012.
- Purkey, S. G. and Johnson, G. C.: Warming of Global Abyssal and Deep Southern Ocean Waters between the 1990s and 2000s: Contributions to Global Heat and Sea Level Rise Budgets, *J. Cli-*

- mate, 23, 6336–6351, <https://doi.org/10.1175/2010JCLI3682.1>, 2010.
- Ramírez, F., Afán, I., Davis, L. S., and Chiaradia, A.: Climate impacts on global hot spots of marine biodiversity, *Science Advances*, 3, e1601198, <https://doi.org/10.1126/sciadv.1601198>, 2017.
- Rhein, M., Rintoul, S. R., Aoki, S., Campos, E., Chambers, D., Feely, R. A., Gulev, S., Johnson, G. C., Josey, S. A., Kostianoy, A., Mauritzen, C., Roemmich, D., Talley, L. D., and Wang, F.: Observations: Ocean, in: *Climate Change 2013: The Physical Science Basis, Contribution of Working Group I to the Fifth Assessment Report of the Intergovernmental Panel on Climate Change*, edited by: Stocker, T. F., Qin, D., Plattner, G.-K., Tignor, M., Allen, S. K., Boschung, J., Nauels, A., Xia, Y., Bex, V., and Midgley, P. M., Cambridge University Press, Cambridge, United Kingdom and New York, NY, USA, 255–316, <https://doi.org/10.1017/CBO9781107415324.010>, 2013.
- Rhein, M., Steinfeldt, R., Huhn, O., Sültenfuß, J., and Breckenfelder, T.: Greenland Submarine Melt Water Observed in the Labrador and Irminger Sea, *Geophys. Res. Lett.*, 45, 510–570, <https://doi.org/10.1029/2018GL079110>, 2018.
- Richter-Menge, J., Druckenmiller, M. L., and Jeffries, M. (Eds.): *Arctic Report Card*, 2019, available at: <https://www.arctic.noaa.gov/Report-Card> (last access: 7 August 2020), 2019.
- Rignot, E., Mouginot, J., Scheuchl, B., van den Broeke, M., van Wessem, M. J., and Morlighem, M.: Four decades of Antarctic Ice Sheet mass balance from 1979–2017, *P. Natl. Acad. Sci. USA*, 116, 1095, <https://doi.org/10.1073/pnas.1812883116>, 2019.
- Riser, S. C., Freeland, H. J., Roemmich, D., Wijffels, S., Troisi, A., Belbéoch, M., Gilbert, D., Xu, J., Pouliquen, S., Thresher, A., Le Traon, P.-Y., Maze, G., Klein, B., Ravichandran, M., Grant, F., Poulain, P.-M., Suga, T., Lim, B., Sterl, A., and Jayne, S. R.: Fifteen years of ocean observations with the global Argo array, *Nat. Clim. Change*, 6, 145–153, <https://doi.org/10.1038/nclimate2872>, 2016.
- Roemmich, D. and Gilson, J.: The 2004–2008 mean and annual cycle of temperature, salinity, and steric height in the global ocean from the Argo Program, *Prog. Oceanogr.*, 82, 81–100, <https://doi.org/10.1016/j.pocean.2009.03.004>, 2009.
- Roy, S., Harris, R. N., Rao, R. U. M., and Chapman, D. S.: Climate change in India inferred from geothermal observations, *J. Geophys. Res.-Earth*, 107, ETG 5-1–ETG 5-16, <https://doi.org/10.1029/2001JB000536>, 2002.
- Santer, B. D., Solomon, S., Wentz, F. J., Fu, Q., Po-Chedley, S., Mears, C., Painter, J. F., and Bonfils, C.: Tropospheric Warming Over The Past Two Decades, *Sci. Rep.*, 7, 2336, <https://doi.org/10.1038/s41598-017-02520-7>, 2017.
- Santer, B. D., Po-Chedley, S., Zelinka, M. D., Cvijanovic, I., Bonfils, C., Durack, P. J., Fu, Q., Kiehl, J., Mears, C., Painter, J., Pallotta, G., Solomon, S., Wentz, F. J., and Zou, C.-Z.: Human influence on the seasonal cycle of tropospheric temperature, *Science*, 361, eaas8806, <https://doi.org/10.1126/science.aas8806>, 2018.
- Schweiger, A., Lindsay, R., Zhang, J., Steele, M., Stern, H., and Kwok, R.: Uncertainty in modeled Arctic sea ice volume, *J. Geophys. Res.-Oceans*, 116, C00D06, <https://doi.org/10.1029/2011JC007084>, 2011.
- Schweiger, A. J., Wood, K. R., and Zhang, J.: Arctic Sea Ice Volume Variability over 1901–2010: A Model-Based Reconstruction, *J. Climate*, 32, 4731–4752, <https://doi.org/10.1175/JCLI-D-19-0008.1>, 2019.
- Seneviratne, S., Lüthi, D., Litschi, M., and Schär, C.: Land-atmosphere coupling and climate change in Europe, *Nature*, 443, 205–209, <https://doi.org/10.1038/nature05095>, 2006.
- Seneviratne, S., Donat, M., Mueller, B., and Alexander, L.: No pause in the increase of hot temperature extremes, *Nat. Clim. Change*, 4, 161–163, <https://doi.org/10.1038/nclimate2145>, 2014.
- Seneviratne, S. I., Corti, T., Davin, E. L., Hirschi, M., Jaeger, E. B., Lehner, I., Orlowsky, B., and Teuling, A. J.: Investigating soil moisture–climate interactions in a changing climate: A review, *Earth-Sci. Rev.*, 99, 125–161, <https://doi.org/10.1016/j.earscirev.2010.02.004>, 2010.
- Serreze, M. C. and Barry, R. G.: Processes and impacts of Arctic amplification: A research synthesis, *Global Planet. Change*, 77, 85–96, <https://doi.org/10.1016/J.GLOPLACHA.2011.03.004>, 2011.
- Shepherd, A., Fricker, H. A., and Farrell, S. L.: Trends and connections across the Antarctic cryosphere, *Nature*, 558, 223–232, <https://doi.org/10.1038/s41586-018-0171-6>, 2018a.
- Shepherd, A., Ivins, E. R., Rignot, E., Smith, B., Van den Broeke, M. R., Velicogna, I., Whitehouse, P. L., Briggs, K. H., Joughin, I., Krinner, G., Nowicki, S., Payne, A. J., Scambos, T. A., Schlegel, N., A. G., Agosta, C., Ahlström, A. P., Babonis, G., Barletta, V. R., Blazquez, A., Bonin, J., Csatho, B., Cullather, R. I., Felikson, D., Fettweis, X., Forsberg, R., Gallée, H., Gardner, A. S., Gilbert, L., Groh, A., Gunter, B., Hanna, E., Harig, C., Helm, V., Horvath, A., Horwath, M., Khan, S., Kjeldsen, K. K., Konrad, H., Langen, P., Lecavalier, B., Loomis, B., Luthcke, S. B., McMillan, M., Melini, D., Mernild, S., Mohajerani, Y., Moore, P., Mouginot, J., Moyano, G., Muir, A., Nagler, T., Nield, G., Nilsson, J., Noël, B. P. Y., Otsuka, I., Pattle, M. E., Peltier, W. R., Pie, N., Rietbroek, R., Rott, H., Sandberg Sørensen, L., Sasgen, I., Save, H., Scheuchl, B., Schrama, E. J. O., Schröder, L., Seo, K.-W., Simonsen, S., Slater, T., Spada, G., Sutterly, T. C., Talpe, M., Tarasov, L., Van de Berg, W. J., Van der Wal, W., Van Wessem, J. M., Vishwakarma, B. D., Wiese, D., and Wouters, B.: Mass balance of the Antarctic Ice Sheet from 1992 to 2017, *Nature*, 558, 219–222, <https://doi.org/10.1038/s41586-018-0179-y>, 2018b.
- Shepherd, A., Ivins, E., Rignot, E., Smith, B., van den Broeke, M., Velicogna, I., Whitehouse, P., Briggs, K., Joughin, I., Krinner, G., Nowicki, S., Payne, T., Scambos, T., Schlegel, N., Geruo, A., Agosta, C., Ahlström, A., Babonis, G., Barletta, V. R., and IMBIE team: Mass balance of the Greenland Ice Sheet from 1992 to 2018, *Nature*, 579, 233–239, <https://doi.org/10.1038/s41586-019-1855-2>, 2019.
- Sherwood, S. C. and Huber, M.: An adaptability limit to climate change due to heat stress, *P. Natl. Acad. Sci. USA*, 107, 9552, <https://doi.org/10.1073/pnas.0913352107>, 2010.
- Shi, J.-R., Xie, S.-P., and Talley, L. D.: Evolving Relative Importance of the Southern Ocean and North Atlantic in Anthropogenic Ocean Heat Uptake, *J. Climate*, 31, 7459–7479, <https://doi.org/10.1175/JCLI-D-18-0170.1>, 2018.
- Smerdon, J. E. and Stieglitz, M.: Simulating heat transport of harmonic temperature signals in the Earth’s shallow subsurface: Lower-boundary sensitivities, *Geophys. Res. Lett.*, 33, L14402, <https://doi.org/10.1029/2006GL026816>, 2006.

- Steiner, A., Ladstädter, F., Randel, W. J., Maycock, A. C., Claud, C., Fu, Q., Gleisner, H., Haimberger, L., Ho, S.-P., Keckhut, P., Leblanc, T., Mears, C., Polvani, L., Santer, B., Schmidt, T., Sofieva, V., Wing, R., and Zou, C.-Z.: Observed temperature changes in the troposphere and stratosphere from 1979 to 2018, *J. Climate*, 33, 8165–8194, <https://doi.org/10.1175/JCLI-D-19-0998.1>, 2020.
- Stevens, C. W.: Subsurface investigation of shallow-water permafrost located within the near-shore zone of the Mackenzie Delta, Northwest Territories, Canada, University of Calgary, 2007.
- Stevens, M. B., González-Rouco, J. F., and Beltrami, H.: North American climate of the last millennium: Underground temperatures and model comparison, *J. Geophys. Res.-Earth*, 113, F01008, <https://doi.org/10.1029/2006JF000705>, 2008.
- Stieglitz, M. and Smerdon, J. E.: Characterizing Land–Atmosphere Coupling and the Implications for Subsurface Thermodynamics, *J. Climate*, 20, 21–37, <https://doi.org/10.1175/JCLI3982.1>, 2007.
- Storto, A., Masina, S., Simoncelli, S., Iovino, D., Cipollone, A., Drevillon, M., Drillet, Y., Schuckman, K., Parent, L., Garric, G., Greiner, E., Desportes, C., Zuo, H., Balmaseda, M., and Peterson, K.: The added value of the multi-system spread information for ocean heat content and steric sea level investigations in the CMEMS GREP ensemble reanalysis product, *Clim. Dynam.*, 53, 287–312, <https://doi.org/10.1007/s00382-018-4585-5>, 2018.
- Storto, A., Alvera-Azcárate, A., Balmaseda, M. A., Barth, A., Chevallier, M., Counillon, F., Domingues, C. M., Drevillon, M., Drillet, Y., Forget, G., Garric, G., Haines, K., Hernandez, F., Iovino, D., Jackson, L. C., Lellouche, J.-M., Masina, S., Mayer, M., Oke, P. R., and Zuo, H.: Ocean Reanalyses: Recent Advances and Unsolved Challenges, *Front. Mar. Sci.*, 6, 418, <https://doi.org/10.3389/fmars.2019.00418>, 2019.
- Straneo, F. and Cenedese, C.: The Dynamics of Greenland’s Glacial Fjords and Their Role in Climate, *Annu. Rev. Mar. Sci.*, 7, 89–112, <https://doi.org/10.1146/annurev-marine-010213-135133>, 2015.
- Straneo, F., Adusumilli, S., Slater, D., Timmermanns, M., Marzeion, B., and Schweiger, A.: Inventory of Earth’s ice loss and associated energy uptake from 1979 to 2017, *Geophys. Res. Lett.*, in review, 2020.
- Suman, A., Dyer, F., and White, D.: Late Holocene temperature variability in Tasmania inferred from borehole temperature data, *Clim. Past*, 13, 559–572, <https://doi.org/10.5194/cp-13-559-2017>, 2017.
- Trenberth, K. E.: The ocean is warming, isn’t it?, *Nature*, 465, p. 304, <https://doi.org/10.1038/465304a>, 2010.
- Trenberth, K. E.: Understanding climate change through Earth’s energy flows, *J. Roy. Soc. New Zeal.*, 50, 331–347, <https://doi.org/10.1080/03036758.2020.1741404>, 2020.
- Trenberth, K. E. and Fasullo, J. T.: Tracking Earth’s Energy, *Science*, 328, 316–317, <https://doi.org/10.1126/science.1187272>, 2010.
- Trenberth, K. E. and Fasullo, J. T.: Applications of an Updated Atmospheric Energetics Formulation, *J. Climate*, 31, 6263–6279, <https://doi.org/10.1175/JCLI-D-17-0838.1>, 2018.
- Trenberth, K. E., Fasullo, J. T., and Shepherd, T. G.: Attribution of climate extreme events, *Nat. Clim. Change*, 5, 725–730, <https://doi.org/10.1038/nclimate2657>, 2015.
- Trenberth, K. E., Fasullo, J. T., and Balmaseda, M. A.: Earth’s Energy Imbalance, *J. Climate*, 27, 3129–3144, <https://doi.org/10.1175/JCLI-D-13-00294.1>, 2014.
- Trenberth, K. E., Fasullo, J. T., von Schuckmann, K., and Cheng, L.: Insights into Earth’s Energy Imbalance from Multiple Sources, *J. Climate*, 29, 7495–7505, <https://doi.org/10.1175/JCLI-D-16-0339.1>, 2016.
- Trenberth, K. E., Cheng, L., Jacobs, P., Zhang, Y., and Fasullo, J.: Hurricane Harvey Links to Ocean Heat Content and Climate Change Adaptation. *Earth’s Future*, 6, 730–744, <https://doi.org/10.1029/2018EF000825>, 2018.
- UN: United Nations Framework Convention on Climate Change, FCCC/INFORMAL/84 GE.05-62220 (E) 200705, available at: <https://unfccc.int/resource/docs/convkp/conveng.pdf> (last access: 7 August 2020), 1992.
- UN: The Paris Agreement, available at: https://unfccc.int/sites/default/files/english_paris_agreement.pdf (last access: 7 August 2020), 2015.
- UNGA: The future we want, Resolution adopted by the General Assembly on 27 July 2012, A/RES/66/288, 2012.
- UNGA: Transforming our world: the 2030 Agenda for Sustainable Development, Resolution adopted by the General Assembly on 25 September 2015, A/RES/70/1, 2015.
- Vanderkelen, I., van Lipzig, N. P. M., Lawrence, D. M., Drovers, B., Golub, M., Gosling, S. N., Janssen, A. B. G., Marcé, R., Schmied, H. M., Perroud, M., Pierson, D., Pokhrel, Y., Satoh, Y., Schewe, J., Seneviratne, S. I., Stepanenko, V. M., Tan, Z., Woolway, R. I., and Thiery, W.: Global Heat Uptake by Inland Waters, *Geophys. Res. Lett.*, 47, e2020GL087867, <https://doi.org/10.1029/2020GL087867>, 2020.
- Vasseur, G., Bernard, P., Van de Meulebrouck, J., Kast, Y., and Jolivet, J.: Holocene paleotemperatures deduced from geothermal measurements, *Palaeogeogr. Palaeoclimatol.*, 43, 237–259, [https://doi.org/10.1016/0031-0182\(83\)90013-5](https://doi.org/10.1016/0031-0182(83)90013-5), 1983.
- Verdoya, M., Chiozzi, P., and Pasquale, V.: Thermal log analysis for recognition of ground surface temperature change and water movements, *Clim. Past*, 3, 315–324, <https://doi.org/10.5194/cp-3-315-2007>, 2007.
- von Schuckmann, K. and Le Traon, P.-Y.: How well can we derive Global Ocean Indicators from Argo data?, *Ocean Sci.*, 7, 783–791, <https://doi.org/10.5194/os-7-783-2011>, 2011.
- von Schuckmann, K., Sallée, J.-B., Chambers, D., Le Traon, P.-Y., Cabanes, C., Gaillard, F., Speich, S., and Hamon, M.: Consistency of the current global ocean observing systems from an Argo perspective, *Ocean Sci.*, 10, 547–557, <https://doi.org/10.5194/os-10-547-2014>, 2014.
- von Schuckmann, K., Palmer, M. D., Trenberth, K. E., Cazenave, A., Chambers, D., Champollion, N., Hansen, J., Josey, S. A., Loeb, N., Mathieu, P.-P., Meyssignac, B., and Wild, M.: An imperative to monitor Earth’s energy imbalance, *Nat. Clim. Change*, 6, 138–144, <https://doi.org/10.1038/nclimate2876>, 2016.
- von Schuckmann, K., Le Traon, P.-Y., Alvarez-Fanjul, E., Axel, L., Balmaseda, M., Breivik, L.-A., Brewin, R. J. W., Bricaud, C., Drevillon, M., Drillet, Y., Dubois, C., Embury, O., Etienne, H., Sotillo, M. G., Garric, G., Gasparin, F., Gutknecht, E., Guinehut, S., Hernandez, F., and Verbrugge, N.: The Copernicus Marine Environment Monitoring Service

- Ocean State Report, *J. Oper. Oceanogr.*, 9(sup2), s235–s320, <https://doi.org/10.1080/1755876X.2016.1273446>, 2017.
- von Schuckmann, K., Le Traon, P.-Y., Smith, N., Pascual, A., Brasseur, P., Fennel, K., Djavidnia, S., Aaboe, S., Fanjul, E. A., Autret, E., Axell, L., Aznar, R., Benincasa, M., Bentamy, A., Boberg, F., Bourdallé-Badie, R., Nardelli, B. B., Brando, V. E., Bricaud, C., and Zuo, H.: Copernicus Marine Service Ocean State Report, *J. Oper. Oceanogr.*, 11(sup1), S1–S142, <https://doi.org/10.1080/1755876X.2018.1489208>, 2018.
- von Schuckmann, K., Cheng, L., Palmer, M. D., Hansen, J., Tasone, C., Aich, V., Adusumilli, S., Beltrami, H., Boyer, T., Cuesta-Valero, F. J., Desbruyères, D., Domingues, C., García-García, A., Gentile, P., Gilson, J., Gorfer, M., Haimberger, L., Ishii, M., Johnson, G. C., Killick, R., King, B. A., Kirchengast, G., Kolodziejczyk, N., Lyman, J., Marzeion, B., Mayer, M., Monier, M., Monselesan, D. P., Purkey, S., Roemmich, D., Schweiger, A., Seneviratne, S. I., Shepherd, A., Slater, D. A., Steiner, A. K., Straneo, F., Timmermanns, M.-L., and Wijffels, S. E.: Heat stored in the Earth system: Where does the energy go? Version 2, World Data Center for Climate (WDCC) at DKRZ, https://doi.org/10.26050/WDCC/GCOS_EHI_EXP_v2, 2020.
- Wang, G., Cheng, L., Abraham, J., and Li, C.: Consensuses and discrepancies of basin-scale ocean heat content changes in different ocean analyses, *Clim. Dynam.*, 50, 2471–2487, <https://doi.org/10.1007/s00382-017-3751-5>, 2018.
- Wang, X., Key, J., Kwok, R., and Zhang, J.: Comparison of Arctic Sea Ice Thickness from Satellites, Aircraft, and PIOMAS Data, *Remote Sensing*, 8, 1–17, <https://doi.org/10.3390/rs8090713>, 2016.
- Watts, N., Amann, M., Arnell, N., Ayeb-Karlsson, S., Belesova, K., Boykoff, M., Byass, P., Cai, W., Campbell-Lendrum, D., Capstick, S., Chambers, J., Dalin, C., Daly, M., Dasandi, N., Davies, M., Drummond, P., Dubrow, R., Ebi, K. L., Eckelman, M., and Montgomery, H.: The 2019 report of The Lancet Countdown on health and climate change: ensuring that the health of a child born today is not defined by a changing climate, *The Lancet*, 394, 1836–1878, [https://doi.org/10.1016/S0140-6736\(19\)32596-6](https://doi.org/10.1016/S0140-6736(19)32596-6), 2019.
- WCRP Global Sea Level Budget Group: Global sea-level budget 1993–present, *Earth Syst. Sci. Data*, 10, 1551–1590, <https://doi.org/10.5194/essd-10-1551-2018>, 2018.
- Wijffels, S., Roemmich, D., Monselesan, D., Church, J., and Gilson, J.: Ocean temperatures chronicle the ongoing warming of Earth, *Nat. Clim. Change*, 6, 116–118, <https://doi.org/10.1038/nclimate2924>, 2016.
- Wild, M.: The global energy balance as represented in CMIP6 climate models, *Clim. Dynam.*, 55, 553–577, <https://doi.org/10.1007/s00382-020-05282-7>, 2020.
- Willis, J. K., Roemmich, D., and Cornuelle, B.: Interannual variability in upper ocean heat content, temperature, and thermohaline expansion on global scales, *J. Geophys. Res.-Oceans*, 109, <https://doi.org/10.1029/2003JC002260>, 2004.
- Wilson, N., Straneo, F., and Heimbach, P.: Satellite-derived submarine melt rates and mass balance (2011–2015) for Greenland’s largest remaining ice tongues, *The Cryosphere*, 11, 2773–2782, <https://doi.org/10.5194/tc-11-2773-2017>, 2017.
- WMO: WMO Statement on the State of the Global Climate in 2019, available at: https://library.wmo.int/doc_num.php?explnum_id=10211, last access: 7 August 2020.
- Woollings, T., Gregory, J. M., Pinto, J. G., Reyers, M., and Brayshaw, D. J.: Response of the North Atlantic storm track to climate change shaped by ocean–atmosphere coupling, *Nat. Geosci.*, 5, 313–317, <https://doi.org/10.1038/ngeo1438>, 2012.
- Xu, C., McDowell, N. G., Fisher, R. A., Wei, L., Sevanto, S., Christoffersen, B. O., Weng, E., and Middleton, R. S.: Increasing impacts of extreme droughts on vegetation productivity under climate change, *Nat. Clim. Change*, 9, 948–953, <https://doi.org/10.1038/s41558-019-0630-6>, 2019.
- Yang, H., Lohmann, G., Wei, W., Dima, M., Ionita, M., and Liu, J.: Intensification and poleward shift of subtropical western boundary currents in a warming climate, *J. Geophys. Res.-Oceans*, 121, 4928–4945, <https://doi.org/10.1002/2015JC011513>, 2016.
- Zanna, L., Khattiwala, S., Gregory, J. M., Ison, J., and Heimbach, P.: Global reconstruction of historical ocean heat storage and transport, *P. Natl. Acad. Sci. USA*, 116, 1126, <https://doi.org/10.1073/pnas.1808838115>, 2019.
- Zemp, M., Huss, M., Thibert, E., Eckert, N., McNabb, R., Huber, J., Barandun, M., Machguth, H., Nussbaumer, S. U., Gärtner-Roer, I., Thomson, L., Paul, F., Maussion, F., Kutuzov, S., and Cogley, J. G.: Global glacier mass changes and their contributions to sea-level rise from 1961 to 2016, *Nature*, 568, 382–386, <https://doi.org/10.1038/s41586-019-1071-0>, 2019.
- Zhang, J. and Rothrock, D. A.: Modeling Global Sea Ice with a Thickness and Enthalpy Distribution Model in Generalized Curvilinear Coordinates, *Mon. Weather Rev.*, 131, 845–861, [https://doi.org/10.1175/1520-0493\(2003\)131<0845:MGSIIWA>2.0.CO;2](https://doi.org/10.1175/1520-0493(2003)131<0845:MGSIIWA>2.0.CO;2), 2003.
- Zscheischler, J., Westra, S., van den Hurk, B. J. J. M., Seneviratne, S. I., Ward, P. J., Pitman, A., AghaKouchak, A., Bresch, D. N., Leonard, M., Wahl, T., and Zhang, X.: Future climate risk from compound events, *Nat. Clim. Change*, 8, 469–477, <https://doi.org/10.1038/s41558-018-0156-3>, 2018.

AGENDA
NATIONAL CLIMATE TASK FORCE MEETING
Thursday, February 11, 2021

(b) (5)

Pre-read

CLIMATE TASK FORCE CHARTER

From Executive Order 14008: “Tackling the Climate Crisis at Home and Abroad” (January 27, 2021)

Mission and Work. The Climate Task Force shall facilitate the organization and deployment of a Government-wide approach to combat the climate crisis. The Task Force shall facilitate the planning and implementation of key Federal Actions to reduce climate pollution; increase resilience to the impacts of climate change; protect public health; conserve our lands, waters, oceans, and biodiversity; deliver environmental justice; and spur well-paying union jobs and economic growth. As necessary and appropriate, members of the Task Force will engage on these matters with State, local Tribal, and territorial governments; workers and communities; and leaders across the various sectors of our economy.

Prioritizing Actions. To the extent permitted by law, Task Force members shall prioritize action on climate change in their policy-making and budget processes, in their contracting and procurement, and in their engagement with State, local, Tribal, and territorial governments; workers and communities; and leader across all the sectors of our economy.

Membership:

Chair, National Climate Advisor

the Secretary of the Treasury

the Secretary of Defense

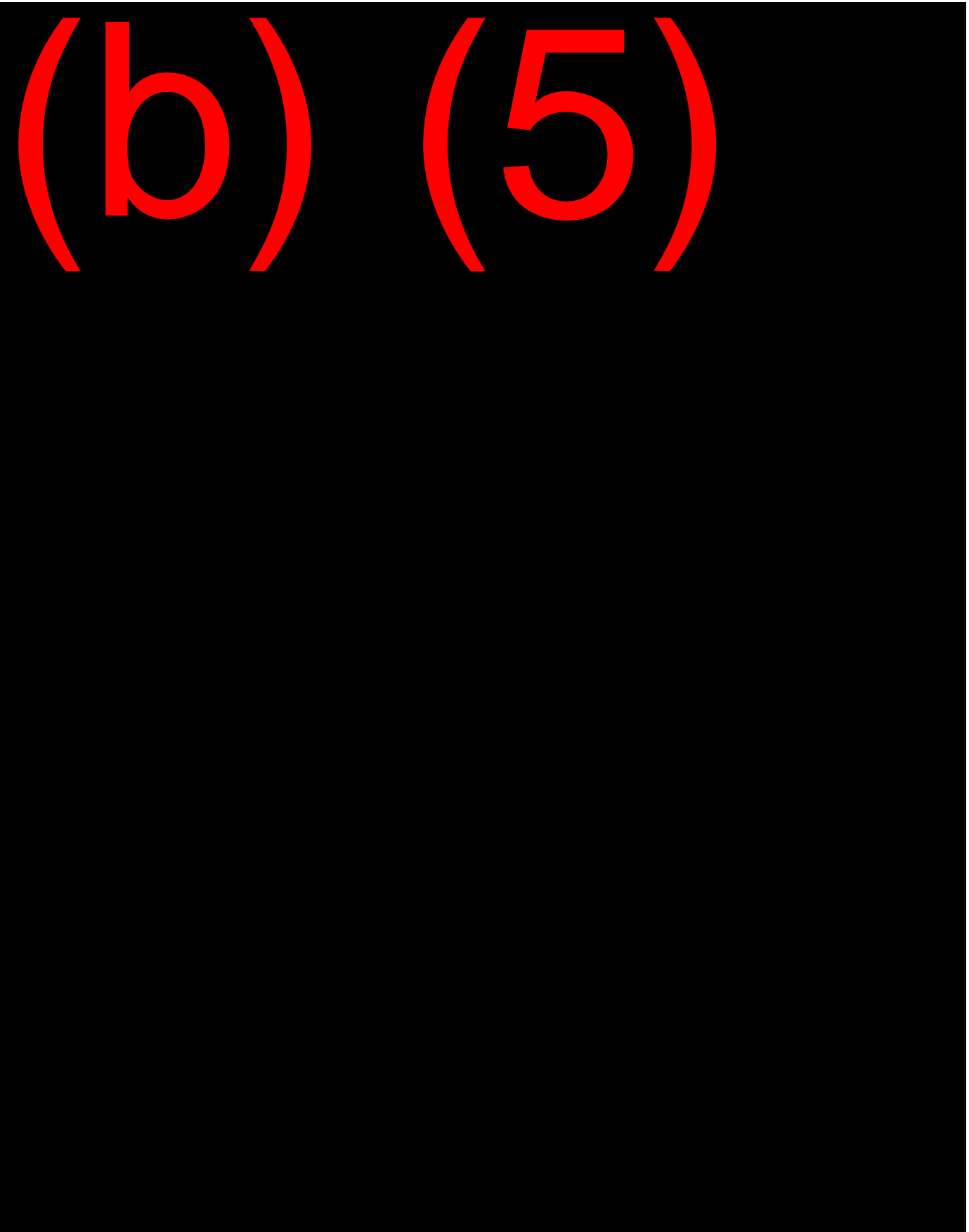
the Attorney General

the Secretary of the Interior

the Secretary of Agriculture

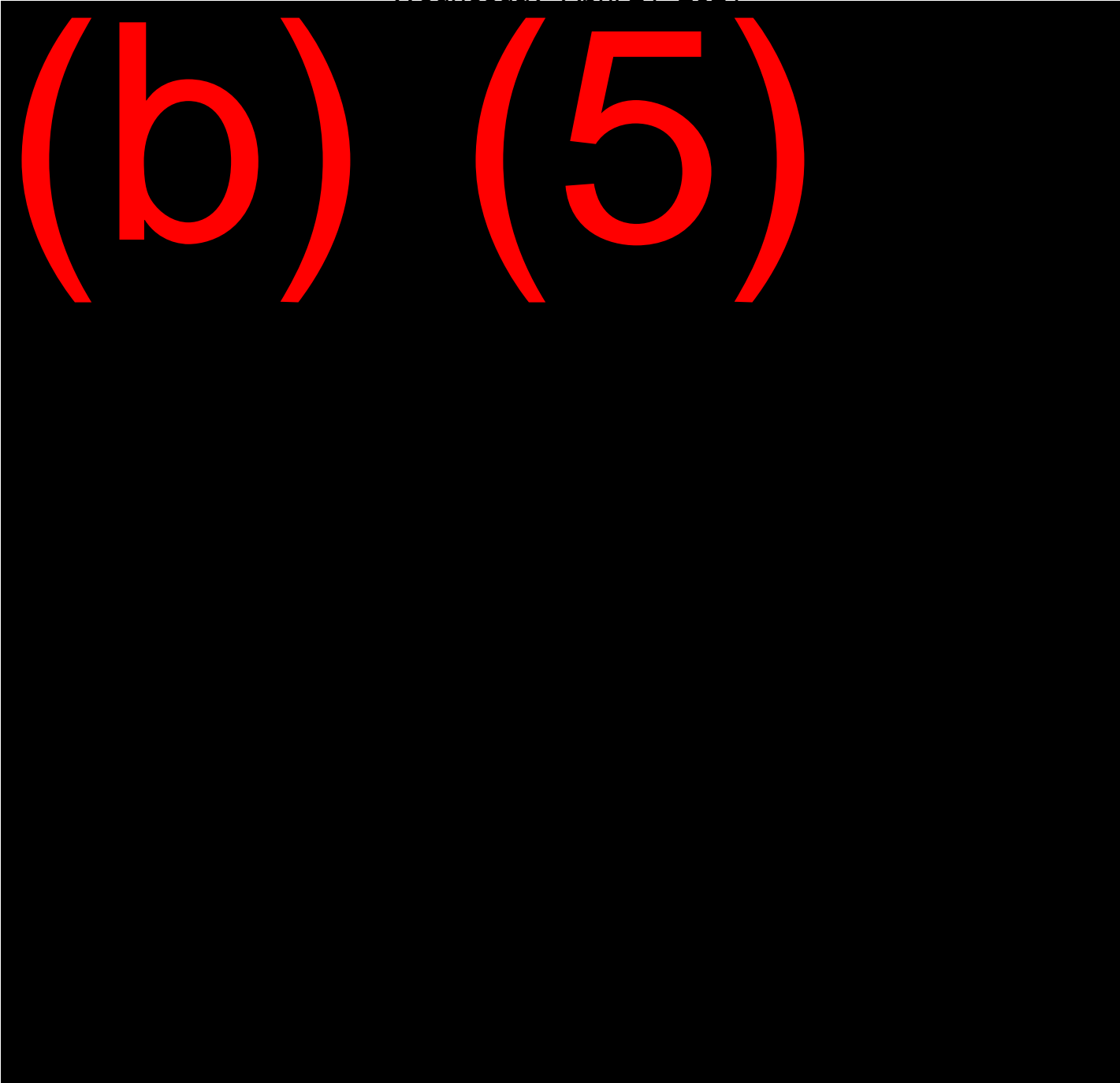
the Secretary of Commerce
the Secretary of Education*
the Secretary of Labor
the Secretary of Health and Human Services
the Secretary of Housing and Urban Development
the Secretary of Transportation
the Secretary of Energy
the Secretary of Homeland Security
the Administrator of General Services
the Chair of the Council on Environmental Quality
the Administrator of the Environmental Protection Agency
the Director of the Office of Management and Budget
the Director of the Office of Science and Technology Policy
the Assistant to the President for Domestic Policy
the Assistant to the President for National Security Affairs
the Assistant to the President for Homeland Security and Counterterrorism
the Assistant to the President for Economic Policy

(b) (5)



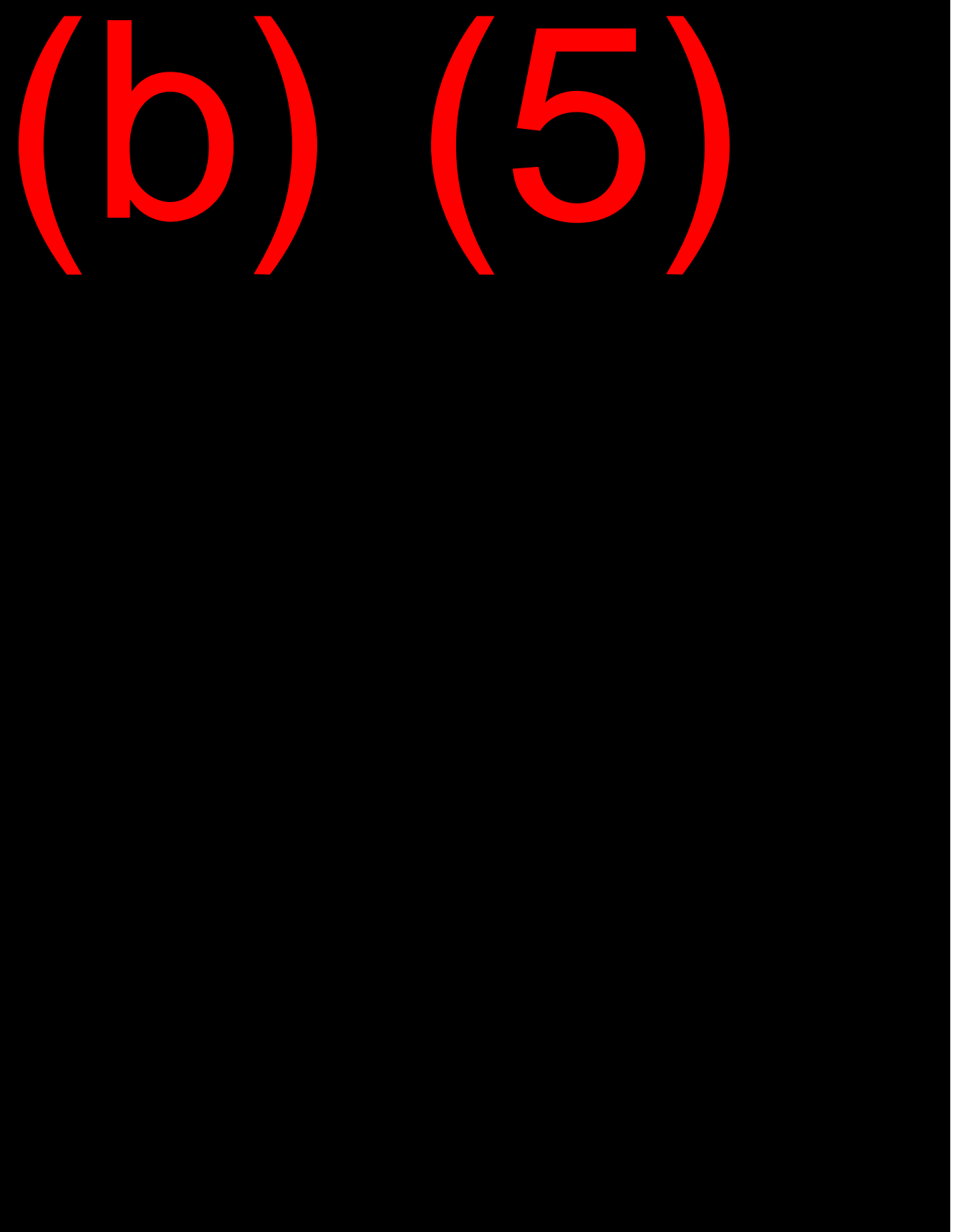
AGENDA
NATIONAL CLIMATE TASK FORCE MEETING
Wednesday April 21, 2021

(b) (5)



Potential Announcements Re Climate | Proposed List: [AGENCY NAME]

(b) (5)





March 22, 2021

Via Email to recipients (for whom we have email addresses; White House National Climate Advisor Gina McCarthy, c/o Maggie Thomas)

White House National Climate Advisor Gina McCarthy
Special Presidential Envoy for Climate John Kerry
The White House
1600 Pennsylvania Avenue, NW
Washington, DC 20500

Re: United States' Nationally Determined Contribution and Best Scientific Standards for Protecting Children's Fundamental Rights

Dear White House National Climate Advisor Gina McCarthy, Special Presidential Envoy for Climate John Kerry, and Members of the National Climate Task Force,

By April 22, 2021, you will release the United States Nationally Determined Contribution (NDC), and set US energy and climate policy for the next ten years, with implications far beyond 2030. We write in the interest of our Nation's youth and posterity to petition for an NDC commensurate with the best available science and consistent with protecting the fundamental constitutional rights of children, such as children within environmental justice communities, including communities of color, low-income communities, and indigenous communities. The premier scientific experts on the planet are clear on three points:

1. Earth energy imbalance (and more global warming) can only be stopped by returning the atmospheric CO₂ concentration to below 350 ppm by 2100. This is the best scientific standard for "stabilization of greenhouse gas concentrations in the atmosphere at a level that would prevent dangerous anthropogenic interference with the climate system. . . . within a time-frame" sufficient to protect life and liberties, and with which to align our Nation's NDC.¹
2. Current increased average temperatures of 1.1°C are already dangerous. Aiming for temperature targets of even more heat at 1.5°C to 2°C stokes more danger and is exponentially more catastrophic for our children and posterity.
3. "Net Zero" emissions is a shell game with little accountability, detached from a precise standard for protection and prevention. Laws and policies, like NDCs, must separate emission allowances and reductions from sequestration efforts and measure them independent of one another.²

¹ UNFCCC, Art. 2.

² D. McLaren et al., *Beyond "Net-Zero": A Case for Separate Targets for Emissions Reduction and Negative Emissions*, Front. Clim. (2019).

First, scientists state the “Earth energy imbalance (EEI) is the most critical number defining the prospects for continued global warming and climate change.”³ “Stabilization of climate . . . requires that EEI be reduced to approximately zero to achieve Earth’s system quasi-equilibrium.”⁴ The measured EEI from 2010-2018 is $0.87 \pm 0.12 \text{ Wm}^{-2}$. Returning CO₂ concentrations to below 350 ppm would restore the energy balance of Earth by allowing as much heat to escape into space as Earth retains, an important historic balance that has kept our planet in the sweet spot for the past 10,000 years, supporting stable sea levels and coastlines, enabling productive agriculture, and allowing humans and other species to thrive.⁵

With just 1°C of warming, glaciers in all regions of the world are melting at accelerating rates, as are the Greenland and Antarctic ice sheets, causing seas to rise.⁶ From 1994 to 2017, the Earth lost 28 trillion tonnes of ice, with the rate of ice loss increasing by 57% compared to the 1990s.⁷ The paleo-climate record shows the last time atmospheric CO₂ levels were over 400 ppm, the seas were 70 feet higher than they are today and heating consistent with CO₂ concentrations as low as 450 ppm may have been enough to melt almost all of Antarctica.⁸ The last time the ice sheets were stable was when the atmospheric CO₂ level was <350 ppm prior to 1986. Similarly, scientists believe we can protect marine life and prevent massive bleaching and die-off of coral reefs only by rapidly returning CO₂ levels to below 350 ppm.⁹

Second, EEI and CO₂ standards should dictate emission reduction targets, leaving temperature and sea level rise measurements as useful indicators of whether governments are de- or re-stabilizing the climate system. However, the global average temperature increase allowance on the Earth’s surface of 1.5°C to 2°C is based on “political science,” backed by fossil fuel companies, not the “physical science” of climate stabilization. Scientific experts are clear that current levels of heating of 1.1°C above preindustrial temperatures are already too dangerous to sustain over time for human health, drought, extreme weather events and property damage, biodiversity loss, food and water shortages, and economic loss. The 2018 IPCC Special Report on 1.5°C said allowing **a temperature rise of 1.5°C “is not considered ‘safe’** for most nations, communities, ecosystems, and sectors and poses

³ Karina von Schuckmann et al., *Heat Stored in the Earth System: Where Does the Energy Go?*, 12 Earth Syst. Sci. Data. 2013 (2020) (written by 38 international experts, including lead IPCC authors).

⁴ *Id.*

⁵ James Hansen, *Storms of My Grandchildren* 166 (2009).

⁶ M. Zemp et al., *Global Glacier Mass Changes and their Contributions to Sea-Level Rise from 1961-2016*, Nature (2019); B. Menounos et al., *Heterogeneous Changes in Western North American Glaciers Linked to Decadal Variability in Zonal Wind Strength*, Geophysical Research Letters (2018).

⁷ T. Slater et al., *Earth’s Ice Imbalance*, 15 The Cryosphere 233 (2021).

⁸ James E. Hansen, *Declaration in Support of Plaintiffs, Juliana v. United States*, No. 6:15-cv-01517-TC, 14 (D. Or. Aug. 12, 2015); IPCC, *Chapter 6.3.2, What Does the Record of the Mid-Pliocene Show?*, in Climate Change 2007: The Physical Science Basis (2007); Dowsett & Cronin, *High Eustatic Sea Level During the Middle Pliocene: Evidence from the Southeastern U.S. Atlantic Coastal Plain*, Geology (1990); N.J. Shackleton et al., *Pliocene Stable Isotope Stratigraphy of Site 846*, Proceedings of the Ocean Drilling Program, Scientific Results (1995); see also James Hansen et al., *Ice Melt, Sea Level Rise and Superstorms: Evidence from Paleoclimate Data, Climate Modeling, and Modern Observations that 2 °C Global Warming Could be Dangerous*, 16 Atmos. Chem. & Phys. 3761 (2016).

⁹ J. Veron et al., *The Coral Reef Crisis: The Critical Importance of <350 ppm CO₂*, 58 Marine Pollution Bulletin 1428 (2009).

significant risks to natural and human systems as compared to current warming of 1°C (*high confidence*).”¹⁰ Simply put—more heat is deadly.

Third, the politically popular concept of “net zero” allows governments to zero out a percentage of ongoing CO₂ emissions by counting them as “sequestered” through removal processes, such as biogenic or natural sequestration in terrestrial carbon sinks (called the LULUCF sector), leaving a smaller amount of source “net emissions” to be reduced. However, in order to align emissions and sequestration with a <350 ppm standard, carbon removed through natural sequestration in sinks must be counted separately and used to draw down the excess CO₂ already in the atmosphere from cumulative US historic emissions, not to provide a negative credit or offset for ongoing and new US emissions. Indeed, **all gross US emissions, not only net emissions, need to be swiftly reduced to near zero (not net zero) by 2050**. Three countries that set NDCs in 2020 all tier their emission reduction commitments by 2030 to “net emissions” without specifying the precise percentage of actual gross emissions that will cease. If the US takes that same approach, it will authorize ongoing emissions at levels with dangerous consequences for children and future generations. According to *Net Zero America*, which was funded in part by BP and ExxonMobil, there are several “net zero by 2050” scenarios that allow the US to continue high levels of oil and gas production for domestic consumption and exports, policies that are plainly incompatible with climate stabilization and correcting EEI.

US energy and climate policy should set emission levels consistent with a 350 ppm standard. It is scientifically defensible and technically and economically feasible to reduce total US emissions by 80% by 2030 and 96-100% by 2050 while simultaneously enhancing biogenic sequestration capacity of sinks and separately accounting for sinks as a drawdown of US historic cumulative CO₂ emissions.¹¹ Both are vital. By linking US emission reductions to “net emissions” you would authorize ~12% of US emissions to continue in perpetuity, leaving only ~88% to be addressed.¹² As the capacity of sinks for sequestration improve, this policy would allow even higher levels of ongoing emissions, without addressing the issue of excess atmospheric CO₂ that must be drawn down to restore EEI and prevent multi-meter sea level rise. There is no scientific basis for doing this, when the Nation’s sequestration capacity in sinks must be counted toward carbon drawdown from *cumulative historic* CO₂ emissions, not ongoing and new annual emissions.

According to the 2019 draft US inventory, total gross US greenhouse gas emissions were 6,577.2 million metric tons of carbon dioxide equivalent (MMT CO_{2e}).¹³ An 80%

¹⁰ J. Roy et al., *Sustainable Development, Poverty Eradication and Reducing Inequalities*, in *Global Warming of 1.5°C*. An IPCC Special Report on the impacts of global warming of 1.5°C above pre-industrial levels and related global greenhouse gas emission pathways, in the context of strengthening the global response to the threat of climate change, sustainable development, and efforts to eradicate poverty, at 447 (2018) (emphasis added); see also James Hansen et al., *Assessing “Dangerous Climate Change”: Required Reduction of Carbon Emissions to Protect Young People, Future Generations and Nature*, 8 PLOS ONE e81648 (2013).

¹¹ Mark Jacobson et al., *100% Clean and Renewable Wind, Water, and Sunlight (WWS) All-Sector Energy Roadmaps for the 50 United States*, Energy & Environ Sci (2015); B. Haley et al., *350 ppm Pathways for the United States* (2019); James Williams et al., *Carbon-Neutral Pathways for the United States*, 2 AGU Advances e2020AV000284 (2021)

¹² In 2019, US net emissions (5,788.3 MMT CO_{2e}) were 88% of total emissions (6,577.2 MMT CO_{2e}). US EPA, *Draft Inventory of U.S. Greenhouse Gas Emissions and Sinks 1990-2018*, ES-9 (2021).

¹³ US EPA, *Draft Inventory of U.S. Greenhouse Gas Emissions and Sinks: 1990-2019*, ES-4 (2021). Emissions from Wood Biomass, Ethanol, and Biodiesel Consumption are not included in this number. *Id.* ES-9, fn. A.

reduction in total U.S. emissions would result in gross emission levels of 1,315.4 MMT CO₂e by 2030. In 2019, “[t]he primary greenhouse gas emitted by human activities in the United States was CO₂, representing approximately 80.2 percent of total greenhouse gas emissions. The largest source of CO₂, and of overall greenhouse gas emissions, was fossil fuel combustion [primarily from transportation and power generation].”¹⁴

Separately, the US should commit to increase terrestrial sequestration in carbon sinks by up to 50% by improving land management policies and practices to increase actual carbon sink sequestration from 2019 levels of 788.9 MMT CO₂e, which is a decline in sequestration from 1990 at 900.8 MMT CO₂e. US sinks have capacity to sequester ~414 MMT CO₂ more per year than current stocks.¹⁵ The NDC should commit to a 2030 target of increasing existing terrestrial carbon removal sequestration by at least 25% and up to 50%.

As National Climate Advisor McCarthy said, “Right now we are robbing young people of their future.” Any NDC that aligns with 1.5°C or 2°C, or a misleading “net zero” emissions allowance not aligned with a <350 ppm standard, will continue to rob children of their future and be subject to challenge in our courts. This is the moment to align human laws and policies with nature’s laws and protect our children from the climate crisis as Executive Order 14008 and the Constitution require. There is simply no more time for delay. The solutions are at hand.

We represent the youth of America from all communities on the climate crisis, and we respectfully request your attention on the science to ensure that your policies conform thereto.

Sincerely,
/s/
Julia Olson
Executive Director and Chief Legal Counsel

Andrea Rodgers
Senior Litigation Attorney

Liz Lee
Government Affairs Attorney

Nate Bellinger
Staff Attorney

Philip Gregory
Of Counsel

Our Children’s Trust

Our Children’s Trust is the world’s only nonprofit public interest law firm that provides strategic, campaign-based legal services to youth from diverse backgrounds to secure their legal rights to a safe climate, including the 21 youth plaintiffs in Juliana v. United States.

¹⁴ US EPA, *Draft Inventory of U.S. Greenhouse Gas Emissions and Sinks: 1990-2019*, ES-9.

¹⁵ Expert Report of G. Philip Robertson, *Juliana v. United States*, No. 6:15-cv-01517-TC (D. Or. Aug. 12, 2015); J.E. Fargione et al., *Negative Emission Technologies and Reliable Sequestration: A Research Agenda*, National Academies of Sciences, Engineering, and Medicine, Chapter 3 (2019).

cc:

Members of the National Climate Task Force

Janet Yellen, Secretary of the Treasury

Lloyd Austin, Secretary of Defense

Merrick Garland, Attorney General

Deb Haaland, Secretary of the Interior

Tom Vilsack, Secretary of Agriculture

Gina Raimondo, Secretary of Commerce

Miguel Cardona, Secretary of Education

Al Stewart, Acting Secretary of Labor

Xavier Becerra, Secretary of Health and Human Services

Marcia Fudge, Secretary of Housing and Urban Development

Pete Buttigieg, Secretary of Transportation

Jennifer Granholm, Secretary of Energy

Alejandro Mayorkas, Secretary of Homeland Security

Katy Kale, Acting Administrator of General Services

Matt Lee-Ashley, Acting Chair of the Council on Environmental Quality

Michael Regan, Administrator of the Environmental Protection Agency

Steve Jurczyk, Acting Administrator of the National Aeronautics and Space Administration

Rob Fairweather, Acting Director of the Office of Management and Budget

Kei Koizumi, Acting Director of the Office of Science and Technology Policy

Susan Rice, Assistant to the President for Domestic Policy

Jake Sullivan, Assistant to the President for National Security Affairs

Elizabeth Sherwood-Randall, Assistant to the President for Homeland Security and
Counterterrorism

Brian Deese, Assistant to the President for Economic Policy



Young people's burden: requirement of negative CO₂ emissions

James Hansen¹, Makiko Sato¹, Pushker Kharecha¹, Karina von Schuckmann², David J. Beerling³, Junji Cao⁴, Shaun Marcott⁵, Valerie Masson-Delmotte⁶, Michael J. Prather⁷, Eelco J. Rohling^{8,9}, Jeremy Shakun¹⁰, Pete Smith¹¹, Andrew Lacis¹², Gary Russell¹², and Reto Ruedy^{12,13}

¹Climate Science, Awareness and Solutions, Columbia University Earth Institute, New York, NY 10115, USA

²Mercator Ocean, 10 Rue Hermes, 31520 Ramonville St Agne, France

³Leverhulme Centre for Climate Change Mitigation, University of Sheffield, Sheffield, S10 2TN, UK

⁴Key Lab of Aerosol Chemistry and Physics, SKLLQG, Institute of Earth Environment, Xi'an, 710061, China

⁵Department of Geoscience, 1215 W. Dayton St., Weeks Hall, University of Wisconsin-Madison, Madison, WI 53706, USA

⁶Institut Pierre Simon Laplace, Laboratoire des Sciences du Climat et de

l'Environnement (CEA-CNRS-UVSQ) Université Paris Saclay, Gif-sur-Yvette, France

⁷Earth System Science Department, University of California at Irvine, CA, USA

⁸Research School of Earth Sciences, The Australian National University, Canberra, 2601, Australia

⁹Ocean and Earth Science, University of Southampton, National Oceanography Centre, Southampton, SO14 3ZH, UK

¹⁰Department of Earth and Environmental Sciences, Boston College, Chestnut Hill, MA 02467, USA

¹¹Institute of Biological and Environmental Sciences, University of Aberdeen, 23 St Machar Drive, Aberdeen, AB24 3UU, UK

¹²NASA Goddard Institute for Space Studies, New York, NY 10025, USA

¹³SciSpace LLC, 2880 Broadway, New York, NY 10025, USA

Correspondence to: James Hansen (jeh1@columbia.edu)

Received: 22 September 2016 – Discussion started: 4 October 2016

Revised: 29 May 2017 – Accepted: 8 June 2017 – Published: 18 July 2017

Abstract. Global temperature is a fundamental climate metric highly correlated with sea level, which implies that keeping shorelines near their present location requires keeping global temperature within or close to its preindustrial Holocene range. However, global temperature excluding short-term variability now exceeds +1 °C relative to the 1880–1920 mean and annual 2016 global temperature was almost +1.3 °C. We show that global temperature has risen well out of the Holocene range and Earth is now as warm as it was during the prior (Eemian) interglacial period, when sea level reached 6–9 m higher than today. Further, Earth is out of energy balance with present atmospheric composition, implying that more warming is in the pipeline, and we show that the growth rate of greenhouse gas climate forcing has accelerated markedly in the past decade. The rapidity of ice sheet and sea level response to global temperature is difficult to predict, but is dependent on the magnitude of warming. Targets for limiting global warming thus, at minimum, should aim to avoid leaving global temperature at Eemian or higher levels for centuries. Such targets now require “negative emissions”, i.e., extraction of CO₂ from the air. If phasedown of fossil fuel emissions begins soon, improved agricultural and forestry practices, including reforestation and steps to improve soil fertility and increase its carbon content, may provide much of the necessary CO₂ extraction. In that case, the magnitude and duration of global temperature excursion above the natural range of the current interglacial (Holocene) could be limited and irreversible climate impacts could be minimized. In contrast, continued high fossil fuel emissions today place a burden on young people to undertake massive technological CO₂ extraction if they are to limit climate change and its consequences. Proposed methods of extraction such as bioenergy with carbon capture and storage (BECCS) or air capture of CO₂ have minimal

estimated costs of USD 89–535 trillion this century and also have large risks and uncertain feasibility. Continued high fossil fuel emissions unarguably sentences young people to either a massive, implausible cleanup or growing deleterious climate impacts or both.

1 Introduction

The United Nations 1992 Framework Convention on Climate Change (United Nations, 1992) stated its objective as “stabilization of GHG concentrations in the atmosphere at a level that would prevent dangerous anthropogenic interference with the climate system”. The 15th Conference of the Parties (Copenhagen Accord, 2009) concluded that this objective required a goal to “reduce global emissions so as to hold the increase of global temperature below 2 °C”. The 21st Conference of the Parties (Paris Agreement, 2015), currently ratified by 148 nations, aims to strengthen the global response to the climate change threat by “[h]olding the increase in the global average temperature to well below 2 °C above the pre-industrial levels and pursuing efforts to limit the temperature increase to 1.5 °C above the pre-industrial levels”.

Global surface temperature has many merits as the principal metric for climate change, but additional metrics, such as atmospheric CO₂ amount and Earth's energy imbalance, help refine targets for avoiding dangerous human-made climate change. Paleoclimate data and observations of Earth's present energy imbalance led Hansen et al. (2008, 2013a, 2016) to recommend reducing CO₂ to less than 350 ppm, with the understanding that this target must be adjusted as CO₂ declines and empirical data accumulate. The 350 ppm CO₂ target is moderately stricter than the 1.5 °C warming target. The near-planetary energy balance anticipated at 350 ppm CO₂ implies a global temperature close to recent values, i.e., about +1 °C relative to preindustrial.

We advocate pursuit of this goal within a century to limit the period with global temperature above that of the current interglacial period, the Holocene.¹ Limiting the period and magnitude of temperature excursion above the Holocene range is crucial to avoid strong stimulation of slow feedbacks. Slow feedbacks include ice sheet disintegration and thus sea level rise, which is probably the most threatening climate impact, and release of greenhouse gases (GHGs) via such mechanisms as thawing tundra and loss of soil carbon. Holocene climate stability allowed sea level to be stable for the past several millennia (Kopp et al., 2016) as civilizations developed. But there is now a danger that temperature rises so far above the Holocene range that slow feedbacks are activated to a degree that continuing climate change will be out

of humanity's control. Both the 1.5 °C and 350 ppm targets require rapid phasedown of fossil fuel emissions.

Today, global fossil fuel emissions continue at rates that make these targets increasingly improbable (Fig. 1 and Appendix A1). On a per capita historical basis the US is 10 times more accountable than China and 25 times more accountable than India for the increase in atmospheric CO₂ above its preindustrial level (Hansen and Sato, 2016). In response, a lawsuit (Juliana et al. vs. United States, 2016, hereafter J. et al. vs. US, 2016) was filed against the United States asking the US District Court, District of Oregon, to require the US government to produce a plan to rapidly reduce emissions. The suit requests that the plan reduce emissions at the 6 % yr⁻¹ rate that Hansen et al. (2013a) estimated as the requirement for lowering atmospheric CO₂ to a level of 350 ppm. At a hearing in Eugene Oregon on 9 March 2016 the United States and three interveners (American Petroleum Institute, National Association of Manufacturers, and the American Fuels and Petrochemical Association) asked the court to dismiss the case, in part based on the argument that the requested rate of fossil fuel emissions reduction was beyond the court's authority. Magistrate Judge Coffin stated that he found “the remedies aspect of the plaintiff's complaint [to be] *troublesome*”, in part because it involves “a separation of powers issue”. But he also noted that some of the alleged climate change consequences, if accurate, could be considered “beyond the pale”, and he rejected the motion to dismiss the case. Judge Coffin's ruling was certified, as required, by a second judge (Aiken, 2016) on 9 September 2016, and, barring a settlement that would be overseen by the court, the case is expected to proceed to trial in late 2017. It can be anticipated that the plausibility of achieving the emission reductions needed to stabilize climate will be a central issue at the remedy stage of the trial.

Urgency of initiating emissions reductions is well recognized (IPCC, 2013, 2014; Huntingford et al., 2012; Friedlingstein et al., 2014; Rogelj et al., 2016a) and was stressed in the paper (Hansen et al., 2013a) used in support of the lawsuit J. et al. vs. US (2016). It is also recognized that the goal to keep global warming less than 1.5 °C likely requires negative net CO₂ emissions later this century if high global emissions continue in the near term (Fuss et al., 2014; Anderson, 2015; Rogelj et al., 2015; Sanderson et al., 2016). The Intergovernmental Panel on Climate Change (IPCC) reports (IPCC, 2013, 2014) do not address environmental and ecological feasibility and impacts of large-scale CO₂ removal, but recent studies (Smith et al., 2016; Williamson,

¹ By Holocene we refer to the preindustrial portion of the present interglacial period. As we will show, the rapid warming of the past century has brought temperature above the range in the prior 11 700 years of the Holocene.

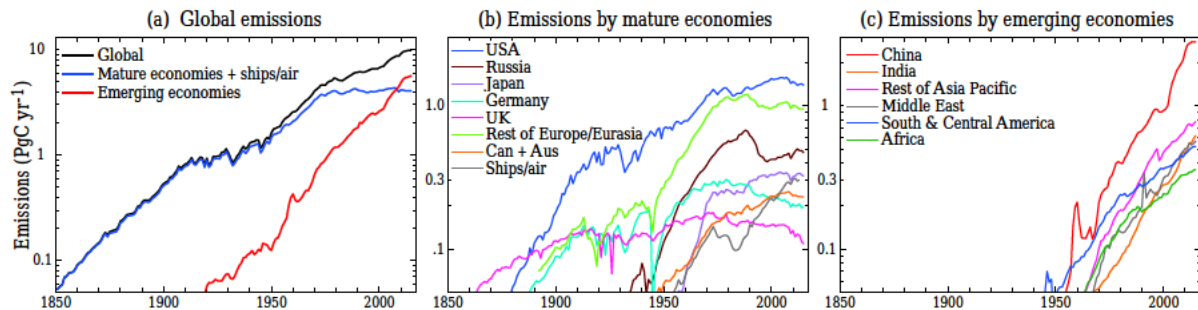


Figure 1. Fossil fuel (and cement manufacture) CO₂ emissions (note log scale) based on Boden et al. (2016) with BP data used to infer 2014–2015 estimates. Europe/Eurasia is Turkey plus the Boden et al. categories Western Europe and Centrally Planned Europe. Asia Pacific is sum of Centrally Planned Asia, Far East and Oceania. Middle East is Boden et al. (2016) Middle East less Turkey. Russia is Russian Federation since 1992 and 60 % of USSR in 1850–1991. Ships/air is sum of bunker fuels of all nations. Can + Aus is the sum of emissions from Canada and Australia.

2016) are taking up this crucial issue and raising the question of whether large-scale negative emissions are even feasible.

Our aim is to contribute to understanding of the required rate of CO₂ emissions reduction via an approach that is transparent to non-scientists. We consider potential drawdown of atmospheric CO₂ by reforestation and afforestation, the potential for improved agricultural practices to store more soil carbon, and potential reductions of non-CO₂ GHGs that could reduce human-made climate forcing.² Quantitative examination reveals the merits of these actions to partly offset demands on fossil fuel CO₂ emission phasedown, but also their limitations, thus clarifying the urgency of government actions to rapidly advance the transition to carbon-free energies to meet the climate stabilization targets they have set.

We first describe the status of global temperature change and then summarize the principal climate forcings that drive long-term climate change. We show that observed global warming is consistent with knowledge of changing climate forcings, Earth's measured energy imbalance, and the canonical estimate of climate sensitivity,³ i.e., about 3 °C global warming⁴ for doubled atmospheric CO₂. For clarity we make global temperature calculations with our simple climate model, which we show (Appendix A2) has a transient climate sensitivity near the midpoint of the sensitivity of models illustrated in Fig. 10.20a of IPCC (2013). The standard climate sensitivity and climate model do not in-

clude effects of “slow” climate feedbacks such as change in ice sheet size. There is increasing evidence that some slow feedbacks can be triggered within decades, so they must be given major consideration in establishing the dangerous level of human-made climate interference. We thus incorporate consideration of slow feedbacks in our analysis and discussion, even though precise specification of their magnitude and timescales is not possible. We present updates of GHG observations and find a notable acceleration during the past decade of the growth rate of GHG climate forcing. For future fossil fuel emissions we consider both the representative concentration pathway (RCP) scenarios used in Climate Model Intercomparison Project 5 (CMIP5) IPCC studies, and simple emission growth rate changes that help evaluate the plausibility of needed emission changes. We use a Green's function calculation of global temperature with canonical climate sensitivity for each emissions scenario, which yields the amount of CO₂ that must be extracted from the air – effectively the climate debt – to return atmospheric CO₂ to less than 350 ppm or limit global warming to less than 1.5 °C above preindustrial levels. We discuss alternative extraction technologies and their estimated costs, and finally we consider the potential alleviation of CO₂ extraction requirements that might be obtained via special efforts to reduce non-CO₂ GHGs.

2 Global temperature change

The framing of human-caused climate change by the Paris Agreement uses global mean surface temperature as the metric for assessing dangerous climate change. We have previously argued the merits of additional metrics, especially Earth's energy imbalance (Hansen et al., 2005; von Schuckmann et al., 2016) and atmospheric CO₂ amount (Hansen et al., 2008). Earth's energy imbalance integrates over all climate forcings, known and unknown, and informs us where climate is heading, because it is this imbalance that drives

²A climate forcing is an imposed change in Earth's energy balance, measured in W m⁻². For example, Earth absorbs about 240 W m⁻² of solar energy, so if the Sun's brightness increases 1 % it is a forcing of +2.4 W m⁻².

³Climate sensitivity is the response of global average surface temperature to a standard forcing, with the standard forcing commonly taken to be doubled atmospheric CO₂, which is a forcing of about 4 W m⁻² (Hansen et al., 2005).

⁴IPCC (2013) finds that 2 × CO₂ equilibrium sensitivity is likely in the range 3 ± 1.5 °C, as was estimated by Charney et al. (1979). Median sensitivity in recent model inter-comparisons is 3.2 °C (Andrews et al., 2012; Vial et al., 2013).

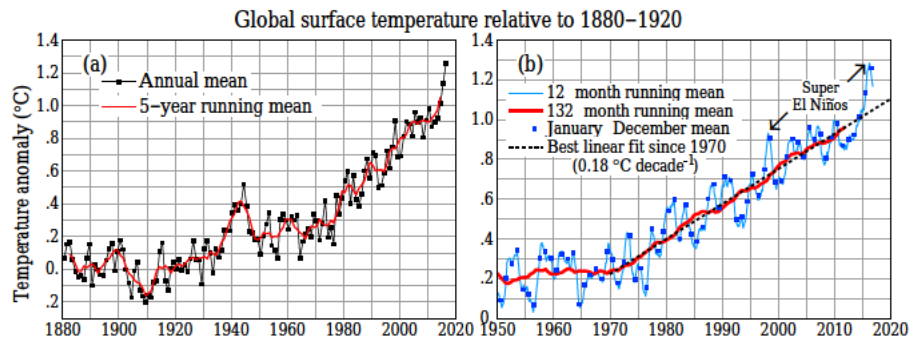


Figure 2. Global surface temperature relative to 1880–1920 based on GISTEMP data (Appendix A3). (a) Annual and 5-year means since 1880, (b) 12- and 132-month running means since 1970. Blue squares in (b) are calendar year (January–December) means used to construct (a). Panel (b) uses data through April 2017.

continued warming. The CO₂ metric has merit because CO₂ is the dominant control knob on global temperature (Lacis et al., 2010, 2013), including paleo-temperature change (cf. Fig. 28 of Hansen et al., 2016). Our present paper uses these alternative metrics to help sharpen determination of the dangerous level of global warming, and to quantify actions that are needed to stabilize climate. We here use global temperature as the principal metric because several reasons of concern are scaled to global warming (O'Neill et al., 2017), including specifically the potential for slow feedbacks such as ice sheet melt and permafrost thaw. The slow feedbacks, whose timescales depend on how strongly the climate system is being forced, will substantially determine the magnitude of climate impacts and affect how difficult the task of stabilizing climate will be.

Quantitative assessment of both ongoing and paleo-temperature change is needed to define acceptable limits on human-made interference with climate, with paleoclimate especially helpful for characterizing long-term ice sheet and sea level response to temperature change. Thus, we examine the modern period with near-global instrumental temperature data in the context of the current and prior (Holocene and Eemian) interglacial periods, for which less precise proxy-based temperatures have recently emerged. The Holocene, over 11 700 years in duration, had relatively stable climate, prior to the remarkable warming in the past half century. The Eemian, which lasted from about 130 000 to 115 000 years ago, was moderately warmer than the Holocene and experienced sea level rise to heights 6–9 m (20–30 ft) greater than today.

2.1 Modern temperature

The several analyses of temperature change since 1880 are in close agreement (Hartmann et al., 2013). Thus, we can use the current GISTEMP analysis (see Supplement), which is updated monthly and available (<http://www.columbia.edu/~mhs119/temperature/>).

The popular measure of global temperature is the annual-mean global mean value (Fig. 2a), which is publicized at the end of each year. However, as discussed by Hansen et al. (2010), the 12-month running mean global temperature is more informative and removes monthly “noise” from the record just as well as the calendar year average. For example, the 12-month running mean for the past 67 years (Fig. 2b) defines clearly the super-El Niños of 1997–1998 and 2015–2016 and the 3-year cooling after the Mount Pinatubo volcanic eruption in the early 1990s.

Global temperature in 2014–2016 reached successive record high levels for the period of instrumental data (Fig. 2). Temperature in the latter 2 years was partially boosted by the 2015–2016 El Niño, but the recent warming is sufficient to remove the illusion of a hiatus of global surface warming after the 1997–1998 El Niño (Appendix A4).

The present global warming rate, based on a linear fit for 1970–present (dashed line in Fig. 2b) is +0.18 °C per decade.⁵ The period since 1970 is the time with high growth rate of GHG climate forcing, which has been maintained at approximately +0.4 W m⁻² decade⁻¹ (see Sect. 6 below)⁶ causing Earth to be substantially out of energy balance (Cheng et al., 2017). The energy imbalance drives global warming, so unless and until there is substantial change in the rate of added climate forcing we expect the underlying warming to continue at a comparable rate.

Global temperature defined by the linear fit to temperature since 1970 now exceeds 1 °C⁷ relative to the 1880–1920 mean (Fig. 2b), where the 1880–1920 mean provides our best estimate of “preindustrial” temperature (Ap-

⁵ Extreme end points affect linear trends, but if the 2016 temperature is excluded the calculated trend (0.176 °C decade⁻¹) still rounds to 0.18 °C decade⁻¹.

⁶ As forcing additions from chlorofluorocarbons (CFCs) and CH₄ declined, CO₂ growth increased (Sect. 6).

⁷ It is 1.05 °C for linear fit to 132-month running mean, but can vary by a few hundredths of a degree depending on the method chosen to remove short-term variability.

pendix A5). At the rate of $0.18^{\circ}\text{C decade}^{-1}$ the linear trend line of global temperature will reach $+1.5^{\circ}\text{C}$ in about 2040 and $+2^{\circ}\text{C}$ in the late 2060s. However, the warming rate can accelerate or decelerate, depending on policies that affect GHG emissions, developing climate feedbacks, and other factors discussed below.

2.2 Temperature during current and prior interglacial periods

Holocene temperature has been reconstructed at centennial-scale resolution from 73 globally distributed proxy temperature records by Marcott et al. (2013). This record shows a decline of 0.6°C from early Holocene maximum temperature to a “Little Ice Age” minimum in the early 1800s (that minimum being better defined by higher resolution data of Abram et al., 2016). Concatenation of the modern and Holocene temperature records (Fig. 3; Appendix A5) assumes that 1880–1920 mean temperature is 0.1°C warmer than the Little Ice Age minimum (Abram et al., 2016). The early Holocene maximum in the Marcott et al. (2013) data thus reaches $+0.5^{\circ}\text{C}$ relative to the 1880–1920 mean of modern data. The formal 95 % confidence bounds to Holocene temperature (Marcott et al., 2013) are $\pm 0.25^{\circ}\text{C}$ (blue shading in Fig. 3b), but total uncertainty is larger. Specifically, Liu et al. (2014) points out a bias effect caused by seasonality in the proxy temperature reconstruction. Correction for this bias will tend to push early Holocene temperatures lower, increasing the gap between today's temperature and early Holocene temperature (Marcott and Shakun, 2015).

We emphasize that comparisons of current global temperature with the earlier Holocene must bear in mind the centennial smoothing inherent in the Holocene data (Marcott et al., 2013). Thus, the temperature in an anomalous single year such as 2016 is not an appropriate comparison. However, the temperature in 2016 based on the 1970–present linear trend (at least 1°C relative to the 1880–1920 mean) does provide a meaningful comparison. The trend line reduces the effect of interannual variability, but the more important point is that Earth's energy imbalance assures that this temperature will continue to rise unless and until the global climate forcing begins to decline. In other words, we know that mean temperature over the next several decades will not be lower than 1°C .

We conclude that the modern trend line of global temperature crossed the early Holocene (smoothed) temperature maximum ($+0.5^{\circ}\text{C}$) in about 1985. This conclusion is supported by the accelerating rate of sea level rise, which approached 3 mm yr^{-1} at about that date (Hansen et al., 2016 show a relevant concatenation of measurements in their Fig. 29). Such a high rate of sea level rise, which is 3 m per millennium, far exceeds the prior rate of sea level rise in the last six millennia of the Holocene (Lambeck et al., 2014). Note that near stability of sea level in the latter half of the Holocene as global temperature fell about 0.5°C , prior to

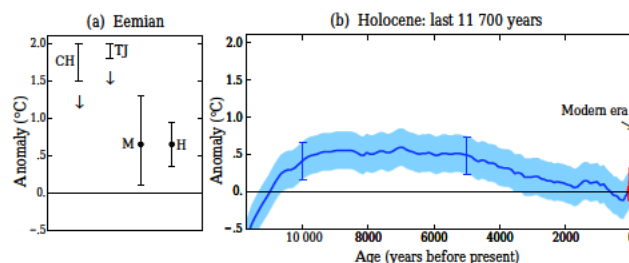


Figure 3. Estimated average global temperature for (a) last interglacial (Eemian) period (Clark and Huybers, 2009; Turney and Jones, 2010; McKay et al., 2011; Hoffman et al., 2017) and (b) centennially smoothed Holocene (Marcott et al., 2013) temperature and the 11-year mean of modern data (Fig. 2), as anomalies relative to 1880–1920. Vertical downward arrows indicate likely overestimates (see text).

rapid warming of the modern era (Fig. 3), is not inconsistent with that global cooling. Hemispheric solar insolation anomalies in the latter half of the Holocene favored ice sheet growth in the Northern Hemisphere and ice sheet decay in Antarctica (Fig. 27a, Hansen et al., 2016), but the Northern Hemisphere did not become cool enough to reestablish ice sheets on North America or Eurasia. There was a small increase in Greenland ice sheet mass (Larsen et al., 2015), but this was presumably at least balanced by Antarctic ice sheet mass loss (Lambeck et al., 2014).

The important point is that global temperature has risen above the centennially smoothed Holocene range. Global warming is already having substantial adverse climate impacts (IPCC, 2014), including extreme events (NAS, 2016). There is widespread agreement that 2°C warming would commit the world to multi-meter sea level rise (Levermann et al., 2013; Dutton et al., 2015; Clark et al., 2016). Sea level reached 6–9 m higher than today during the Eemian (Dutton et al., 2015), so it is particularly relevant to know how global mean Eemian temperature compares to the preindustrial level and thus to today.

McKay et al. (2011) estimated peak Eemian annual global ocean sea surface temperature (SST) as $+0.7 \pm 0.6^{\circ}\text{C}$ relative to late Holocene temperature, while models, as described by Masson-Delmotte et al. (2013), give more confidence to the lower part of that range. Hoffman et al. (2017) report the maximum Eemian annual global SST as $+0.5 \pm 0.3^{\circ}\text{C}$ relative to 1870–1889, which is $+0.65^{\circ}\text{C}$ relative to 1880–1920. The response of surface air temperature (SAT) over land is twice as large as the SST response to climate forcings in 21st century simulations with models (Collins et al., 2013), in good agreement with observed warming in the industrial era (Appendix A3 this paper, Fig. A3a). The ratio of land SAT change to SST change is reduced only to ~ 1.8 after 1000 years in climate models (Fig. A6, Appendix A6). This implies that, because land covers $\sim 30\%$ of the globe, SST warmings should be multiplied by 1.24–

1.3 to estimate global temperature change. Thus, the McKay et al. (2011) and Hoffman et al. (2017) data are equivalent to a global Eemian temperature of just under +1 °C relative to the Holocene. Clark and Huybers (2009) and Turney and Jones (2010) estimated global temperature in the Eemian as 1.5–2 °C warmer than the Holocene (Fig. 3), but Bakker and Renssen (2014) point out two biases that may cause this range to be an overestimate. Bakker and Renssen (2014) use a suite of models to estimate that the assumption that maximum Eemian temperature was synchronous over the planet overestimates Eemian temperature by 0.4 ± 0.3 °C – a feature supported by a lack of synchronicity of warmest conditions in assessments with improved synchronization of records (Govin et al., 2015) – and that they also suggest that a possible seasonal bias of proxy temperature could make the total overestimate as large as 1.1 ± 0.4 °C. Given uncertainties in the corrections, it becomes a matter of expert judgment. Dutton et al. (2015) conclude that the best estimate for Eemian temperature is +1 °C relative to preindustrial. Consistent with these estimates and the discussion of Masson-Delmotte et al. (2013), we assume that maximum Eemian temperature was +1 °C relative to preindustrial with an uncertainty of at least 0.5 °C.

These considerations raise the question of whether 2 °C, or even 1.5 °C, is an appropriate target to protect the well-being of young people and future generations. Indeed, Hansen et al. (2008) concluded that “if humanity wishes to preserve a planet similar to that on which civilization developed and to which life on Earth is adapted, ... CO₂ will need to be reduced ... to at most 350 ppm, but likely less than that”, and further “if the present overshoot of the target CO₂ is not brief, there is a possibility of seeding irreversible catastrophic effects”.

A danger of 1.5 or 2 °C targets is that they are far above the Holocene temperature range. If such temperature levels are allowed to long exist they will spur “slow” amplifying feedbacks (Hansen et al., 2013b; Rohling et al., 2013; Masson-Delmotte et al., 2013), which have potential to run out of humanity's control. The most threatening slow feedback likely is ice sheet melt and consequent significant sea level rise, as occurred in the Eemian, but there are other risks in pushing the climate system far out of its Holocene range. Methane release from thawing permafrost and methane hydrates is another potential feedback, for example, but the magnitude and timescale of this is unclear (O'Connor et al., 2010; Quiquet et al., 2015).

Here we examine the fossil fuel emission reductions required to restore atmospheric CO₂ to 350 ppm or less, so as to keep global temperature close to the Holocene range, in addition to the canonical 1.5 and 2 °C targets. Quantitative investigation requires consideration of Earth's energy imbalance, changing climate forcings, and climate sensitivity.

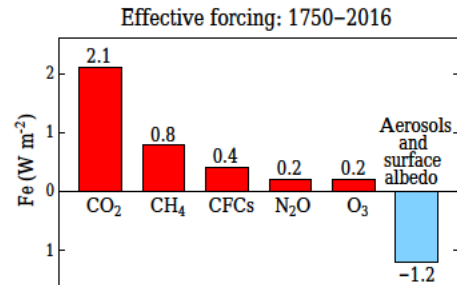


Figure 4. Estimated effective climate forcings (update through 2016 of Fig. 28b of Hansen et al., 2005, which are consistent with estimates of Myhre et al., 2013, in the most recent IPCC report, IPCC, 2013). Forcings are based on observations of each gas, except simulated CH₄-induced changes of O₃ and stratospheric H₂O included in the CH₄ forcing. Aerosols and surface albedo change are estimated from historical scenarios of emissions and land use. Oscillatory and intermittent natural forcings (solar irradiance and volcanoes) are excluded. CFCs include not only chlorofluorocarbons, but all Montreal Protocol trace gases (MPTGs) and other trace gases (OTGs). Uncertainties (for 5–95 % confidence) are 0.6 W m^{-2} for total GHG forcing and 0.9 W m^{-2} for aerosol forcing (Myhre et al., 2013).

3 Global climate forcings and Earth's energy imbalance

The dominant human-caused drivers of climate change are changes of atmospheric GHGs and aerosols (Fig. 4). GHGs absorb Earth's infrared (heat) radiation, thus serving as a “blanket” warms Earth's surface by reducing heat radiation to space. Aerosols, fine particles/droplets in the air that cause visible air pollution, both reflect and absorb solar radiation, but reflection of solar energy to space is their dominant effect, so they cause a cooling that partly offsets GHG warming. Estimated forcings (Fig. 4), an update of Fig. 28b of Hansen et al. (2005), are similar to those of Myhre et al. (2013) in the most recent IPCC report (IPCC, 2013).⁸

Climate forcings in Fig. 4 are the planetary energy imbalance that would be caused by the preindustrial-to-present change in each atmospheric constituent, if the climate were held fixed at its preindustrial state (Hansen et al., 2005). The CH₄ forcing includes its indirect effects, as increasing atmospheric CH₄ causes tropospheric ozone (O₃) and stratospheric water vapor to increase (Myhre et al., 2013). Uncertainties, discussed by Myhre et al. (2013), are typically 10–15 % for GHG forcings. The aerosol forcing uncertainty, described by a probability distribution function (Boucher et al., 2013), is of order 50 %. Our estimate of aerosol plus surface albedo forcing (-1.2 W m^{-2}) differs from the -1.5 W m^{-2}

⁸Our GHG forcings, calculated with formulae of Hansen et al. (2000), yield a CO₂ forcing 6.7 % larger than the central IPCC estimate (Table 8.2 of Myhre et al., 2013) for the CO₂ change from 1750 to 2011. For all well-mixed (long-lived) GHGs we obtain 3.03 W m^{-2} , which is within the IPCC range $2.83 \pm 0.29 \text{ W m}^{-2}$.

of Hansen et al. (2005), as discussed below, but both are within the range of the distribution function of Boucher et al. (2013).

Positive net forcing (Fig. 4) causes Earth to be temporarily out of energy balance, with more energy coming in than going out, which drives slow global warming. Eventually Earth will become hot enough to restore planetary energy balance. However, because of the ocean's great thermal inertia (heat capacity), full atmosphere–ocean response to the forcing requires a long time: atmosphere–ocean models suggest that even after 100 years only 60–75 % of the surface warming for a given forcing has occurred, the remaining 25–40 % still being “in the pipeline” (Hansen et al., 2011; Collins et al., 2013). Moreover, we outline in the next section that global warming can activate “slow” feedbacks, such as changes of ice sheets or melting of methane hydrates, so the time for the system to reach a fully equilibrated state is even longer.

GHGs have been increasing for more than a century and Earth has partially warmed in response. Earth's energy imbalance is the portion of the forcing that has not yet been responded to. This imbalance thus defines additional global warming that will occur without further change in forcings. Earth's energy imbalance can be measured by monitoring ocean subsurface temperatures, because almost all excess energy coming into the planet goes into the ocean (von Schuckmann et al., 2016). Most of the ocean's heat content change occurs in the upper 2000 m (Levitus et al., 2012), which has been well measured since 2005, when the distribution of Argo floats achieved good global coverage (von Schuckmann and Le Traon, 2011). Here we update the von Schuckmann and Le Traon (2011) analysis with data for 2005–2015 (Fig. 5) finding a decade-average 0.7 W m^{-2} heat uptake in the upper 2000 m of the ocean. Addition of the smaller terms raises the imbalance to $+0.75 \pm 0.25 \text{ W m}^{-2}$ averaged over the solar cycle (Appendix A7).

4 Climate sensitivity and feedbacks

Climate sensitivity has been a fundamental issue at least since the 19th century, when Tyndall (1861) and Arrhenius (1896) stimulated interest in the effect of CO₂ change on climate. Evaluation of climate sensitivity involves the full complexity of the climate system, as all components and processes in the system are free to interact on all timescales. Tyndall and Arrhenius recognized some of the most important climate feedbacks on both fast and slow timescales. The amount of water vapor in the air increases with temperature, which is an amplifying feedback because water vapor is a very effective greenhouse gas; this is a “fast” feedback, because water vapor amount in the air adjusts within days to temperature change. The area covered by glaciers and ice sheets is a prime “slow” feedback; it, too, is an amplifying feedback, because the darker surface exposed by melting ice absorbs more sunlight.

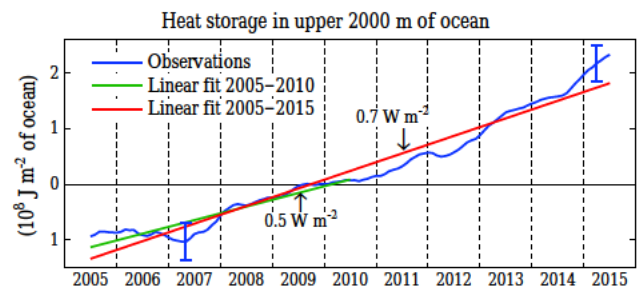


Figure 5. Ocean heat uptake in the upper 2 km of ocean during 11 years from 2005 to 2015 using analysis method of von Schuckmann and Le Traon (2011). Heat uptake in W m^{-2} (0.5 and 0.7) refers to global (ocean + land) area – i.e., it is the contribution of the upper ocean to the heat uptake averaged over the entire planet.

Diminishing climate feedbacks also exist. Cloud-cover changes, for example, can either amplify or reduce climate change (Boucher et al., 2013). Thus, it is not inherent that amplifying feedbacks should be dominant, but climate models and empirical data concur that amplifying feedbacks dominate on both short and long timescales, as we will discuss. Amplifying feedbacks lead to large climate change in response to even weak climate forcings such as ice age cycles caused by small perturbations of Earth's orbit, and still larger climate change occurs on even longer timescales in response to gradual changes in the balance between natural sources and sinks of atmospheric CO₂ (Zachos et al., 2001; Royer et al., 2012; Franks et al., 2014).

4.1 Fast-feedback climate sensitivity

Doubled atmospheric CO₂, a forcing of $\sim 4 \text{ W m}^{-2}$, is a standard forcing in studies of climate sensitivity. Charney et al. (1979) concluded that equilibrium sensitivity, i.e., global warming after a time sufficient for the planet to restore energy balance with space, was $3 \pm 1.5^\circ\text{C}$ for $2 \times \text{CO}_2$ or $0.75^\circ\text{C} (\text{W m}^{-2})^{-1}$ forcing. The Charney analysis was based on climate models in which ice sheets and all long-lived GHGs (except for the specified CO₂ doubling) were fixed. The climate sensitivity thus inferred is the “fast-feedback” climate sensitivity. The central value found in a wide range of modern climate models (Flato et al., 2013) remains 3°C for $2 \times \text{CO}_2$.

The possibility of unknown unknowns in models would keep the uncertainty in the fast-feedback climate sensitivity high, if it were based on models alone, but as discussed by Rohling et al. (2012a), paleoclimate data allow narrowing of the uncertainty. Ice sheet size and the atmospheric amount of long-lived GHGs (CO₂, CH₄, N₂O) under natural conditions change on multi-millennial timescales. These changes are so slow that the climate is in quasi-equilibrium with the changing surface condition and long-lived GHG amounts. Thus, these changing boundary conditions, along with knowledge

of the associated global temperature change, allow empirical assessment of the fast-feedback climate sensitivity. The central result agrees well with the model-based climate sensitivity estimate of 3 °C for 2 × CO₂ (Rohling et al., 2012b), with an uncertainty that is arguably 1 °C or less (Hansen et al., 2013b).

The ocean has great heat capacity (thermal inertia), so it takes decades to centuries for Earth's surface temperature to achieve most of its fast-feedback response to a change in climate forcing (Hansen et al., 1985). Thus, Earth has only partly responded to the human-made increase in GHGs in the air today, the planet must be out of energy balance with the planet gaining energy (via reduced heat radiation to space), and more global warming is “in the pipeline”.

A useful check on understanding of ongoing climate change is provided by the consistency of the net climate forcing (Fig. 4), Earth's energy imbalance, observed global warming, and climate sensitivity. Observed warming since 1880–1920 is 1.05 °C⁹ based on the linear fit to the 132-month running mean (Fig. 2b), which limits bias from short-term oscillations. Global warming between 1700 and 1800 as well as 1880 and 1920 was ~0.1 °C (Abram et al., 2016; Hawkins et al., 2017; Marcott et al., 2013), so 1750–2015 warming is ~1.15 °C. Taking climate sensitivity as 0.75 °C (W m⁻²)⁻¹ forcing, global warming of 1.15 °C implies that 1.55 W m⁻² of the total 2.5 W m⁻² forcing has been “used up” to cause observed warming. Thus, 0.95 W m⁻² forcing should remain to be responded to – i.e., the expected planetary energy imbalance is 0.95 W m⁻², which is reasonably consistent with the observed 0.75 ± 0.25 W m⁻². If we instead take the aerosol + surface albedo forcing as -1.5 W m⁻², as estimated by Hansen et al. (2005), the net climate forcing is 2.2 W m⁻² and the forcing not responded to is 0.65 W m⁻², which is also within the observational error of Earth's energy imbalance.

4.2 Slow climate feedbacks

Large glacial-to-interglacial climate oscillations occur on timescales of tens and hundreds of thousands of years, with atmospheric CO₂ amount and the size of ice sheets (and thus sea level) changing almost synchronously on these timescales (Masson-Delmotte et al., 2013). It is readily apparent that these climate cycles are due to small changes in Earth's orbit and the tilt of its spin axis, which alter the geographical and seasonal distribution of sunlight striking Earth.

⁹The IPCC (2013; p. 37 of Technical Summary) estimate of warming for 1880–2012 is 0.85 °C (range 0.65 to 1.06 °C). While within that range, our value is higher because (1) use of 4-year longer period, (2) warming in the past few years eliminates the effect on the 1970–present trend from a seeming 1998–2012 warming hiatus, and (3) the GISTEMP analysis has greater coverage of the large Arctic warming than the other analyses (Fig. TS.2, p. 39 of IPCC, 2013).

The large climate response is a result of two amplifying feedbacks: (1) atmospheric GHGs (mainly CO₂ but accompanied by CH₄ and N₂O), which increase as Earth warms and decrease as it cools (Ciais et al., 2013), thus amplifying the temperature change, and (2) the size of ice sheets, which shrink as Earth warms and grow as it cools, thus changing the amount of absorbed sunlight in the sense that also amplifies the climate change. For example, 20 000 years ago most of Canada and parts of the US were covered by an ice sheet, and sea level was about 130 m (~400 ft) lower than today. Global warming of ~5 °C between the last glacial maximum and the Holocene (Masson-Delmotte et al., 2013) is accounted for almost entirely by radiative forcing caused by decrease in ice sheet area and increase in GHGs (Lorius et al., 1990; Hansen et al., 2007).

The glacial–interglacial timescale is set by the timescale of the weak orbital forcings. Before addressing the crucial issue of the inherent timescale of slow feedbacks, we need to say more about the two dominant slow feedbacks, described above as ice sheets and GHGs.

The ice sheet feedback works mainly via the albedo (reflectivity) effect. A shrinking ice sheet exposes darker ground and warming darkens the ice surface by increasing the area and period with wet ice, thus increasing the ice grain size and increasing the surface concentration of light-absorbing impurities (Tedesco et al., 2016). The ice albedo effect is supplemented by a change in surface albedo in ice-free regions due to vegetation changes. This vegetation albedo effect provides a significant amplification of warming as Earth's temperature increases from its present climate state, because dark forests tend to replace tundra or sparse low-level vegetation in large areas of Eurasia and North America (Lunt et al., 2010).

The GHG feedback on glacial–interglacial timescales is 75–80 % from CO₂ change; N₂O and CH₄ account for 20–25 % (Lorius et al., 1990; Hansen et al., 2007; Masson-Delmotte et al., 2013). In simple terms, the ocean and land release more of these gases as the planet becomes warmer. Mechanisms that control GHG release as Earth warms, and GHG drawdown as Earth cools, are complex, including many processes that affect the distribution of carbon, among the ocean, atmosphere, and biosphere (Yu et al., 2016; Ciais et al., 2013, and references therein). Release of carbon from methane hydrates and permafrost contributed to climate change in past warm periods (Zachos et al., 2008; DeConto et al., 2012) and potentially could have a significant effect in the future (O'Connor et al., 2010; Schädel et al., 2016).

Paleoclimate data help assess the possible timescale for ice sheet change. Ice sheet size, judged from sea level, varies almost synchronously with temperature for the temporal resolution available in paleoclimate records, but Grant et al. (2012) find that sea level change lags temperature change by 1–4 centuries. Paleoclimate forcing, however, is both weak and very slow, changing on millennial timescales. Hansen (2005, 2007) argues on heuristic grounds that the much faster and stronger human-made climate forcing pro-

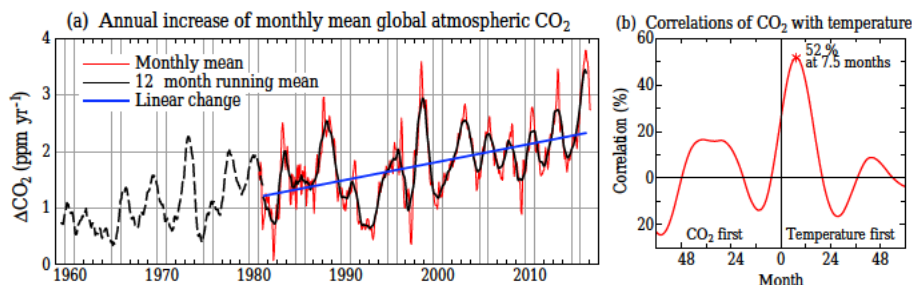


Figure 6. (a) Global CO₂ annual growth based on NOAA data (<http://www.esrl.noaa.gov/gmd/ccgg/trends/>). Dashed curve is for a single station (Mauna Loa). Red curve is monthly global mean relative to the same month of prior year; black curve is 12-month running mean of red curve. (b) CO₂ growth rate is highly correlated with global temperature, with the CO₂ change lagging global temperature change by 7–8 months.

jected this century with continued high fossil fuel emissions, equivalent to doubling atmospheric CO₂, would likely lead to substantial ice sheet collapse and multi-meter sea level rise on the timescale of a century. Modeling supports this conclusion, as Pollard et al. (2015) found that addition of hydro-fracturing and cliff failure to their ice sheet model not only increased simulated sea level rise from 2 to 17 m in response to 2 °C ocean warming but also accelerated the time for multi-meter change from several centuries to several decades. Ice sheet modeling of Applegate et al. (2015) explicitly shows that the timescale for large ice sheet melt decreases dramatically as the magnitude of warming increases. Hansen et al. (2016), based on a combination of climate modeling, paleo-data, and modern observations, conclude that continued high GHG emissions would likely cause multi-meter sea level rise within 50–150 years.

The GHG feedback plays a leading role in determining the magnitude of paleoclimate change and there is reason to suspect that it may already be important in modern climate. Rising temperatures increase the rate of CO₂ and CH₄ release from drying soils, thawing permafrost (Schädel et al., 2016; Schuur et al., 2015) and warming continental shelves (Kvenvolden, 1993; Judd et al., 2002), and affect the ocean carbon cycle as noted above. Crowther et al. (2016) synthesize results of 49 field experiments across North America, Europe and Asia, inferring that every 1 °C global mean soil surface warming can cause a 30 PgC soil carbon loss and suggesting that continued high fossil fuel emissions might drive 2 °C soil warming and a 55 PgC soil carbon loss by 2050. Although this analysis admits large uncertainty, such large soil carbon loss could wreak havoc with efforts to achieve the net soil and biospheric carbon storage that is likely necessary for climate stabilization, as we discuss in subsequent sections.

Recent changes of GHGs result mainly from industrial and agricultural emissions, but they also include any existing climate feedback effects. CO₂ and CH₄ are the largest forcings (Fig. 4), so it is especially important to examine their ongoing changes.

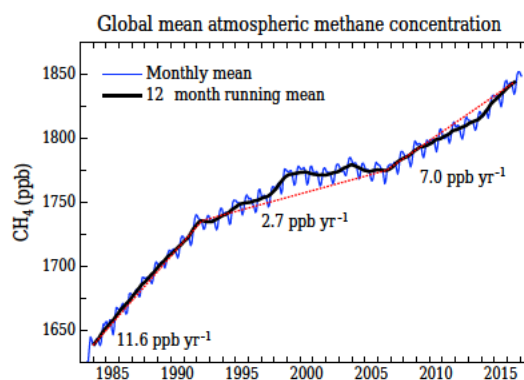


Figure 7. Global CH₄ from Dlugokencky (2016), NOAA/ESRL (http://www.esrl.noaa.gov/gmd/ccgg/trends_ch4/). End months for three indicated slopes are January 1984, May 1992, August 2006, and February 2017.

5 Observed CO₂ and CH₄ growth rates

Annual increase in atmospheric CO₂, averaged over a few years, grew from less than 1 ppm yr⁻¹ 50 years ago to more than 2 ppm yr⁻¹ today (Fig. 6), with global mean CO₂ now exceeding 400 ppm (Betts et al., 2016). Growth of atmospheric CO₂ is about half of fossil fuel CO₂ emissions as discussed in Appendix A8 and illustrated in Fig. A8. The large oscillations of annual growth are correlated with global temperature and with the El Niño/La Niña cycle, as discussed in Appendix A8. Recent global temperature anomalies peaked in February 2016, so as expected the CO₂ growth rate has been declining for the past several months (Fig. 6a).

Atmospheric CH₄ stopped growing between 1998 and 2006, indicating that its sources were nearly in balance with the atmospheric oxidation sink, but growth resumed in the past decade (Fig. 7). CH₄ growth averaged 10 ppb yr⁻¹ in 2014–2016, almost as fast as in the 1980s. Likely reasons for the recent increased growth of CH₄ are discussed in Appendix A8.

The continued growth of atmospheric CO₂ and reaccelerating growth of CH₄ raise important questions related to prospects for stabilizing climate. How consistent with reality are scenarios for phasing down climate forcing when tested by observational data? What changes to industrial and agricultural emissions are required to stabilize climate? We address these issues below.

6 GHG climate forcing growth rates and emission scenarios

Insight is obtained by comparing the growth rate of GHG climate forcing based on observed GHG amounts with past and present GHG scenarios. We examine forcings of IPCC Special Report on Emissions Scenarios (IPCC SRES, 2000) used in the 2001 AR3 and 2007 AR4 reports (Fig. 8a) and RCP scenarios (Moss et al., 2010; Meinshausen et al., 2011a) used in the 2013 IPCC AR5 report (Fig. 8b). We include the “alternative scenario” of Hansen et al. (2000) in which CO₂ and CH₄ emissions decline such that global temperature stabilizes near the end of the century.¹⁰ We use the same radiation equations for observed GHG amounts and scenarios, so errors in the radiation calculations do not alter the comparison. Equations for GHG forcings are from Table 1 of Hansen et al. (2000) with the CH₄ forcing using an efficacy factor 1.4 to include effects of CH₄ on tropospheric O₃ and stratospheric H₂O (Hansen et al., 2005).

The growth of GHG climate forcing peaked at $\sim 0.05 \text{ W m}^{-2} \text{ yr}^{-1}$ ($5 \text{ W m}^{-2} \text{ century}^{-1}$) in 1978–1988, then falling to a level 10–25 % below IPCC SRES (2000) scenarios during the first decade of the 21st century (Fig. 8a). The decline was due to (1) decline of the airborne fraction of CO₂ emissions (Fig. A8), (2) slowdown of CH₄ growth (Fig. 7), and (3) the Montreal Protocol, which initiated phase-out of the production of gases that destroy stratospheric ozone, primarily chlorofluorocarbons (CFCs).

The 2013 IPCC RCP scenarios (Fig. 8b) use observed GHG amounts up to 2005 and diverge thereafter, fanning out into an array of potential futures driven by assumptions about energy demand, fossil fuel prices, and climate policy, chosen to be representative of an extensive literature on possible emissions trajectories (Moss et al., 2010; van Vuuren et al., 2011; Meinshausen et al., 2011a, b). Numbers on the RCP scenarios (8.5, 6.0, 4.5 and 2.6) refer to the GHG climate forcing (W m^{-2}) in 2100.

Scenario RCP2.6 has the world moving into negative growth (net contraction) of GHG forcing 25 years from now (Fig. 8b), through rapid reduction of GHG emissions, along

¹⁰This scenario is discussed by Hansen and Sato (2004). CH₄ emissions decline moderately, producing a small negative forcing. CO₂ emissions (not captured and sequestered) are assumed to decline until in 2100 fossil fuel emissions just balance uptake of CO₂ by the ocean and biosphere. CO₂ emissions continue to decline after 2100.

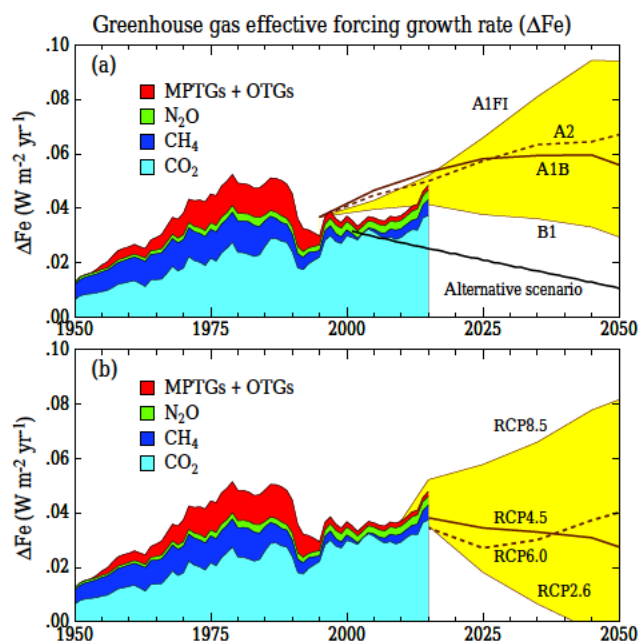


Figure 8. GHG climate forcing annual growth rate (ΔF_e) with historical data being 5-year running means, except 2015 is a 3-year mean. Panel (a) includes scenarios used in IPCC AR3 and AR4 reports, and panel (b) has AR5 scenarios. GHG amounts are from NOAA/ESRL Global Monitoring Division. O₃ changes are not fully included, as they are not well measured, but its tropospheric changes are partially included via the effective CH₄ forcing. Effective climate forcing (F_e), MPTGs and OTGs are defined in the Fig. 4 caption.

with CO₂ capture and storage. Already in 2015 there is a huge gap between reality and RCP2.6. Closing the gap (0.01 W m^{-2}) between actual growth of GHG climate forcing in 2015 and RCP2.6 (Fig. 8b), with CO₂ alone, would require extraction from the atmosphere of more than 0.7 ppm of CO₂ or 1.5 PgC due to the emissions gap of a single year (2015). We discuss the plausibility and estimated costs of scenarios with CO₂ extraction in Sect. 9.

As a complement to RCP scenarios, we define scenarios with focus on the dominant climate forcing, CO₂, with its changes defined simply by percent annual emission decrease or increase. Below (Sect. 10.1 and Appendix A13) we conclude that efforts to limit non-CO₂ forcings could keep their growth small or even slightly negative, so a focus on long-lived CO₂ is appropriate. Thus, for the non-CO₂ GHGs we use RCP6.0, a scenario with small changes of these gases. For CO₂ we consider rates -6 , -3 \% yr^{-1} , constant emissions, and $+2 \text{ \% yr}^{-1}$; emissions stop increasing in the $+2 \text{ \% yr}^{-1}$ case when they reach 25 Gt yr^{-1} (Fig. 9a). Scenarios with decreasing emissions are preceded by constant emissions for 2015–2020, in recognition that some time is required to achieve policy change and implementation. Note the similarity of RCP2.6 with -3 \% yr^{-1} , RCP4.5 with constant emissions, and RCP8.5 with $+2 \text{ \% yr}^{-1}$ (Fig. 9).

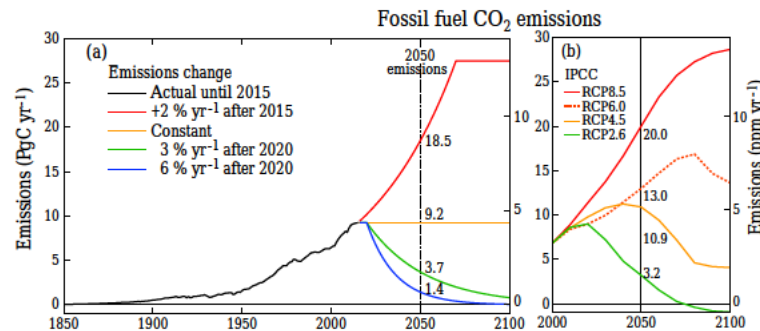


Figure 9. Fossil fuel emission scenarios. (a) Scenarios with simple specified rates of emission increase or decrease. (b) IPCC (2013) RCP scenarios. Note: 1 ppm atmospheric CO₂ is ~ 2.12 GtC.

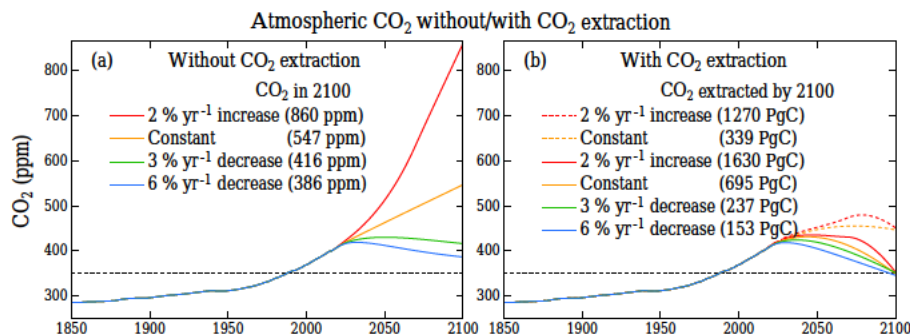


Figure 10. (a) Atmospheric CO₂ for Fig. 9a emission scenarios. (b) Atmospheric CO₂ including effect of CO₂ extraction that increases linearly after 2020 (after 2015 in +2 % yr⁻¹ case).

7 Future CO₂ for assumed emission scenarios

We must model Earth's carbon cycle, including ocean uptake of carbon, deforestation, forest regrowth and carbon storage in the soil, for the purpose of simulating future atmospheric CO₂ as a function of the fossil fuel emission scenario. Fortunately, the convenient dynamic-sink pulse-response function version of the well-tested Bern carbon cycle model (Joos et al., 1996) does a good job of approximating more detailed models, and it produces a good match to observed industrial-era atmospheric CO₂. Thus, we use this relatively simple model, described elsewhere (Joos et al., 1996; Kharecha and Hansen, 2008, and references therein), to examine the effect of alternative fossil fuel use scenarios on the growth or decline of atmospheric CO₂. Assumptions about emissions in the historical period are given in Appendix A9.

Figure 10a shows the simulated atmospheric CO₂ for the baseline emission cases (Fig. 9a). These cases do not include active CO₂ removal. Five additional cases including CO₂ removal (Fig. 10b) achieve atmospheric CO₂ targets of either 350 or 450 ppm in 2100, with cumulative removal amounts listed in parentheses (Fig. 10b). The rate of CO₂ extraction in all cases increases linearly from zero in 2010 to the value in 2100 that achieves the atmospheric CO₂ target (350 or 450 ppm). The amount of CO₂ that must be

extracted from the system exceeds the difference between the atmospheric amount without extraction and the target amount (e.g., constant CO₂ emissions and no extraction yield 547 ppm for atmospheric CO₂ in 2100), but to achieve a target of 350 ppm the required extraction is 328 ppm, not 547–350 = 197 ppm. The well-known reason (Cao and Caldeira, 2010) is that ocean outgassing increases and vegetation productivity and ocean CO₂ uptake decrease with decreasing atmospheric CO₂, as explored in a wide range of Earth system models (Jones et al., 2016).

8 Simulations of global temperature change

Analysis of future climate change, and policy options to alter that change, must address various uncertainties. One useful way to treat uncertainty is to use results of many models and construct probability distributions (Collins et al., 2013). Such distributions have been used to estimate the remaining budget for fossil fuel emissions for a specified likelihood of staying under a given global warming limit and to compare alternative policies for limiting climate forcing and global warming (Rogelj et al., 2016a, b).

Our aim here is a fundamental, transparent calculation that clarifies how future warming depends on the rate of fossil fuel emissions. We use best estimates for basic uncertain

quantities such as climate sensitivity. If these estimates are accurate, actual temperature should have about equal chances of falling higher or lower than the calculated value. Important uncertainties in projections of future climate change include climate sensitivity, the effects of ocean mixing and dynamics on the climate response function discussed below, and aerosol climate forcing. We provide all defining data so that others can easily repeat calculations with alternative choices.

One clarification is important for our present paper. The climate calculations in this section include only fast-feedbacks, which is also true for most climate simulations by the scientific community for IPCC (2013). This is not a limitation for the past, i.e., for the period 1850–present, because we employ measured GHG changes, which include any GHG change due to slow feedbacks. Also, we know that ice sheets did not change significantly in size in that period; there may have been some change in Greenland's albedo and expansion of forests in the Northern Hemisphere (Pearson et al., 2013), but those feedbacks so far have only a small global effect. However, this limitation to fast feedbacks may soon become important; it is only in the past few decades that global temperature rose above the prior Holocene range and only in the past 2 years that it shot far above that range. This limitation must be borne in mind when we consider the role of slow feedbacks in establishing the dangerous level of warming.

We calculate global temperature change T at time t in response to any climate forcing scenario using the Green's function (Hansen, 2008)

$$T(t) = \int_{1850}^t R(t-t') [dF(t')/dt'] dt' + F_v \times R(t-1850), \quad (1)$$

where $R(t')$ is the product of equilibrium global climate sensitivity and the dimensionless climate response function (percent of equilibrium response), $dF(t')/dt'$ is the annual increment of the net forcing, and F_v is the negative of the average volcanic aerosol forcing during the few centuries preceding 1850. $F_v \times R(t)$ is a small correction term that prevents average volcanic aerosol activity from causing a long-term cooling – i.e., it accounts for the fact that the ocean in 1850 was slightly cooled by prior volcanoes. We take $F_v = 0.3 \text{ W m}^{-2}$, the average stratospheric aerosol forcing for 1850–2015. The assumed-constant pre-1850 volcanic aerosols caused a constant cooling up to 1850, which gradually decreases to zero after 1850 and is replaced by post-1850 time-dependent volcanic cooling; note that $T(1850) = 0^\circ\text{C}$. We use the “intermediate” response function in Fig. 5 of Hansen et al. (2011), which gives good agreement with Earth's measured energy imbalance. The response function is 0.15, 0.55, 0.75 and 1 at years 1, 10, 100 and 2000 with these values connected linearly in log (year). This defined response function allows our results to be exactly reproduced, or altered with alternative choices for climate forcings, climate sensitivity and response function. Forcings that we use are tabulated in Appendix A10.

We use equilibrium fast-feedback climate sensitivity $0.75^\circ\text{C} (\text{W m}^{-2})^{-1}$ (3°C for $2 \times \text{CO}_2$). This is consistent with climate models (Collins et al., 2013; Flato et al., 2013) and paleoclimate evidence (Rohling et al., 2012a; Masson-Delmotte et al., 2013; Bindoff and Stott, 2013). We use RCP6.0 for the non-CO₂ GHGs.

We take tropospheric aerosol plus surface albedo forcing as -1.2 W m^{-2} in 2015, presuming the aerosol and albedo contributions to be -1 and -0.2 W m^{-2} , respectively. We assume a small increase this century as global population rises and increasing aerosol emission controls in emerging economies tend to be offset by increasing development elsewhere, so aerosol + surface forcing is -1.5 W m^{-2} in 2100. The temporal shape of the historic aerosol forcing curve (Table A10) is from Hansen et al. (2011), which in turn was based on the Novakov et al. (2003) analysis of how aerosol emissions have changed with technology change.

Historic stratospheric aerosol data (Table A10, annual version), an update of Sato et al. (1993), include moderate 21st century aerosol amounts (Bourassa et al., 2012). Future aerosols, for realistic variability, include three volcanic eruptions in the rest of this century with properties of the historic Agung, El Chichón and Pinatubo eruptions, plus a background stratospheric aerosol forcing of -0.1 W m^{-2} . This leads to mean stratospheric aerosol climate forcing of -0.3 W m^{-2} for remainder of the 21st century, similar to the mean stratospheric aerosol forcing for 1850–2015 (Table A10). Reconstruction of historical solar forcing (Coddington et al., 2016; Kopp et al., 2016), based on data in Fig. A11, is extended with an 11-year cycle.

Individual and net climate forcings for the several fossil fuel emission reduction rates are shown in Fig. 11a and c. Scenarios with linearly growing CO₂ extraction at rates required to yield 350 or 450 ppm airborne CO₂ in 2100 are in Fig. 11b and d. These forcings and the assumed climate response function define expected global temperature for the entire industrial era considered here (Fig. 12). We extended the global temperature calculations from 2100 to 2200 by continuing the $\% \text{ yr}^{-1}$ change in CO₂ emissions. In the cases with CO₂ extraction we kept the GHG climate forcing fixed in the 22nd century, which meant that large CO₂ extraction continued in cases with continuing high emissions; for example, the case with constant emissions that required extraction of 695 PgC during 2020–2100 required further extraction of $\sim 900 \text{ PgC}$ during 2100–2200. Even the cases with annual emission reductions -6 and $-3 \% \text{ yr}^{-1}$ required small extractions to compensate for back-flux of CO₂ from the ocean that accumulated there historically.

A stark summary of alternative futures emerges from Fig. 12a. If emissions grow $2 \% \text{ yr}^{-1}$, modestly slower than the $2.6 \% \text{ yr}^{-1}$ growth of 2000–2015, warming reaches $\sim 4^\circ\text{C}$ by 2100. Warming is about 2°C if emissions are constant until 2100. Furthermore, both scenarios launch

Earth onto a course of more dramatic change well beyond the initial $2\text{--}3^\circ\text{C}$ global warming, because (1) warming con-

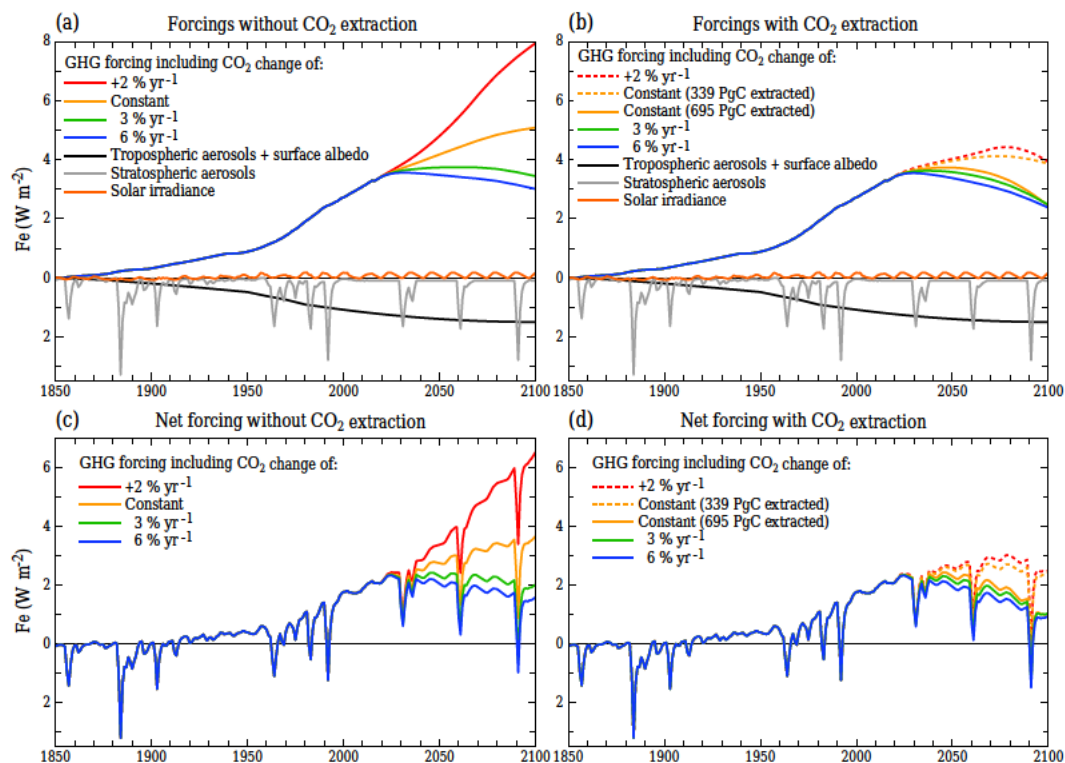


Figure 11. Climate forcings used in our climate simulations; F_e is effective forcing, as discussed in connection with Fig. 4. (a) Future GHG forcing uses four alternative fossil fuel emission growth rates. (b) GHG forcings are altered based on CO₂ extractions of Fig. 10.

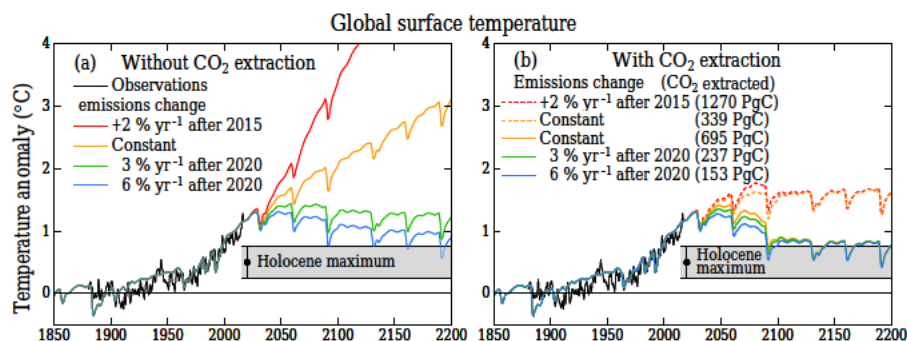


Figure 12. Simulated global temperature for Fig. 11 forcings. Observations as in Fig. 2. Temperature zero-point is the 1880–1920 mean temperature for both observations and model. Gray area is 2σ (95 % confidence) range for centennially smoothed Holocene maximum, but there is further uncertainty about the magnitude of the Holocene maximum, as noted in the text and discussed by Liu et al. (2014).

tinues beyond 2100 as the planet is still far from equilibrium with the climate forcing, and (2) warming of 2–3 °C would unleash strong slow feedbacks, including melting of ice sheets and increases of GHGs.

The most important conclusion from Fig. 12a is the proximity of results for the cases with emission reductions of 6 and 3 % yr^{−1}. Although Hansen et al. (2013a) called for emission reduction of 6 % yr^{−1} to restore CO₂ to 350 ppm by 2100, that rate of reduction may have been regarded as implausibly steep by a federal court in 2012, when it declined

to decide whether the US was violating the public trust by causing or contributing to dangerous climate change (Alec L. v. Jackson, 2012). Such a concern is less pressing for emission reductions of 3 % yr^{−1}. Note that reducing global emissions at a rate of 3 % yr^{−1} (or more steeply) maintains global warming at less than 1.5 °C above preindustrial temperature.

However, end-of-century temperature still rises 0.5 °C or more above the prior Holocene maximum with consequences for slow feedbacks that are difficult to foresee. Desire to minimize sea level rise spurs the need to get global tem-

perature back into the Holocene range. That goal preferably should be achieved on the timescale of a century or less, because paleoclimate evidence indicates that the response time of sea level to climate change is 1–4 centuries (Grant et al., 2012, 2014) for natural climate change, and if anything the response should be faster to a stronger, more rapid human-made climate forcing. The scenarios that reduce CO₂ to 350 ppm succeed in getting temperature back close to the Holocene maximum by 2100 (Fig. 12b), but they require extractions of atmospheric CO₂ that range from 153 PgC in the scenario with 6 % yr⁻¹ emission reductions to 1630 PgC in the scenario with +2 % yr⁻¹ emission growth.

Scenarios ranging from constant emissions to +2 % yr⁻¹ emissions growth can be made to yield 450 ppm in 2100 via extraction of 339–1270 PgC from the atmosphere (Fig. 10b). However, these scenarios still yield warming more than 1.5 °C above the preindustrial level (more than 1 °C above the early Holocene maximum). Consequences of such warming and the plausibility of extracting such huge amounts of atmospheric CO₂ are considered below.

9 CO₂ extraction: estimated cost and alternatives

Extraction of CO₂ from the air, also called negative emissions or carbon dioxide removal (CDR), is required if large, long-term excursion of global temperature above its Holocene range is to be averted, as shown above. In estimating the cost and plausibility of CO₂ extraction we distinguish between (1) carbon extracted from the air by improved agricultural and forestry practices, and (2) additional “technological extraction” by intensive negative emission technologies.

We assume that improved practices will aim at optimizing agricultural and forest carbon uptake via relatively natural approaches, compatible with the land delivering a range of ecosystem services (Smith, 2016; Smith et al., 2016). In contrast, proposed technological extraction and storage of CO₂ generally does not have co-benefits and remains unproven at relevant scales (NAS, 2015a). Improved practices have local benefits in agricultural yields and forest products and services (Smith et al., 2016), which may help minimize net costs. The intended nationally determined contributions (INDCs) submitted by 189 countries include carbon drawdown through land use plans (United Nations, 2016) with aggregate removal rate of $\sim 2 \text{ PgCO}_2 \text{ yr}^{-1}$ ($\sim 0.55 \text{ PgC yr}^{-1}$) after 2020. These targets are not the maximum possible drawdown, as they are only about a third of amounts Smith (2016) estimated as “realistic”.

Developed countries recognize a financial obligation to less developed countries that have done little to cause climate change (Paris Agreement 2015).¹¹ We suggest that at least part of developed country support should be chan-

neled through agricultural and forestry programs, with continual evaluation and adjustment to reward and encourage progress (Bustamante et al., 2014). Efforts to minimize non-CO₂ GHGs can be included in the improved practices program.

Here, we do not estimate the cost of CO₂ extraction obtained via the “improved agricultural and forestry practices”,¹² because that would be difficult given the range of activities it is likely to entail, and because it is not necessary for reaching the conclusion that total CO₂ extraction costs will be high due to the remaining requirements for technological extraction. However, we do estimate the potential magnitude of CO₂ extraction that might be achievable via such improved practices, as that is needed to quantify the required amount of “technological extraction” of CO₂. Finally, we compare costs of extraction with estimated costs of mitigation measures that could limit the magnitude of required extraction, while admitting that there is large uncertainty in both extraction and mitigation cost estimates.

9.1 Estimated cost of CO₂ extraction

Hansen et al. (2013a) suggested a goal of 100 PgC extraction in the 21st century, which would be almost as large as estimated net emissions from historic deforestation and land use (Ciais et al., 2013). Hansen et al. (2013a) assumed that 100 PgC was about as much as could be achieved via relatively natural reforestation and afforestation (Canadell and Raupach, 2008) and improved agricultural practices that increase soil carbon (Smith, 2016).

Here we first reexamine whether a concerted global effort on carbon storage in forests and soil might have potential to provide a carbon sink substantially larger than 100 PgC this century. Smith et al. (2016) estimate that reforestation and afforestation together have carbon storage potential of about 1.1 PgC yr^{-1} . However, as forests mature, their uptake of atmospheric carbon decreases (termed “sink saturation”), thereby limiting CO₂ drawdown. Taking 50 years as the average time for tropical, temperate and boreal trees to experience sink saturation yields 55 PgC as the potential storage in forests this century.

but with the funds directed to the international “improved practices” programs.

¹²A comment is in order about the relation of “improved agricultural and forestry practices” with an increased role of biofuels in climate mitigation. Agriculture, forestry and other land use have potential for important contributions to climate change mitigation (Smith et al., 2014). However, first-generation biofuel production and use (which is usually based on edible portions of feedstocks, such as starch) is not inherently carbon-neutral; indeed, it is likely carbon-positive, as has been illustrated in specific quantitative analyses for corn ethanol in the United States (Searchinger et al., 2008; DeCicco et al., 2016). The need for caution regarding the role of biofuels in climate mitigation is discussed by Smith et al. (2014).

¹¹ Another conceivable source of financial support for CO₂ drawdown might be legal settlements with fossil fuel companies, analogous to penalties that courts have imposed on tobacco companies,

Smith (2016) shows that soil carbon sequestration and soil amendment with biochar compare favorably with other negative emission technologies with less impact on land use, water use, nutrients, surface albedo, and energy requirements, but understanding of and literature on biochar are limited (NAS, 2015a). Smith (2016) estimates that soil carbon sequestration has potential to store 0.7 PgC yr⁻¹. However, as with carbon storage in forest, there is a saturation effect. A commonly used 20-year saturation time (IPCC, 2006) would yield 14 PgC soil carbon storage, while an optimistic 50-year saturation time would yield 35 PgC. Use of biochar to improve soil fertility provides additional carbon storage of up to 0.7–1.8 PgC yr⁻¹ (Woelf et al., 2010; Smith, 2016). Larger industrial-scale biochar carbon storage is conceivable, but belongs in the category of intensive negative emission technologies, discussed below, whose environmental impacts and costs require scrutiny. We conclude that 100 PgC is an appropriate ambitious estimate for potential carbon extraction via a concerted global-scale effort to improve agricultural and forestry practices with carbon drawdown as a prime objective.

Intensive negative emission technologies that could yield greater CO₂ extraction include (1) burning of biofuels, most commonly at power plants, with capture and sequestration of resulting CO₂ (Creutzig et al., 2015), and (2) direct air capture of CO₂ and sequestration (Keith, 2009; NAS, 2015a), and (3) grinding and spreading of minerals such as olivine to enhance geological weathering (Taylor et al., 2016). However, energy, land and water requirements of these technologies impose economic and biophysical limits on CO₂ extraction (Smith et al., 2016).

The popular concept of bioenergy with carbon capture and storage (BECCS) requires large areas and high fertilizer and water use, and may compete with other vital land use such as agriculture (Smith, 2016). Costs estimates are ~USD 150–350 (tC)⁻¹ for crop-based BECCS (Smith et al., 2016).

Direct air capture has more limited area and water needs than BECCS and no fertilizer requirement, but it has high energy use, has not been demonstrated at scale, and cost estimates exceed those of BECCS (Socolow et al., 2011; Smith et al., 2016). Keith et al. (2006) have argued that, with strong research and development support and industrial-scale pilot projects sustained over decades, it may be possible to achieve costs ~USD 200 (tC)⁻¹, thus comparable to BECCS costs; however, other assessments are higher, reaching USD 1400–3700 (tC)⁻¹ (NAS, 2015a).

Enhanced weathering via soil amendment with crushed silicate rock is a candidate negative emission technology that also limits coastal ocean acidification as chemical products liberated by weathering increase land–ocean alkalinity flux (Kohler et al., 2010; Taylor et al., 2016). If two-thirds of global croplands were amended with basalt dust, as much as 1–3 PgC yr⁻¹ might be extracted, depending on application rate (Taylor et al., 2016), but energy costs of mining, grinding and spreading likely reduce this by 10–25 %

(Moosdorf et al., 2014). Such large-scale enhanced weathering is speculative, but potential co-benefits for temperate and tropical agroecosystems could affect its practicality, and may put some enhanced weathering into the category of improved agricultural and forestry practices. Benefits include crop fertilization that increases yield and reduces use and cost of other fertilizers, increasing crop protection from insect herbivores and pathogens thus decreasing pesticide use and cost, neutralizing soil acidification to improve yield, and suppression of GHG (N₂O and CO₂) emissions from soils (Edwards et al., 2017; Kantola et al., 2017). Against these benefits, we note potential negative impacts of air and water pollution caused by the mining, including downstream environmental consequences if silicates are washed into rivers and the ocean, causing increased turbidity, sedimentation, and pH, with unknown impacts on biodiversity (Edwards et al., 2017). Cost of enhanced weathering might be reduced by deployment with reforestation and afforestation and with crops used for BECCS; this could significantly enhance the combined carbon sequestration potential of these methods.

For cost estimates, we first consider restoration of airborne CO₂ to 350 ppm in 2100 (Fig. 10b), which would keep global warming below 1.5 °C and bring global temperature back close to the Holocene maximum by the end of the century (Fig. 12b). This scenario keeps the temperature excursion above the Holocene level small enough and brief enough that it has the best chance of avoiding ice sheet instabilities and multi-meter sea level rise (Hansen et al., 2016). If fossil fuel emission phasedown of 6 % yr⁻¹ had begun in 2013, as proposed by Hansen et al. (2013a), this scenario would have been achieved via the hypothesized 100 PgC carbon extraction from improved agricultural and forestry practices.

We examine here scenarios with 6 and 3 % yr⁻¹ emission reduction starting in 2021, as well as scenarios with constant emissions and +2 % yr⁻¹ emission growth starting in 2016 (Figs. 10b and 12b). The –6 and –3 % yr⁻¹ scenarios leave a requirement to extract 153 and 237 PgC from the air during this century. Constant emission and +2 % yr emission scenarios yield extraction requirements of 695 and 1630 PgC to reach 350 ppm CO₂ in 2100.

Total CO₂ extraction requirements for these scenarios are given in Fig. 10. Cost estimates here for extraction use amounts 100 Pg less than in Fig. 10 under assumption that 100 PgC can be stored via improved agricultural and forestry practices. Shortfall of this 100 PgC goal will increase our estimated costs accordingly, as will the cost of the improved agricultural and forestry program.

Given a CO₂ extraction cost of USD 150–350 (tC)⁻¹ for intensive negative emission technologies (Fig. 3f of Smith et al., 2016), the 53 PgC additional extraction required for the scenario with 6 % yr⁻¹ emission reduction would cost USD 8–18.5 trillion, thus USD 100–230 billion per year if spread uniformly over 80 years. We cannot rule out possible future reduction in CO₂ extraction costs, but given the energy requirements for removal and the already optimistic

lower limit on our estimate, we do not speculate further about potential cost reduction.

In contrast, continued high emissions, between constant emissions and $+2\% \text{ yr}^{-1}$, would require additional extraction of 595–1530 PgC (Fig. 10b) at a cost of USD 89–535 trillion or 1.1–6.7 trillion per year over 80 years.¹³ Such extraordinary cost, along with the land area, fertilizer and water requirements (Smith et al., 2016) suggest that, rather than the world being able to buy its way out of climate change, continued high emissions would likely force humanity to live with climate change running out of control with all the consequences that would entail.

9.2 Mitigation alternative

High costs of CO₂ extraction raise the question of how these costs compare to the alternative: taking actions to mitigate climate change by reducing fossil fuel CO₂ emissions. The Stern Review (Stern, 2006; Stern and Taylor, 2007) used expert opinion to produce an estimate for the cost of reducing emissions to limit global warming to about 2 °C. Their central estimate was 1 % of gross domestic product (GDP) per year, thus about USD 800 billion per year. They argued that this cost was much less than likely costs of future climate damage if high emissions continue, unless we apply a high “discount rate” to future damage, which has ethical implications in its treatment of today's young people and future generations. However, their estimated uncertainty of the cost is $\pm 3\%$, i.e., the uncertainty is so large as to encompass GDP gain.

Hsu (2011) and Ackerman and Stanton (2012) argue that economies are more efficient if the price of fossil fuels better reflects costs to society, and thus GDP gain is likely with an increasing carbon price. Mankiw (2009) similarly suggests that a revenue-neutral carbon tax is economically beneficial. Hansen (2009, 2014) advocates an approach in which a gradually rising carbon fee is collected from the fossil fuel industry with the funds distributed uniformly to citizens. This approach provides incentives to business and the public that drive the economy toward energy efficiency, conservation, renewable energies and nuclear power. An economic study of this carbon-fee-and-dividend policy in the US (Nystrom and Luckow, 2014) supports the conclusion that GDP increases as the fee rises steadily. These studies refute the common argument that environmental protection is damaging to economic prosperity.

We can also compare CO₂ extraction cost with the cost of carbon-free energy infrastructure. Global energy consumption in 2015 was 12.9 Gtoe¹⁴ with coal providing 30 % of

global energy and almost 45 % of global fossil fuel CO₂ emissions (BP, 2016). Most coal use, and its increases, is in Asia, especially China and India. Carbon-free replacement for coal energy is expected to be some combination of renewables (including hydropower) and nuclear power. China is leading the world in installation of wind, solar and nuclear power, with new nuclear power in 2015 approximately matching the sum of new solar and wind power (BP, 2016). For future decarbonization of electricity it is easiest to estimate the cost of the nuclear power component, because nuclear power can replace coal for baseload electricity without the need for energy storage or major change to national electric grids. Recent costs of Chinese and South Korean light water reactors are in the range USD 2000–3000 per kilowatt (Chinese Academy of Engineering, 2015; Lovering et al., 2016). Although in some countries reactor costs stabilized or declined with repeated construction of the same reactor design, in others costs have risen for a variety of reasons (Lovering et al., 2016). Using USD 2500 per kilowatt as reactor cost and assuming 85 % capacity factor (percent uptime for reactors) yields a cost of USD 10 trillion to produce 20 % of present global energy use (12.9 Gtoe). Note that 20 % of current global energy use is a huge amount (Fig. 13), exceeding the sum of present hydropower (6.8 %), nuclear (4.4 %), wind (1.4 %), solar (0.4 %), and other renewable energies (0.9 %).

We do not suggest that new nuclear power plants on this scale will or necessarily should be built. Rather we use this calculation to show that mitigation costs are not large in comparison to costs of extracting CO₂ from the air. Renewable energy costs have fallen rapidly in the past 2–3 decades with the help of government subsidies, especially renewable portfolio standards that require utilities to achieve a specified fraction of their power from renewable sources. Yet fossil fuel use continues to be high, at least in part because fossil fuel prices do not include their full cost to society. Rapid and economic movement to non-fossil energies would be aided by a rising carbon price, with the composition of energy sources determined by competition among all non-fossil energy sources, as well as energy efficiency and conservation. Sweden provides a prime example: it has cut per capita emissions by two-thirds since the 1990s while doubling per capita income in a capitalistic framework that embodies free-market principles (Pierrehumbert, 2016).

Mitigation of climate change deserves urgent priority. We disagree with assessments such as “the world will probably have only two choices if it wants to stay below 1.5 °C of warming. It must either deploy carbon dioxide removal on an enormous scale or use solar geoengineering” (Parker and Geden, 2016). While we reject 1.5 °C as a safe target – it is likely warmer than the Eemian and far above the Holocene range – Fig. 12 shows that fossil fuel emission reduction of $3\% \text{ yr}^{-1}$ beginning in 2021 yields maximum global warming $\sim 1.5\text{ °C}$ for climate sensitivity 3 °C for $2 \times \text{CO}_2$, with neither CO₂ removal nor geoengineering. These calculations

¹³For reference, the United Nations global peacekeeping budget is about USD 10 billion per year. National military budgets are larger: the 2015 USA military budget was USD 596 billion and the global military budget was USD 1.77 trillion (SIPRI, 2016).

¹⁴Gtoe is gigatons oil equivalent; 1 Gtoe, is 41.868 EJ (exajoule = 10^{18} J) or 11 630 TWh (terawatt hours).

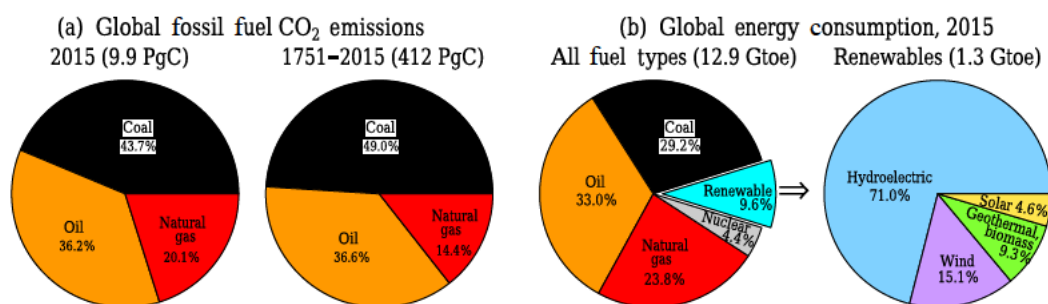


Figure 13. (a) Global fossil fuel emissions data from Boden et al. (2017) for 1751–2014 are extended to 2015 using BP (2016) data. (b) Global primary energy consumption data from BP (2016); energy accounting method is the substitution method (Macknick, 2011).

show that mitigation – reduction of fossil fuel emissions – is very effective. We know no persuasive scientific reason to a priori reject as implausible a rapid phasedown of fossil fuel emissions.

10 Non-CO₂ GHGs, aerosols and purposeful climate intervention

10.1 Non-CO₂ GHGs

The annual increment in GHG climate forcing is growing, not declining. The increase is more than 20 % in just the past 5 years (Fig. 8). Resurgence of CH₄ growth is partly responsible, but CO₂ is by far the largest contributor to growth of GHG climate forcing (Fig. 8). Nevertheless, given the difficulty and cost of reducing CO₂, we must ask about the potential for reducing non-CO₂ GHGs. Could realistic reductions of these other gases substantially alter the CO₂ abundance required to meet a target climate forcing?

We conclude, as discussed in Appendix A13, that a net decrease in climate forcing by non-CO₂ GHGs of perhaps -0.25 W m^{-2} relative to today is plausible, but we must note that this is a dramatic change from the growing abundances, indeed accelerating growth, of these gases today. Achievement of this suggested negative forcing requires (i) successful completion of planned phase-out of MPTGs (-0.23 W m^{-2}), (ii) absolute reductions of CH₄ forcing by 0.12 W m^{-2} from its present value, and (iii) N₂O forcing increasing by only 0.1 W m^{-2} . Achieving this net negative forcing of -0.25 W m^{-2} for non-CO₂ gases would allow CO₂ to be 365 ppm, rather than 350 ppm, while yielding the same total GHG forcing. Absolute reduction of non-CO₂ gases is thus helpful but does not alter the requirement for rapid fossil fuel emission reductions. Moreover, this is an optimistic scenario that is unlikely to occur in the absence of a reduction of CO₂, which is needed to limit global warming and thus avoid amplifying GHG feedbacks.

10.2 Aerosols and purposeful climate intervention

Human-made aerosols today are believed to cause a large, albeit poorly measured, negative climate forcing (Fig. 4) of the order of -1 W m^{-2} with uncertainty of at least 0.5 W m^{-2} (Fig. 7.19, Boucher et al., 2013). Fossil fuel burning is only one of several human-caused aerosol sources (Boucher et al., 2013). Given that human population continues to grow, and that human-caused climate effects such as increased desertification can lead to increased aerosols, we do not anticipate a large reduction in the aerosol cooling effect, even if fossil fuel use declines. Rao et al. (2017) suggest that future aerosol amount will decline due to technological advances and global action to control emissions. We are not confident of such a decline, as past controls have been at least matched by increasing emissions in developing regions, and global population continues to grow. However, to the extent that Rao et al. (2017) projections are borne out, they will only strengthen the conclusions of our present paper about the threat of climate change for young people and the burden of decreasing GHG amounts in the atmosphere.

Recognition that aerosols have a cooling effect, combined with the difficulty of restoring CO₂ to 350 ppm or less, inevitably raises the issue of purposeful climate intervention, also called geoengineering, and specifically solar radiation management (SRM). The cooling mechanism receiving greatest attention is injection of SO₂ into the stratosphere (Budyko, 1974; Crutzen, 2006), thus creating sulfuric acid aerosols that mimic the effect of volcanic aerosol cooling. That idea and others are discussed in a report of the US National Academy of Sciences (NAS, 2015b) and references therein. We limit our discussion to the following summary comments.

Such purposeful intervention in nature, an attempt to mitigate effects of one human-made pollutant with another, raises additional practical and ethical issues. Stratospheric aerosols, for example, could deplete stratospheric ozone and/or modify climate and precipitation patterns in ways that are difficult to predict with confidence, while doing nothing to alleviate ocean acidification caused by rising CO₂; we note that Keith et al. (2016) suggest alternative aerosols that would limit the

impact on ozone. However, climate intervention also raises issues of global governance, and introduces the possibility of sudden global consequences if aerosol injection is interrupted (Boucher et al., 2013). Despite these issues, it is apparent that cooling by aerosols, or other methods that alter the amount of sunlight absorbed by Earth, could be effective more quickly than the difficult process of removing CO₂ from the air. Thus, we agree with the NAS (2015b) conclusion that research is warranted to better define the climate, economic, political, ethical, legal and other dimensions of potential climatic interventions.

In summary, although research on climate interventions is warranted, the possibility of geoengineering can hardly be seen as alleviating the overall burden being placed on young people by continued high fossil fuel emissions. We concur with the assessment (NAS, 2015b) that such climate interventions are no substitute for the reduction of carbon dioxide emissions needed to stabilize climate and avoid deleterious consequences of rapid climate change.

11 Discussion

Global temperature is now far above its range during the preindustrial Holocene, attaining at least the warmth of the Eemian period, when sea level reached +6–9 m relative to today. Also, Earth is now out of energy balance, implying that more warming will occur, even if atmospheric GHG amounts are stabilized at today's level. Furthermore, the GHG climate forcing is not only still growing, the growth rate is actually accelerating, as shown in Fig. 14, which is extracted from data in our Fig. 8.

This summary, based on real-world data for temperature, planetary energy balance, and GHG changes, differs from a common optimistic perception of progress toward stabilizing climate. That optimism may be based on the lowered warming target in the Paris Agreement (2015), slowdown in the growth of global fossil fuel emissions in the past few years (Fig. A1), and falling prices of renewable energies, but the hard reality of the climate physics emerges in Figs. 2, 5, 8 and 14. Although the scenarios employed in climate simulations for the most recent IPCC study (AR5) include cases with rapidly declining GHG growth, the scenarios do nothing to alter reality, which reveals that GHG growth rates not only remain high, they are accelerating.

The need for prompt action implied by these realities may not be a surprise to the relevant scientific community, because paleoclimate data revealed high climate sensitivity and the dominance of amplifying feedbacks. However, effective communication with the public of the urgency to stem human-caused climate change is hampered by the inertia of the climate system, especially the ocean and the ice sheets, which respond rather slowly to climate forcings, thus allowing future consequences to build up before broad public concern awakens. Some effects of human-caused global warm-

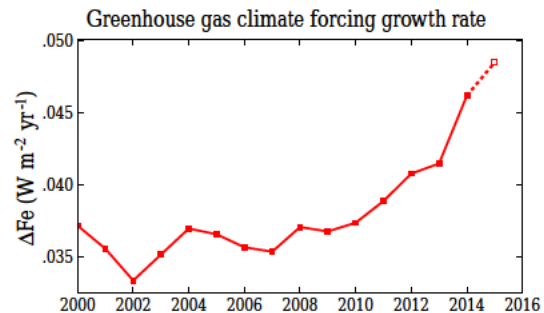


Figure 14. Recent growth rate of total GHG effective climate forcing; points are 5-year running means, except for 2015, which is a 3-year mean. See Fig. 8 for individual gases.

ing are now unavoidable, but is it inevitable that sea level rise of many meters is locked in, and, if so, on what timescale? Precise unequivocal answers to such questions are not possible. However, useful statements can be made.

First, the inertia and slow response of the climate system also allow the possibility of actions to limit the climate response by reducing human-caused climate forcing in coming years and decades. Second, the response time itself depends on how strongly the system is being forced; specifically, the response might be much delayed with a weaker forcing.

For example, studies suggesting multi-meter sea level rise in a century assume continued high fossil fuel emissions this century (Hansen et al., 2016) or at least a 2 °C SST increase (DeConto and Pollard, 2016). Ice sheet response time decreases rapidly in models as the forcing increases, because processes such as hydrofracturing and collapse of marine-terminating ice cliffs spur ice sheet disintegration (Pollard et al., 2015). All amplifying feedbacks, including atmospheric water vapor, sea ice cover, soil carbon release and ice sheet melt could be reduced by rapid emissions phasedown. This would reduce the risk of climate change running out of humanity's control and provide time to assess the climate response, develop relevant technologies, and consider further purposeful actions to limit and/or adapt to climate change.

Concern exists that large sea level rise may be inevitable, because of numerous ice streams on Antarctica and Greenland with inward-sloping beds (beds that deepen upstream) subject to runaway marine ice sheet instability (Mercer, 1978; Schoof, 2007, 2010). Some ice stream instabilities may already have been triggered (Rignot et al., 2014), but the number of ice streams affected and the timescale of their response may differ strongly depending on the magnitude of the forcing (DeConto and Pollard, 2016). Sea level rise this century of say half a meter to a meter, which may be inevitable even if emissions decline, would have dire consequences, yet these are dwarfed by the humanitarian and economic disasters that would accompany sea level rise of several meters (McGranahan et al., 2007). Given the increasing proportion of global population living in coastal areas (Hal-

legatte et al., 2013), there is potential for forced migrations of hundreds of millions of people, dwarfing prior refugee humanitarian crises, challenging global governance (Biermann and Boas, 2010) and security (Gemenne et al., 2014).

Global temperature is a useful metric, because increasing temperature drives amplifying feedbacks. Global ocean temperature is a major factor affecting ice sheet size, as indicated by both model studies (Pollard et al., 2015) and paleoclimate analyses (Overpeck et al., 2006; Hansen et al., 2016). Eemian ocean warmth, probably not more than about +0.7 °C warmer than preindustrial conditions (McKay et al., 2011; Masson-Delmotte et al., 2013; Sect. 2.2 above), corresponding to global warmth about +1 °C relative to preindustrial, led to sea level 6–9 m higher than today. This implies that, in the long run, the El Niño-elevated 2016 temperature of +1.3 °C relative to preindustrial temperature, and even the (+1.05 °C) underlying trend to date without the El Niño boost, is probably too high for maintaining our present coastlines.

We conclude that the world has already overshoot appropriate targets for GHG amount and global temperature, and we thus infer an urgent need for (1) rapid phasedown of fossil fuel emissions, (2) actions that draw down atmospheric CO₂, and (3) actions that, at minimum, eliminate net growth of non-CO₂ climate forcings. These tasks are formidable and, with the exception of the Montreal Protocol agreement on hydrofluorocarbons (HFCs) that will halt the growth of their climate forcing (Appendix A13), they are not being pursued globally. Actions at citizen, city, state and national levels to reduce GHG emissions provide valuable experience and spur technical developments, but without effective global policies the impact of these local efforts is reduced by the negative feedback caused by reduced demand for and price of fossil fuels.

Our conclusion that the world has overshoot appropriate targets is sufficiently grim to compel us to point out that pathways to rapid emission reductions are feasible. Peters et al. (2013) note that Belgium, France and Sweden achieved emission reductions of 4–5 % yr⁻¹ sustained over 10 or more years in response to the oil crisis of 1973. These rates were primarily a result of nuclear power build programs, which historically has been the fastest route to carbon-free energy (Fig. 2 of Cao et al., 2016). These examples are an imperfect analogue, as they were driven by a desire for energy independence from oil, but present incentives are even more comprehensive. Peters et al. (2013) also note that a continuous shift from coal to natural gas led to sustained reductions of 1–2 % yr⁻¹ in the UK in the 1970s and in the 2000s, 2 % yr⁻¹ in Denmark in 1990–2000s, and 1.4 % yr⁻¹ in the USA since 2005. Furthermore, these examples were not aided by the economy-wide effect of a rising carbon fee or tax (Hsu, 2011; Ackerman and Stanton, 2012; Hansen, 2014), which encourages energy efficiency and carbon-free energies.

In addition to CO₂ emission phase-out, large CO₂ extraction from the air is needed and a halt of growth of non-CO₂

climate forcings to achieve the temperature stabilization of our scenarios. Success of both CO₂ extraction and non-CO₂ GHG controls requires a major role for developing countries, given that they have been a large source of recent deforestation (IPCC, 2013) and have a large potential for reduced emissions. Ancillary benefits of the agricultural and forestry practices needed to achieve CO₂ drawdown, such as improved soil fertility, advanced agricultural practices, forest products, and species preservation, are of interest to all nations. Developed nations have a recognized obligation to assist nations that have done little to cause climate change yet suffer some of the largest climate impacts. If economic assistance is made partially dependent on verifiable success in carbon drawdown and non-CO₂ mitigation, this will provide incentives that maximize success in carbon storage. Some activities, such as soil amendments that enhance weathering, might be designed to support both CO₂ and other GHG drawdown.

Considering our conclusion that the world has overshoot the appropriate target for global temperature, and the difficulty and perhaps implausibility of negative emissions scenarios, we would be remiss if we did not point out the potential contribution of demand-side mitigation that can be achieved by individual actions as well as by government policies. Numerous studies (e.g. Hedenhus et al., 2014; Popp et al., 2010) have shown that reduced ruminant meat and dairy products is needed to reduce GHG emissions from agriculture, even if technological improvements increase food yields per unit farmland. Such climate-beneficial dietary shifts have also been linked to co-benefits that include improved sustainability and public health (Bajzelj et al., 2014; Tilman and Clark, 2014). Similarly, Working Group 3 of IPCC (2014) finds “robust evidence and high agreement” that demand-side measures in the agriculture and land use sectors, especially dietary shifts, reduced food waste, and changes in wood use have substantial mitigation potential, but they remain under-researched and poorly quantified.

There is no time to delay. CO₂ extraction required to achieve 350 ppm CO₂ in 2100 was ~100 PgC if 6 % yr⁻¹ emission reductions began in 2013 (Hansen et al., 2013a). Required extraction is at least ~150 PgC in our updated scenarios, which incorporate growth of emissions in the past 4 years and assume that emissions will continue at approximately current levels until a global program of emission reductions begins in 4 years (in 2021 relative to 2020; see Figs. 9 and 10 for reduction rates). The difficulty of stabilizing climate was thus markedly increased by a delay in emission reductions of 8 years, from 2013 to 2021. Nevertheless, if rapid emission reductions are initiated soon, it is still possible that at least a large fraction of required CO₂ extraction can be achieved via relatively natural agricultural and forestry practices with other benefits. On the other hand, if large fossil fuel emissions are allowed to continue, the scale and cost of industrial CO₂ extraction, occurring in conjunction with a deteriorating climate and costly dislocations, may

become unmanageable. Simply put, the burden placed on young people and future generations may become too heavy to bear.

Data availability. Data used to create all the figures are available at <https://doi.org/10.5281/zenodo.823301> (Hansen et al., 2017). Our Eq. (1) is used to compute the temperature change in Fig. 12. Continual updates of the data are available at http://www.columbia.edu/~mhs119/Burden_figures/.

Appendix A: Additional figures, tables and explanatory information

A1 Fossil fuel CO₂ emissions

CO₂ emissions from fossil fuels in 2015 were only slightly higher than in 2014 (Fig. A1). Such slowdowns are common, usually reflecting the global economy. Given rising global population and the fact that nations such as India are still at early stages of development, the potential exists for continued emissions growth. Fundamental changes in energy technology are needed for the world to rapidly phase down fossil fuel emissions.

Emissions are growing rapidly in emerging economies; while growth slowed in China in the past 2 years, emissions remain high (Fig. 1). The Kyoto Protocol (1997), a policy instrument of the Framework Convention (United Nations, 1992), spurred emission reductions in some nations, and the collapse of the Soviet Union caused a large decrease in emissions by Russia (Fig. 1b). However, growth of international ship and air emissions (Fig. 1b) largely offset these reductions and the growth rate of global emissions actually accelerated from 1.5 % yr⁻¹ in 1973–2000 to ~2.5 % yr⁻¹ after 2000 (Fig. A1). China is now the largest source of fossil fuel emissions, followed by the US and India, but on a per capita historical basis the US is 10 times more accountable than China and 25 times more accountable than India for the increase in atmospheric CO₂ above its preindustrial level (Hansen and Sato, 2016). Tabular data for Figs. 1 and A1 are available on the web page <http://www.columbia.edu/~mhs119/Burden>.

A2 Transient climate response to cumulative CO₂ emissions (TCRE)

The transient climate response (TCR), defined as the global warming at year 70 in response to a 1 % yr⁻¹ CO₂ increase, for our simple Green's function climate model is 1.89 °C with energy imbalance of 1.52 W m⁻² at that point; this TCR is in the middle of the range reported in the IPCC AR5 report (IPCC, 2013). We calculate the transient climate response to cumulative carbon emissions (TCRE) of our climate plus carbon cycle model as in Sect. 10.8.4 of IPCC (2013), i.e., $TCRE = TCR \times CAF/C_0$, where C_0 = preindustrial atmospheric CO₂ mass = 590 PgC and $CAF = C_{atm}/C_{sum}$, C_{atm} = atmospheric CO₂ mass minus C_0 and C_{sum} = cumulative CO₂ emissions (all evaluated at year 2100).

We find $TCRE = 1.54$ °C per 1000 PgC at 2100 with constant emissions (which yields cumulative emissions of 1180 PgC at 2100, which is near the midpoint of the range assessed by IPCC, i.e., 0.8 to 2.5 °C per 1000 PgC (IPCC, 2013). Our two cases with rapidly declining emissions never achieve 1000 PgC emissions, but TCRE can still be computed using the IPCC formulae, yielding $TCRE = 1.31$ and

1.25 °C per 1000 PgC at 2100 for the cases of –3 and –6 % yr⁻¹ respective emission reductions. As expected, the rapid emission reductions substantially reduce the temperature rise in 2100.

A3 Observed temperature data and analysis method

We use the current Goddard Institute for Space Studies global temperature analysis (GISTEMP), described by Hansen et al. (2010). The analysis combines data from (1) meteorological station data of the Global Historical Climatology Network (GHCN) described by Peterson and Vose (1997) and Menne et al. (2012), (2) Antarctic research station data reported by the Scientific Committee on Antarctic Research (SCAR), (<http://www.antarctica.ac.uk/met/READER>), and (3) ocean surface temperature measurements from the NOAA Extended Reconstructed Sea Surface temperature (ERSST) (Smith et al., 2008; Huang et al., 2015).

Surface air temperature change over land is about twice SST change (Fig. A3a), and thus global temperature change is 1.3 times larger than the SST change. Note that the Arctic Ocean and parts of the Southern Ocean are excluded in the calculations because of inadequate data, but these regions are also not sampled in most paleo-analyses and the excluded areas are small. Land area included covers 29 % of the globe and ocean area included covers 65 % of the globe.

The present analysis uses GHCN.v3.3.0 (Menne et al., 2012) for land data and ERSST.v4 for sea surface temperature (Huang et al., 2015). The update from GHCN.v2 used in our 2010 analysis to GHCN.v3 had negligible effect on global temperature change over the past century (see graph at http://www.columbia.edu/~mhs119/Temperature/GHCN_V3vsV2/). However, the adjustments to SST to produce ERSST.v4 have a noticeable effect, especially in the period 1939–1945, as shown by the difference between the two data sets (lower graph in Fig. A3b). This change is of interest mainly because it increases the magnitude of an already unusual global temperature fluctuation in the 1940s, making the 1939–1945 global temperature maximum even more pronounced than it was in ERSST.v3 data. Thompson et al. (2008) show that two natural sources of variability, the El Niño–Southern Oscillation and (possibly related) unusual winter Arctic warmth associated with advection over high Northern Hemisphere latitudes, partly account for global warmth of 1939–1945, and they suggest that the sharp cooling after 1945 is a data flaw, due to a rapid change in the mix of data sources (bucket measurements and engine room intake measurements) and a bias between these that is not fully accounted for.

Huang et al. (2015) justify the changes made to obtain version 4 of ERSST, the changes including more complete input data in ICOADS Release 2.5, buoy SST bias adjustments not present in version 3, updated ship SST bias adjustments using Hadley Nighttime Marine Air Temperature ver-

sion 2 (HadNMat2), and revised low-frequency data filling in data-sparse regions using nearby observations. ERSST.v4 is surely an improvement in the record during the past half century, when spatial and temporal data coverages are best. On the other hand, the largest changes between v3 and v4 are in 1939–1945, coinciding with World War II and changes in the mix of data sources. Several hot spots appear in the Southern Hemisphere ocean during WWII in the v4 data, and then disappear after the war (Fig. A3c). These hot spots coincide with the locations of large SST changes between v3 and v4 (Fig. A3c), which leads us to suspect that the magnitude of the 1940s global warming maximum (Fig. 2) is exaggerated; i.e., it is partly spurious. We suggest that this warming spike warrants scrutiny in the next version of the SST analysis. However, the important point is that these data adjustments and uncertainties are small in comparison with the long-term warming. Adjustments between ERSST.v3b and ERSST.v4 increase global warming over the period 1950–2015 by about 0.05 °C, which is small compared with the ~ 1 °C global warming during that period. The effect of the adjustments on total global warming between the beginning of the 20th century and 2015 is even smaller (Fig. A3b).

A4 Recent global warming rate

Recent warming removes the illusion of a hiatus of global warming since the 1997–1998 El Niño (Fig. 2). Several studies, including Trenberth and Fasullo (2013), England et al. (2014), Dai et al. (2015), Rajaratnam et al. (2015) and Medhaug et al. (2017), have showed that temporary plateaus are consistent with expected long-term warming due to increasing atmospheric GHGs. Other analyses of the 1998–2013 plateau illuminate the roles of unforced climate variability and natural and human-caused climate forcings in climate change, with the Interdecadal Pacific Oscillation (a recurring pattern of ocean–atmosphere climate variability) playing a major role in the warming slowdown (Kosaka and Xie, 2013; Huber and Knutti, 2014; Meehl et al., 2014; Fyfe et al., 2016; Medhaug et al., 2017).

A5 Coincidence of 1880–1920 mean and preindustrial global mean temperatures

The Framework Convention (United Nations, 1992) and Paris Agreement (2015) define goals relative to “preindustrial” temperature, but do not define that period. We use 1880–1920, the earliest time with near-global coverage of instrumental data, as the zero-point for temperature anomalies. Although human-caused increases of GHGs would be expected to have caused a small warming by then, that warming was at least partially balanced by cooling from larger than average volcanic activity in 1880–1920. Extreme Little Ice Age conditions may have been ~ 0.1 °C cooler than the 1880–1920 mean (Abram et al., 2016), but the Little Ice Age is inappropriate to define preindustrial because the deep

ocean temperature did not have time to reach equilibrium. Thus, preindustrial global temperature has uncertainty of at least 0.1 °C, and the 1880–1920 period, which has the merit of near-global data, yields our best estimate of preindustrial temperature.

A6 Land vs. ocean warming at equilibrium

Observations (Fig. A3a) show surface air temperature (SAT) over land increasing almost twice as much as sea surface temperature (SST) during the past century. This large difference is likely partly due to the thermal inertia of the ocean, which has not fully responded to the climate forcing due to increasing GHGs. However, land warming is heavily modulated by the ocean temperature, so land temperature too has not achieved its equilibrium response.

We use long climate model simulations to examine how much the ratio of land SAT change over ocean SST change (the observed quantities) is modified as global warming approaches its equilibrium response. This ratio is ~ 1.8 in years 901–1000 of doubled CO₂ simulations (Fig. A6) for two versions of GISS modelE-R (Schmidt et al., 2014; Hansen et al., 2016).

A7 Earth's energy imbalance

Hansen et al. (2011) inferred an Earth energy imbalance with the solar cycle effect removed of $+0.75 \pm 0.25 \text{ W m}^{-2}$, based on an imbalance of 0.58 W m^{-2} during the 2005–2010 solar minimum, based on the analysis of von Schuckmann and Le Traon (2011) for heat gain in the upper 2 km of the ocean and estimates of small heat gains by the deep ocean, continents, atmosphere, and net melting of sea ice and land ice. The von Schuckmann and Le Traon (2011) analysis for 2005–2015 (Fig. 5) yields a decade-average 0.7 W m^{-2} heat uptake in the upper 2 km of the ocean; addition of the smaller terms raises the imbalance to at least $+0.8 \text{ W m}^{-2}$ for 2005–2015, consistent with the recent estimate of $+0.9 \pm 0.1 \text{ W m}^{-2}$ by Trenberth et al. (2016) for 2005–2015. Other recent analyses including the most up-to-date corrections for ocean instrumental biases yield $+0.4 \pm 0.1 \text{ W m}^{-2}$ by Cheng et al. (2017) for the period 1960–2015 and $+0.7 \pm 0.1 \text{ W m}^{-2}$ by Dieng et al. (2017) for the period 2005–2013. We conclude that the estimate of $+0.75 \pm 0.25 \text{ W m}^{-2}$ for the current Earth energy imbalance averaged over the solar cycle is still valid.

A8 CO₂ and CH₄ growth rates

Growth of airborne CO₂ is about half of fossil fuel CO₂ emissions (Fig. A8), the remaining portion of emissions being the net uptake by the ocean and biosphere (Ciais et al., 2013). Here we use the Keeling et al. (1973) definition of airborne fraction, which is the ratio of quantities that are known with good accuracy: the annual increase in CO₂ in the atmosphere

and the annual amount of CO₂ injected into the atmosphere by fossil fuel burning. The data reveal that, even as fossil fuel emissions have increased by a factor of 4 over the past half century, the ocean and biosphere have continued to take up about half of the emissions (Fig. A8, right-hand scale). This seemingly simple relation between emissions and atmospheric CO₂ growth is not predictive as it depends on the growth rate of emissions being maintained, which is not true in cases with major changes in the emission scenario, so we use a carbon cycle model in Sect. 7 to compute atmospheric CO₂ as a function of emission scenario.

Oscillations of annual CO₂ growth are correlated with global temperature and with the El Niño/La Niña cycle.¹⁵ Correlations (Fig. 6) are calculated for the 12-month running means, which effectively remove the seasonal cycle and monthly noise. Maxima of the CO₂ growth rate lag global temperature maxima by 7–8 months (Fig. 6b) and lag Niño3.4 (latitudes 5° N–5° S, longitudes 120–170° W) temperature by ~10 months. These lags imply that the current CO₂ growth spike (Fig. 6 uses data through January 2017), associated with the 2015–2016 El Niño, is well past its maximum, as Niño3.4 peaked in December 2015 and the global temperature anomaly peaked in February 2016.

CH₄ growth rate has varied over the past two decades, probably driven primarily by changes in emissions, as observations of CH₃CCl₃ show very little change in the atmospheric sink for CH₄ (Montzka et al., 2011; Holmes et al., 2013). Recent box-model inversions of the CH₄–CH₃CCl₃ system have argued for large fluctuations in the atmospheric sink over this period but there is no identified cause for such changes (Rigby et al., 2017; Turner et al., 2017; Prather and Holmes, 2017). Future changes in the sink could lead to increased atmospheric CH₄ separate from emission changes, but this effect is difficult to project and not included in the RCP scenarios (Voulgarakis et al., 2013).

Carbon isotopes provide a valuable constraint (Saunio et al., 2016) that aids analysis of which CH₄ sources¹⁶ contribute to the CH₄ growth resurgence in the past decade (Fig. 7). Schaefer et al. (2016) conclude that the growth was primarily biogenic, thus not fossil fuel, and located outside the tropics, most likely ruminants and rice agriculture. Such an increasing biogenic source is consistent with effects of increasing population and dietary changes (Tilman and Clark,

2014). Nisbet et al. (2016) concur with Schaefer et al. (2016) that the CH₄ growth is from biogenic sources, but from the latitudinal distribution of growth they conclude that tropical wetlands¹⁷ have been an important contributor to the CH₄ increase. Their conclusion that increasing tropical precipitation and temperature may be major factors driving CH₄ growth suggests the possibility that the slow climate-methane amplifying feedback might already be significant. There is also concern that global warming will lead to a massive increase in CH₄ emissions from methane hydrates and permafrost (O'Connor et al., 2010), but as yet there is little evidence for a substantial increase in emissions from hydrates or permafrost either now or over the last 1 000 000 years (Berchet et al., 2016; Warwick et al., 2016; Quiquet et al., 2015).

Schwietzke et al. (2016) use isotopic constraints to show that the fossil fuel contribution to atmospheric CH₄ is larger than previously believed, but total fossil fuel CH₄ emissions are not increasing. This conclusion is consistent with the above studies, and it does not contradict evidence of increased fossil fuel CH₄ emissions at specific locations (Turner et al., 2016). A recent inverse model study, however, contradicts the satellite studies and finds no evidence for increased US emissions (Bruhwiler et al., 2017). The recent consortium study of global CH₄ emissions finds with top-down studies that the recent increase is likely due to biogenic (natural and human sources) sources in the tropics, but it is difficult to attribute the magnitude of the rise to tropical wetlands alone (Saunio et al., 2017).

A9 CO₂ emissions in historical period

For land use CO₂ emissions in the historical period, we use the values labeled Houghton/2 by Hansen et al. (2008), which were shown in the latter publication to yield good agreement with observed CO₂. We use fossil fuel CO₂ emissions data for 1850–2013 from Boden et al. (2016). BP (2016) fuel consumption data for 2013–2015 are used for the fractional annual changes of each nation to allow extension of the Boden analysis through 2015. Emissions were almost flat from 2014 to 2015, due to economic slowdown and increased use of low-carbon energies, but, even if a peak in global emissions is near, substantial decline of emissions is dependent on acceleration in the transformation of energy production and use (Jackson et al., 2016).

A10 Tables of effective climate forcings, 1850–2100

CO₂, CH₄ and N₂O forcings are calculated with analytic formulae of Hansen et al. (2000). CH₄ forcing includes the factor 1.4 to convert adjusted forcing to effective forcing, thus incorporating the estimated effect of a CH₄ increase on tropospheric ozone and stratospheric water vapor. Our CH₄ ad-

¹⁵One mechanism for greater than normal atmospheric CO₂ growth during El Niños is the impoverishment of nutrients in equatorial Pacific surface water and thus reduced biological productivity that result from reduced upwelling of deep water (Chavez et al., 1999). However, the El Niño/La Niña cycle seems to have an even greater impact on atmospheric CO₂ via the terrestrial carbon cycle through effects on the water cycle, temperature, and fire, as discussed in a large body of literature (referenced, for example, by Schwalm et al., 2011).

¹⁶Estimated human-caused CH₄ sources (Ciais et al., 2013) are fossil fuels (29 %), biomass/biofuels (11 %), waste and landfill (23 %), ruminants (27 %) and rice (11 %).

¹⁷Wetlands compose a majority of natural CH₄ emissions and are estimated to be equivalent to about 36 % of the anthropogenic source (Ciais et al., 2013).

justed forcing is significantly ($\sim 17\%$) higher than the values in IPCC (2013), but ($\sim 9\%$) smaller than values of Etminan et al. (2017). Our factor of 1.4 to convert direct radiative forcing to effective forcing is in the upper portion of the indirect effects discussed by Myhre et al. (2013), so our net CH₄ forcing agrees with Etminan et al. (2017) within uncertainties.

A11 Solar irradiance

Solar irradiance has been measured from satellites since the late 1970s. Figure A11 is a composite of several satellite-measured time series. Data through 28 February 2003 are an update of Frohlich and Lean (1998) obtained from the Physikalisch Meteorologisches Observatorium Davos, World Radiation Center. Subsequent update is from University of Colorado Solar Radiation & Climate Experiment (SORCE). Historical total solar irradiance reconstruction is available at <http://lasp.colorado.edu/home/sorce/data/tsi-data/>. Data sets are concatenated by matching the means over the first 12 months of SORCE data. Monthly sunspot numbers support the conclusion that the solar irradiance in the current solar cycle is significantly lower than in the three preceding solar cycles.

The magnitude of the change in solar irradiance from the prior solar cycle to the current solar cycle is of the order of -0.1 W m^{-2} , which is not negligible but small compared with greenhouse gas climate forcing. On the other hand, the variation of solar irradiance from solar minimum to solar maximum is of the order of 0.25 W m^{-2} , so the high solar irradiance in 2011–2015 contributes to the increase in Earth's energy imbalance between 2005 and 2010 as well as 2010 and 2015.

A12 Alternative scenario

Simulated global temperature for the climate forcings of the “alternative scenario” discussed in Sect. 6 are shown in Fig. A12. The climate model, with sensitivity 3°C for doubled CO₂, is the same as used for Fig. 12.

A13 Non-CO₂ GHGs

CO₂ is the dominant forcing in future climate scenarios. Growth of non-CO₂ GHG climate forcing is likely to be even smaller, relative to CO₂ forcing, than in recent decades (Fig. 8) if there is a strong effort to limit climate change. Indeed, recent agreement to use the Montreal Protocol (2016) to phase down production of minor trace gases, the hydrofluorocarbons (HFCs), should cause annually added forcing of Montreal Protocol trace gases (MPTGs) + other trace gases (OTGs) (red region in Fig. 8) to become near zero or slightly negative, thus at least partially off-setting growth of other non-CO₂ GHGs, especially N₂O.

Methane (CH₄) is the largest climate forcing other than CO₂ (Fig. 4). The CH₄ atmospheric lifetime is only about 10 years (Prather et al., 2012), so there is potential to reduce this climate forcing rapidly if CH₄ sources are reduced. Our climate simulations, based on the RCP6.0 non-CO₂ GHG scenarios, follow an optimistic path in which CH₄ increases moderately in the next few decades to 1650 ppb in 2070 and then decreases rapidly to 1650 ppb in 2100, yielding a forcing change of -0.1 W m^{-2} . However, the IPCC (Kirtman et al., 2013) uses a more modern chemical model projection for the RCP anthropogenic emissions and gives a less beneficial view with a decrease to only 1734 ppb and a forcing change of -0.03 W m^{-2} . RCP2.6 makes a more optimistic assumption: that CH₄ will decline monotonically to 1250 ppb in 2100, yielding a forcing of -0.3 W m^{-2} (relative to today's 1800 ppb CH₄), but the IPCC projections of RCP2.6 reduce this to -0.2 W m^{-2} (Kirtman et al., 2013).

Observed atmospheric CH₄ amount (Fig. A13a) is diverging on the high side of these optimistic scenarios. The downward offset (~ 20 ppb) of CH₄ scenarios relative to observations (Fig. A13a) is due to the fact that RCP scenarios did not include a data adjustment that was made in 2005 to match a revised CH₄ standard scale (E. Dlugokencky, personal communication, 2016), but observed CH₄ is also increasing more rapidly than in most scenarios. Reversal of CH₄ growth is made difficult by increasing global population, the diverse and widely distributed nature of agricultural sources, and global warming “in the pipeline”, as these trends create an underlying tendency for increasing CH₄. The discrepancy between observed and assumed CH₄ growth could also be due in part to increased natural sources or changes in the global OH sink (Dlugokencky et al., 2011; Turner et al., 2017). Evidence for increased natural sources in a warmer climate is suggested by glacial–interglacial CH₄ increases of the order of 300 ppb, and contributions to observed fluctuations cannot be ruled out on the basis of recent budgets (Ciais et al., 2013).

Methane emissions from rice agriculture and ruminants potentially could be mitigated by changing rice growing methods (Epule et al., 2011) and inoculating ruminants (Eckard et al., 2010; Beil, 2015), but that would require widespread adoption of new technologies at the farmer level. California, in implementing a state law to reduce GHG emissions, hopes to dramatically cut agricultural CH₄ emissions (see <http://www.arb.ca.gov/cc/scopingplan/scopingplan.htm>), but California has one of the most technological and regulated agricultural sectors in the world. It is not clear that this level of management can occur in the top agricultural CH₄ emitters like China, India and Brazil. Methane leaks from fossil fuel mining, transportation and use can be reduced; indeed, percentage leakage from conventional fossil fuel mining and fuel use has declined substantially in recent decades (Schwietzke et al., 2016), but there is danger of increased leakage with expanded shale gas ex-

traction (Caulton et al., 2014; Petron et al., 2013; Howarth, 2015; Kang et al., 2016).

Observed N₂O growth is exceeding all scenarios (Fig. A13b). Major quantitative gaps remain in our understanding of the nitrogen cycle (Kroeze and Bouwman, 2011), but fertilizers are clearly a principal cause of N₂O growth (Röckmann and Levin, 2005; Park et al., 2012). More efficient use of fertilizers could reduce N₂O emissions (Liu and Zhang, 2011), but considering the scale of global agriculture, and the fact that fixed N is an inherent part of feeding people, there will be pressure for continued emissions at least comparable to present emissions. In contrast, agricultural CH₄ emissions are inadvertent and not core to food production. Given the current imbalance (emissions exceeding atmospheric losses by about 30 %; Prather et al., 2012) and the long N₂O atmospheric lifetime (116 ± 9 years; Prather et al., 2015) it is nearly inevitable that N₂O will continue to increase this century, even if emissions growth is checked. There can be no expectation of an N₂O decline that offsets the need to reduce CO₂.

The Montreal Protocol has stifled and even reversed growth of specific trace gases that destroy stratospheric ozone and cause global warming (Prather et al., 1996; Newman et al., 2009). The anticipated benefit over the 21st century is a drop in climate forcing of -0.23 W m^{-2} (Prather et al., 2013). Protocol amendments that add other gases such as HFCs are important; forcings of these gases are small today, but without the protocol their potential for growth is possibly as large as $+0.2 \text{ W m}^{-2}$ (Prather et al., 2013).

We conclude that a 0.25 W m^{-2} decrease in climate forcing by non-CO₂ GHGs is plausible, but requires a dramatic change from the growing abundances of these gases today. Achievement requires (i) successful phase-out of MPTGs (-0.23 W m^{-2}), (ii) reduction of CH₄ forcing by 0.12 W m^{-2} , and (iii) limiting N₂O increase to 0.1 W m^{-2} . A net negative forcing of -0.25 W m^{-2} for non-CO₂ gases would allow CO₂ to be 365 ppm, rather than 350 ppm, while yielding the same total GHG forcing. Thus, potential reduction of non-CO₂ gases is helpful, but it does not alter the need for rapid fossil fuel emission reduction.

Table A1. (a) Effective forcings (W m⁻²) in 1850–2015 relative to 1850. (b) Effective forcing (W m⁻²) in 2016–2100 relative to 1850.

Year	CO ₂	CH ₄ ^a	CFCs ^b	N ₂ O	O ₃ ^c	TA + SA ^d	Volcano ^e	Solar	Net
(a)									
1850	0.000	0.000	0.000	0.000	0.000	0.000	−0.083	0.000	−0.083
1860	0.024	0.013	0.000	0.004	0.004	−0.029	−0.106	0.032	−0.058
1870	0.048	0.027	0.000	0.008	0.009	−0.058	−0.014	0.048	0.068
1880	0.109	0.041	0.000	0.011	0.014	−0.097	−0.026	−0.049	0.003
1890	0.179	0.058	0.000	0.014	0.018	−0.146	−0.900	−0.070	−0.847
1900	0.204	0.077	0.001	0.017	0.023	−0.195	−0.040	−0.063	0.024
1910	0.287	0.115	0.002	0.022	0.026	−0.250	−0.072	−0.043	0.087
1920	0.348	0.160	0.003	0.029	0.032	−0.307	−0.215	−0.016	0.034
1930	0.425	0.206	0.004	0.037	0.036	−0.364	−0.143	0.014	0.215
1940	0.494	0.247	0.005	0.043	0.045	−0.424	−0.073	0.037	0.374
1950	0.495	0.291	0.009	0.052	0.056	−0.484	−0.066	0.055	0.408
1960	0.599	0.365	0.027	0.061	0.078	−0.621	−0.106	0.102	0.505
1970	0.748	0.461	0.076	0.075	0.097	−0.742	−0.381	0.093	0.427
1980	0.976	0.568	0.185	0.097	0.115	−0.907	−0.108	0.169	1.095
1990	1.227	0.659	0.303	0.125	0.117	−0.997	−0.141	0.154	1.447
2000	1.464	0.695	0.347	0.150	0.117	−1.084	−0.048	0.173	1.814
2005	1.619	0.651	0.356	0.162	0.123	−1.125	−0.079	0.019	1.770
2010	1.766	0.710	0.364	0.177	0.129	−1.163	−0.082	0.028	1.929
2015	1.927	0.730	0.373	0.195	0.129	−1.199	−0.100	0.137	2.192
(b)									
2016	1.942	0.698	0.367	0.192	0.130	−1.207	−0.100	0.097	2.119
2020	2.074	0.702	0.373	0.201	0.130	−1.234	−0.100	−0.008	2.139
2030	2.347	0.708	0.343	0.226	0.130	−1.296	−1.057	−0.008	1.393
2040	2.580	0.735	0.301	0.254	0.123	−1.350	−0.100	0.027	2.569
2050	2.803	0.766	0.267	0.288	0.117	−1.396	−0.100	0.062	2.807
2060	3.017	0.791	0.243	0.322	0.111	−1.433	−1.208	0.097	1.940
2070	3.222	0.804	0.229	0.358	0.105	−1.462	−0.100	0.132	3.289
2080	3.421	0.792	0.215	0.391	0.098	−1.484	−0.100	0.167	3.500
2090	3.614	0.722	0.199	0.427	0.091	−1.495	−1.240	0.167	2.484
2100	3.801	0.619	0.191	0.456	0.085	−1.500	−0.100	0.167	3.719

^a CH₄: CH₄-induced changes of tropospheric O₃ and stratospheric H₂O are included. ^b CFCs: this includes all GHGs except CO₂, CH₄, N₂O and O₃. ^c O₃: half of troposphere O₃ forcing + stratosphere O₃ forcing from IPCC (2013). ^d TA + SA: tropospheric aerosols and surface albedo forcings combined. ^e Volcano: volcanic forcing is zero when there are no stratospheric aerosols. Annual data are available at <http://www.columbia.edu/~mhs119/Burden/>.

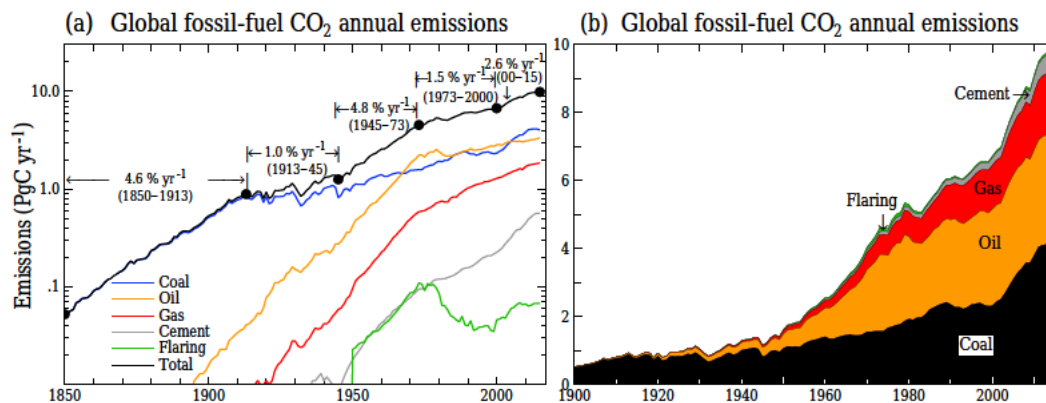


Figure A1. CO₂ emissions from fossil fuels and cement use based on Boden et al. (2017) through 2014, extended using BP (2016) energy consumption data. Panel (a) is log scale and (b) is linear. Growth rates r in (a) for an n -year interval are from $(1 + r)^n$ with end values being 3-year means to minimize noise.

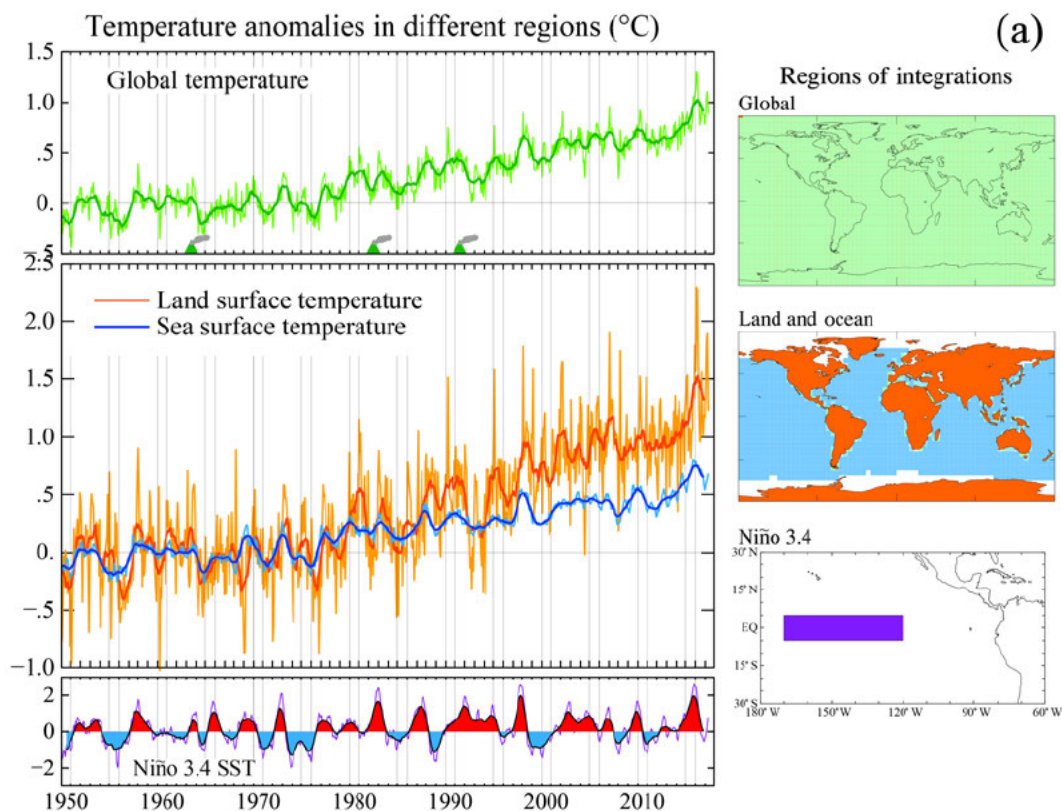


Figure A2.

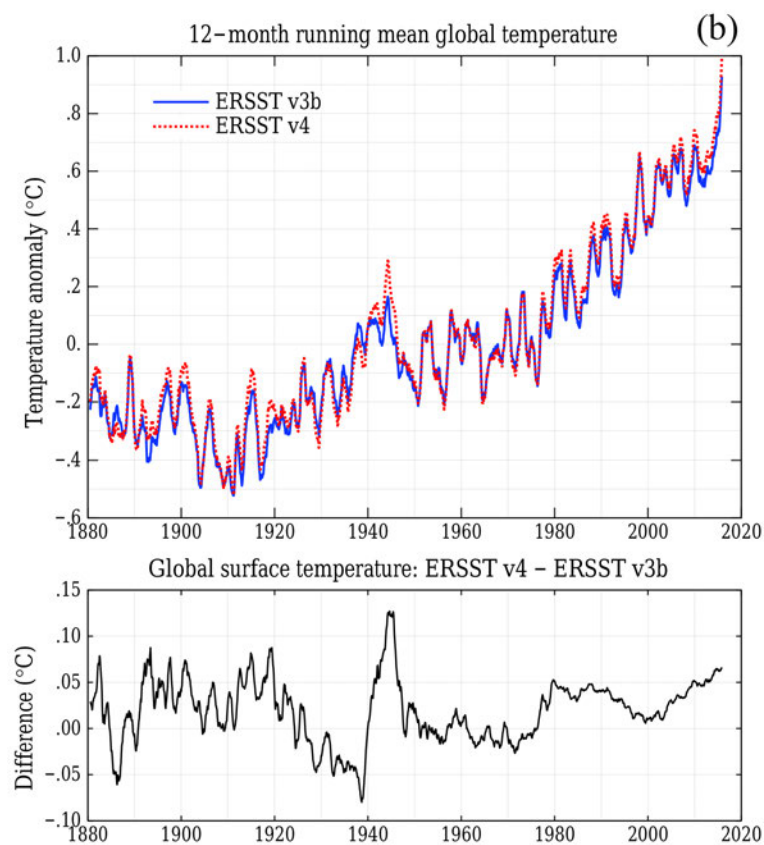


Figure A2.

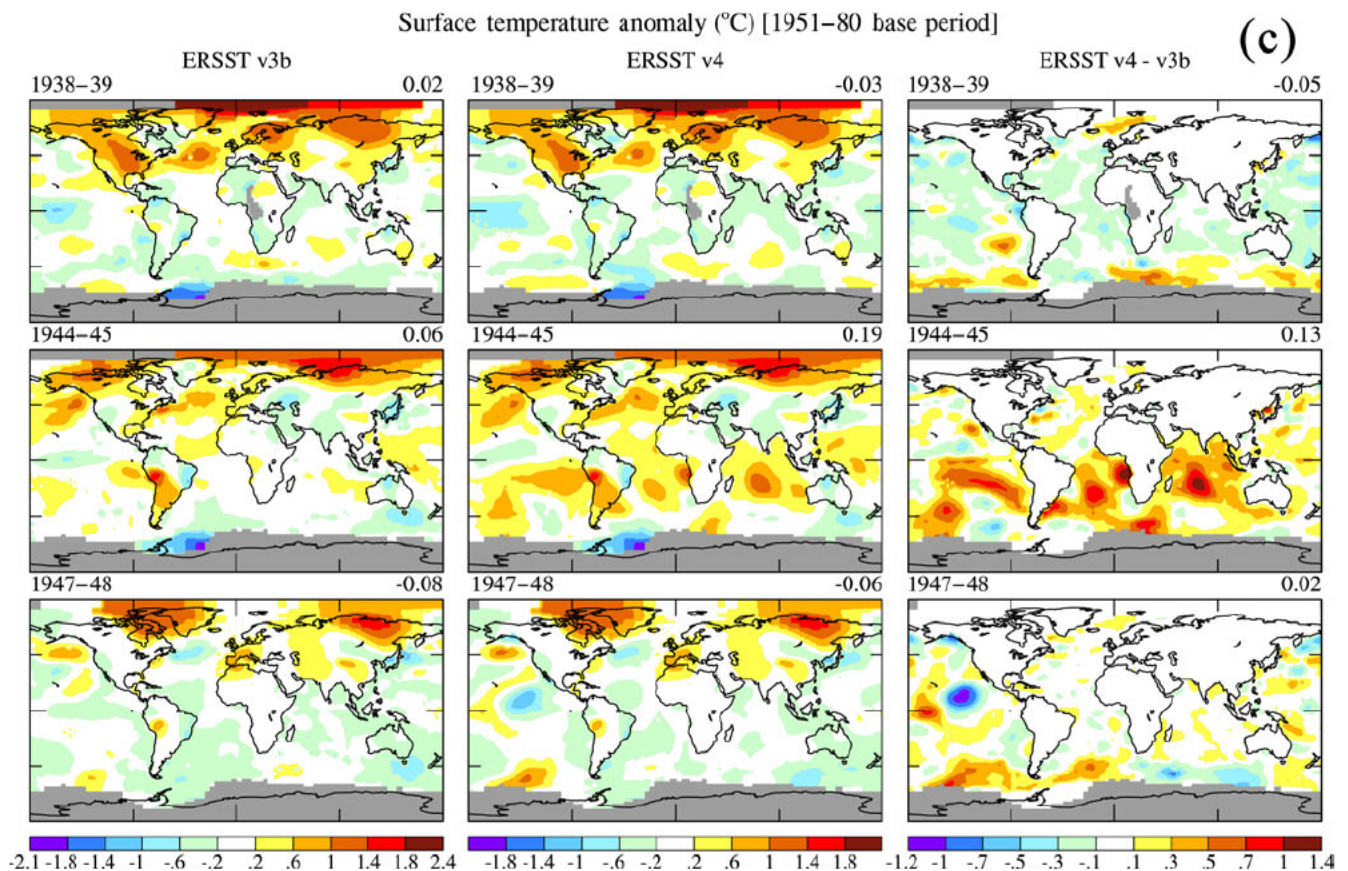


Figure A2. (a) Monthly (thin lines) and 12-month running mean (thick lines or filled colors for Niño 3.4) global, global land, sea surface, and Niño 3.4 temperatures. Temperatures are relative to 1951–1980 base period for the current GISTEMP analysis, which uses NOAA ERSST.v4 for sea surface temperature. (b) Global surface temperature relative to 1951–1980 in the GISTEMP analysis, comparing the current analysis using NOAA ERSST.v4 for sea surface temperature with results using ERSST.v3b. (c) Temperature anomalies in three periods relative to 1951–1980 comparing results obtained using ERSST.v3b (left column panels), ERSST.v4 (center column panels), and their difference (right column panels).

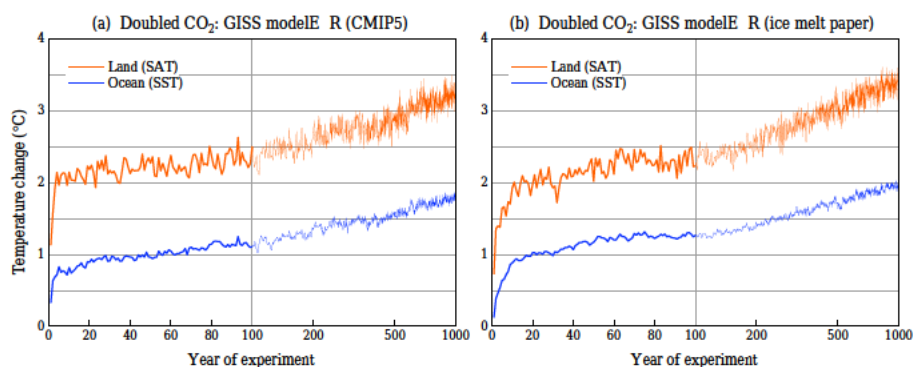


Figure A3. 1000-year temperature response in two versions of GISS modelE-R. (a) Version used for CMIP5 simulations (Schmidt et al., 2014), which has higher resolution (40-layer atmosphere at $2^\circ \times 2.5^\circ$, 32-layer ocean at $1^\circ \times 1.25^\circ$); (b) version used by Hansen et al. (2016), which has coarse resolution (20-layer atmosphere at $4^\circ \times 5^\circ$, 12-layer ocean at $4^\circ \times 5^\circ$) and includes two significant improvements to small-scale ocean mixing (see Sect. 3.2 of Hansen et al., 2016).

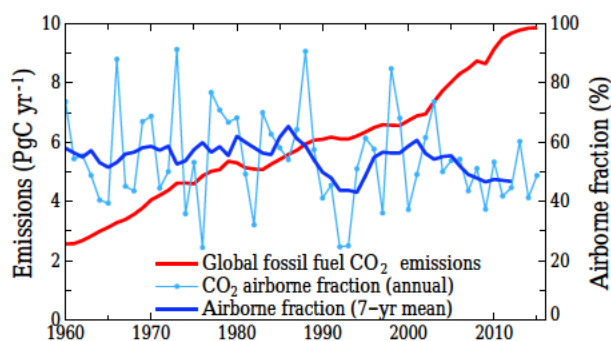


Figure A4. Fossil fuel CO₂ emissions (left scale) and airborne fraction, i.e., the ratio of observed atmospheric CO₂ increase to fossil fuel CO₂ emissions.

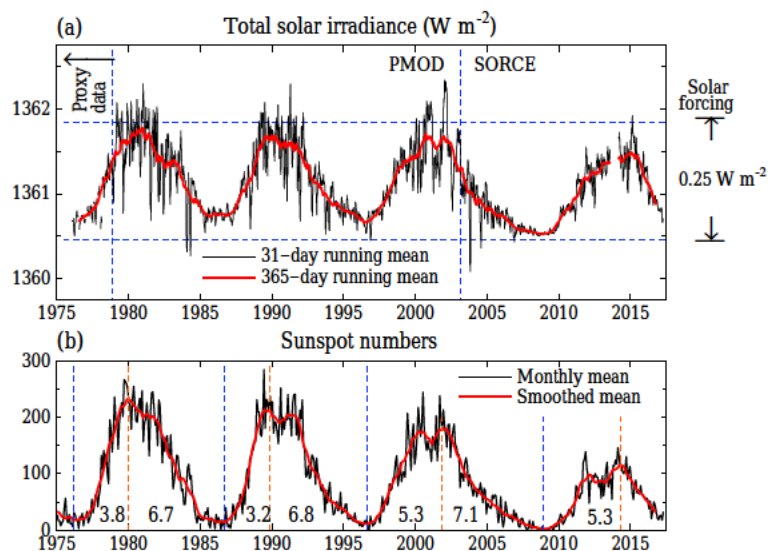


Figure A5. Solar irradiance and sunspot number in the era of satellite data. Left scale is the energy passing through an area perpendicular to Sun–Earth line. Averaged over Earth's surface the absorbed solar energy is $\sim 240 \text{ W m}^{-2}$, so the full amplitude of the measured solar variability is $\sim 0.25 \text{ W m}^{-2}$.

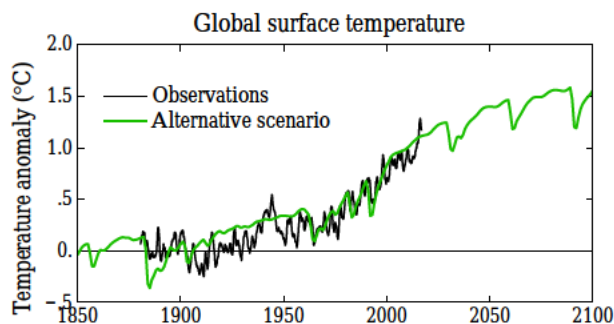


Figure A6. Simulated global temperature with historical climate forcings to 2000 followed by the alternative scenario. Historical climate forcings are discussed in the main text.

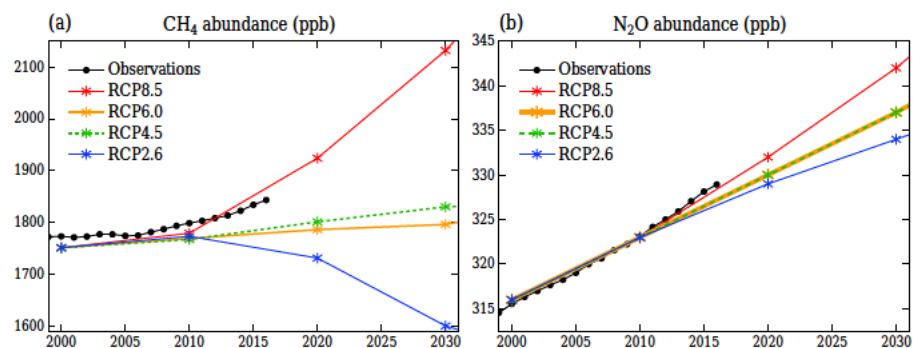


Figure A7. Comparison of observed CH₄ and N₂O amounts with RCP scenarios. RCP6.0 and 4.5 scenarios for N₂O overlap. Observations are from NOAA/ESRL Global Monitoring Division. Natural sources and feedbacks not included in RCP scenarios may contribute to observed growth (see Sect. 11).

Competing interests. The authors declare that they have no conflict of interest.

Disclosure

The first author (James Hansen) notes that he is a plaintiff in the lawsuit *Juliana et al. vs. United States*.

Acknowledgements. Support of the Climate Science, Awareness and Solutions program was provided by the Durst family, the Grantham Foundation for Protection of the Environment, Jim and Krisann Miller, Gary Russell, Gerry Lenfest, the Flora Family Foundation, Elisabeth Mannschott, Alexander Totic and Hugh Perrine, which is gratefully acknowledged. David J. Beerling acknowledges funding through a Leverhulme Trust Research Centre Award (RC-2015-029). Eelco J. Rohling acknowledges support from Australian Laureate Fellowship FL12 0100050.

We appreciate the generosity, with data and advice, of Tom Boden, Ed Dlugokencky, Robert Howarth, Steve Montzka, Larissa Nazarenko and Nicola Warwick; the thoughtful reviews of the anonymous reviewers and several SC commenters (SCs are short comments published in response to the discussion version of our paper); and assistance of the editor, James Dyke.

Edited by: James Dyke

Reviewed by: three anonymous referees

References

- Abram, N. J., McGregor, H. V., Tierney, J. E., Evans, M. N., McKay, N. P., Kaufman, D. S., and PAGES 2k Consortium: Early onset of industrial-era warming across the oceans and continents, *Nature*, 536, 411–418, <https://doi.org/10.1038/nature19082>, 2016.
- Ackerman, F. and Stanton, E. A.: Climate risks and carbon prices: revising the social cost of carbon, *Economics E-J.*, 6, 1–25, 2012.
- Aiken, A.: Opinion and Order, Case No. 6:15-cv-01517-TC in United States District Court, District of Oregon, Eugene Division, 54 pp., Judge Aiken's Opinion and Order is available at: http://www.columbia.edu/~jeh1/mailings/2016/20161111_EmpathicRulingbyJudgeAiken.pdf, last access: 10 November 2016.
- Alec L v. Jackson DDC, No. 11-CV-02235, 12/14/11, United States District Court, District of Columbia, 31 May 2012.
- Anderson, K.: Talks in the city of light generate more heat, *Nature*, 528, 437, 2015.
- Andrews, T., Gregory, J., Webb, M., and Taylor, K.: Forcing, feedbacks and climate sensitivity in CMIP5 coupled atmosphere-ocean climate models, *Geophys. Res. Lett.*, 39, L09712, <https://doi.org/10.1029/2012GL051607>, 2012.
- Applegate, P. J., Parizek, B. R., Nicholas, R. E., Alley, R. B., and Keller, K.: Increasing temperature forcing reduces the Greenland Ice Sheet's response time scale, *Clim. Dynam.*, 45, 2001–2011, 2015.
- Arrhenius, S.: On the influence of carbonic acid in the air upon the temperature on the ground, *Phil. Mag.*, 41, 237–276, 1896.
- Bajzelj, B., Richards, K. S., Allwood, J. M., Smith, P., Dennis, J. S., Curmi, E., and Gilligan, C. A.: Importance of food-demand management for climate mitigation, *Nat. Clim. Change*, 4, 924–929, 2014.
- Bakker, P. and Renssen, H.: Last interglacial model-data mismatch of thermal maximum temperatures partially explained, *Clim. Past*, 10, 1633–1644, <https://doi.org/10.5194/cp-10-1633-2014>, 2014.
- Beil, L.: Getting creative to cut methane from cows, *Science News*, 188, 22–25, 2015.
- Berchet, A., Bousquet, P., Pison, I., Locatelli, R., Chevallier, F., Paris, J.-D., Dlugokencky, E. J., Laurila, T., Hatakka, J., Viisanen, Y., Worthy, D. E. J., Nisbet, E., Fisher, R., France, J., Lowry, D., Ivakhov, V., and Hermansen, O.: Atmospheric constraints on the methane emissions from the East Siberian Shelf, *Atmos. Chem. Phys.*, 16, 4147–4157, <https://doi.org/10.5194/acp-16-4147-2016>, 2016.
- Betts, R. A., Jones, C. D., Knight, J. R., Keeling, R. F., and Kennedy, J. J.: El Niño and a record CO₂ rise, *Nat. Clim. Change*, 6, 806–810, 2016.
- Biermann, F. and Boas, I.: Preparing for a warmer world: towards a global governance system to protect climate refugees, *Global Environ. Polit.*, 10, 60–88, 2010.
- Bindoff, N. L. and Stott, P. A.: Detection and attribution of climate change: from global to regional, in: *Climate Change 2013: The Physical Science Basis*, edited by: Stocker, T. F., Qin, D., Plattner, G.-K., Tignor, M., Allen, S. K., Boschung, J., Nauels, A., Xia, Y., Bex, V., and Midgley, P. M., Cambridge University Press, Cambridge, UK, 2013.
- Boden, T. A., Marland, G., and Andres, R. J.: Global, Regional, and National Fossil-Fuel CO₂ Emissions, Carbon Dioxide Information Analysis Center, Oak Ridge National Laboratory, Oak Ridge, Tennessee, USA, https://doi.org/10.3334/CDIAC/00001_V2017, 2017.
- Boucher, O., Randall, D., Artaxo, P., Bretherton, C., Fiengold, G., Forster, P., Kerminen, V.-M., Kondo, Y., Liao, H., Lohmann, U., Rasch, P., Satheesh, S. K., Sherwood, S., Stevens, B., and Zhang, X. Y.: Clouds and aerosols, in: *Climate Change 2013: The Physical Science Basis*, edited by: Stocker, T. F., Qin, D., Plattner, G.-K., Tignor, M., Allen, S. K., Boschung, J., Nauels, A., Xia, Y., Bex, V., and Midgley, P. M., Cambridge University Press, Cambridge, UK, 2013.
- Bourassa, A. E., Robock, A., Randel, W. J., Deshler, T., Rieger, L. A., Lloyd, N. D., Llewellyn, E. J., and Degenstein, D. A.: Large volcanic aerosol load in the stratosphere linked to Asian Monsoon transport, *Science*, 337, 78–81, 2012.
- BP: 2016 BP Statistical Review of World Energy, available at: <http://www.bp.com/en/global/corporate/energy-economics/statistical-review-of-world-energy.html>, last access: 23 June 2016.
- Bruhwyler, L. M., Basu, S., Bergamaschi, P., Bousquet, P., Dlugokencky, E., Houweling, S., Ishizawa, M., Kim, H.-S., Locatelli, R., Maksyutov, S., Montzka, S., Pandey, S., Patra, P. K., Petron, G., Saunois, M., Sweeney, C., Schwietzke, S., Tans, P., and Weatherhead, E. C.: US CH₄ emissions from oil and gas production: Have recent large increases been detected?, *J. Geophys. Res.-Atmos.*, 122, 4070–4083, <https://doi.org/10.1002/2016JD026157>, 2017.
- Budyko, M. I.: *Izmeniya Klimata, Gidrometeoroizdat*, Leningrad, 1974.

- Bustamante, M., Robledo-Abad, C., Harper, R., Mbow, C., Ravindranath, N. H., Sperling, F., Haberl, H., de Siqueira Pinto, A., and Smith, P.: Co-benefits, trade-offs, barriers and policies for greenhouse gas mitigation in the Agriculture, Forestry and Other Land Use (AFOLU) sector, *Global Change Biol.*, 20, 3270–3290, <https://doi.org/10.1111/gcb.12591>, 2014.
- Canadell, J. G. and Raupach, M. R.: Managing forests for climate change mitigation, *Science*, 320, 1456–1457, 2008.
- Cao, J., Cohen, A., Hansen, J., Lester, R., Peterson, P., and Xu, H.: China–U.S. cooperation to advance nuclear power, *Science*, 353, 547–548, 2016.
- Cao, L. and Caldeira, K.: Atmospheric carbon dioxide removal: long-term consequences and commitment, *Environ. Res. Lett.*, 5, 024011, <https://doi.org/10.1088/1748-9326/5/2/024011>, 2010.
- Caulton, D. R., Shepson, P. B., Santoro, R. L., Sparks, J. P., Howarth, R. W., Ingrassia, A. R., Cambaliza, M. O. L., Sweeney, C., Karion, A., Davis, K. J., Strim, B. H., Montzka, S. A., and Miller, B. R.: Toward a better understanding and quantification of methane emissions from shale gas development, *P. Natl. Acad. Sci. USA*, 111, 6237–6242, 2014.
- Charney, J., Arakawa, A., Baker, D., Bolin, B., Dickinson, R., Goody, R., Leith, C., Stommel, H., and Wunsch, C.: Carbon Dioxide and Climate: A Scientific Assessment, *Natl. Acad. Sci. Press*, Washington, D.C., USA, p. 33, 1979.
- Chavez, F. P., Strutton, P. G., Friederich, G. E., Feely, R. A., Feldman, G. C., Foley, D. G., and McPhaden, M. J.: Biological and chemical response of the Equatorial Pacific Ocean to the 1997–98 El Niño, *Science*, 286, 2126–2131, 1999.
- Cheng, L., Trenberth, K., Fasullo, J., Boyer, T., Abraham, J., and Zhu, J.: Improved estimates of ocean heat content from 1960–2015, *Sci. Adv.*, 3, e1601545, <https://doi.org/10.1126/sciadv.1601545>, 2017.
- Chinese Academy of Engineering: Re-studying the nuclear development in China, 1st Edn., Tsinghua University Press, Tsinghua, 2015.
- Ciais, P., Sabine, C., Bala, G., Bopp, L., Brovkin, V., Canadell, J., Chhabra, A., DeFries, R., Galloway, J., Heimann, M., Jones, C., Le Quéré, C., Myneni, R. B., Piao, S., and Thornton, P.: Carbon and other biogeochemical cycles, in: *Climate Change 2013: The Physical Science Basis*, edited by: Stocker, T. F., Qin, D., Plattner, G.-K., Tignor, M., Allen, S. K., Boschung, J., Nauels, A., Xia, Y., Bex, V., and Midgley, P. M., Cambridge University Press, Cambridge, UK, 2013.
- Clark, P. U. and Huybers, P.: Interglacial and future sea level, *Nature*, 462, 856–857, 2009.
- Clark, P. U., Shakun, J. D., Marcott, S. A., Mix, A. C., Eby, M., Kulp, S., Levermann, A., Milne, G. A., Pfister, P. L., Santer, B. D., Schrag, D. P., Solomon, S., Stocker, T. F., Strauss, B. H., Weaver, A. J., Winkelmann, R., Archer, D., Bard, E., Goldner, A., Lambeck, K., Pierrehumbert, R. T., and Plattner, G. K.: Consequences of twenty-first-century policy for multi-millennial climate and sea-level change, *Nat. Clim. Change*, 6, 360–369, 2016.
- Coddington, O., Lean, J. L., Pilewskie, P., Snow, M., and Lindholm, D.: A solar irradiance climate data record, *B. Am. Meteorol. Soc.*, 97, 1265–1282, <https://doi.org/10.1175/BAMS-D-14-00265.1>, 2016.
- Collins, M., Knutti, R., Arblaster, J., Dufresne, J. L., Fichefet, T., Friedlingstein, P., Gao, X., Gutowski, W. J., Johns, T., Krinner, G., Shongwe, M., Tebaldi, C., Weaver, A., and Wehner, M.: Long-term climate change: Projections, commitments and irreversibility, in: *Climate Change 2013: The Physical Basis*, edited by: Stocker, T. F., Qin, D., Plattner, G.-K., Tignor, M., Allen, S. K., Boschung, J., Nauels, A., Xia, Y., Bex, V., and Midgley, P. M., Cambridge University Press, Cambridge, UK, 2013.
- Copenhagen Accord: United Nations Framework Convention on Climate Change, Draft decision available at: http://unfccc.int/meetings/copenhagen_dec_2009/items/5262.php (last access: 9 September 2016), 2009.
- Creutzig, F., Ravindranath, N. H., Berndes, G., Bolwig, S., Bright, R., Cherubini, F., Chum, H., Corbera, E., Delucchi, M., Faaij, A., Fargione, J., Haberl, H., Heath, G., Lucon, O., Plevin, R., Popp, A., Robledo-Abad, C., Rose, S., Smith, P., Stromman, A., and Suh, S.: Bioenergy and climate change mitigation: an assessment, *GCB Bioenergy*, 7, 916–944, 2015.
- Crowther, T. W., Todd-Brown, K. E., Rowe, C. W., Wieder, W. R., Carey, J. C., Machmuller, M. B., Snoek, B. L., Fang, S., Zhou, G., Allison, S. D., Blair, J. M., Bridgman, S. D., Burton, A. J., Carrillo, Y., Reich, P. B., Clark, J. S., Classen, A. T., Dijkstra, F. A., Elberling, B., Emmett, B. A., Estiarte, M., Frey, S. D., Guo, J., Harte, J., Jiang, L., Johnson, B. R., Kröel-Dulay, G., Larsen, K. S., Laudon, H., Lavalée, J. M., Luo, Y., Lupascu, M., Ma, L. N., Marhan, S., Michelsen, A., Mohan, J., Niu, S., Pendall, E., Peñuelas, J., Pfeifer-Meister, L., Poll, C., Reinsch, S., Reynolds, L. L., Schmidt, I. K., Sistla, S., Sokol, N. W., Templer, P. H., Treseder, K. K., Welker, J. M., and Bradford, M. A.: Quantifying global soil carbon losses in response to warming, *Nature*, 540, 104–108, 2016.
- Crutzen, P. J.: Albedo enhancement by stratospheric sulfur injections: A contribution to resolve a policy dilemma?, *Climatic Change*, 77, 211–219, 2006.
- Dai, A., Fyfe, J. C., Xie, S. P., and Dai, X.: Decadal modulation of global surface temperature by internal climate variability, *Nat. Clim. Change*, 5, 555–559, <https://doi.org/10.1038/nclimate2605>, 2015.
- DeCicco, J. M., Liu, D. Y., Hoo, J., Krishnan, R., Kurthen, A., and Wang, L.: Carbon balance effects of U.S. biofuel production and use, *Climatic Change*, 138, 667–680, 2016.
- DeConto, R. M. and Pollard, D.: Contribution of Antarctica to past and future sea-level rise, *Nature*, 531, 591–597, 2016.
- DeConto, R. M., Galeotti, S., Pagani, M., Tracy, D., Schaefer, K., Zhang, T., Pollard, D., and Beerling, D. J.: Past extreme warming events linked to massive carbon release from thawing permafrost, *Nature*, 484, 87–91, 2012.
- Dieng, H. B., Cazenave, A., Meyssignac, B., von Schuckmann, K., and Palanisamy, H.: Sea and land temperatures, ocean heat content, Earth's energy imbalance and net radiative forcing over the recent years, *Int. J. Climatol.*, <https://doi.org/10.1002/joc.4996>, 2017.
- Dragokkenky, E. J.: Global CH₄ data, NOAA/ESRL, available at: http://www.esrl.noaa.gov/gmd/ccgg/trends_ch4/, last access: 13 September 2016.
- Dragokkenky, E. J., Nisbet, E. G., Fisher, R., and Lowry, D.: Global atmospheric methane: budget, changes and dangers, *Philos. T. Roy. Soc. A*, 369, 2058–2072, 2011.
- Dutton, A., Carlson, A. E., Long, A. J., Milne, G. A., Clark, P. U., DeConto, R., Horton, B. P., Rahmstorf, S., and Raymo, M. E.: Sea-level rise due to polar ice-sheet

- mass loss during past warm periods, *Science*, 349, 153, <https://doi.org/10.1126/science.aaa4019>, 2015.
- Eckard, R. J., Grainger, C., and de Klein, C. A. M.: Strategies to reduce methane emissions from farmed ruminants grazing on pasture, *Livestock Science*, 130, 47–56, 2010.
- Edwards, D. P., Lim, F., James, R. H., Pearce, C. R., Scholes, J., Freckleton, R. P., and Beerling, D. J.: Climate change mitigation: potential benefits and pitfalls of enhanced rock weathering in tropical agriculture, *Biol. Lett.*, 13, <https://doi.org/10.1098/rsbl.2016.0715>, 2017.
- England, M. H., McGregor, S., Spence, P., Meehl, G. A., Timmermann, A., Cai, W., Gupta, A. S., McPhaden, M. J., Purich, A., and Santoso, A.: Recent intensification of wind-driven circulation in the Pacific and the ongoing warming hiatus, *Nat. Clim. Change*, 4, 222–227, <https://doi.org/10.1038/nclimate2106>, 2014.
- Epule, E. T., Peng, C., and Mafany, N. M.: Methane emissions from paddy rice fields: strategies towards achieving a win-win sustainability scenario between rice production and methane reduction, *J. Sustain. Dev.*, 4, 188–196, 2011.
- Etminan, M., Myhre, G., Highwood, E. J., and Shine, K. P.: Radiative forcing of carbon dioxide, methane, and nitrous oxide: A significant revision of the methane radiative forcing, *Geophys. Res. Lett.*, 43, 12614–12623, <https://doi.org/10.1002/2016GL071930>, 2017.
- Flato, G., Marotzke, J., Abiodun, B., Braconnot, P., Chou, S. C., Collins, W., Cox, P., Driouech, F., Emori, S., Eyring, V., Forest, C., Gleckler, P., Guilyardi, E., Jakob, C., Kattsov, V., Reason, C., and Rummukainen, M.: Evaluation of Climate Models, in: *Climate Change 2013: The Physical Science Basis*, edited by: Stocker, T. F., Qin, D., Plattner, G.-K., Tignor, M., Allen, S. K., Boschung, J., Nauels, A., Xia, Y., Bex, V., and Midgley, P. M., Cambridge University Press, Cambridge, UK, 2013.
- Franks, P. J., Royer, D. L., Beerling, D. J., Van de Water, P. K., Cantrill, D. J., Barbour, M. M., and Berry, J. A.: New constraints on atmospheric CO₂ concentration for the Phanerozoic, *Geophys. Res. Lett.*, 41, 4685–4694, 2014.
- Friedlingstein, P., Andrew, R. M., Rogelj, J., Peters, G. P., Canadell, J. G., Knutti, R., Luderer, G., Raupach, M. R., Schaeffer, M., van Vuuren, D. P., and Le Quéré, C.: Persistent growth of CO₂ emissions and implications for reaching climate targets, *Nat. Geosci.*, 1, 457–461, 2014.
- Frohlich, C. and Lean, J.: The Sun's total irradiance: cycles and trends in the past two decades and associated climate change uncertainties, *Geophys. Res. Lett.*, 25, 4377–4380, 1998.
- Fuss, S., Canadell, J. G., Peters, G. P., Tavoni, M., Andrew, R. M., Ciais, P., Jackson, R. B., Jones, C. D., Kraxner, F., Nakicenovic, N., Le Quere, C., Raupach, M. R., Sharifi, A., Smith, P., and Yamagata, Y.: Betting on negative emissions, *Nat. Clim. Change*, 4, 850–853, 2014.
- Fyfe, J. C., Meehl, G. A., England, M. H., Mann, M. E., Santer, B. D., Flato, G. M., Hawkins, E., Gillett, N. P., Xie, S., Kosaka, Y., and Swart, N. C.: Making sense of the early-2000s warming slowdown, *Nat. Clim. Change*, 6, 224–228, 2016.
- Gemenne, F., Barnett, J., Adger, W. N., and Dabelko, G. D.: Climate and security: evidence, emerging risks, and a new agenda, *Climatic Change*, 123, 1–9, 2014.
- Govin, A., Capron, E., Tzedakis, P. C., Verheyden, S., Ghaleb, B., Hillaire-Marcel, C., St-Onge, G., Stoner, J. S., Bassinot, F., Bazin, L., Blunier, T., Combourieu-Nebout, N., El Ouahabi, A., Gentry, D., Gersonde, R., Jimenez-Amat, P., Landais, A., Martrat, B., Masson-Delmotte, V., Parrenin, F., Seidenkrantz, M. S., Veres, D., Waelbroeck, C., and Zahn, R.: Sequence of events from the onset to the demise of the Last Interglacial: Evaluating strengths and limitations of chronologies used in climatic archives, *Quaternary Sci. Rev.*, 129, 1–36, 2015.
- Grant, K. M., Rohling, E. J., Bar-Matthews, M., Ayalon, A., Medina-Elizalde, M., Ramsey, C. B., Satow, C., and Roberts, A. P.: Rapid coupling between ice volume and polar temperature over the past 150,000 years, *Nature*, 491, 744–747, 2012.
- Grant, K. M., Rohling, E. J., Ramsey, C. B., Cheng, H., Edwards, R. L., Florindo, F., Heslop, D., Marra, F., Roberts, A. P., Tamisiea, M. E., and Williams, F.: Sea-level variability over five glacial cycles, *Nat. Commun.*, 5, 5076, <https://doi.org/10.1038/ncomms6076>, 2014.
- Hallegatte, S., Green, C., Nicholls, R. J., and Corfee-Morlot, J.: Future flood losses in major coastal cities, *Nat. Clim. Change*, 3, 802–806, 2013.
- Hansen, J.: Climate threat to the planet: implications for energy policy and intergenerational justice, Bjerknes lecture, American Geophysical Union, San Francisco, 17 December 2008, available at: <http://www.columbia.edu/~jeh1/2008/AGUBjerknes20081217.pdf> (last access: 10 August 2016), 2008.
- Hansen, J.: *Storms of My Grandchildren*, Bloomsbury, New York, 304 pp., 2009.
- Hansen, J. and Sato, M.: Greenhouse gas growth rates, *P Natl. Acad. Sci. USA*, 101, 16109–16114, 2004.
- Hansen, J. and Sato, M.: Regional climate change and national responsibilities, *Environ. Res. Lett.*, 11, 034009, <https://doi.org/10.1088/1748-9326/11/3/034009>, 2016.
- Hansen, J., Russell, G., Lacis, A., Fung, I., Rind, D., and Stone, P.: Climate response times: Dependence on climate sensitivity and ocean mixing, *Science*, 229, 857–859, <https://doi.org/10.1126/science.229.4716.857>, 1985.
- Hansen, J., Sato, M., Ruedy, R., Lacis, A., and Oinas, V.: Global warming in the twenty-first century: An alternative scenario, *P. Natl. Acad. Sci. USA*, 97, 9875–9880, 2000.
- Hansen, J., Sato, M., Ruedy, R., Nazarenko, L., Lacis, A., Schmidt, G. A., Russell, G., Aleinov, I., Bauer, M., Bauer, S., Bell, N., Cairns, B., Canuto, V., Chandler, M., Cheng, Y., Del Genio, A., Faluvegi, G., Fleming, E., Friend, A., Hall, T., Jackman, C., Kelley, M., Kiang, N. Y., Koch, D., Lean, J., Lerner, J., Lo, K., Menon, S., Miller, R. L., Minnis, P., Novakov, T., Oinas, V., Perlwitz, J. P., Perlwitz, J., Rind, D., Romanou, A., Shindell, D., Stone, P., Sun, S., Tausnev, N., Thresher, D., Wielicki, B., Wong, T., Yao, M., and Zhang, S.: Efficacy of climate forcings, *J. Geophys. Res.*, 110, D18104, <https://doi.org/10.1029/2005JD005776>, 2005.
- Hansen, J., Sato, M., Kharecha, P., Russell, G., Lea, D. W., and Siddall, M.: Climate change and trace gases, *Philos. T. Roy. Soc. A*, 365, 1925–1954, <https://doi.org/10.1098/rsta.2007.2052>, 2007.
- Hansen, J., Sato, M., Kharecha, P., Beerling, D., Berner, R., Masson-Delmotte, V., Pagani, M., Raymo, M., Royer, D. L., and Zachos, J. C.: Target atmospheric CO₂: Where should humanity aim?, *Open Atmos. Sci. J.*, 2, 217–231, 2008.
- Hansen, J., Ruedy, R., Sato, M., and Lo, K.: Global surface temperature change, *Rev. Geophys.*, 48, RG4004, <https://doi.org/10.1029/2010RG000345>, 2010.

- Hansen, J., Sato, M., Kharecha, P., and von Schuckmann, K.: Earth's energy imbalance and implications, *Atmos. Chem. Phys.*, 11, 13421–13449, <https://doi.org/10.5194/acp-11-13421-2011>, 2011.
- Hansen, J., Kharecha, P., Sato, M., Masson-Delmotte, V., Ackerman, F., Beerling, D. J., Hearty, P. J., Hoegh-Guldberg, O., Hsu, S., Parmesan, C., Rockstrom, J., Rohling, E. J., Sachs, J., Smith, P., Steffen, K., Van Susteren, L. von Schuckmann, K., and Zachos, J. C.: Assessing “dangerous climate change”: Required reduction of carbon emissions to protect young people, future generations and nature, *Plos One*, 8, e81648, <https://doi.org/10.1371/journal.pone.0081648>, 2013a.
- Hansen, J., Sato, M., Russell, G., and Kharecha, P.: Climate sensitivity, sea level and atmospheric carbon dioxide, *Philos. T. Roy. Soc. A*, 371, 20120294, <https://doi.org/10.1098/rsta.2012.0294>, 2013b.
- Hansen, J., Sato, M., Hearty, P., Ruedy, R., Kelley, M., Masson-Delmotte, V., Russell, G., Tselioudis, G., Cao, J., Rignot, E., Velicogna, I., Tormey, B., Donovan, B., Kandiano, E., von Schuckmann, K., Kharecha, P., Legrande, A. N., Bauer, M., and Lo, K.-W.: Ice melt, sea level rise and superstorms: Evidence from paleoclimate data, climate modeling, and modern observations that 2 °C global warming could be dangerous, *Atmos. Chem. Phys.*, 16, 3761–3812, <https://doi.org/10.5194/acp-16-3761-2016>, 2016.
- Hansen, J., Sato, M., Kharecha, P., and von Schuckmann, K.: Young people's burden: Data files, <https://doi.org/10.5281/zenodo.823301>, 2017.
- Hansen, J. E.: A slippery slope: How much global warming constitutes “dangerous anthropogenic interference”? An editorial essay, *Climatic Change*, 68, 269–279, <https://doi.org/10.1007/s10584-005-4135-0>, 2005.
- Hansen, J. E.: Scientific reticence and sea level rise, *Environ. Res. Lett.*, 2, 024002, <https://doi.org/10.1088/1748-9326/2/2/024002>, 2007.
- Hansen, J. E.: Environment and development challenges: the imperative of a carbon fee and dividend The Oxford Handbook of the Macroeconomics of Global Warming, edited by: Bernard, L. and Semmler, W., Oxford University Press, Oxford, <https://doi.org/10.1093/oxfordhb/9780199856978.013.0026>, 2014.
- Hartmann, D. L., Klein Tank, A. M. G., Rusticucci, M., Alexander, L. V., Brönnimann, S., Charabi, Y., Dentener, F. J., Dlugokencky, E. J., Easterling, D. R., Kaplan, A., Soden, B. J., Thorne, P. W., Wild, M., and Zhai, P. M.: Observations: Atmosphere and Surface, in: *Climate Change 2013: The Physical Science Basis*, edited by: Stocker, T. F., Qin, D., Plattner, G.-K., Tignor, M., Allen, S. K., Boschung, J., Nauels, A., Xia, Y., Bex, V., and Midgley, P. M., Cambridge University Press, Cambridge, UK, 2013.
- Hawkins, E., Ortega, P., Suckling, E., Schurer, A., Hegerl, G., Jones, P., Joshi, M., Osborn, T. J., Masson-Delmotte, V., Mignot, J., Thorne, P., and van Oldenborgh, G. J.: Estimating changes in global temperature since the pre-industrial period, *B. Am. Meteorol. Soc.*, <https://doi.org/10.1175/BAMS-D-16-0007.1>, online first, 2017.
- Hedenus, F., Wirsenius, S., and Johansson, D. J. A.: The importance of reduced meat and dairy consumption for meeting stringent climate change targets, *Climatic Change*, 124, 79–91, <https://doi.org/10.1007/s10584-014-1104-5>, 2014.
- Hoffman, J. S., Clark, P. U., Parnell, A. C., and He, F.: Regional and global sea-surface temperatures during the last interglaciation, *Science*, 355, 276–279, 2017.
- Holmes, C. D., Prather, M. J., Søvde, O. A., and Myhre, G.: Future methane, hydroxyl, and their uncertainties: key climate and emission parameters for future predictions, *Atmos. Chem. Phys.*, 13, 285–302, <https://doi.org/10.5194/acp-13-285-2013>, 2013.
- Howarth, R. W.: Methane emissions and climatic warming risk from hydraulic fracturing and shale gas development: implications for policy, *Energy Emission Control Tech.*, 3, 45–54, 2015.
- Hsu, S. L.: *The Case for a Carbon Tax*, Island Press, Washington, D.C., p. 233, 2011.
- Huang, B., Banzon, V. F., Freeman, E., Lawrimore, J., Liu, W., Peterson, T. C., Smith, T. M., Thorne, P. W., Woodruff, S. D., and Zhang, H.-M.: Extended reconstructed sea surface temperature Version 4 (ERSST.v4). Part I: Upgrades and intercomparisons, *J. Climate*, 28, 911–930, 2015.
- Huber, M. and Knutti, R.: Natural variability, radiative forcing and climate response in the recent hiatus reconciled, *Nat. Geosci.*, 7, 651–656, 2014.
- Huntingford, C., Lowe, J. A., Gohar, L. K., Bowerman, N. H., Allen, M. R., Raper, S. C., and Smith, S. M.: The link between a global 2 °C warming threshold and emissions in years 2020, 2050 and beyond, *Environ. Res. Lett.*, 7, 014039, <https://doi.org/10.1088/1748-9326/7/1/014039>, 2012.
- IPCC: Guidelines for National Greenhouse Gas Inventories, in: Vol. 4, Agriculture, Forestry and Other Land Use, edited by: Eggleston, H. S., Buendia, L., Miwa, K., Ngara, T., and Tanabe, K., IGES Japan, <http://www.ipcc-nggip.iges.or.jp/> (last access: September 2016), 2006.
- IPCC – Intergovernmental Panel on Climate Change: *Climate Change 2013*, edited by: Stocker, T., Qin, D., Q., Plattner, G. K., Tignor, M. M. B., Allen, S. K., Boschung, J., Nauels, A., Xia, Y., Bex, V., and Midgley, P. M., Cambridge University Press, Cambridge, 1535 pp., 2013.
- IPCC – Intergovernmental Panel on Climate Change: *Climate Change 2014: Impacts, Adaptation, and Vulnerability*, edited by: Field, C., Barros, V. R., Dokken, D. J., Mach, K. J., and Mastrandrea, M. D., Cambridge University Press, Cambridge, 1132 pp., 2014.
- IPCC SRES – Intergovernmental Panel on Climate Change: *Special Report on Emissions Scenarios*, edited by: Nakicenovic, N. and Swart, R., Cambridge University Press, Cambridge, 2000.
- Jackson, R. B., Canadell, J. G., Le Quere, C., Andrew, R. M., Korsbakken, J. I., Peters, G. P., and Nakicenovic, N.: Reaching peak emissions, *Nat. Clim. Change*, 6, 7–10, 2016.
- Jones, C. D., Ciais, P., Davis, S. J., Friedlingstein, G., Gasser, T., Peter, G. P., Rogelj, J., van Vuuren, D. P., Canadell, J. G., Cowie, A., Jackson, R. B., Jonas, M., Kriegler, E., Littleton, E., Lowe, J. A., Milne, J., Shrestha, G., Smith, P., Torvanger, A., and Wiltshire, A.: Simulating the Earth system response to negative emissions, *Environ. Res. Lett.*, 11, e095012, <https://doi.org/10.1088/1748-9326/11/9/095012>, 2016.
- Joos, F., Bruno, M., Fink, R., Stocker, T. F., Siegenthaler, U., Le Quere, C., and Sarmiento, J. L.: An efficient and accurate representation of complex oceanic and biospheric models of anthropogenic carbon uptake, *Tellus B*, 48, 397–417, 1996.

- Judd, A. G., Hovland, M., Dimitrov, L. I., Garcia, G. S., and Jukes, V.: The geological methane budget at continental margins and its influence on climate change, *Geofluids*, 2, 109–126, 2002.
- Juliana et al. vs. United States: Kelsey Cascadia Rose Juliana et al. v The United States of America; Barack Obama, in his official capacity as President of the United States, et al.; United States District Court, District of Oregon, Eugene Division Case no. 6:15-cv-01517-TC, hearing held on 13 September 2016 on defendant's motion to dismiss case, decision pending, 2016.
- Kang, M., Christian, S., Celia, M. A., Mauzerall, D. L., Bill, M., Miller, A. R., Chen, Y., Conrad, M. E., Darrah, T. H., and Jackson, R. B.: Identification and characterization of high methane-emitting abandoned oil and gas wells, *P. Natl. Acad. Sci. USA*, 113, 13636–13641, <https://doi.org/10.1073/pnas.1605913113>, 2016.
- Kantola, I. B., Masters, M. D., Beerling, D. J., Long, S. P., and DeLucia, E. H.: Potential of global croplands and bioenergy crops for climate change mitigation through deployment for enhanced weathering, *Biol. Lett.*, 13, 20160714, <https://doi.org/10.1098/rsbl.2016.0714>, 2017.
- Keeling, C. D., Whorf, T. P., Wahlen, M., and van der Plicht, J.: Interannual extremes in the rate of rise of atmospheric carbon dioxide since 1980, *Nature*, 375, 666–670, 1973.
- Keith, D. W.: Why capture CO₂ from the atmosphere, *Science*, 325, 1654–1655, 2009.
- Keith, D. W., Ha-Duong, M., and Stolaroff, J. K.: Climate strategy with CO₂ capture from the air, *Climatic Change*, 74, 17–45, 2006.
- Keith, D. W., Weisenstein, D. K., Dykema, J. A., and Keutsch, F. N.: Stratospheric solar geoengineering without ozone loss, *P. Natl. Acad. Sci. USA*, 113, 14910–14914, <https://doi.org/10.1073/pnas.1615572113>, 2016.
- Kharecha, P. A. and Hansen, J. E.: Implications of “peak oil” for atmospheric CO₂ and climate, *Global Biogeochem. Cy.*, 22, GB3012, <https://doi.org/10.1029/2007GB003142>, 2008.
- Kirtman, B., Power, S. B., Adedoyin, J. A., Boer, G. J., Bojariu, R., Camilloni, I., Doblas-Reyes, F. J., Fiore, A. M., Kimoto, M., Meehl, G. A., Prather, M., Sarr, A., Schär, C., Sutton, R., van Oldenborgh, G. J., Vecchi, G., and Wang, H. J.: Near-term Climate Change: Projections and Predictability, in: *Climate Change 2013: The Physical Science Basis*, edited by: Stocker, T. F., Qin, D., Plattner, G.-K., Tignor, M., Allen, S. K., Boschung, J., Nauels, A., Xia, Y., Bex, V., and Midgley, P. M., Cambridge University Press, Cambridge, UK, 2013.
- Kohler, P., Hartman, J., and Wolf-Gladrow, D. A.: Geoengineering potential of artificially enhanced silicate weathering of olivine, *P. Natl. Acad. Sci. USA*, 107, 20228–20233, 2010.
- Kopp, G., Krivova, N., Lean, J., and Wu, C. J.: The Impact of the Revised Sunspot Record on Solar Irradiance Reconstructions, *Solar Physics*, 291, 2951–2965, <https://doi.org/10.1007/s11207-016-0853-x>, 2016.
- Kopp, R. E., Kemp, A. C., Bittermann, K., Horton, B. P., Donnelly, J. P., Gehrels, W. R., Hay, C. C., Mitrovica, J. X., Morrow, E. D., and Rahmstorf, S.: Temperature-driven global sea-level variability in the Common Era, *P. Natl. Acad. Sci. USA*, 113, E1434–E1441, 2016.
- Kosaka, Y. and Xie, S. P.: Recent global-warming hiatus tied to equatorial Pacific surface cooling, *Nature*, 501, 403–407, 2013.
- Kroeze, C. and Bouwman, L.: The role of nitrogen in climate change, *Curr. Opin. Environ. Sustain.*, 3, 279–280, 2011.
- Kvenvolden, K. A.: Gas hydrates – Geological perspective and global change, *Rev. Geophys.*, 31, 173–187, 1993.
- Kyoto Protocol: available at: http://unfccc.int/kyoto_protocol/items/2830.php (last access: 9 September 2016), 1997.
- Lacis, A. A., Schmidt, G. A., Rind, D., and Ruedy, R. A.: Atmospheric CO₂: Principal control knob governing Earth's temperature, *Science*, 330, 356–359, <https://doi.org/10.1126/science.1190653>, 2010.
- Lacis, A. A., Hansen, J. E., Russell, G. L., Oinas, V., and Jonas, J.: The role of long-lived greenhouse gases as principal LW control knob that governs the global surface temperature for past and future climate change, *Tellus B*, 65, 19734, <https://doi.org/10.3402/tellusb.v65i0.19734>, 2013.
- Lambeck, K., Rouby, H., Purcell, A., Sun, Y., and Sambridge, M.: Sea level and global ice volumes from the Last Glacial Maximum to the Holocene, *P. Natl. Acad. Sci. USA*, 111, 15296–15303, 2014.
- Larsen, N. K., Kjær, K. H., Lecavalier, B., Bjørk, A. A., Colding, S., Huybrechts, P., Jakobsen, K. E., Kjeldsen, K. K., Knudsen, K.-L., Odgaard, B. V., and Olsen, J.: The response of the southern Greenland ice sheet to the Holocene thermal maximum, *Geology*, 43, 291–294, <https://doi.org/10.1130/G36476.1>, 2015.
- Levermann, A., Clark, P. U., Marzeion, B., Milne, G. A., Pollard, D., Radic, V., and Robinson, A.: The multimillennial sea-level commitment of global warming, *P. Natl. Acad. Sci. USA*, 110, 13745–13750, <https://doi.org/10.1073/pnas.1219414110>, 2013.
- Levitus, S., Antonov, J. I., Boyer, T. P., Baranova, O. K., Garcia, H. E., Locarnini, R. A., Mishonov, A. V., Regan, J. R., Seidov, D., Yarosh, E. S., and Zweng, M. M.: World ocean heat content and thermocline sea level change (0–2000 m), 1955–2010, *Geophys. Res. Lett.*, 39, L10603, <https://doi.org/10.1029/2012GL051106>, 2012.
- Liu, X. and Zhang, F.: Nitrogen fertilizer induced greenhouse gas emissions in China, *Curr. Opin. Environ. Sustain.*, 3, 407–413, 2011.
- Liu, Z., Zhu, J., Rosenthal, Y., Zhang, X., Otto-Bliesner, B. L., Timmermann, A., Smith, R. S., Lohmann, G., Zheng, W., and Timm, O. E.: The Holocene temperature conundrum, *P. Natl. Acad. Sci. USA*, 111, E3501–E3505, <https://doi.org/10.1073/pnas.1407229111>, 2014.
- Lorius, C., Jouzel, J., Raynaud, D., Hansen, J., and Le Treut, H.: The ice-core record: Climate sensitivity and future greenhouse warming, *Nature*, 347, 139–145, <https://doi.org/10.1038/347139a0>, 1990.
- Lovering, J. R., Yip, A., and Nordhaus, T.: Historical construction costs of global nuclear power reactors, *Energy Policy*, 91, 371–382, 2016.
- Lunt, D. J., Haywood, A. M., Schmidt, G. A., Salzmann, U., Valdes, P. J., and Dowsett, H. J.: Earth system sensitivity inferred from Pliocene modelling and data, *Nat. Geosci.*, 3, 60–64, 2010.
- Macknick, J.: Energy and CO₂ emission data uncertainties, *Carbon Manage.*, 2, 189–205, 2011.
- Mankiw, N. G.: Smart taxes: an open invitation to join the Pigou club, *Eastern Econ. J.*, 35, 14–23, 2009.
- Marcott, S. A. and Shakun, J. D.: Holocene climate change and its context for the future, *PAGES*, 23, 28, 2015.

- Marcott, S. A., Shakun, J. D., Clark, P. U., and Mix, A. C.: A reconstruction of regional and global temperature for the last 11,300, *Science*, 339, 1198–1201, 2013.
- Masson-Delmotte, V., Schulz, M., Abe-Ouchi, A., Beer, J., Ganopolski, A., Gonzalez Rouco, J. F., Jansen, E., Lambeck, K., Luterbacher, J., Naish, T., Osboorn, T., Otto-Bliesner, B., Quinn, T., Ramekh, R., Rojas, M., Shao, X., and Timmermann, A.: Information from paleoclimate archives, in: *Climate Change 2013: The Physical Science Basis*, edited by: Stocker, T. F., Qin, D., Plattner, G.-K., Tignor, M., Allen, S. K., Boschung, J., Nauels, A., Xia, Y., Bex, V., and Midgley, P. M., Cambridge University Press, Cambridge, UK, 2013.
- McGranahan, G., Balk, D., and Anderson, B.: The rising tide: assessing the risks of climate change and human settlements in low elevation coastal zones, *Environ. Urban.*, 19, 17–37, 2007.
- McKay, N. P., Overpeck, J. T., and Otto-Bliesner, B. L.: The role of ocean thermal expansion in Last Interglacial sea level rise, *Geophys. Res. Lett.*, 38, L14605, <https://doi.org/10.1029/2011GL048280>, 2011.
- Medhaug, I., Stolpe, M. B., Fischer, E. M. and Knutti, R.: Reconciling controversies about the 'global warming hiatus', *Nature*, 545, 41–47, 2017.
- Meehl, G. A., Teng, H., and Arblaster, J. M.: Climate model simulations of the observed early-2000s hiatus of global warming, *Nat. Clim. Change*, 4, 898–902, <https://doi.org/10.1038/nclimate2357>, 2014.
- Meinshausen, M., Smith, S. J., Calvin, K., Daniel, J. S., Kainuma, M. L. T., Lamarque, J. F., Matsumoto, K., Montzka, S. A., Raper, S. C. B., Riahi, K., Thomson, A., Velders, G. J. M., and van Vuuren, D. P. P.: The RCP greenhouse gas concentrations and their extensions from 1765 to 2300, *Climatic Change*, 109, 213–241, 2011a.
- Meinshausen, M., Wigley, T. M. L., and Raper, S. C. B.: Emulating atmosphere–ocean and carbon cycle models with a simpler model, *MAGICC6 – Part 2: Applications*, *Atmos. Chem. Phys.*, 11, 1457–1471, <https://doi.org/10.5194/acp-11-1457-2011>, 2011b.
- Menne, M. J., Durre, I., Vose, R. S., Gleason, B. E., and Houston, T. G.: An overview of the Global Historical Climatology Network–Daily database, *J. Atmos. Ocean Tech.*, 29, 897–910, 2012.
- Mercer, J. H.: West Antarctic ice sheet and CO₂ greenhouse effect: a threat of disaster, *Nature*, 271, 321–325, 1978.
- Montreal Protocol: The Montreal Protocol on Substances that Deplete the Ozone Layer, available at: <http://www.ozone.unep.org/>, last access: 19 June 2016.
- Montzka, S. A., Krol, M., Dlugokencky, E., Hall, B., Jockel, P., and Lelieveld, J.: Small interannual variability of global atmospheric hydroxyl, *Science*, 331, 67–69, 2011.
- Moosdorf, N., Renforth, P., and Hartmann, J.: Carbon dioxide efficiency of terrestrial enhanced weathering, *Environ. Sci. Technol.*, 48, 4809–4816, 2014.
- Moss, R. H., Edmonds, J. A., Hibbard, K. A., Manning, M. R., Rose, S. K., van Vuuren, D. P., Carter, T. R., Emori, S., Kainuma, M., Kram, T., Meehl, G. A., Mitchell, J. F. B., Nakicenovic, N., Riahi, K., Smith, S. J., Stouffer, R. J., Thomson, A. M., Weyant, J. P., and Wilbanks, T. J.: The next generation of scenarios for climate change research and assessment, *Nature*, 463, 747–756, 2010.
- Myhre, G., Shindell, D., Breon, F., Collins, W., Fuglestad, J., Huang, J., Koch, D., Lamarque, J. F., Lee, D., Mendoza, B., Nakajima, T., Robock, A., Stephens, G., Takemura, T., and Zhang, H.: Anthropogenic and natural climate forcing, in: *Climate Change 2013: The Physical Science Basis*, edited by: Stocker, T. F., Qin, D., Plattner, G.-K., Tignor, M., Allen, S. K., Boschung, J., Nauels, A., Xia, Y., Bex, V., and Midgley, P. M., Cambridge University Press, Cambridge, UK, 2013.
- NAS – National Academy of Sciences: Climate Intervention: Carbon Dioxide Removal and Reliable Sequestration, Washington, D.C., 154 pp., <https://doi.org/10.17226/18805>, 2015a.
- NAS – National Academy of Sciences: Climate Intervention: Reflecting Sunlight to Cool Earth, Washington, D.C., 234 pp., <https://doi.org/10.17226/18988>, 2015b.
- NAS – National Academy of Sciences: Attribution of Extreme Weather Events in the Context of Climate Change, National Academies Press, Washington, D.C., <https://doi.org/10.17226/21852>, 2016.
- Newman, P. A., Oman, L. D., Douglass, A. R., Fleming, E. L., Frith, S. M., Hurwitz, M. M., Kawa, S. R., Jackman, C. H., Krotkov, N. A., Nash, E. R., Nielsen, J. E., Pawson, S., Stolarski, R. S., and Velders, G. J. M.: What would have happened to the ozone layer if chlorofluorocarbons (CFCs) had not been regulated?, *Atmos. Chem. Phys.*, 9, 2113–2128, <https://doi.org/10.5194/acp-9-2113-2009>, 2009.
- Nisbet, E. G., Dlugokencky, E. J., Manning, M. R., Lowry, D., France, J. L., Michel, S. E., Miller, J. B., White, J. W. C., Vaughn, B., Bousquet, P., Pyle, J. A., Warwick, N. J., Cain, M., Brownlow, R., Zazzeri, G., Lanoiselle, M., Mannin, A. C., Gloor, E., Worthy, D. E. J., Brunke, E. G., Labuschagne, C., Wolff, E. W., and Ganesan, A. L.: Rising atmospheric methane: 2007–2014 growth and isotopic shift, *Global Biogeochem. Cy.*, 30, 1356–1370, 2016.
- Novakov, T., Ramanathan, V., Hansen, J. E., Kirchstetter, T. W., Sato, M., Sinton, J. E., and Sathaye, J. A.: Large historical changes of fossil-fuel black carbon aerosols, *Geophys. Res. Lett.*, 30, 1324, <https://doi.org/10.1029/2005JD005977>, 2003.
- Nystrom, S., and Luckow, M. S.: The economic, climate, fiscal, power, and demographic impact of a national fee-and-dividend carbon tax, *Regional Economic Modeling, Inc.*, Washington, D.C., 126 pp., <http://bit.ly/1srHy3X> (last access: January 2017), 2014.
- O'Connor, F. M., Boucher, O., Gedney, N., Jones, C. D., Folberth, G. A., Coppel, R., Friedlingstein, P., Collins, W. J., Chappellaz, J., Ridley, J., and Johnson, C. E.: Possible role of wetlands, permafrost, and methane hydrates in the methane cycle under future climate change, *Rev. Geophys.*, 48, RG4005, <https://doi.org/10.1029/2010RG000326>, 2010.
- O'Neill, B. C., Oppenheimer, M., Warren, R., Hallegatte, S., Kopp, R. E., Portner, H. O., Scholes, R., Birkmann, J., Foden, W., Licker, R., Mach, K. J., Marbaix, P., Mastrandrea, M. D., Price, J., Takahashi, K., van Ypersele, J. P., and Yohe, G.: IPCC reasons for concern regarding climate change risks, *Nat. Clim. Change*, 7, 28–37, 2017.
- Overpeck, J. T., Otto-Bliesner, B. L., Miller, G. H., Muhs, D. R., Alley, R. B., and Kiehl, J. T.: Paleoclimatic evidence for future ice-sheet instability and rapid sea-level rise, *Science*, 311, 1747–1750, 2006.
- Paris Agreement: UNFCCC secretariat, available at http://unfccc.int/paris_agreement/items/9485.php (last access: 21 April 2017), 2015.

- Park, S., Croteau, P., Boering, K. A., Etheridge, D. M., Ferretti, D., Fraser, P. J., Kim, K. R., Krummel, P. B., Langenfelds, R. L., van Ommen, T. D., Steele, L. P., and Trudinger, C. M.: Trends and seasonal cycles in the isotopic composition of nitrous oxide since 1940, *Nat. Geosci.*, 5, 261–265, 2012.
- Parker, A. and Geden, O.: No fudging on geoengineering, *Nat. Geosci.*, 9, 859–860, <https://doi.org/10.1038/ngeo2851>, 2016.
- Pearson, R. G., Phillips, S. J., Loranty, M. M., Beck, P. S. A., Damoulas, T., Knight, S. J., and Goetz, S. J.: Shifts in Arctic vegetation and associated feedbacks under climate change, *Nat. Clim. Change*, 3, 673–677, 2013.
- Peters, G. P., Andrew, R. M., Boden, T., Canadell, J. G., Ciais, P., Le Quéré, C., Marland, G., Raupach, M. R., and Wilson, C.: The challenge to keep global warming below 2 °C, *Nat. Clim. Change*, 3, 4–6, 2013.
- Peterson, T. C. and Vose, R.: An overview of the global historical climatology network temperature database, *B. Am. Meteorol. Soc.*, 78, 2837–2849, 1997.
- Petron, G., Frost, G. J., Trainer, M. K., Miller, B. R., Dlugokencky, E. J., and Tans, P.: Reply to comment on “Hydrocarbon emissions characterization in the Colorado Front Range – A pilot study” by Michael A. Levi, *J. Geophys. Res.-Atmos.*, 118, 236–242, <https://doi.org/10.1029/2012JD018487>, 2013.
- Pierrehumbert, R.: How to decarbonize? Look to Sweden, *Bull. Atom. Sci.*, 72, 105–111, 2016.
- Pollard, D., DeConto, R. M., and Alley, R. B.: Potential Antarctic ice sheet retreat driven by hydrofracturing and ice cliff failure, *Earth Planet. Sc. Lett.*, 412, 112–121, 2015.
- Popp, A., Lotze-Campen, H., and Bodirsky, B.: Food consumption, diet shifts and associated non-CO₂ greenhouse gases, *Global Environ. Change*, 20, 451–462, 2010.
- Prather, M., Midgley, P., Rowland, F. S., and Stolarski, R.: The ozone layer: the road not taken, *Science*, 381, 551–554, 1996.
- Prather, M., Flato, G., Friedlingstein, P., Jones, C., Lamarque, J. F., Liao, H., and Rasch, P.: Annex II: Climate System Scenario Tables, in: *Climate Change 2013: The Physical Science Basis*, edited by: Stocker, T., Qin, D. Q., Plattner, G. K., Tignor, M. M. B., Allen, S. K., Boschung, J., Nauels, A., Xia, Y., Bex, V., and Midgley, P. M., Cambridge University Press, Cambridge, 1395–1445, 2013.
- Prather, M. J. and Holmes, C. D.: Overexplaining or underexplaining methane's role in climate change, *P. Natl. Acad. Sci. USA*, 114, 5324–5326, <https://doi.org/10.1073/pnas.1704884114>, 2017.
- Prather, M. J., Holmes, C. D., and Hsu, J.: Reactive greenhouse gas scenarios: systematic exploration of uncertainties and the role of atmospheric chemistry, *Geophys. Res. Lett.*, 39, L09803, <https://doi.org/10.1029/2012GL051440>, 2012.
- Prather, M. J., Hsu, J., Deluca, N. M., Jackman, C. H., Oman, L. D., Douglass, A. R., Fleming, E. L., Strahan, S. E., Steenrod, S. D., Sovde, O. A., Isaksen, I. S. A., Froidevaux, L., and Funke, B.: Measuring and modeling the lifetime of nitrous oxide including its variability, *J. Geophys. Res.-Atmos.*, 120, 5693–5705, 2015.
- Quiquet, A., Archibald, A. T., Friend, A. D., Chappellaz, J., Levine, J. G., Stone, E. J., Telford, P. J., and Pyle, J. A.: The relative importance of methane sources and sinks over the Last Interglacial period and into the last glaciation, *Quaternary Sci. Rev.*, 112, 1–16, 2015.
- Rajaratnam, B., Romano, J., Tsiang, M., and Diffenbaugh, N. S.: Debunking the climate hiatus, *Climatic Change*, 133, 129–140, 2015.
- Rao, S., Klimont, Z., Smith, S. J., Van Dingenen, R., Dentener, F., Bouwman, L., Riahi, K., Amann, M., Bodirsky, B. L., van Vuuren, D. P., Reis, L. A., Calvin, K., Drouet, L., Fricko, O., Fujimori, S., Gernaat, D., Havlik, P., Harmsen, M., Hasegawa, T., Heyes, C., Hilaire, J., Luderer, G., Masui, T., Stehfest, E., Strefler, J., van der Sluis, S., and Tavoni, M.: Future air pollution in the Shared Socio-economic Pathways, *Global Environ. Change*, 42, 346–358, 2017.
- Rigby, M., Montzk, S. A., Prinn, R. G., White, J. W. C., Younga, D., O'Doherty, S., Lunta, M. F., Ganesane, A. L., Manning, A. J., Simmonds, P. G., Salameh, P. K., Harthg, C. M., Mühleg, J., Weiss, R. F., Fraser, P. J., Steele, L. P., Krummel, P. B., McCullocha, A., and Park, S.: Role of atmospheric oxidation in recent methane growth, *P. Natl. Acad. Sci. USA*, 114, 5373–5377, <https://doi.org/10.1073/pnas.1616426114>, 2017.
- Rignot, E., Mouginot, J., Morlighem, M., Seroussi, H., and Scheuchl, B.: Widespread, rapid grounding line retreat of Pine Island, Thwaites, Smith, and Kohler glaciers, West Antarctica, from 1992 to 2011, *Geophys. Res. Lett.*, 41, 3502–3509, 2014.
- Röckmann, T. and Levin, I.: High-precision determination of the changing isotopic composition of atmospheric N₂O from 1990 to 2002, *J. Geophys. Res.-Atmos.*, 110, D21304, <https://doi.org/10.1029/2005jd006066>, 2005.
- Rogelj, J., Luderer, G., Pietzcker, R. C., Kriegler, E., Schaeffer, M., Krey, V., and Riahl, K.: Energy system transformations for limiting end-of-century warming to below 1.5 °C, *Nat. Clim. Change*, 5, 519–527, 2015.
- Rogelj, J., den Elzen, M., Hohne, N., Franzen, T., Fekete, H., Winkler, H., Schaeffer, R., Sha, F., Rishi, K., and Meinshausen, M.: Paris Agreement climate proposals need a boost to keep warming well below 2 °C, *Nature*, 534, 631–639, 2016a.
- Rogelj, J., Schaeffer, M., Friedlingstein, P., Gillett, N. P., van Vuuren, D. P., Riahi, K., Allen, M., and Knutti, R.: Differences between carbon budget estimates unraveled, *Nat. Clim. Change*, 534, 631–639, 2016b.
- Rohling, E. J., Sluijs, A., Dijkstra, H., Köhler, P., van de Wal, R. S., von der Heydt, A., Beerling, D., Berger, A., Bijl, P., Crucifix, M., DeConto, R., Drijfhout, S., Fedorov, A., Foster, G., Ganopolski, A., Hansen, J., Hönlisch, B., Hooghiemstra, H., Huber, M., Huybers, P., Knutti, R., Lea, D., Lourens, L. J., Lunt, D., Masson-Delmotte, V., Medina-Elizalde, M., Otto-Bliesner, B., Pagani, M., Pälike, H., Renssen, H., Royer, D., Siddall, M., Valdes, P., Zachos, J. C., and Zeebe, R. E.: Making sense of palaeoclimate sensitivity, *Nature*, 491, 683–691, <https://doi.org/10.1038/nature11574>, 2012a.
- Rohling, E. J., Medina-Elizade, M., Shepherd, J. G., Siddall, M., and Stanford, J. D.: Sea surface and high-latitude temperature sensitivity to radiative forcing of climate over several glacial cycles, *J. Climate*, 25, 1635–1656, 2012b.
- Rohling, E. J., Haigh, I. D., Foster, G. L., Roberts, A. P., and Grant, K. M.: A geological perspective on potential future sea-level rise, *Scient. Rep.*, 3, 3461, <https://doi.org/10.1038/srep03461>, 2013.
- Royer, D. L., Pagani, M., and Beerling, D. J.: Geobiological constraints on Earth system sensitivity to CO₂ during the Cretaceous and Cenozoic, *Geobiology*, 10, 298–310, 2012.

- Sanderson, B. M., O'Neill, B. C., and Tebaldi, C.: What would it take to achieve the Paris temperature targets?, *Geophys. Res. Lett.*, 43, 7133–7142, <https://doi.org/10.1002/2016GL069563>, 2016.
- Sato, M., Hansen, J. E., McCormick, M. P., and Pollack, J. B.: Stratospheric aerosol optical depths, 1850–1990, *J. Geophys. Res.*, 98, 22987–22994, <https://doi.org/10.1029/93JD02553>, 1993.
- Saunois, M., Jackson, R. B., Bousquet, P., Poulter, B., and Canadell, J. G.: The growing role of methane in anthropogenic climate change, *Environ. Res. Lett.*, 11, 120207, <https://doi.org/10.1088/1748-9326/11/12/120207>, 2016.
- Saunois, M., Bousquet, P., Poulter, B., Peregón, A., Ciais, P., Canadell, J. G., Dlugokencky, E. J., Etiope, G., Bastviken, D., Houweling, S., Janssens-Maenhout, G., Tubiello, F. N., Castaldi, S., Jackson, R. B., Alexe, M., Arora, V. K., Beerling, D. J., Bergamaschi, P., Blake, D. R., Brailsford, G., Bruhwiler, L., Crevoisier, C., Crill, P., Covey, K., Frankenberg, C., Gedney, N., Höglund-Isaksson, L., Ishizawa, M., Ito, A., Joos, F., Kim, H.-S., Kleinen, T., Krummel, P., Lamarque, J.-F., Langenfelds, R., Locatelli, R., Machida, T., Maksyutov, S., Melton, J. R., Morino, I., Naik, V., O'Doherty, S., Parmentier, F.-J. W., Patra, P. K., Peng, C., Peng, S., Peters, G. P., Pison, I., Prinn, R., Ramonet, M., Riley, W. J., Saito, M., Santini, M., Schroeder, R., Simpson, I. J., Spahni, R., Takizawa, A., Thornton, B. F., Tian, H., Tohjima, Y., Viovy, N., Voulgarakis, A., Weiss, R., Wilton, D. J., Wiltshire, A., Worthly, D., Wunch, D., Xu, X., Yoshida, Y., Zhang, B., Zhang, Z., and Zhu, Q.: Variability and quasi-decadal changes in the methane budget over the period 2000–2012, *Atmos. Chem. Phys. Discuss.*, <https://doi.org/10.5194/acp-2017-296>, in review, 2017.
- Schädel, C., Bader, M. K.-F., Schuur, E. A. G., Biasi, C., Bracho, R., Čapek, P., De Baets, S., Diáková, K., Ernakovich, J., Estop-Aragones, C., Graham, D. E., Hartley, I. P., Iversen, C. M., Kane, E., Knoblauch, C., Lupascu, M., Martikainen, P. J., Natali, S. M., Norby, R. J., O'Donnell, J. A., Chowdhury, T. R., Šantrůčková, H., Shaver, G., Sloan, V. L., Treat, C. C., Turetsky, M. R., Waldrop, M. P., and Wickland, K. P.: Potential carbon emissions dominated by carbon dioxide from thawed permafrost soils, *Nat. Clim. Change*, 6, 950–953, <https://doi.org/10.1038/nclimate3054>, 2016.
- Schaefer, H., Mikaloff Fletcher, S. E., Veidt, C., Lassey, K. R., Brailsford, G. W., Bromley, T. M., Dlugokencky, E. J., Michel, S. E., Miller, J. B., Levin, I., Lowe, D. C., Martin, R. J., Vaughn, B. H., and White, J. W. C.: A 21st century shift from fossil-fuel to biogenic methane emissions indicated by ¹³CH₄, *Science*, 352, 80–84, 2016.
- Schmidt, G. A., Kelley, M., Nazarenko, L., Ruedy, R., Russell, G. L., Aleinov, I., Bauer, M., Bauer, S. E., Bhat, M. K., Bleck, R., Canuto, V., Chen, Y.-H., Cheng, Y., Clune, T. L., Del Genio, A., de Fainchtein, R., Faluvegi, G., Hansen, J. E., Healy, R. J., Kiang, N. Y., Koch, D., Lacis, A. A., LeGrande, A. N., Lerner, J., Lo, K. K., Matthews, E. E., Menon, S., Miller, R. L., Oinas, V., Oloso, A. O., Perlwitz, J. P., Puma, M. J., Putman, W. M., Rind, D., Romanou, A., Sato, M., Shindell, D. T., Sun, S., Syed, R. A., Tausnev, N., Tsigaridis, K., Unger, N., Voulgarakis, A., Yao, M.-S., and Zhang, J.: Configuration and assessment of the GISS ModelE2 contributions to the CMIP5 archive, *J. Adv. Model. Earth Syst.*, 6, 141–184, <https://doi.org/10.1002/2013MS000265>, 2014.
- Schoof, C.: Ice sheet grounding line dynamics: steady states, stability, and hysteresis, *J. Geophys. Res.*, 112, F03S28, <https://doi.org/10.1029/2006JF000664>, 2007.
- Schoof, C.: Beneath a floating ice shelf, *Nat. Geosci.*, 3, 450–451, 2010.
- Schuur, E. A. G., McGuire, A. D., Schädel, C., Grosse, G., Harden, J. W., Hayes, D. J., Hugelius, G., Koven, C. D., Kuhry, P., Lawrence, D. M., Natali, S. M., Olefeldt, D., Romanovsky, V. E., Schaefer, K., Turetsky, M. R., Treat, C. C., and Vonk, J. E.: Climate change and the permafrost carbon feedback, *Nature*, 520, 171–179, 2015.
- Schwalm, C. R., Williams, C. A., Schaefer, K., Baker, I., Collatz, G. J., and Rödenbeck, C.: Does terrestrial drought explain global CO₂ flux anomalies induced by El Niño?, *Biogeosciences*, 8, 2493–2506, <https://doi.org/10.5194/bg-8-2493-2011>, 2011.
- Schwietzke, S., Sherwood, O. A., Bruhwiler, L. M. P., Miller, J. B., Etiope, G., Dlugokencky, E. J., Michel, S. E., Arling, V. A., Vaughn, B. H., White, J. W. C., and Tans, P. P.: Upward revision of global fossil fuel methane emissions based on isotope database, *Nature*, 538, 88–91, 2016.
- Searchinger, T., Heimlich, R., Houghton, R. A., Dong, F., Elobeid, A., Fabiosa, J., Tokgoz, S., Hayes, D., and Yu, T.-H.: Use of U.S. croplands for biofuels increases greenhouse gases through emissions from land-use change, *Science*, 319, 1238–1240, 2008.
- SIPRI – Stockholm International Peace Research Institute: SIPRI Military Expenditure Database, available at: <https://www.sipri.org/databases/milex>, last access: 17 September 2016.
- Smith, P.: Soil carbon sequestration and biochar as negative emission technologies, *Global Change Biol.*, 22, 1315–1324, 2016.
- Smith, P., Bustamante, M., Ahammad, H., Clark, H., Dong, H., Elsiddig, E. A., Haberl, H., Harper, R., House, J. Jafari, M., Masera, O., Mbaw, C., Ravindranath, N. H., Rice, C. W., Abad, C. R., Romanovskaya, A., Sperling, F., and Tubiello, F. N.: Agriculture, Forestry and Other Land Use (AFOLU), in: *Climate Change 2014: Mitigation of Climate Change, Contribution of Working Group III to the Fifth Assessment Report of the Intergovernmental Panel on Climate Change*, edited by: Edenhofer, O., Pichs-Madruga, R., Sokona, Y., Minx, J. C., Farahani, E., Kadner, S., Seyboth, K., Adler, A., Baum, I., Brunner, S., Eickemeier, P., Kriemann, B., Savolainen, J., Schlömer, S., von Stechow, C., and Zwickel, T., Cambridge University Press, Cambridge, UK, 2014.
- Smith, P., Davis, S. J., Creutzig, F., Fuss, S., Minx, J., Gavrielle, B., Kato, E., Jackson, R. B., Cowie, A., Kriegler, E., van Vuuren, D. P., Rogelj, J., Ciais, P., Milne, J., Canadell, J. G., McCollum, D., Peters, G., Andrew, R., Krey, V., Shrestha, G., Friedlingstein, P., Gasser, T., Grubler, A., Heidug, W. K., Jonas, M., Jones, C. D., Kraxner, F., Littleton, E., Lowe, J., Moreira, J. R., Nakicenovic, N., Obersteiner, M., Patwardhan, A., Rogner, M., Rubin, E., Sharifi, A., Torvanger, Asbjørn, Yamagata, Y., Edmonds, J., and Yongsung, C.: Biophysical and economic limits to negative CO₂ emissions, *Nat. Clim. Change*, 6, 42–50, 2016.
- Smith, T. M., Reynolds, R. W., and Lawrimore, J.: Improvements to NOAA's historical merged land-ocean surface temperature analysis (1880–2006), *J. Climate*, 21, 2283–2296, 2008.
- Socolow, R., Desmond, M. J., Aines, R., Blackstock, J. J., Bolland, O., Kaarsberg, T., Lewis, N., Mazzotti, M., Pfeffer, A., Sirola, J. J., Sawyer, K., Smit, B., and Wilcox, J.: Direct air capture of

- CO₂ with chemicals: a technology assessment for the APS Panel on Public Affairs, American Physical Society, Office of Public Affairs, Washington, D.C., 2011.
- Stern, N.: The economics of Climate Change: The Stern Review, Cambridge University Press, Cambridge, 2006.
- Stern, N. and Taylor, C.: Climate change: risk, ethics, and the Stern review, *Science*, 317, 203–204, 2007.
- Taylor, L. L., Quirk, J., Thorley, R. M. S., Kharecha, P. A., Hansen, J., Ridgwell, A., Lomas, M. R., Banwart, S. A., and Beerling, D. J.: Enhanced weathering strategies for stabilizing climate and averting ocean acidification, *Nat. Clim. Change*, 6, 402–406, 2016.
- Tedesco, M., Doherty, S., Fettweis, X., Alexander, P., Jeyaratnam, J., and Stroeve, J.: The darkening of the Greenland ice sheet: trends, drivers, and projections (1981–2100), *The Cryosphere*, 10, 477–496, <https://doi.org/10.5194/tc-10-477-2016>, 2016.
- Thompson, D. W. J., Kennedy, J. J., Wallace, J. M., and Jones, P. D.: A large discontinuity in the mid-twentieth century in observed global-mean surface temperature, *Nature*, 453, 646–649, <https://doi.org/10.1038/nature06982>, 2008.
- Tilman, D. and Clark, M.: Global diets link environmental sustainability and human health, *Nature*, 515, 518–522, 2014.
- Trenberth, K. E. and Fasullo, J. T.: An apparent hiatus in global warming?, *Earth's Future*, 1, 19–32, <https://doi.org/10.1002/2013EF000165>, 2013.
- Trenberth, K. E., Fasullo, J., von Schuckmann, K., and Cheng, L.: Insights into Earth's energy imbalance from multiple sources, *J. Climate*, 29, 7495–7505, <https://doi.org/10.1175/JCLI-D-16-0339.1>, 2016.
- Turner, A. J., Jacob, D. J., Benmergui, J., Wofsy, S. C., Maasakkers, J. D., Butz, A., Hasekamp, O., and Biraud, S. C.: A large increase in U.S. methane emissions over the past decade inferred from satellite data and surface observations, *Geophys. Res. Lett.*, 43, 2218–2224, <https://doi.org/10.1002/2016GL067987>, 2016.
- Turner, A. J., Frankenberg, C., Wennberg, P. O., and Jacob, D. J.: Ambiguity in the causes for decadal trends in atmospheric methane and hydroxyl, *P. Natl. Acad. Sci. USA*, 114, 1–6, 2017.
- Turney, C. S. M. and Jones, R. T.: Does the Agulhas Current amplify global temperatures during super-interglacials?, *J. Quatern. Sci.*, 25, 839–843, 2010.
- Tyndall, J.: On the absorption and radiation of heat by gases and vapours, and on the physical connexion of radiation, absorption, and conduction – The Bakerian Lecture, *Phil. Mag.*, 22, 273–285, 1861.
- United Nations: Framework Convention on Climate Change (UNFCCC), United Nations, New York, NY, available at: http://unfccc.int/essential_background/items/6036.php (last access: 3 March 2016), 1992.
- United Nations: UNFCCC Technical Annex – Aggregate effect of the intended nationally determined contributions: an update, available at: http://unfccc.int/focus/indc_portal/items/9240.php (last access: January 2017), 2016.
- van Vuuren, D. P., Edmonds, J., Kainuma, M., Riahi, K., Thomson, A., Hibbard, K., Hurtt, G. C., Kram, T., Krey, V., Lamarque, J.-F., Masui, T., Meinshausen, M., Nakicenovic, N., Smith, S. J., and Rose, S. K.: The representative concentration pathways: an overview, *Climatic Change*, 109, 5–31, 2011.
- Vial, J., Dufresne, J. L., and Bony, S.: On the interpretation of inter-model spread in CMIP5 climate sensitivity estimates, *Clim. Dynam.*, 41, 3339–3362, <https://doi.org/10.1007/s00382-013-1725-9>, 2013.
- von Schuckmann, K. and Le Traon, P. Y.: How well can we derive Global Ocean Indicators from Argo data?, *Ocean Sci.*, 7, 783–791 <https://doi.org/10.5194/os-7-783-2011>, 2011.
- von Schuckmann, K., Palmer, M. D., Trenberth, K. E., Cazenave, A., Chamber, D., Champollion, N., Hansen, J., Josey, S. A., Loeb, N., Mathieu, P. P., Meyssignac, B., and Wild, M.: An imperative to monitor Earth's energy imbalance, *Nat. Clim. Change*, 6, 138–144, 2016.
- Voulgarakis, A., Naik, V., Lamarque, J.-F., Shindell, D. T., Young, P. J., Prather, M. J., Wild, O., Field, R. D., Bergmann, D., Cameron-Smith, P., Cionni, I., Collins, W. J., Dalsøren, S. B., Doherty, R. M., Eyring, V., Faluvegi, G., Folberth, G. A., Horowitz, L. W., Josse, B., MacKenzie, I. A., Nagashima, T., Plummer, D. A., Righi, M., Rumbold, S. T., Stevenson, D. S., Strode, S. A., Sudo, K., Szopa, S., and Zeng, G.: Analysis of present day and future OH and methane lifetime in the ACCMIP simulations, *Atmos. Chem. Phys.*, 13, 2563–2587, <https://doi.org/10.5194/acp-13-2563-2013>, 2013.
- Warwick, N. J., Cain, M. L., Fisher, R., France, J. L., Lowry, D., Michel, S. E., Nisbet, E. G., Vaughn, B. H., White, J. W. C., and Pyle, J. A.: Using $\delta^{13}\text{C}\text{-CH}_4$ and $\delta\text{D}\text{-CH}_4$ to constrain Arctic methane emissions, *Atmos. Chem. Phys.*, 16, 14891–14908, <https://doi.org/10.5194/acp-16-14891-2016>, 2016.
- Williamson, P.: Scrutinize CO₂ removal methods, *Nature*, 530, 153–155, 2016.
- Woolf, D., Amonette, J. E., Street-Perrott, F. A., Lehmann, J., and Joseph, S.: Sustainable biochar to mitigate global climate change, *Nat. Commun.*, 1, 56, <https://doi.org/10.1038/ncomms1053>, 2010.
- Yu, J., Menviel, L., Jin, Z. D., Thornalley, D. J. R., Barker, S., Marino, G., Rohling, E. J., Cai, Y., Zhang, F., Wang, X., Dai, Y. Chen, P., and Broecker, W. S.: Sequestration of carbon in the deep Atlantic during the last glaciation, *Nat. Geosci.*, 9, 319–324, 2016.
- Zachos, J. C., Pagani, M., Sloan, L., Thomas, E., and Billups, K.: Trends, rhythms, and aberrations in global climate 65 Ma to present, *Science*, 292, 686–693, 2001.
- Zachos, J. C., Dickens, G. R., and Zeebe, R. E.: An early Cenozoic perspective on greenhouse warming and carbon-cycle dynamics, *Nature*, 451, 279–283, 2008.